Modelling the response of ice sheets to climatic change and topography

Andrew Robert Kerr

Doctor of Philosophy
University of Edinburgh
1993

Declaration

I hereby declare that this thesis has been composed by myself and the work within it is my own, except where otherwise referenced.

Andrew Robert Kerr

Abstract

The aim of this project is to investigate the influence of climate and topography on ice sheets in maritime environments. Numerical models are adapted to simulate the behaviour of the climate and ice sheets in southern Chile and Scotland during the last glaciation. The climate model relates climatic variables to snow accumulation and ablation using an energy balance model. The ice sheet model is based on the continuity equation for ice thickness and relates surface mass exchange to ice thickness and flow. Subsequently, a simple topography model is developed to examine the critical transition between glaciers and ice sheets.

The net mass balance gradient in maritime regions is primarily sensitive to temperature and precipitation. Ice sheet initiation is strongly influenced by the adjacent ocean's temperature, which affects the delicate balance between decreasing precipitation and decreasing temperature. In Chile, expanded glaciation reflects an equatorward movement of the prevailing westerlies, though the postulated migration of precipitation belts implies that the maximum depression of the snowline is unlikely to have been contemporaneous at different latitudes. In Scotland, ice sheets appear to be triggered by the southward movement of the North Atlantic polar front. These model results imply that maritime regions require a reduction in the ocean temperature, whilst retaining sufficient precipitation, and a surface topography susceptible to ice sheet growth, as necessary conditions for initiating ice sheets. The configuration and altitude of upland topography determines the point of initiation of ice masses and controls the threshold between stable upland glaciers and the growth of an ice sheet. Model results indicate that this threshold is a fold catastrophe. Thus, the topography acts as a filter between climate and the response of a glacier, which undermines the use of proxy ice volume data as proxy climate indicators, while topographic evolution leads to a powerful feedback between topography, climate and ice over Quaternary time scales.

Acknowledgements

I am indebted to my supervisor, David Sugden, for his critical input, encouragement, and enthusiasm, without which this thesis would not have been written.

I would like to thank J. Oerlemans, A.J.Payne, N.R.J. Hulton, and J.F. Nye for contributing useful ideas to my research, and to all the computing staff at the Department of Geography, University of Edinburgh, for technical support.

Thank you also to all those at the Department of Geography who have made my time in Edinburgh so enjoyable, and to Kathy Foster and Caroline MacMillan for love and companionship. Finally, my gratitude goes to my family for their moral and financial support.

This research has been sponsored by the Natural Environment Research Council for which I am grateful.

Table of Contents

Table of Figures

Chapter 4

Paper I:

Paper II:

Chapter 5:

Paper III:

List of Tables

Frontispiece: Mt. Foraker, Alaska at sunset

Chapter One:
Introduction and Principal Themes

1.1 Aim

The aim of this thesis is to investigate the influence of climate and topography on ice sheets in maritime environments. This is accomplished using numerical models which endeavour to represent the climate and ice sheets mathematically. The models are employed to simulate events from specific case studies as a means of understanding the dominant processes and relationships operating within each system. There are three specific objectives:

1) To simulate the climate of southern Chile at the last glacial maximum to investigate the modification of climate required to accord with palaeo-environmental evidence.

2) To simulate the Loch Lomond stadial ice cap in Scotland to examine the climatic and topographic conditions which facilitate ice sheet initiation.

3) To explore the sensitivity of ice sheet evolution to the regional configuration of mountains. This involves deriving a numerical criterion for subglacial topography and calculating the effect of different topographic configurations.

1.2 Background and Scope

The rationale for studying this subject is to understand the interactions between different subsystems of global climate as a means of understanding global climatic change; in this case, the focus is on the role of maritime climates and subglacial topography in determining ice sheet evolution. An appreciation of the links and feedbacks between these and other subsystems is required to understand long term climatic change. The deductive methods used for understanding and predicting short term climatic change, or weather, are not applicable to long term climatic change because of its non-linear response to forcing. One alternative is to reconstruct past climatic fluctuations to investigate the response of these subsystems to forcing and hence provide an understanding of their links and feedbacks. Past climates are reconstructed by synthesising the available information which includes biological, chemical, and geomorphologic records, and in the last millennium, historical chronicles. The ambiguous nature of the data necessitates the use of numerical models to explore and simulate the possible interactions between different elements of the climatic system, and so test our understanding of how it operates.

The study of past climates assumes that complex variations can be deduced from a set of mathematical equations which are derived from the basic physical laws of conservation of mass, energy, and momentum. Given the complexity of global climate, which has processes embedded in a hierarchy of spatial and temporal scales ranging from microscopic to global, no one model can hope to encompass the natural world in its

entirety. Instead, a model focuses on a narrow range of scales, and events occurring outwith this band are assumed to be either extraneous to the model or to act as boundary conditions for the model. Clearly, the initial dilemma is to select the appropriate variables for the model. This depends on the objectives of the work, which define the scale of interest, and the precision to which the relevant natural processes can be represented mathematically (Saltzman,1983).

Evidence suggests that during the Quaternary era, global climate has fluctuated between warm periods, such as the present, and cold periods, such as the last glacial maximum 18,000 years ago. These prominent changes have generated sufficient evidence for a detailed investigation into their origins, and this has led to a spate of theoretical and observational studies into many facets of the climatic change involved. This thesis is concerned with two aspects of the Quaternary climatic fluctuations. The first is the interface between maritime climates and ice sheets, which has ramifications for ideas concerning the alteration of oceanic currents during glacial periods (Broeker and Denton,1989). It is a reasonable assumption that maritime ice sheets are particularly sensitive to climatic change because of their proximity to oceans, and thus are affected by ocean temperature changes and the availability of moisture. The second is the interface between ice and the regional configuration of mountains, which acts as a filter between regional climate and the response of a glacier or ice sheet.

Investigating the behaviour of maritime ice sheets depends on correctly modelling the climate-ice sheet interface. This requires an appreciation of the factors which influence regional climate and the influence exerted by glaciers or ice sheets on local climate. The prime source of energy which drives the regional climatic system is the sun. The energy reaching a point on the earth's surface depends on factors such as the solar output, the earth's orbital configuration and axial rotation, and geographical location. Atmospheric and oceanic circulations redistribute the energy and thus moderate the imbalance of energy reaching the surface. Consequently, one method of modelling global climate, developed by Budyko (1969) and Sellers (1969), is to examine the energy balance of the earth, and formulate the energy budget in terms of surface temperature. The energy balance is reduced to simple mathematical equations by averaging small scale processes and empirically determining key variables which affect the overall energy flux. More recent and sophisticated versions of energy balance models include seasonal cycles and a more realistic geography of continental and oceanic regions (North et al.,1981; Crowley and North,1991).

These models indicate that for a range of solar output, including the present day value, there are three possible steady state global mean temperatures. These correspond to a small volume of ice, a large volume of ice, and completely ice covered (figure 1.1).

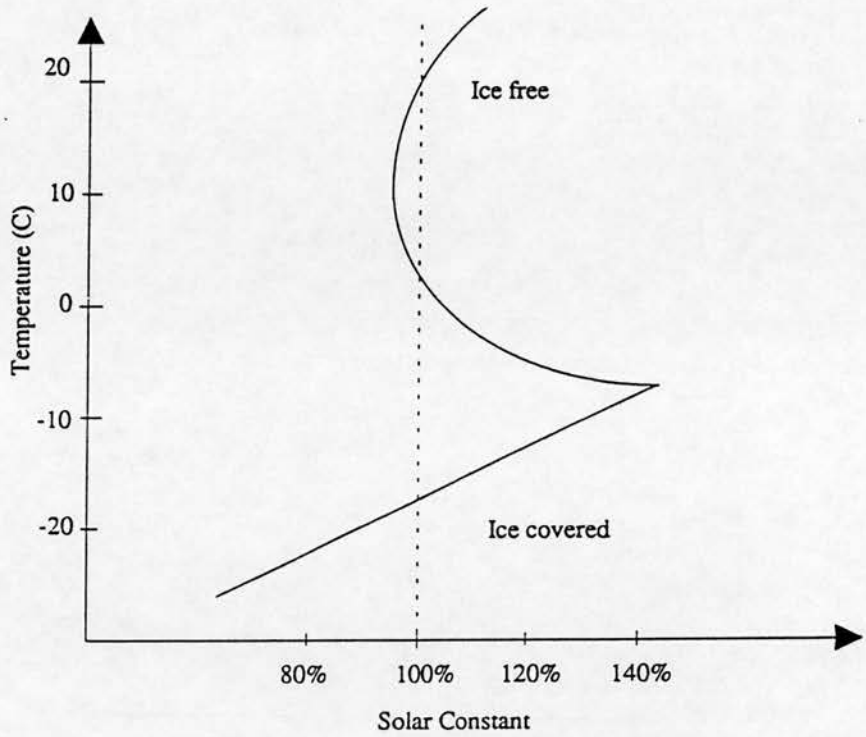

Figure 1.1 Steady state global mean temperatures for a range of solar output.

The intermediate state has no physical relevance since it is in an unstable steady state; small perturbations force the climate back to the lower or upper branches. The model results imply that a drop in the solar constant of a few percent from the present value leads to a catastrophic drop in global temperature to the only remaining equilibrium state, that of an ice covered earth. If this was to occur then the solar output would have to rise to almost one and a half times its present value to return to a non-glaciated earth. However, there is no evidence that the earth has been totally glaciated in recent geological times, and this insight has led to the realisation that non-equilibrium, or unstable, models are required to explain Quaternary glaciations. In other words, the climate is regulated through the existence of feedbacks on different spatial and temporal scales which prevent the climate from approaching the equilibrium states postulated by the energy balance models. In response a number of oscillating models have been

developed incorporating different physical feedbacks. These include ice sheet dynamics (Weertman,1976; Birchfield,1977; Källen et al.,1979; Budd and Smith,1981) in conjunction with deep ocean temperature (Sergin,1979), isostasy (Birchfield et al.,1981; Ghil and LeTreut,1981; Oerlemans,1980b; Peltier,1982; Pollard,1982), sea ice extent (Saltzman and Sutera,1984; Saltzman et al.,1984), and deep ocean circulation (Broeker and Denton,1989).

The growth and decay of ice sheets is driven by the balance between mass input (accumulation) and mass output (ablation). Generally the models force ice sheets either by prescribing the accumulation and ablation directly, or by incorporating an energy balance model which derives surface temperature and hence the mass balance of the ice sheet. Of course, the interface between the atmosphere and the ice surface is far more complicated than is manifest with the simple regional energy balance models. The mass and energy budgets of glaciers or ice sheets depend on factors such as the radiation budget, temperature, precipitation, and turbulent fluxes, and these have contrasting sensitivities depending on the climatic regime (Kuhn,1981,1984,1989; Oerlemans and Hoogendoorn,1989).

A number of models, of varying degrees of sophistication, have been developed to examine the detailed variations of energy and mass budgets over an ice surface. A fundamental problem has been the acquisition of detailed data from glaciers to test the models. This problem of data acquisition can be reduced by the erudite use of empirical simplifications of the relevant fluxes to parameters that can be readily measured. Braithwaite (1984) attempts to derive a statistical relationship between a glacier's equilibrium line, which is the altitude at which annual mass input balances mass output, and the glacier's altitudinal mass balance profile. However, he concludes that further climatic information is required to constrain the correlation. More productive has been the use of degree day methods, which sets the ablation proportional to the sum of positive daily temperatures, to calculate mass balance variations from meteorological variables (Braithwaite and Olesen,1989; Ambach and Kuhn,1989). However, such an approach is unable to discriminate between different climatic factors which are likely to vary disproportionately during long term climatic change. Hence a more process oriented approach is required.

Oerlemans (1992) develops a model, originally derived by Oerlemans and Hoogendorn (1989), which calculates the altitudinal profile of mass balance for Alpine glaciers from the three primary influences of surface energy and mass budgets. These are;

firstly, external factors such as solar output or the orbital configuration of the earth; secondly, regional climatic conditions such as temperature and precipitation; and thirdly, local factors such as altitude, slope, and aspect. The model is adapted for Greenland and used for sensitivity studies of glacial mass balance (Oerlemans,1991). The advantage of such process oriented models is that they explicitly calculate the effect of factors such as temperature and precipitation, the value of which are notoriously difficult to constrain in palaeoclimatic models.

The first aim of the present work is to investigate the change in maritime climates required to initiate and grow ice sheets; here, the climate and ice sheet are coupled by linking three separate models. A zonally averaged energy balance model is used to calculate the surface temperature in the desired region. The effect of changes to the solar output or the orbital configuration of the earth is included. The regional temperature cycle thus derived is then used as input to the second model, the surface energy balance model based on that of Oerlemans (1992). This latter model calculates the glacial mass balance profile for the region. The glacial mass balance profile is used as input to the third model, the ice sheet model, which is based on the models of Mahaffy (1976), Budd and Smith (1981) and Payne (1988). It uses the continuity equation of ice to obtain ice sheet extent from the glacial mass balance and derivations for ice deformation and sliding.

The second aim of the thesis is to examine the role of mountains on ice sheet evolution. Oerlemans and van der Veen (1984) note the existence of a fold catastrophe in the ice sheet - climate system when mountains are present, because potentially there are multiple configurations of ice surface elevation and hence interactions with the climate. It is concluded that one high plateau is more important than a few high but steep-sided mountain ranges in initiating and growing ice sheets. Examples of fold catastrophes are common and include the transition from valley glaciers to ice sheets (Hindmarsh,1990), ice sheet evolution over medium scale topography (Oerlemans,1981; Payne and Sugden,1990), and the coalescence of ice sheet domes. The catastrophic jumps at these topographic thresholds occur as the system jumps to more stable states, and depend on the response time of the glacier to climatic forcing. The evolution through time may then become unpredictable (Hindmarsh,1990).

The ice sheet model used to investigate climate - ice interactions is not suitable for examining the role of mountains because the assumptions required to calculate glacial dynamics are not applicable over steep terrain. Instead, sensitivity experiments conducted here suggest a simpler formulation of the processes involved with glacial dynamics and

climate may be acceptable. The complexity of the overall system is reduced by the use of simple ice sheet and climate models. It is assumed that ice deforms perfectly plastically to an applied stress, which depends only on the angle of the slope. The climate is simplified by assuming a glacier has a mass balance profile with a fixed altitudinal gradient which can only change by raising or lowering the equilibrium line. The sensitivity experiments in this thesis are thus a first step in assigning a numerical criterion to the configuration of mountains, which determines their relative susceptibility to ice sheet initiation and growth. Ultimately, a measure of the two control variables, the configuration of mountains and the glacial mass balance profile, will provide a means of calculating steady state ice volumes for an arbitrary geographical region.

1.3 Methodology

This thesis uses numerical models of natural systems to elucidate the factors which influence the interfaces between three domains: the atmosphere, the cryosphere, and the lithosphere. To have confidence in the implications of the models' results an appropriate modelling methodology must be utilised. In this work, models are used to simulate inferred climatic changes to examine whether such changes can lead to the resulting ice sheet evolution. Model output is tested against independent evidence from the relevant region.

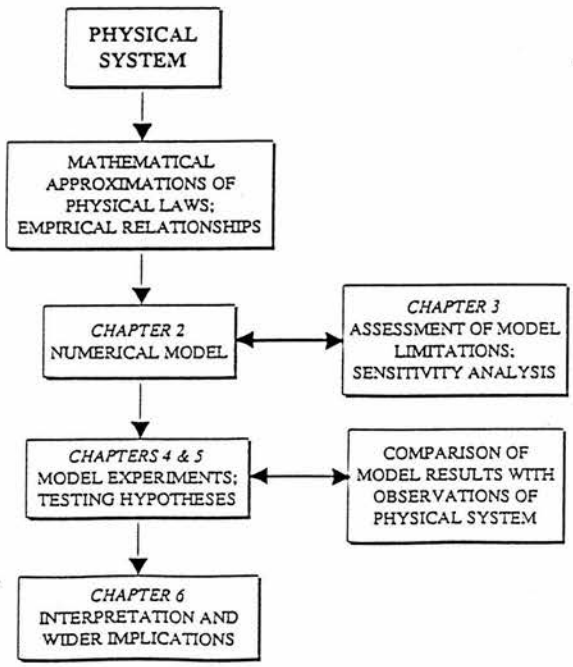

Figure 1.2 The modelling strategy employed in this thesis.

Model Construction

The construction of a model involves three different stages; choosing the variables, assigning values to the variables, and tuning the variables to simulate the real world. The choice of variable depends on which processes are perceived to be important in the system of interest. This is influenced by the relationships between components within the system and the interface between the system and other related domains. The first step is to draw a boundary around the system of interest to separate the causes (or independent variables) and effects (or dependent variables) of perturbations to the system. Since different variables are important at different spatial and temporal scales, identifying and isolating the system of interest substantially narrows the potential choice of variables. The continuum of mass, energy, and momentum exchange which operates in nature must be sub-divided into a discrete approximation of the exact, instantaneous values of variables to solve the relevant equations. The main approach used to achieve this is to rely on averaged values for the different variables. This process of averaging introduces numerical errors which fundamentally constrain the simulation of reality by the model.

Variables can be split into two categories depending on the scale at which they operate relative to the scale of the system of interest. The response (or relaxation) time of a variable is the time taken to return to an equilibrium state after a perturbation. If the averaging period of a variable or system in the model is very much larger than its response time then the variable or system may be assumed to be in a steady state. Its value does not change in time over that averaging period except in the form of stochastic perturbations about the mean value. However, if the averaging period is shorter than the response time, the boundary condition is always changing and a prognostic, or time dependent model is required (Saltzman, 1985). Ice sheets have response times of thousands of years and hence fall into the latter category with regard to global climatic fluctuations. Other climatic components have different response times and may fall into either category. For example, inter-annual variations are assumed not to force long term climate (though James and James (1989) indicate this may not be strictly true), so fall into the former category, while decadal averages of glacial mass balance can affect ice sheet evolution and must be considered in a time-dependent manner. Thus processes with short response times, such as the atmosphere, are assumed to be in a quasi-equilibrium state with processes with longer response times, such as an ice sheet surface. However, Saltzman (1985) argues that the non-linear nature of the climatic system means that it is

unlikely that a detailed understanding of climatic components with short response times will ever provide a measure of the fluxes or processes involved in long term climatic change. These long term mass and energy fluxes are below our resolution and occur as a result of a small disequilibrium between processes with different response times. This sets fundamental limits to our knowledge of the evolution of the whole climatic system.

It is still possible to examine potential feedbacks within and between climatic domains by determining the necessary conditions for an event to occur. Thus the choice of variables for the model will include both time-dependent processes and time-averaged processes which are perceived to be important. If these fail to simulate the reconstructed event then it suggests either that other processes are important or that the values assigned to variables in the model are incorrect.

Assigning numerical values to variables is the second stage of model construction and proceeds from two related standpoints. Firstly, the physical processes underlying a particular relationship may be well known but the process may be too detailed to be incorporated into the model. For example, inter-seasonal variations in climate are well documented but in the context of ice sheet evolution are little more than noise to the underlying signal, or trend, of climate. Hence these variations are ignored by assuming some mean seasonal variation, perhaps with a superimposed stochastic component.

The second approach to quantifying variables occurs when a knowledge of the underlying physical process is sketchy or non existent. In this case a purely empirical relationship is developed between variables. Since this is not causal it must be assumed that the conditions which led to the original observations are invariant spatially and temporally. If these were to change there is no justification for assuming that the empirical relationship remains valid. A common example is the latitudinal variation of cloud cover which is used in planetary albedo calculations but poorly constrained physically. By using simple empirical relationships modellers reduce the freedom of the model to adapt realistically to new conditions.

Since relationships between variables are often complex and affected by external factors, the use of an assigned mean value will inevitably lead to errors. For example, the use of a cubic power in the Glen flow law for ice is a gross simplification of the strain on ice resulting from an applied stress. The actual strain will depend on factors such as the temperature of the ice, the grain size, the orientation of the grains, and the impurities in the ice (Paterson,1981). However, testing models of ice sheet extent using a cubic power in the Glen flow law produces the best fit with independent evidence. This parameter is

thus a useful generalisation of the complex processes involved in ice flow but it is not applicable to all flow phenomena, such as large ice streams. If large ice streams are adjudged to be irrelevant to the evolution of the overall system then it is justifiable to use the generalisations. If not, a more detailed approach to the problem is necessary.

These difficulties lead to a somewhat arbitrary approach since one physical system may be represented by a multitude of numerical models, each emphasising slightly different components of the system depending on the objectives of the work and the bias of the worker. For example, this thesis aims to examine the ice sheet - climate interface but is not overly concerned with the complexities of ice sheet dynamics, and relies on rather simple derivations of the relevant equations. This re-emphasises the point that no one model can hope to encompass the entire range of processes operating on different spatial and temporal scales in the natural world. Rather, the model is a tool to tackle a specific problem.

The final procedure for constructing the model is to tune the variables to simulate the real world. This is intimately connected with the previous procedures since the choice of variables and their values establishes the precision to which the models simulate the real world. The values of the variables are adjusted to ensure the output represents observations of reality. If the model is based on accurate equations deduced from the fundamental laws of physics, then one might expect it to simulate reality without the need for tuning. Unfortunately, the need to simplify processes empirically and the process of averaging variables spatially and temporally leads to a model which can only simulate the real world approximately. The parameters used in the simplifying and averaging processes can be very sensitive to small changes in value, and this affects model output. The best solution appears to be to tune, or adjust, model parameter values to simulate independent evidence accurately. Once these values have been set one must assume that the prevailing conditions do not change. This substantially restricts the freedom of the model to respond to forcing which is outwith the range for which it was tuned. It implies that the inclusion of fewer tuned parameters in the model leads to a more realistic response. Unfortunately, at whatever scale is chosen some averaging and simplifying is necessary and the non-linear nature of the global climate system ensures that model output will soon diverge from the observed reality. The best procedure is to reduce the number of tuning parameters to a minimum and attempt to construct a model which is relatively insensitive to the value of tuned parameters.

Model Testing and Analysis

The uncertainties in construction mean that the model must be tested to verify that it is a sufficiently accurate representation of the system under investigation. Testing the models involves two procedures. The first is the comparison between model output and independent evidence from the physical system under investigation. The model must be constructed in such a way that the output can be tested against available data. The absence of these data, or production of model output which is untestable, will severely restrict the model's value. However, it is still possible to examine the sensitivity of the parameters within the system. For example, it has been suggested that the solar output has varied over millennia and affected global climate. Unfortunately, there is no method of testing this proposition and the idea remains unsubstantiated. On the other hand it is possible to determine the sensitivity of global climate to a change in solar output with the appropriate model. The model does not seek to predict the temporal evolution of solar output, merely examine the relative importance of its variability in comparison with other climatic variables.

The second procedure is to assess the quality of the data used to test the model. There are four separate issues concerned with the accuracy and availability of test data. Firstly, the availability of test data will predetermine the design and use of the model. A separate data set is required from that used to construct the model, in order to avoid a circular argument. The second issue is whether the test data are representative of the system under investigation. This depends on the sampling procedure and determines whether the model output can be measured statistically. The third issue concerns the accuracy of the test data. There is likely to be both an intrinsic error of measurement and an error of interpretation. This latter error is especially probable in disciplines such as geomorphology, which rely on dominant paradigms to provide an interpretation of convoluted data. Finally, it is difficult to test empirically-derived parameters which are not directly based on physical processes.

By means of illustration, if an ice sheet model is independently tested against the extent of an existing ice sheet, such as the Greenland ice sheet, and then used to examine the evolution of former ice sheets, a number of assumptions are implicit in the results. Of the four issues noted above the first and third are concerned with the availability and accuracy of test data. With this example, it can be assumed that the existing ice sheet extent is well documented. The fourth issue concerns the physical processes from which empirical parameters are derived, and in this example it is assumed that the ice sheet

model is a sufficiently good representation of ice dynamics. The only problem then concerns the representation of the test data. Since ice sheets vary in time, a single snapshot of ice sheet extent is not particularly helpful, even with well resolved climatic data, since we do not know if the ice sheet is in equilibrium with the climate. Without further information it would be difficult to state with confidence that the ice sheet model could simulate ice sheet evolution through time. Furthermore, it is assumed that the factors which force ice sheet extent are the same now as previously. As Boulton and Jones (1979) noted with the example of deformable beds under Pleistocene ice sheets, this may not be the case.

A model that satisfies the tests is not necessarily a good simplification of the real world. Rather, it is a sufficiently good representation of the system to simulate the available test data. More detailed test data may constrain a model more closely but unless the model is built to the exact specifications of the system it can never simulate the entire system at every level of resolution. Ultimately there is a trade off between the accuracy to which the model simulates a system and the complexity of the model. Unfortunately, with non-linear systems such as the climate, increasing the complexity of the model indefinitely will not necessarily increase the accuracy of the model output, since numerical errors are propagated through the model from the finest level of resolution.

Once a model has satisfied the tests the next procedure is to analyse the model. Sensitivity analysis is the process of systematically varying model parameters to examine their sensitivity within the model. Ideally the most sensitive parameters are those that are directly derived from physical processes rather than those derived from empirical simplifications of such relationships. These latter parameters often rely on optimisation, or tuning, to produce meaningful results and therefore rely on assumptions of invariance over space and time. Furthermore, they may not represent any particular physical process and are difficult to test. If the parameters which are schematic simplifications of the real world turn out to be highly sensitive then there is a case for attempting to reformulate either the model or the parameter simplification, since any error of input will be compounded during the model run. In the worst case a particular parameter to which the model is sensitive may just be an artefact of the model's construction and bear no resemblance to the real world. For example, the use of ice calving parameters based only on water depth can lead to unstable behaviour in the ice sheet model which is not reflected in reality. This may be because the model cannot account for sub-grid scale factors such as topographic pinning points.

In this thesis each parameter is varied about its most likely value by a fixed percentage of their actual value, usually 10% or 20%, unless the parameter has a large uncertainty attached to its value, in which case the variation is proportionately larger. Certain parameters are interdependent and in these cases the minimum error of one depends on the value of another, so the analysis assesses the effect both of varying constants individually and as an associated pair or group.

Model Experiments

Once a model has been verified by tests and analysed it can be used in experiments as a means to understanding the dominant processes and relationships operating within the system. In this thesis two case studies are used to examine the interface between maritime climates and ice sheets. The first is used to investigate the climatic factors involved in the modification of maritime climates during glacial periods. The second is used to examine the necessary climatic and topographic configurations required to initiate ice sheet growth.

The first case study is an investigation of the climatic changes occurring in southern Chile between glacial and interglacial periods. It is a useful case study for examining the sensitivity of maritime climates for two reasons. Firstly, the geographical location means the climate is governed by the prevailing Westerlies which circulate the globe between Antarctica and the southern hemisphere land masses. Chile is dominated by the Andean Cordillera to its east and the Pacific Ocean to the west, so the climatic effect of the rest of South America is small (Miller,1976). Furthermore the Patagonian ice fields are narrow so the modification of climate during a glacial cycle can be examined without involving the complicated feedbacks which occur between a large ice sheet and the climate. Secondly, there is sufficient palaeo-environmental evidence to delimit different climatic zones and reconstruct regional climatic changes (Heusser,1989c; Markgraf,1989a).

The second case study is the initiation of the Loch Lomond stadial ice cap which existed in Scotland approximately 12,500 to 9,500 years BP. There are two reasons for using this as a case study. Firstly, its geographical location and size mean that it was likely to be sensitive to ocean temperature changes. It would therefore respond to changes in the North Atlantic circulation which are believed to be crucial in global climatic change. Secondly, there is a large body of data concerning the Late Devensian stadial climate for Britain (e.g.Lowe and Walker,1984) and the North Atlantic (Ruddiman

et al.,1980). The climate is relatively well known while field evidence provides an independent test of the model simulation. Normally, testing theories about the growth of an ice sheet is difficult since evidence is destroyed by the succeeding maximum. However, the Loch Lomond glaciation in Scotland appears to represent a truncated glaciation with an abrupt transition from full glacial to interglacial conditions. It is therefore an excellent region for testing theories concerning the necessary modification of climate required to initiate ice sheets.

The final objective of the thesis is to examine the role of the sub-glacial topography on ice sheet evolution. Since the ice sheet model cannot represent the diverse topographic configurations in detail, a case study is not employed. Instead, hypothetical situations are created using highly simplified models to examine the sensitivity of particular facets of the system. Although these ideas are related to evidence from other models, no attempt is made to simulate real world situations.

1.4 Thesis Structure

This chapter defines the aims and scope of the thesis and examines the methodology underpinning the use of mathematical models to explain and understand global climatic change. This involves considering the logical implications of using abstract models to explain natural phenomena and the epistemological limitations of conclusions inferred from model results. The models' construction, testing, analysis, and ultimately their application to case studies is reviewed.

The second chapter details the construction of the models. Different domains of the climatic system are reduced to and represented by mathematical equations which are either derived empirically or deduced from the fundamental laws of physics. The mathematical foundations behind the derivation of these equations is discussed.

The relationship between model output and reality, and hence the significance of the results, is examined in chapter 3. The strengths and limitations of the models are assessed and the sensitivity of each parameter is examined. This process indicates which parameters primarily affect results, either by their intrinsic sensitivity or because their value is poorly constrained by testing.

Chapter 4 comprises two papers. This approach, though entailing some repetition, provides a more coherent structure for the two case studies. The first uses the climate model to examine factors which influence the snowline in a maritime climate. This is accomplished by identifying the climatic modification required to explain palaeo-

environmental data using southern Chile as a case study. The second paper links the ice sheet and climate models to ascertain the climatic change and topographic configuration required to initiate an ice sheet in a maritime climate. The Loch Lomond stadial ice cap in Scotland is used as a case study.

Chapter 5 also consists of two papers. The first is a paper which reviews the role of topography on the interactions between climate and ice. This includes an appraisal of the effect of both the underlying bedrock topography and the evolving surface topography of an ice sheet. The second paper details some experiments with a highly simplified climate and ice sheet model to explore the effect of topographic configurations on ice sheet evolution. This takes the form of sensitivity experiments on different facets of topography in order to obtain a criterion of its role on ice sheets. The non-linear jump in ice volume observed in the experiments is related to catastrophe theory.

The final chapter summarises the thesis and assesses the wider implications of the work.

Chapter Two:
The Models

2.1 Introduction

This chapter elucidates the construction of the climate and ice sheet models and assesses their respective merits and flaws. This demands an awareness of the exact requirements of the models, the quality of the data, and the relative precision by which each physical process is mathematically represented.

The southern Chile case study employs a surface energy balance model to simulate the climate inferred from palaeoecological evidence during the last glacial maximum. The model was developed to calculate the glacial mass balance of mid-latitude alpine glaciers (Oerlemans,1992) and here is adapted to calculate the glacial mass balance of different regions of Chile. This surface energy balance model is extended with a regional energy balance model and coupled to an ice sheet model for the Loch Lomond stadial case study. The regional energy balance model calculates an annual temperature cycle from regional energy fluxes. This addition provides a means of examining regional climatic fluctuations and the climatic sensitivity to factors such as orbitally induced changes in solar output. The output of the climate model is a glacial mass balance profile, which relates climatic variables to an altitudinal budget of snow accumulation and ablation over one year. This is used as the climatic input to the ice sheet model which calculates the ensuing ice fluxes to provide a measure of ice thickness and extent.

Clearly, the crux of this thesis is not the construction of a unique model for the whole study; rather, it is the adaption and application of existing models to answer the questions posed by the case studies.

2.2 The climate models

To examine the influence of climate on ice sheets the climate model must represent a maritime climate in terms of the glacial input to, and output from, the ice sheet system. This involves relating climatic variables at a specified location to an annually averaged budget of snow accumulation and ablation at different altitudes. This provides a measure of the two parameters which primarily determine the relationship between ice and climate, the snowline and the glacial mass balance profile. The former parameter is the altitude at which snow accumulation exactly balances snow ablation over one year and above which permanent snow cover exists. The latter parameter is the amount of snow accumulated or ablated over one year at different altitudes. This altitudinal gradient is useful for determining the climatic setting and hence the glacial

response to a climatic change (Kuhn,1984; Pelto et al.,1990). The glacial mass balance profile is used to drive the ice sheet model.

2.2.1 The surface mass balance model

The surface mass balance model is taken from Oerlemans (1992) and calculates the accumulation and ablation of snow over a specified altitudinal range. The amount of snow, M, accumulated or ablated in a specific region, and at a particular altitude, is obtained by integrating the surface energy budget, B, and the precipitation, P, over one year:

$$M = \int [-B/L + P]\, \delta t \qquad (2.1)$$

where L is the latent heat of melting at 0°C. The precipitation is assumed to fall as snow below a threshold temperature, which in this case is 2°C. Unless there is a specific seasonal precipitation maximum, precipitation is assumed to fall uniformly during specific precipitation 'events' on every fifth day, and is adjusted to match the annual precipitation total at sea level. Snow melt depends on the energy budget, B. Snow melts if the energy budget, -B/L, is negative, and once snow melts it is assumed not to refreeze. If more snow falls than melts over each time step then there is a net accumulation of snow.

The daily cycle of temperature and radiation is an integral part of the energy balance and is included by integrating with a time step of 30 minutes. The calculation of the integral depends on the value of the surface energy budget, B. This can be partitioned into specific energy fluxes as follows (figure 2.1):

$$B = Q(1-\alpha) + I_\downarrow - I_O + F_S + F_l \qquad (2.2)$$

where Q is the incoming shortwave radiation, α is the albedo, $I_\downarrow$ and I_O are the incoming and outgoing longwave radiation, and F_S and F_l are the turbulent fluxes of sensible and latent heat respectively. This formulation of the energy budget is similar to that employed in the regional energy balance model but is more sophisticated due to the more detailed nature of the input data. Initially, seven parameters must be prescribed from the local climate:

1. Annual temperature cycle
2. Daily temperature range

3. Mean fraction of cloud cover
4. Mean height of cloud base
5. Temperature lapse rate
6. Annual precipitation
7. Altitudinal precipitation gradient

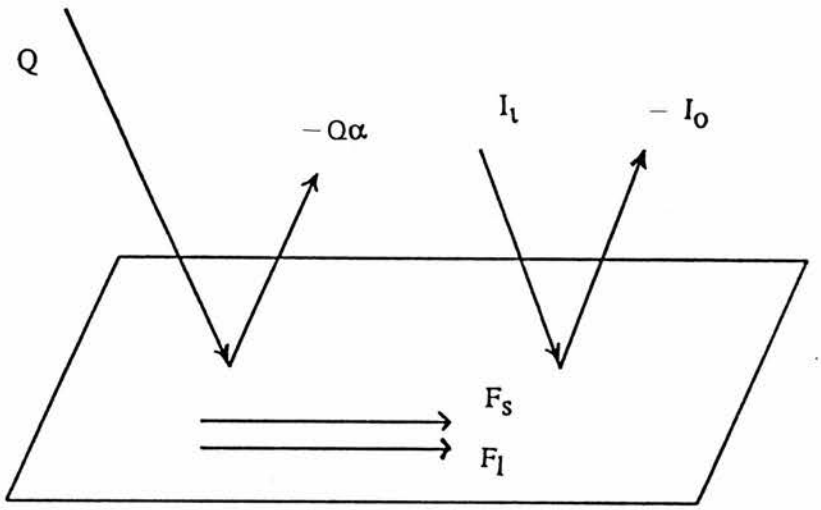

Figure 2.1 The components of the surface energy balance.

The direct incoming shortwave radiation, Q, depends on the solar output, the angular position of the sun, and the transmissivity of the atmosphere, which is obtained by separating the absorption of air, τ_a, and clouds, τ_c. Diffuse shortwave radiation, which is largely determined by the surrounding topography, is an important factor at local scales but is less important regionally. Its variability is below the resolution of the model and so it is not incorporated. The average solar output has been obtained from satellite measurements and is denoted by the solar constant, S, while the angular position of the sun through the year in relation to a flat surface, γ, is obtained with simple trigonometry (Walraven, 1978). The transmissivity of the atmosphere, τ_a, accounts for the scattering and absorption of shortwave radiation by air molecules and is assumed to depend on the altitude of the surface above sea level and the elevation of the sun above the horizon. The

transmissivity of clouds, τ_c, accounts for the scattering and absorption of shortwave radiation by clouds and is assumed to depend on the average cloud cover, n:

$$S = 1353. [1 + 0.034\cos (2\pi N/365)] \text{ W/m}^2 \quad (2.3)$$

$$\tau_a = (0.79 + 0.000024h) [1 - 0.009 (90 - \gamma)] \quad (2.4)$$

$$\tau_c = 1 - (0.41 - 0.000065h) n - 0.37 n^2 \quad (2.5)$$

where h is the altitude in metres, n is cloud cover in tenths, and N is number of days. The total incident shortwave radiation is thus:

$$Q = [S \sin\gamma] \tau_a \tau_c \quad (2.6)$$

The longwave radiation comprises two parts. The outgoing radiation depends on the temperature of the surface. The heat capacity of the surface is not explicitly modelled so the outgoing radiation is set to that of a melting surface of ice. The incoming longwave radiation is assumed to depend on two factors: the contribution from clouds and that from the atmosphere. Both depend on the temperature of the emitting surface. The longwave contribution from the atmosphere is written:

$$I_{at} = \varepsilon_a \sigma \Theta^4_a \quad (2.7)$$

$$\text{where } \varepsilon_a = 0.7 - 0.000025h \quad (2.8)$$

ε_a is the emittance of the atmosphere, Θ_a is the atmospheric temperature, and σ is the Stefan Boltzmann constant. The longwave contribution from the clouds is:

$$I_{cl} = n\varepsilon_{cl} \sigma f \Theta^4_{cl} \quad (2.9)$$

$$\text{where } f = 0.6732 + 0.0024\Theta_{cl} - 0.914\times10^{-5}\Theta^2_{cl} \quad (2.10)$$

n is the cloud cover, ε_{cl} is the cloud emittance, and f is the fraction of emitted black body radiation, which depends on the cloud temperature, Θ_{cl}. Cloud temperature is determined by the mean cloud height and an assumed constant temperature lapse rate.

Thus the total incoming longwave radiation is:

$$I_l = I_{at} + I_{cl} \qquad (2.11)$$

which is determined by three variables: surface air temperature, the mean height of the cloud base, and the average cloud cover.

An appraisal of the surface albedo is important for an accurate determination of the energy budget. It depends on a large number of spatially and temporally heterogeneous variables, and as a result can only be calculated schematically. In the model the albedo is linked to a regional background albedo, α_b, which depends on the altitude, h, relative to the climatic snowline, E:

$$\alpha_b = 0.115 \text{ arctg } (h - E + 300 / 200) + 0.48 \qquad (2.12)$$

This formulation implicitly incorporates the increase in surface albedo with altitude due to the increase of snow cover. The total albedo is:

$$\alpha = \max [0.12; \alpha_{sn} - (\alpha_{sn} - \alpha_{b)} e^{-5\delta} - 0.015Mn] \qquad (2.13)$$

where α_{sn} is the albedo of snow, δ is the depth of snow and Mn is the accumulated seasonal melt. This approach schematically covers a number of factors which are important in the calculation of the surface albedo. The dependence on snow depth stems from the high albedo of fresh snow compared with old snow. Similarly, the dependence on the accumulated melt over the year stems from the general reduction in albedo caused by the increasing quantities of dirt, melting snow and ice on the surface through the summer.

The final components of the energy budget are the turbulent fluxes of sensible and latent heat. These are also related to the climatic snowline since both microscale turbulence and moisture exchange increase down glacier. The sensible heat flux is:

$$F_S = C (\Theta_a - \Theta_S) \qquad (2.14)$$

where Θ_a and Θ_S are the temperature of the atmosphere and surface respectively. C is the exchange coefficient:

$$C = C_E + (E - h) \, dC/dh \qquad (2.15)$$

where Ce and dC/dh are empirically derived constants. The latent heat flux is:

$$F_l = C \, L (q_a - q_s) / c_p \qquad (2.16)$$

where q is the mixing ratio of water vapour, L is the latent heat of vapourisation and c_p is the heat capacity of air.

The energy budget is integrated with the precipitation for three years to obtain the glacial mass balance profile. Three years of integration are required to allow the model output to approach an equilibrium profile, independent of the initial conditions. This is necessary because a climatic snowline must be specified initially to calculate the surface albedo and turbulent fluxes.

2.2.2 The regional energy balance model

The regional energy balance model is developed to calculate the annual temperature cycle at sea level in specified regions, by relating the radiation balance at the surface to a schematic representation of the energy fluxes occurring latitudinally (ie.between latitudinal bands) and zonally (ie.between land and ocean within one latitudinal band).

Assuming global climate is in an equilibrium, the energy budget for a vertical column in the earth's atmosphere is:

$$Q(1 - \alpha) + \text{div} (\text{horizontal heat fluxes}) = I \qquad (2.17)$$

where Q is the incoming shortwave radiation, α is the surface albedo (reflectance), and I is the outgoing longwave radiation.

At any point the absorbed solar radiation is balanced by longwave radiation emitted to space and the divergence of atmospheric and oceanic heat fluxes to cooler areas of the globe. All fluxes are zonally averaged over 10° latitudinal bands. Oceans and land have very different heat capacities and, as a result, annual temperature cycles differ with a comparable radiation budget, so the extent of land and ocean within each latitudinal band is differentiated. To simplify the calculation, the model is reduced to one

latitude zone, with the energy into and out of this zone calculated from the hemispherically averaged energy budget.

The model comprises two sections. Firstly, the surface radiation budget, and secondly, the latitudinal and zonal heat fluxes. The surface radiation budget is:

$$R = Q (1 - \alpha) + I \qquad (2.18)$$

The incoming shortwave radiation, Q, is calculated over the latitudinal band as an average daily quantity, and is reduced to a simple geometrical relationship using trigonometry (Sellers, 1965; Monin,1986).

The net longwave radiation emitted to space, I, is dependent on a number of factors including surface temperature and cloudiness. The formation of clouds depends on atmospheric instabilty and vertical motion, and is controlled by microscale processes (Barry and Chorley, 1987). The regional variance of cloud cover is therefore difficult to quantify, so empirical relationships derived from satellite data are used in models. Here, longwave radiation is expressed in terms of surface temperature and cloudiness, following van den Dool (1980):

$$I_O = A_O + B\theta + CN_O \qquad (2.19)$$

$$I_C = A_C + BT + CN_C \qquad (2.20)$$

where T is the surface temperature of the land, θ is the surface temperature of the ocean, N is the cloud cover as a function of latitude, o and c refer to the ocean and land respectively, and A, B, and C are empirically derived constants.

The planetary albedo varies with the type of surface, the presence of clouds, and the zenith angle of the sun. The former parameter is calculated by assigning empirical values for the open sea, land, snow, and ice, (Raschke et al.,1973) and roughly estimating the respective area of each in the latitude band (Appendix 1). The latter two parameters are appraised using data from van den Dool (1980) on cloud cover and its albedo at different latitudes. Snow and ice are assumed to be present below arbitrarily assigned thresholds of temperature; in this case 2°C.

The second section of the model calculates the energy fluxes between the latitudinal bands and across coastal boundaries. The transfer of heat between the latitudinal bands and across coastal boundaries is assumed to be proportional to the

temperature gradient across them (figure 2.2). Thus an increasing discrepancy in temperature between latitudes, or between land and ocean, will lead to an increasing heat flux which dampens the temperature difference.

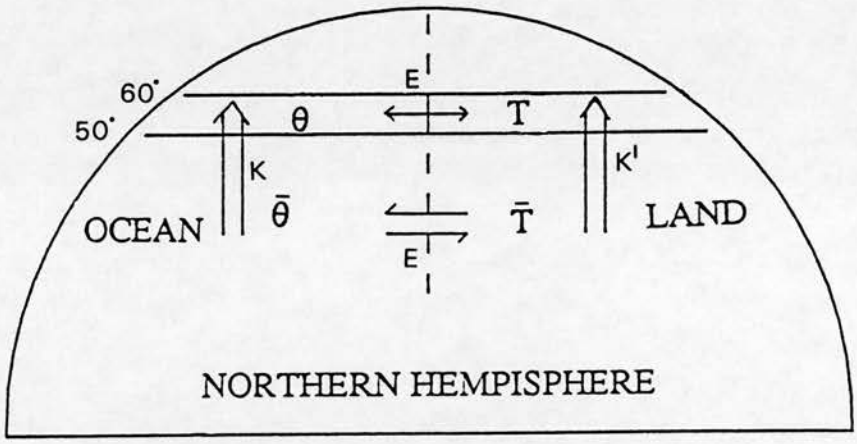

Figure 2.2 The regional energy balance model.

The full equations for the regional energy balance model are:

$$C_o \partial\theta/\delta t = R_o - k\theta + \mu E(T - \theta) \qquad (2.21)$$

$$C_l \partial T/\delta t = R_l - k'T + E(\theta - T) \qquad (2.22)$$

where C is the heat capacity, θ is the ocean temperature, T is the land temperature, R is the surface radiation balance, k is the latitudinal heat flux coefficient, E is the zonal heat flux coefficient, μ is the zonal land ocean fraction, and the subscripts l and o refer to the land and ocean respectively.

This approach to the physical processes in the atmosphere and ocean, coupled with a reliance on empirically derived relationships for the radiation budget, results in model output which is highly sensitive to the value of empirically derived constants. To overcome this problem the model constants are tuned, or optimised, by simulating well constrained data, such as the present climate. The underpinning assumption of this

approach is that the value of the tuned constants remains invariant over time. This will not necessarily hold true if changes in the oceanic and atmospheric circulation occur.

2.2.3 Tuning the regional climate model

Tuning the model was implemented by a systematic variation of specific empirical constants to obtain the best fit simulation of current regional temperature cycles. The comparison between actual data and tuned results was made visually, since the data under consideration had a larger standard deviation of means than the results obtained by modifying the empirical constants. Model output data were tuned to simulate regional temperature cycles in Scotland. Following the Meterological Office (pers.com.;1990) Scotland is split into meteorologically similar regions: the north, the west, and the east (figure 2.3). The regions were allocated different constant values to replicate the contrasting climate across Scotland.

There are four possible tuning parameters. The first is the mean temperature of the hemisphere, which is controlled by the amount of longwave radiation emitted from both land and ocean. The value of the constants, Ac and Ao, determine the overall longwave flux without affecting the relative importance of cloud cover or temperature. Thus the hemispheric mean temperature is tuned by the parameter (Ac + Ao). The second tuning parameter controls the zonal asymmetry of temperature, which is the difference in mean temperature between the land and ocean within one latitudinal band. Again, the value of the constants, Ac and Ao, determine this temperature discrepancy. This parameter is tuned with the parameter (Ac - Ao). The third tuning parameter controls the latitudinal flow of heat from warm to cold regions, and is determined by the value of k. The final tuning parameter controls the exchange of heat between land and ocean within one latitudinal band, and is determined by the value of E.

	Ao	Ac	k	E
North	180	189	6	25
West	180	189	7	21
East	180	189	7	13

Table 2.3 Values of tuning constants in the regional energy balance model.

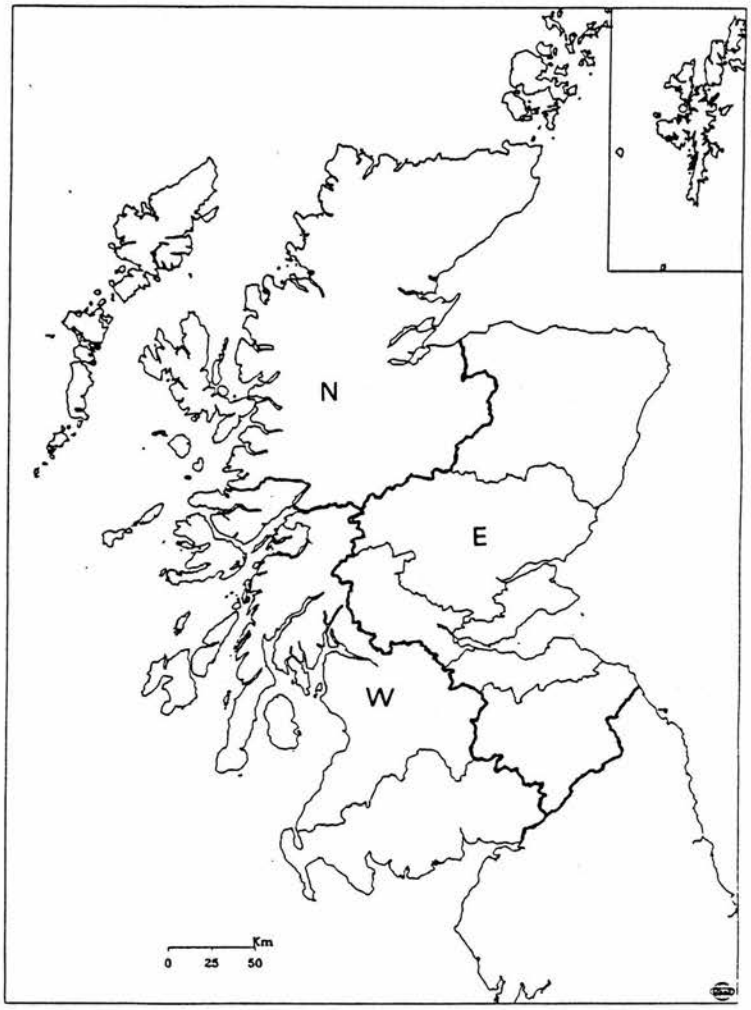

Figure 2.3 The Scottish regions based on Met.O./Carte/D.O./1297A

Regional values of the tuning constants are given in table 2.1. Figure 2.4 shows the comparison between the meteorological data and the tuned model output. The model output is a reasonable fit.

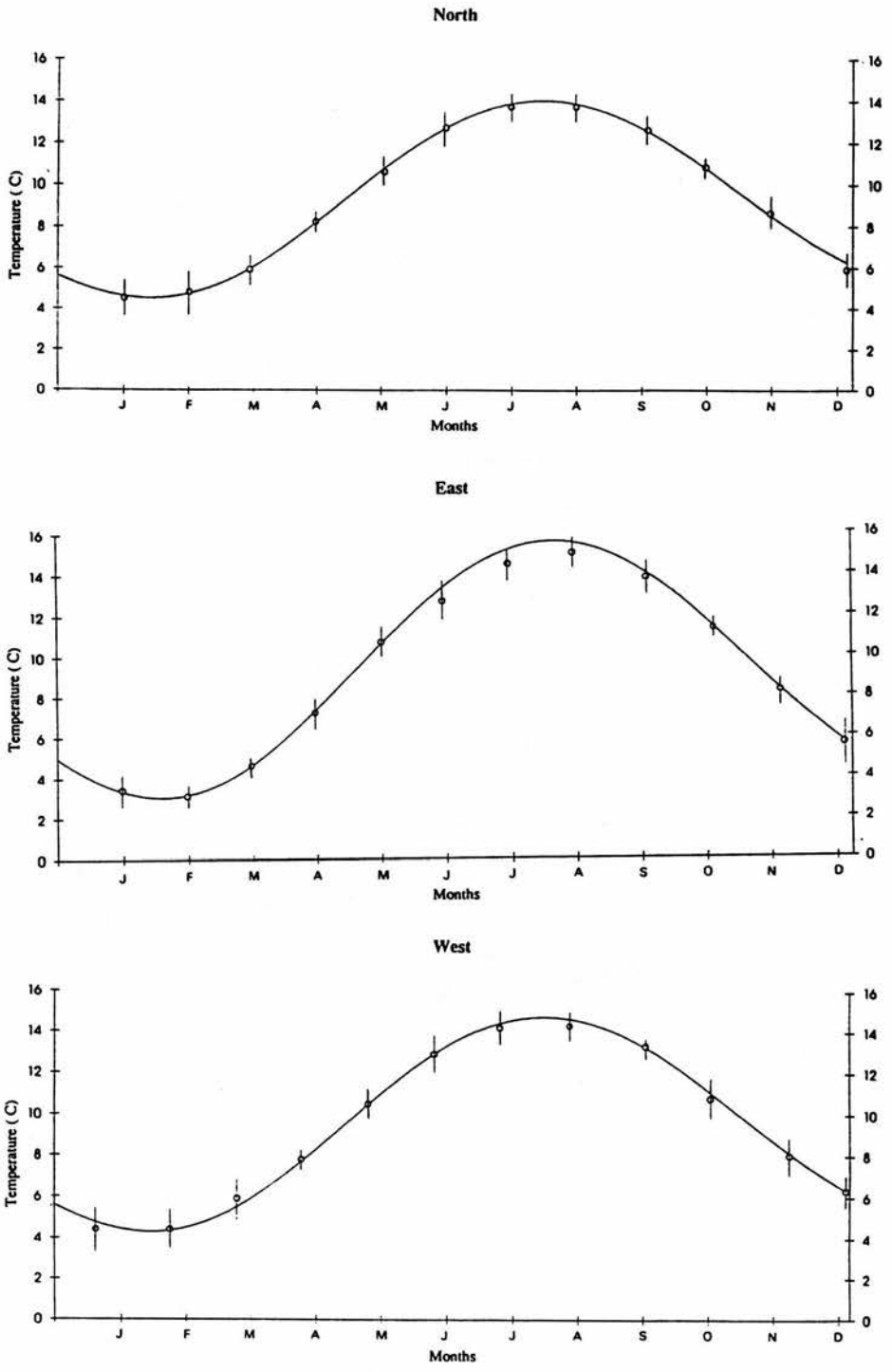

Figure 2.4 Observed and modelled temperature cycles for the Scottish regions.

2.3 The ice sheet model

The ice sheet model is based on the continuity equation for ice thickness and is derived from the model of Mahaffy (1976). It is a two dimensional, non steady state model which is a generalisation of methods used to calculate ice sheet profiles (Nye,1952,1959), and was used to study the Barnes ice cap (Mahaffy,1976), and the initiation of the Laurentide ice sheet (Andrews and Mahaffy, 1976). Subsequently, Budd and Smith (1981,1982) and Payne (1988) developed the model to include more realistic environmental factors to force ice sheet evolution. Budd and Smith (1981,1982) studied the glacial cycles of the Antarctic and Laurentide ice sheets while Payne examined the evolution of the West Antarctic ice sheet (Payne et al., 1989) and the growth of the Loch Lomond ice cap in Scotland (Payne and Sugden,1990). The continuity equation states that the change in ice thickness, h, of a column of ice over a unit of time, t, is equal to the net mass balance at the surface, b, minus the net ice flux, qx and qy, (figure 2.5):

$$\partial h/\partial t = b - [\, \partial q_x/\partial x + \partial q_y/\partial y \,] \qquad (2.23)$$

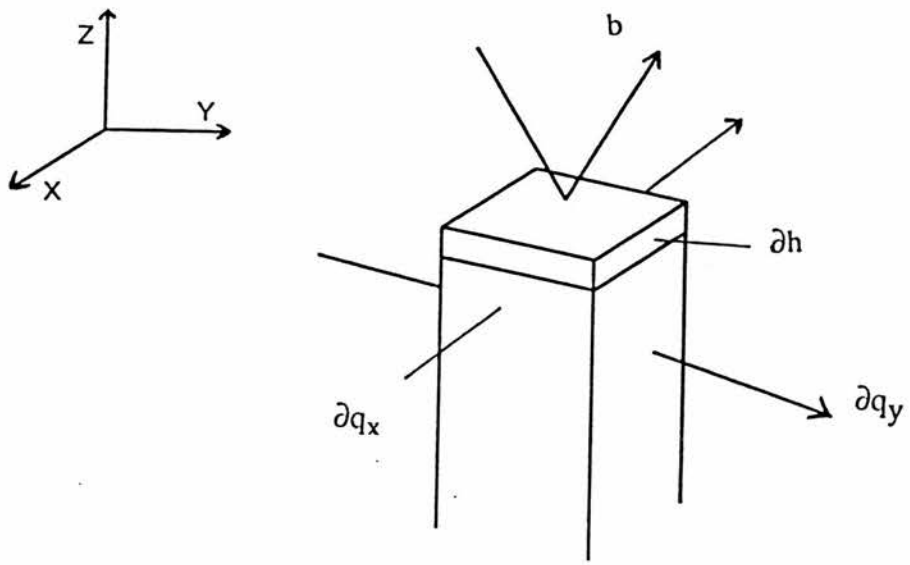

Figure 2.5 The mass balance in a column of ice.

The divergence of the net ice flux depends on two processes: ice deformation and ice sliding.

2.3.1 Ice deformation

The flow of solids is best understood by the application of continuum mechanics. This links the deformational properties of a solid with the fundamental laws of motion. Ice is a polycrystalline solid and has a non linear relationship between an applied stress and the consequent strain over the range of stresses applicable to glaciers. The relationship between the shear stress and shear strain rate for secondary creep in polycrystals is found to be:

$$\varepsilon = A\tau^n \qquad (2.24)$$

where ε is the effective strain rate and τ is the effective stress, which are invariant under any rotation of the coordinate axes (Glen,1955,1958; Nye,1957). Experimental determination of the values of the 'constants', A and n, have found a range of possible values. Values of n range between 1.5 and 4.2 but a mean of 3 is usually taken (Weertman, 1973), and is used throughout this work. The value of A is temperature dependent and follows the Arrhenius relation:

$$A = A_0 \exp(-Q/RT) \qquad (2.25)$$

where Q is the activation energy for creep and has been measured experimentally. It is found to vary with temperatures near the melting point implying that the Arrenhius relation breaks down at this point (Paterson, 1981). The value of A_0 also varies with grain size and the impurity content of ice. Evidently, the complex nature of glacier ice leads to severe difficulties in quantifying the flow of ice for an arbitrary applied stress. It seems sensible to use the mean values of the experimentally determined 'constants' and then assess the sensitivity of these values in comparison with other factors.

In the model the equations governing the stresses on a body of ice are simplified to allow a numerical solution. Three assumptions are made:

1) The deformation is by shear in the x-z plane

2) The variation of the normal stress component with ice depth is very much larger than the variation of vertical shear stress with horizontal distance

3) The inertia of ice permits the omission of acceleration terms so the only relevant force is gravity

The first assumption breaks down at ice margins, in the presence of ice streams, and at the edges of valley glaciers. The second assumption breaks down when surface slopes are low (at ice divides) or when ice thicknesses are small (ice margins). The third assumption breaks down when extensive and compressive flow occurs in the presence of steep, undulating subglacial topography. Longitudinal stresses need to be incorporated to deal with these points and this procedure is discussed in more detail in chapter 5. It follows from the assumptions that the equilibrium equations of stress on a body of ice reduce to:

$$\partial\sigma_x/\partial x + \partial\tau_{xy}/\partial y = 0 \qquad (2.26)$$

$$\partial\sigma_y/\partial y = \rho g \qquad (2.27)$$

$$\partial\tau_{yz}/\partial z + \partial\sigma_z/\partial z = 0 \qquad (2.28)$$

where σ is the normal stress, τ is the shear stress, ρ is the density of ice, and g is gravity. An orthogonal coordinate system is used (figure 2.6).

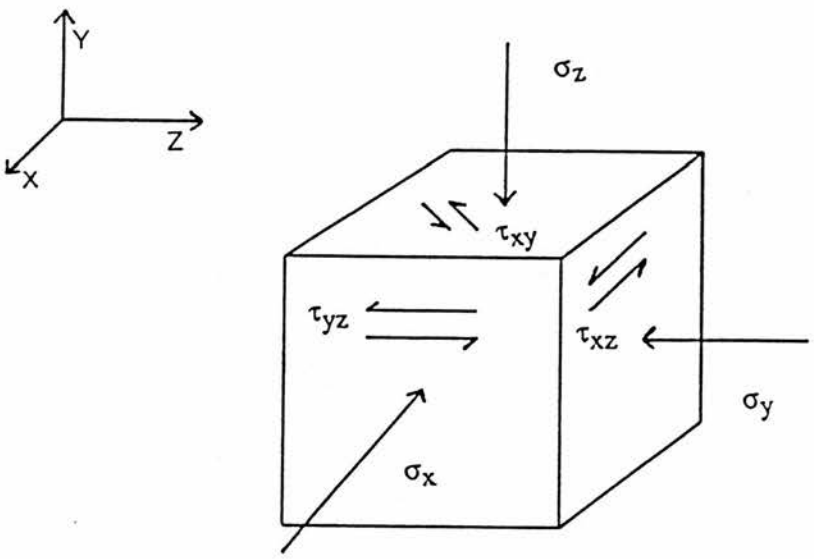

Figure 2.6 The orthogonal system of stresses acting on ice.

The boundary conditions are that the vertical normal stress is equal to the atmospheric pressure, which is taken to be zero, and that the surface supports no shear. The solutions to the equations are:

$$\sigma_y = \sigma_x = \sigma_z = -\rho g (h_s - y) \quad (2.29)$$

$$\tau_{xy} = -\rho g (h_s - y) (\partial h_s / \partial x) \quad (2.30)$$

$$\tau_{yz} = -\rho g (h_s - y) (\partial h_s / \partial z) \quad (2.31)$$

where h_s is the ice surface elevation, and y is the vertical coordinate. The latter two equations only hold for small ice surface slopes when the shear stresses are approximately equal to the shear parallel to the surface. Finally, by assuming that the vertical variation in velocity is very much larger than the horizontal variation in velocity, it can be shown that the ice flux, q, in orthogonal directions from the column of ice is:

$$q_{x,z}(x,z,t) = (-2A/(n+1)) (\rho g)^n \alpha^{n-1} (\partial h_s / \partial x, \partial z) h^{n+2} + hU_s (x,z,t) \quad (2.32)$$

where U_s is the sliding velocity, h_s is the ice thickness, and α is the surface slope in the direction of flow. The value of A is weighted in favour of the lower, shearing layers and averaged over the entire thickness and then assumed to be invariant. The surface slope, α, is:

$$\alpha = \sqrt{[(\partial h_s / \partial x)^2 + (\partial h_s / \partial z)^2]} \quad (2.33)$$

By combining the equations for the flux components, qx and qz, with the continuity equation, it is possible to solve them numerically to obtain ice thickness at a given point. Required inputs are the sub-glacial topography, the initial ice thickness, the spatial variation of mass balance over time, and a relationship for the sliding velocity. A more complete derivation of these equations and their underlying assumptions can be found in Paterson (1980,1981), Hutter (1983), or Lliboutry (1987).

2.3.2 Ice sliding

There are four potential mechanisms for basal sliding in glaciers. The first is regelation which occurs when ice melts in high pressure areas upstream of obstacles and refreezes downstream, with the concurrent transfer of latent heat upstream through the obstacle forcing ice melting. The second process involves enhanced creep caused by the

additional stresses induced by the obstacle which leads to ice preferentially moving over and around obstacles. The former process operates over small obstacles while the latter occurs over larger bedrock irregularities (Weertman,1957). Lliboutry (1968) suggested a third important process, that of sliding over water and air filled cavities between ice and bedrock, since there is less friction in these areas. Finally, Boulton and Jones (1979) indicated the importance of the sub glacial deformation of sediments on glacial flow. However, a generally applicable sliding law is still not in sight; indeed, it has been described (somewhat optimistically) as the last great problem in glaciology (Weertman,1979). This is partly due to the lack of data from the base of glaciers to test ideas, and partly due to the complex nature of the boundary between a rough bed of variable strength and the flow mechanics of the overriding ice.

Ice is only expected to slide when the base of the glacier is at melting point. The temperature at the base can only be calculated if the thermodynamic equations for the ice sheet are solved in conjunction with the ice flow equations. This is mathematically complicated and has only been satisfactorily accomplished when the surface boundary conditions are relatively simple, such as in the Antarctic (Huybrechts,1990).

The model used in this thesis is isothermal so the variation in basal temperatures cannot be calculated and detailed sliding calculations cannot be performed. Instead, sliding velocities are related to the basal shear stress, τ_b, which primarily drives basal sliding, the normal load at the base, Z^*, which primarily inhibits sliding, and an empirically derived multiplication factor, κ_2:

$$Us = \kappa_2 . \tau_b / Z^{*2} \qquad (2.34)$$

The normal load is effectively determined by the ice thickness, while the basal shear stress is calculated in the equations for ice deformation. This derivation implies sliding is proportional to surface slope and inversely proportional to ice thickness. Thus maximum sliding velocities occur at the margin where the ice thickness is smallest and the surface slope is largest, and this allows the ice margin to migrate. Maximum sliding velocities are constrained to be below the maximum observed limits of 2 kilometres/year.

The fluxes of ice used in the continuity equation are obtained by adding the deformation and sliding velocities orthogonally and multiplying by the ice thickness.

2.3.3 Environmental considerations

An ice sheet does not just acquire mass from the atmosphere and disperse it uniformly, it also interacts with the regional environment, often in a seemingly complex manner. These interactions are generally a consequence of the configuration of sub-glacial topography.

Topography forms a crucial external boundary condition in the ice sheet model, influencing where ice can grow and its extent. However, the assumptions employed in deriving the ice flow equations limit the permitted accuracy of the topographic representation in the model. The requirement that ice surface slopes are small and longitudinal stresses are negligible means that mountainous terrain cannot be represented correctly. The topography must be represented in a smoothed form by averaging all topographic altitudes within a grid cell. This has two significant consequences. Firstly, the topographic configuration within the grid cell is replaced by a single mean altitude. In effect, this suppresses the effect of topographic variation on ice flow at a scale beneath that of a grid cell. This problem is discussed in more detail in chapter 5. Secondly, the climate and hence the mass balance is very sensitive to the altitude of the topography. Smoothed topography produces unrealistically low values of accumulation. This problem can be partly circumvented by representing the topography with two gridded data sets (Payne,1988). The first grid contains the mean altitude occurring in each grid cell and is used by the ice sheet model when calculating the ice thickness and flow. The second grid contains the maximum altitude occurring in each grid cell and is used by the climate model to determine the mass balance at each point over the grid. Once the ice thickness has exceeded the difference between the mean and maximum topographic altitudes, the climate model determines the mass balance from the altitude of the ice surface.

The credibility of this approach is dependent on the size of grid cells employed and the configuration of the topography. Large grid cells lead to models with faster computation times or with which a larger area can be covered in the same time. Longer time steps can be used with larger grid cells since they are numerically more stable. However, the more peaked, or Alpine, the topography, the less relevant the model in describing climatic effects or ice flow mechanics.

2.4 The computer model

The preceding equations constitute the mathematical representation of climate and ice sheet behaviour. The equations and the variables are recapitulated in Appendices 1 and 2.

All three models require iterative procedures to obtain output data. The models were tested to ensure that the output converges to a stable value regardless of initial conditions, and that they were numerically stable. In the case of the regional energy balance model the respective land and ocean temperatures are set at the start of the model year. In the surface mass balance model a climatic snowline altitude is required at the start of the year to calculate the albedo and turbulent fluxes. In both climate models, the results converge within three full iterations (model years) to stable values regardless of the initial conditions.

The ice sheet model is more complex since the continuity equation and ice flux calculations depend on partial differentials. The model equations are calculated on the nodes of a rectangular grid of square elements. Partial derivatives are obtained by approximating the value of the relevant function from adjacent nodes. Horizontal derivatives are approximated by a centred difference scheme as follows:

$$\partial H/\partial x \Rightarrow (H_{i+1} - H_{i-1})/\Delta x \qquad (2.35)$$

where the subscript i refers to the x direction, and H is the surface elevation. Equivalent equations are used in the y direction. Time derivatives are approximated by forward differences:

$$\partial H/\partial t = G \Rightarrow H_{t+1} = H_t + \Delta t.G \qquad (2.36)$$

where t is the time step, and G is the horizontal variation in ice flux.

The numerical stability of finite difference schemes such as this one depends on the numerical gradients between grid cells. Large fluctuations in time or space lead to errors in the mathematical approximations and the propagation of high frequency waves through the grid lattice. The former problem is dealt with by ensuring the mass transfer between grid cells is below a critical stability threshold, which depends on the time step employed in the model. This can be related to the maximum possible stable time step (Budd and Jenssen,1975):

$$\Delta t_{max} = (\Delta x)^2 | \alpha' | / (2U'Z'n) \qquad (2.37)$$

where α' is the maximum ice surface slope, U' is the maximum deformation velocity, and Z' is the maximum ice thickness. Smoothing functions to damp non linear instabilities were not necessary in the experiments.

2.5 Summary

The construction of the climate and ice sheet models is based on the perceived mathematical representation of the physical systems. In situations where there are no mathematical derivations from the fundamental laws of conservation and motion, empirical relations are used. The choice of variables is dependent on a subjective assessment of what is, and is not, important at the relevant scales of interest. It also depends on the available data and the accuracy of the empirically derived relationships.

Chapter Three:
Analysing the Models

3.1 Introduction

This chapter details the procedures for analysing the models. Clearly, the ad hoc relationships and mathematical approximations which constitute the models must be assessed before they can be used to make deductive statements concerning the physical system under investigation. This procedure involves sensitivity analysis and operates by systematically varying model parameter values to indicate the relative importance of each parameter within the models. This highlights properties of the models which should be predictable from their construction but, given their complexity, only become apparent when operating the models (Kirkby et al., 1987). It also indicates where efforts in obtaining accurate input data must be concentrated, since sensitive parameters produce large changes in model results for small changes in parameter values. It focuses on the importance of the parameter within the model and the uncertainty attached to its value.

The sensitivity of parameters in the energy balance models is assessed with respect to the resulting effect on the glacial mass balance profile. Each parameter is varied about its calculated or assigned value by a fixed percentage of their actual value, usually 10% and 20%. The variation is proportionately larger if there is a large uncertainty attached to the value of the parameter.

3.2 The surface energy balance model

The surface energy balance model was developed by Oerlemans (1992), and is an extension of work by Oerlemans and Hoogendoorn (1989). Model results successfully simulate data from Alpine glaciers (Oerlemans, 1992) and it has been used to examine the sensitivity of the Greenland ice sheet to climatic change (Oerlemans, 1991). The limitations of the model stem from the necessarily schematic representation of the energy fluxes. Two problems can be distinguished. The first concerns the lack of climatic data over the appropriate averaging period. For example, the long wave radiation calculation requires knowledge of mean cloud cover and the mean height of the cloud base, both of which vary substantially over space and time. It has to be assumed that the variance from the mean value does not materially affect the overall calculation. The second problem concerns the overall formulation of the energy fluxes. The most poorly constrained formulations are those of the surface albedo and the turbulent fluxes. A model of the spatial and temporal variation of the surface albedo does not exist, so the only alternative is to use a scheme which broadly matches empirical observations. Since there are insufficient measurements of surface albedo from southern Chile, and none from the Loch

Lomond stadial, the model can only be applied to these regions because they have a similar climatic and topographic setting to the mid-latitude Alpine glaciers for which the model was developed. The turbulent fluxes determine the transfer of energy from the free atmosphere to the surface and depend on the stability of the atmospheric boundary layer and surface conditions such as temperature, humidity, and roughness (Kuhn,1979,1987). Clearly, these variables can only be quantified at a local scale with in situ measurements, so such refinements cannot be incorporated into the model. Instead, a scheme is utilised which broadly simulates empirical observations (Kuhn, 1979; Gruell and Oerlemans, 1986).

There are four primary divisions within the model which deal with the incoming solar radiation, the long wave radiation, the turbulent fluxes, and regional climatic inputs such as temperature and precipitation. Six prescribed inputs are required: annual temperature cycle, daily temperature cycle, mean cloud cover, mean height of cloud base, temperature lapse rate, and the precipitation at different altitudes. The model was analysed in conjunction with the regional energy balance model, using prescribed inputs for the western Scottish climate.

i) Incoming short-wave radiation

The method of calculating the amount of radiation reaching the earth is taken from Walraven (1978). The effect of the earth's orbital variations can be assessed by changing the mean solar output. This output was varied by up to 5% of its current value, which results in a somewhat larger variation of incoming short-wave radiation than is believed to have occurred in the recent geological past. The effect on the mass balance is striking for its insignificance. A reduction of 2% leads to a linear drop in the net mass balance profile of less than 100 metres (figure 3.1). This result is attributed to the dominant maritime influence on the Scottish climate. Scottish land temperatures depend, to a large degree, on the pervasive influence of the warm waters of the North Atlantic. As a result, the incoming short-wave radiation in Scotland is less significant than the flux of energy from the surrounding ocean.

The amount of radiation reaching the earth's surface depends on its attenuation by the atmosphere. Two parameters, Ta and Tc, are used to quantify the radiative attenuation through air and clouds respectively. A 10% change in the transmissivity of air

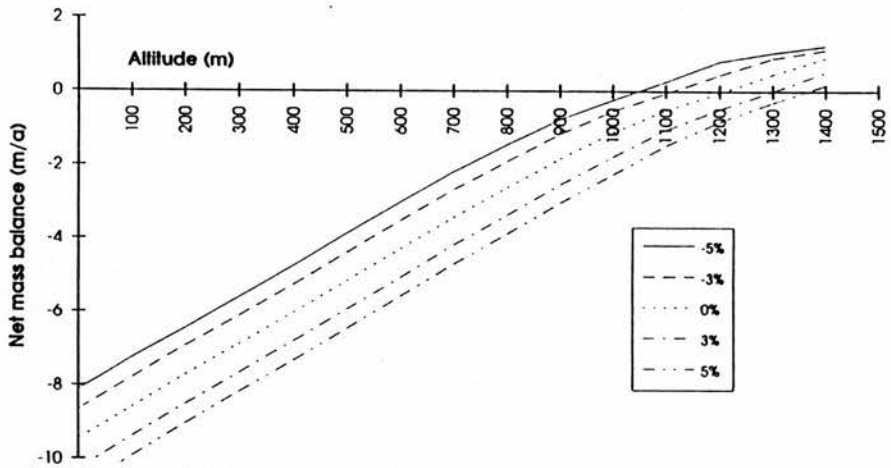

Figure 3.1 Sensitivity to the solar constant.

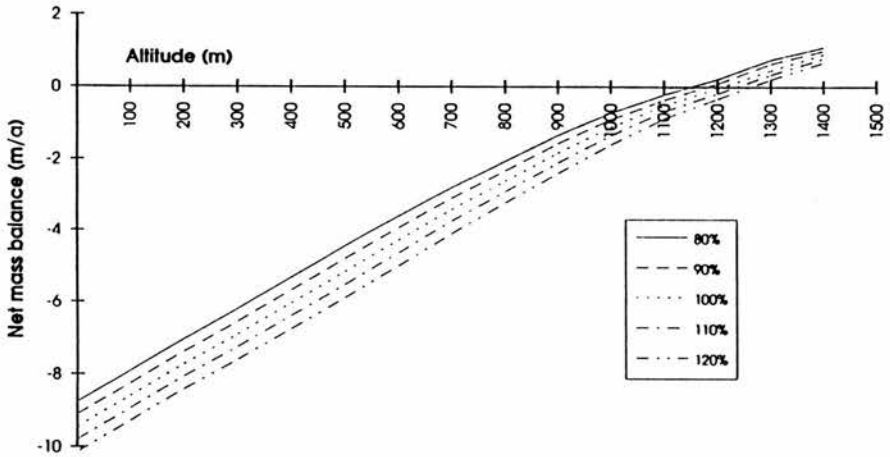

Figure 3.2 Sensitivity to the transmissivity of air.

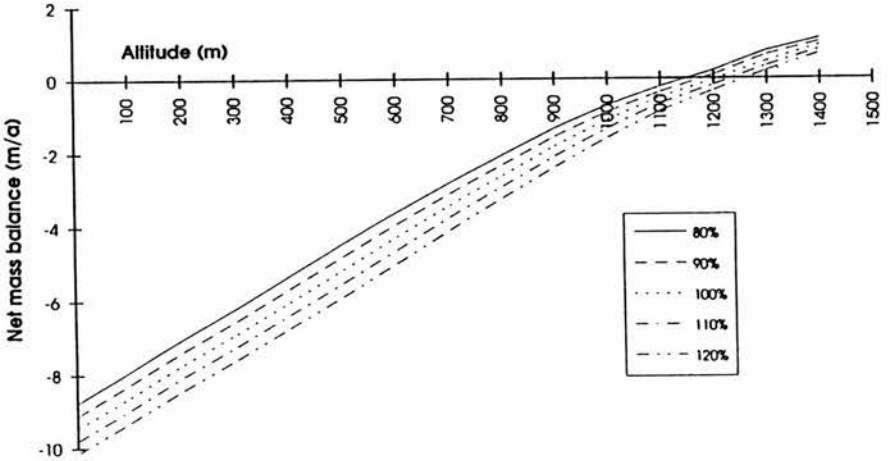

Figure 3.3 Sensitivity to the transmissivity of clouds.

raises or lowers the mass balance profile at the equilibrium line by approximately 30 metres (figure 3.2). Similarly, a change of 10% in the transmissivity of clouds raises or lowers the net mass balance profile by approximately 30 metres (figure 3.3).

The amount of radiation absorbed at the surface depends on the surface albedo. The derivation of surface albedo is more detailed in this model than that used in the regional energy balance model and is based on empirical data from Alpine glaciers. The surface albedo is derived from a regional background albedo, which is linked to the glacial equilibrium line and modified by the presence of snow and the seasonally accumulated snow melt. Three parameters were assessed: the background albedo, the snow albedo, and the overall surface albedo. The background albedo is least sensitive as a change of 10% raises or lowers the mass balance profile by less than 20 metres at the equilibrium line (figure 3.4). There is a proportionately larger change at lower elevations. A 10% change in the mean value of the snow albedo is found to raise or lower the mass balance profile by approximately 50 metres at the equilibrium line but substantially less at lower altitudes, where there is only seasonal snow cover (figure 3.5). The response of the overall surface albedo is similar. A 10% change in the calculated value of the surface albedo raises or lowers the mass balance profile by over 60 metres at the equilibrium line but rather less so at lower elevations (figure 3.6). Although the model is not very sensitive to the surface albedo the value is likely to be poorly constrained.

ii) Long wave radiation

Long wave radiation comprises two parts; the outgoing radiation emitted from the glacier and the incoming radiation emitted from the clouds and atmosphere. The former is assumed to affect the glacier only when ice is melting and thus a constant value is used, which corresponds to a melting surface with an emissivity of 1. The latter is represented by three variables: surface air temperature, cloud cover, and the height of the cloud base. Clearly the spatial and temporal variation of these parameters is such that they can only be represented very crudely.

The assumed long wave radiation emitted from the ice surface was varied about its optimum value and found to be highly sensitive. A 10% increase in its value lowers the equilibrium line by over 150 metres (figure 3.7). However, its value is tightly constrained physically.

Given the extreme uncertainty attached to the mean values of the cloud height and

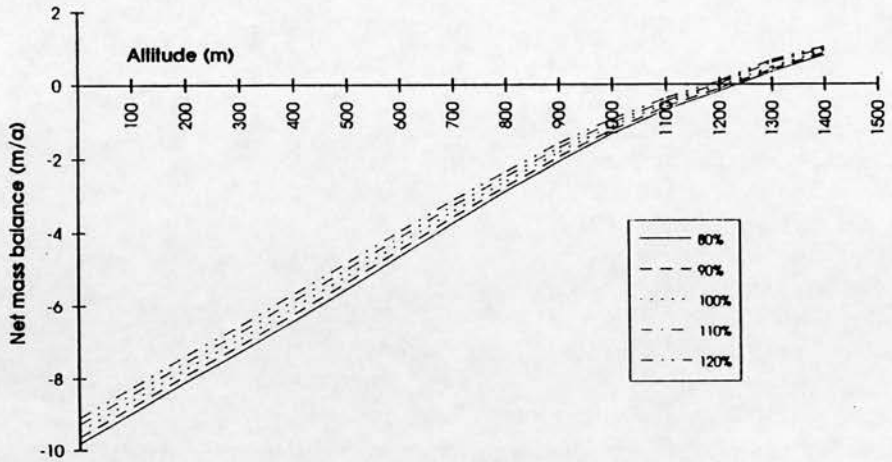

Figure 3.4 Sensitivity to the background albedo.

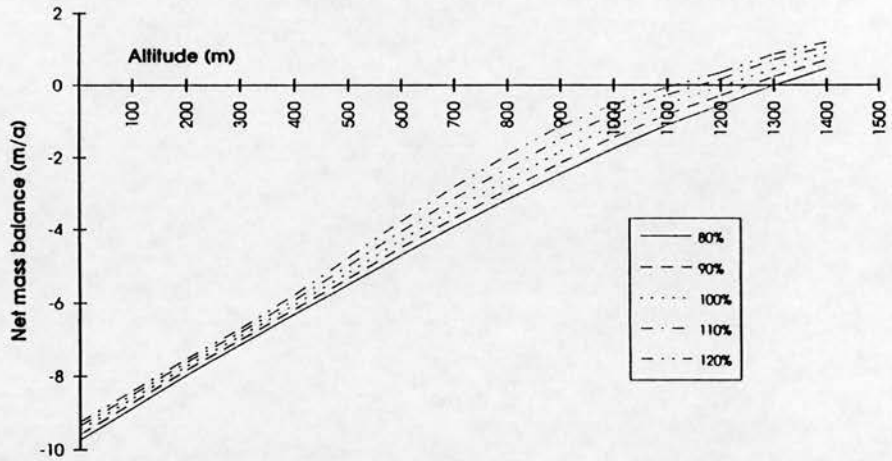

Figure 3.5 Sensitivity to the snow albedo.

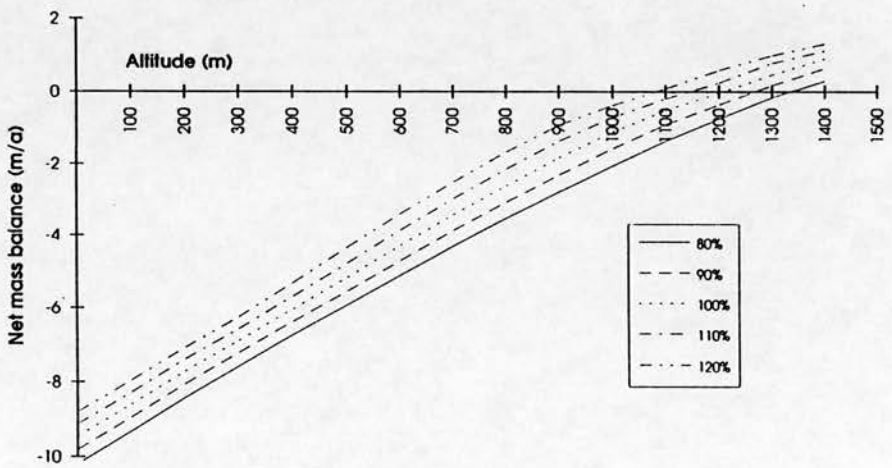

Figure 3.6 Sensitivity to the surface albedo.

cloud cover the parameters were varied over a wide range of possible values. The mean cloud height was varied between 1000 and 4000 metres with an optimum value of 1500 metres. An increase in the cloud height leads to a linear drop in altitude of the net mass balance profile of approximately 25 metres for each additional 1000 metres of cloud height (figure 3.8). The cloud cover was varied between cloud free (n = 0) and totally covered (n = 1), with an optimum value of n = 0.7. Increasing cloud cover raises the mass balance profile non linearly. A 10% increase in cloud cover raises the equilibrium line by approximately 25 metres (figure 3.9).

The remaining three parameters required to calculate the outgoing long wave radiation are representations of the sky emissivity, ε_a, the cloud emittance, ε_{cl}, and the fraction of black body radiation at the temperature of the cloud base, f. A 10% change in the latter parameter raises or lowers the equilibrium line by approximately 30 metres. There is a larger change at lower altitudes (figure 3.10). Similarly, a 10% change in the cloud emittance raises or lowers the equilibrium line by approximately 40 metres, and this change is more pronounced at lower altitudes (figure 3.11). The sky emissivity is assumed to depend only on surface altitude and its value is more sensitive. The equilibrium line altitude is raised or lowered by over 120 metres, with increasing change at lower altitudes (figure 3.12).

iii) Turbulent fluxes

The complex variation of latent and sensible heat fluxes are assumed to be proportional to the contrast in humidity and temperature between the surface and screen height. In general, turbulent fluxes increase down glacier due to increased surface roughness and wind speed (Kondo and Sata,1988) and this is incorporated in the model with an exchange coefficient which decreases linearly with altitude. This formulation requires empirically assigned values for the exchange coefficient at the equilibrium line, Ce, and the altitudinal gradient of the exchange coefficient, dC/dh. Changing these parameters has the effect of rotating the mass balance profile about the equilibrium line, with increasing variation at lower altitudes (figures 3.13 & 3.14). Although the effect on the mass balance is small the value of the fluxes are poorly constrained and so a substantial error is likely.

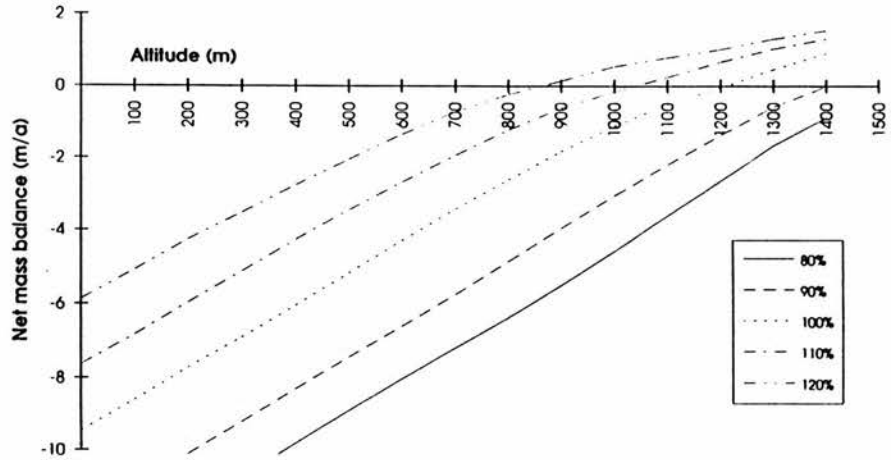

Figure 3.7 Sensitivity to emitted long wave radiation.

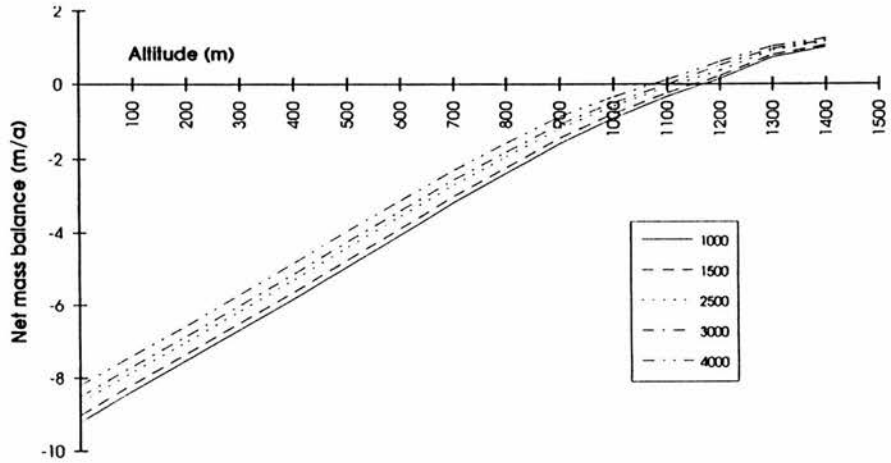

Figure 3.8 Sensitivity to cloud height.

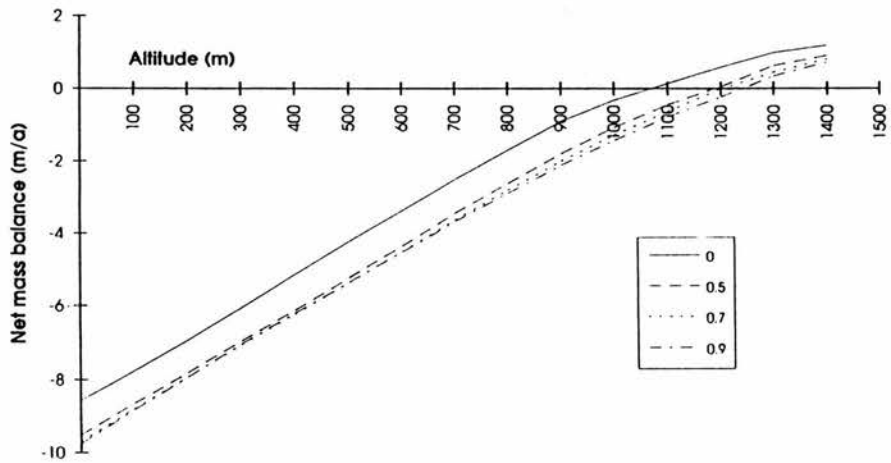

Figure 3.9 Sensitivity to cloud cover.

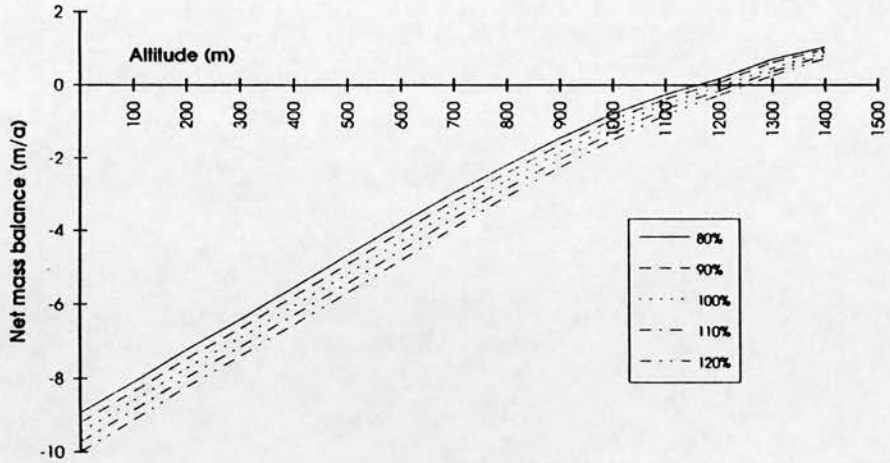

Figure 3.10 Sensitivity to the black body radiation

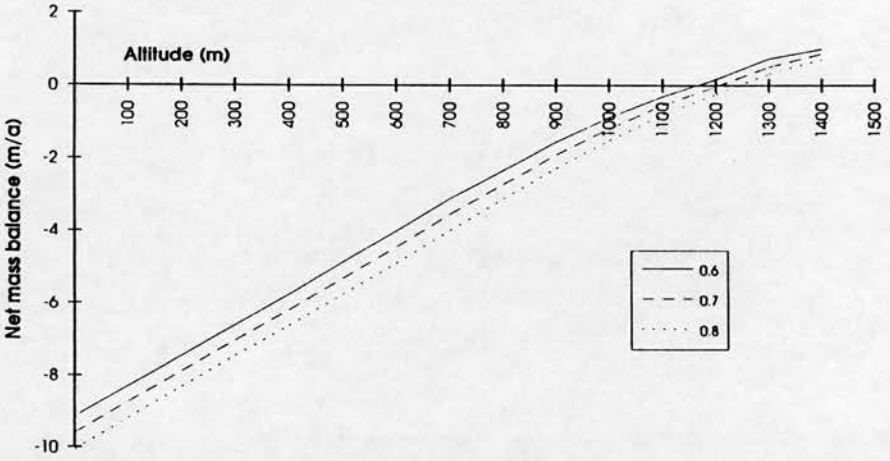

Figure 3.11 Sensitivity to the cloud emittance.

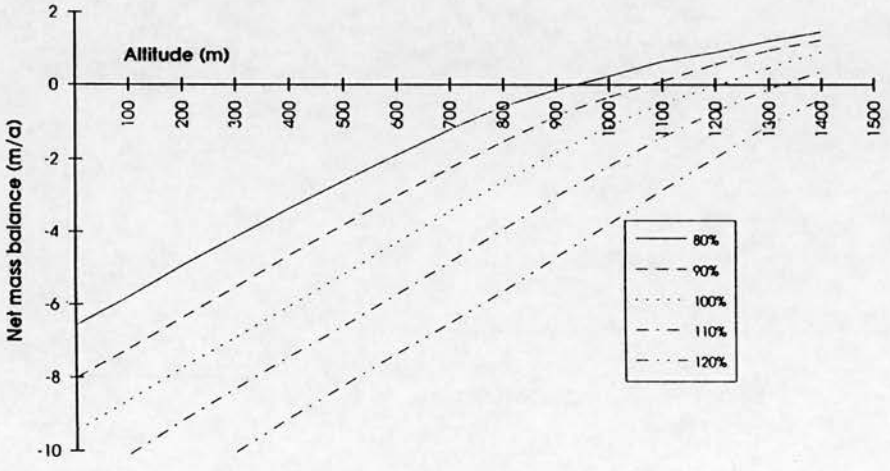

Figure 3.12 Sensitivity to the sky emissivity.

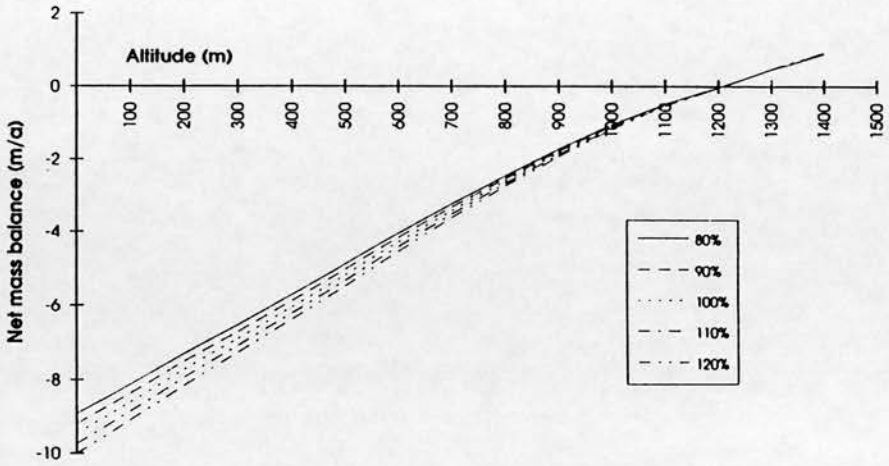

Figure 3.13 Sensitivity of the exchange coefficient.

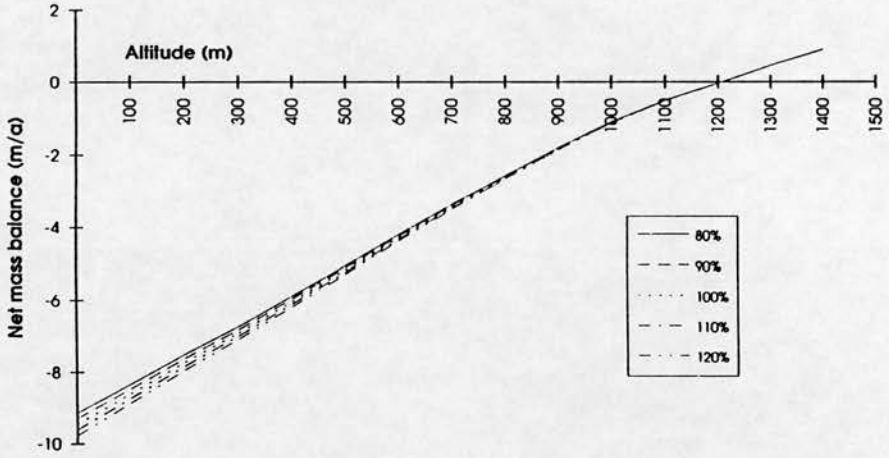

Figure 3.14 Sensitivity to the altitudinal gradient of the exchange coefficient.

iv) Regional climatic inputs

Two crucial inputs are the annual temperature cycle and the precipitation at different altitudes. Increasing precipitation totals lowers the mass balance profile non-linearly because more precipitation, and therefore proportionately more snow, falls at higher altitudes (figure 3.15). A change of 20 centimetres in an annual precipitation total of 1 metre/year changes the equilibrium line by approximately 80 metres. The altitudinal precipitation gradient is also required though in practice it is a poorly constrained parameter. It is less sensitive than the precipitation total as a 10% reduction in the gradient, which reduces the rate of increase of precipitation with altitude, raises the mass balance profile by approximately 40 metres (figure 3.16).

The second important regional climatic factor is the mean annual temperature since it determines the amount of precipitation falling as snow. A rise in the mean temperature of 1°C raises the mass balance profile by over 120 metres (figure 3.17). This sensitivity is also evident with the temperature lapse rate, which is highly variable geographically and seasonally. An increase in the lapse rate of 1°C/km raises the equilibrium line by almost 150 metres and there are progressively larger changes at higher elevations (figure 3.18).

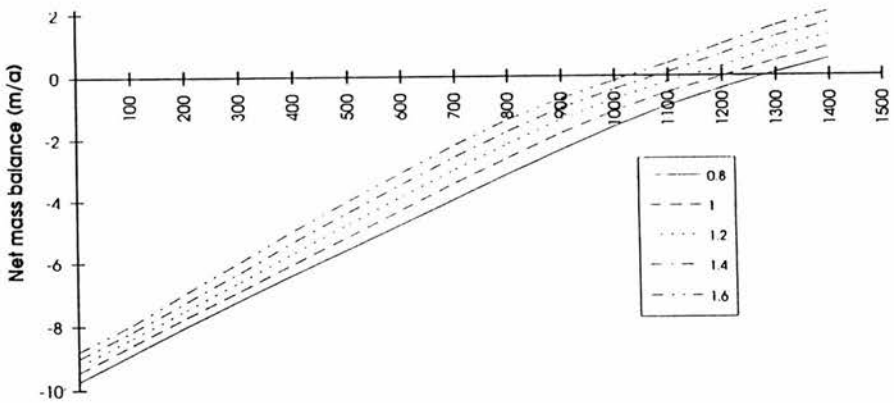

Figure 3.15 Sensitivity to precipitation totals.

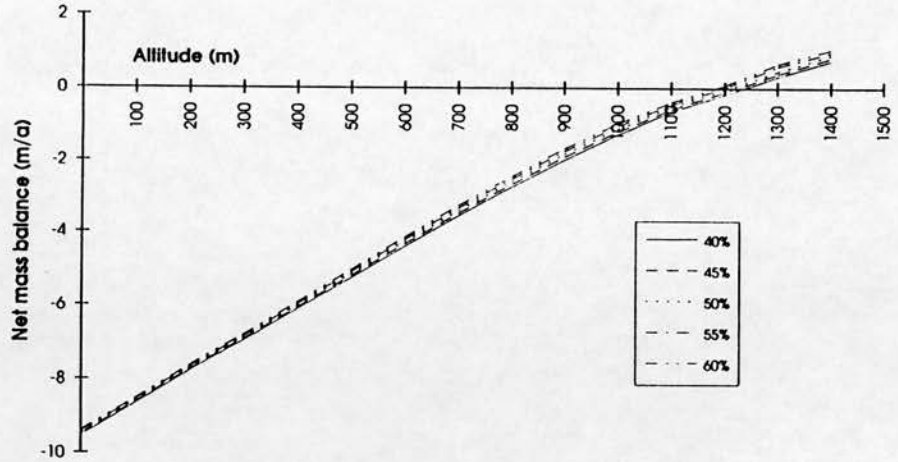

Figure 3.16 Sensitivity to the altitudinal gradient of precipitation.

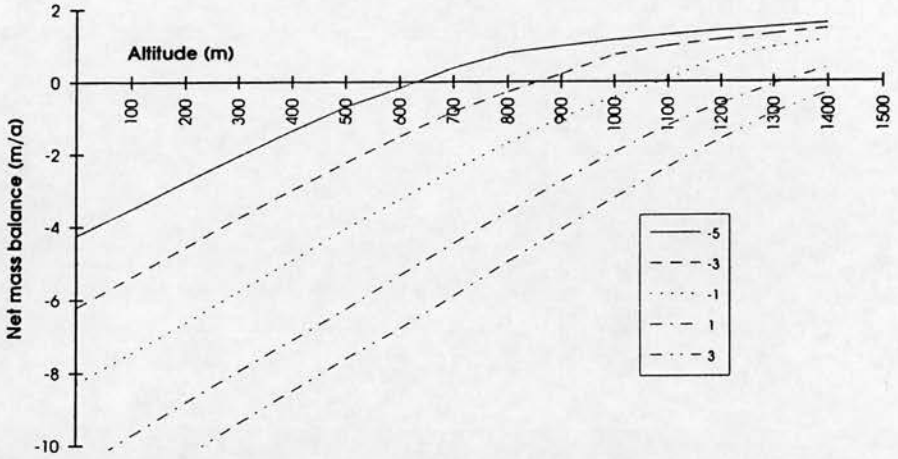

Figure 3.17 Sensitivity to mean annual temperature.

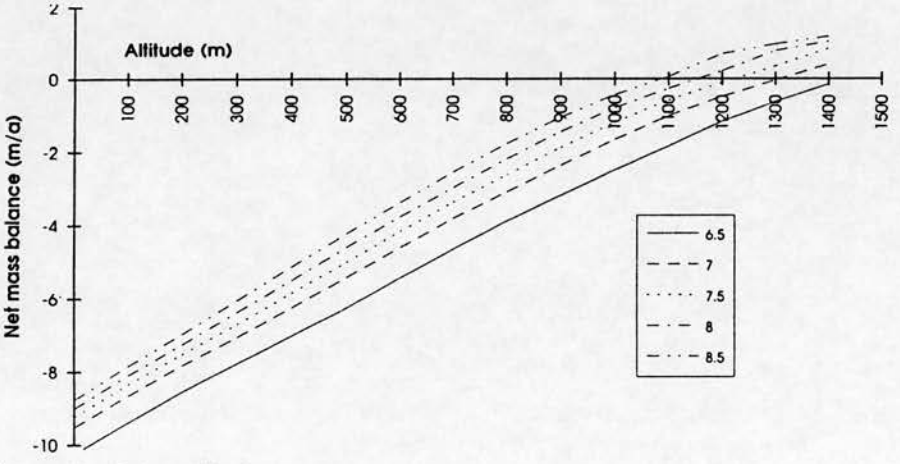

Figure 3.18 Sensitivity to the temperature lapse rate.

3.3 The regional energy balance model

The regional energy balance model is an elementary version of the zonal energy balance models developed in the late 1970's (North et al.,1981; Oerlemans,1980c). The annual temperature cycle of a specified region is obtained from regional energy fluxes but the values of the model parameters are poorly constrained and must be tuned to simulate observed temperatures. As noted earlier this places stringent limits on the utility of the model, though the sensitivity of components of the regional climate can be examined and this provides useful information.

The limitations of the model stem from the large number of empirical relationships. Once these are determined by tuning there is little internal freedom for the model to adapt realistically to new conditions. For example, the earth's orbital cycles change the amount of solar short-wave radiation reaching a specific region, and the sensitivity of the climate to these changes can be investigated with the model. However, if the effect of these changes is to modulate the energy fluxes in the atmosphere and ocean, or vary the regional cloud conditions, the model results are invalidated; it cannot calculate such coupled behaviour because the empirically derived parameter values are only valid for the climatic conditions with which they are tuned. The model therefore provides useful information on the relative sensitivities of components of the regional climate but cannot be expected to simulate the evolution of the regional climate.

There are four primary divisions within the regional energy balance model which are the latitudinal energy flux, the zonal energy flux, the regional albedos, and the long wave radiation.

i) Latitudinal energy flux

The transfer of energy poleward is assumed to be proportional to the thermal gradient across the latitude bands. This poleward flux is established by the value of the latitudinal heat flux parameter, k. There is considerable uncertainty attached to the parameter's optimum value so it was assessed over a wide range of values. Increasing the parameter value increases the poleward heat flux and leads to a warmer annual mean temperature, which raises the mass balance profile. The profile is most sensitive to a modification of the flux parameter when its value is small. A change in value from 1 to 5 raises the equilibrium line by almost 450 metres while a change from 5 to 10 raises the equilibrium line by approximately 350 metres (figure 3.19). Thus the poleward flux is the most sensitive parameter of the model, which reflects the importance of heat carried by

oceanic and atmospheric currents from the south in retaining the temperate climate of western Scotland.

ii) Zonal energy flux

Continental and oceanic regions at comparable latitudes have different annual temperature cycles due to their differing heat capacities, and this leads to an exchange of heat between land and sea. The energy flux is assumed to be proportional to the temperature gradient between them and is established by the zonal heat flux parameter, E. There is considerable uncertainty attached to its optimum value, so it too is assessed over a wide range of values. Increasing the parameter value increases the exchange of heat between land and sea, and this reduces the continental temperature range while increasing the oceanic temperature range. An increase in the value of the zonal heat flux parameter from 1 to 5 increases the equilibrium line altitude by approximately 25 metres and an increase in value from 5 to 10 has a similar effect (figure 3.20). The parameter is less sensitive when used in conjunction with the optimum value of the latitudinal heat flux parameter, since the zonal exchange of energy is subordinated by the poleward heat flux.

iii) Regional albedo

The short-wave radiation input to the system depends on the radiation reaching the surface and the albedo of the surface. The complex geographical and temporal variation in albedo is reduced to a mean value for the ocean and a temperature-dependent range of values for the land. The continental albedo value is more sensitive than the oceanic albedo. A change of 10% from the optimum value of the former raises or lowers the equilibrium line by approximately 100 metres (figure 3.21). A change of 10% in the latter case raises or lowers the equilibrium line by under 30 metres (figure 3.22). The sensitivity of the continental albedo reflects the wide variation between the albedo for snow and land.

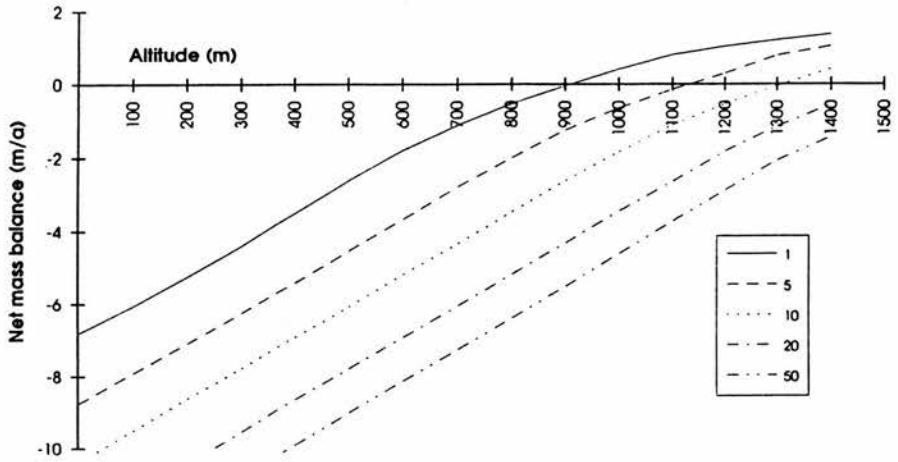

Figure 3.19 Sensitivity to the poleward heat flux parameter, k.

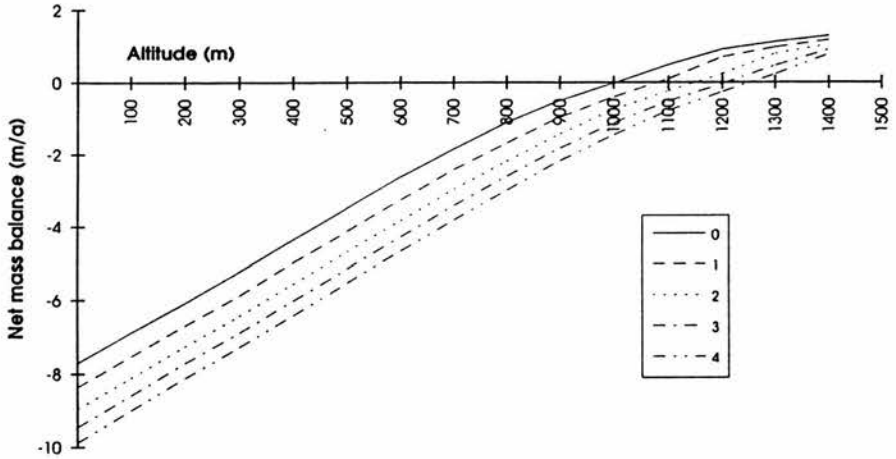

Figure 3.20 Sensitivity to the zonal heat flux parameter, E.

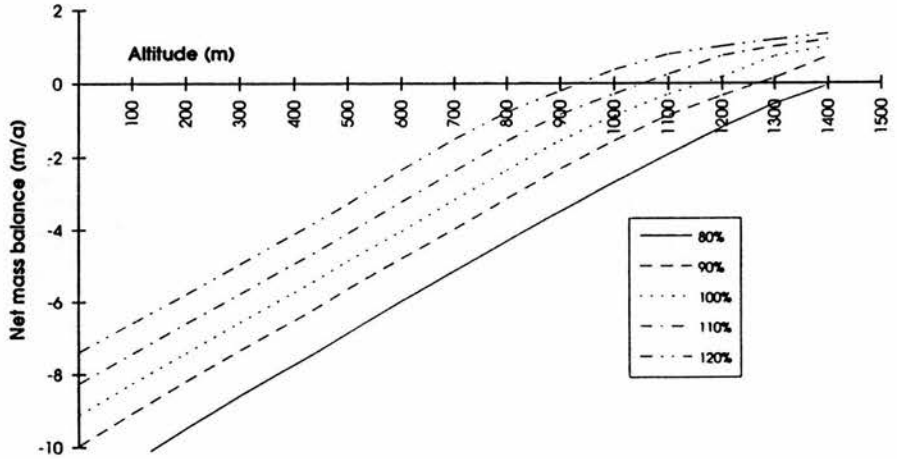

Figure 3.21 Sensitivity to the continental albedo.

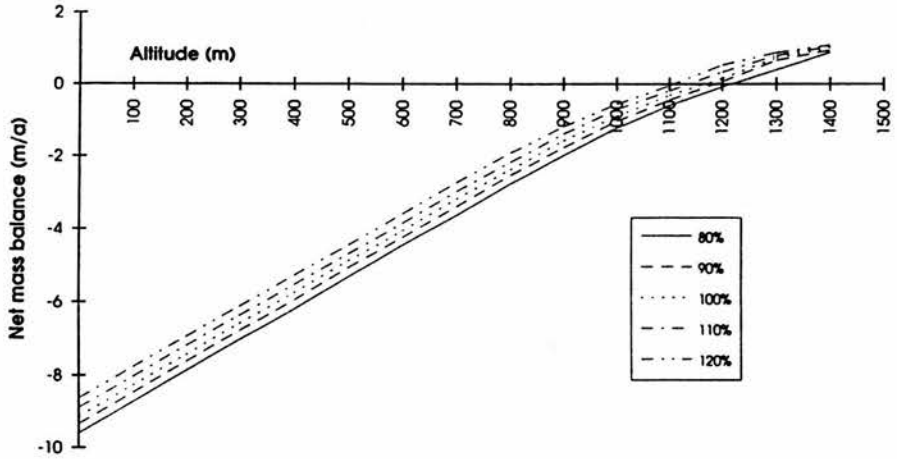

Figure 3.22 Sensitivity to the oceanic albedo.

iv) Long wave radiation

Observed values of long wave radiation are related to surface temperature and cloud cover with an equation containing three empirically derived parameters. The long wave output from continental and oceanic regions are distinguished by using different values for one of these parameters, Ac and Ao. The parameters, Ac and Ao, are sensitive parameters and are used to tune model output to current regional temperature cycles. Increasing the value of 'Ac' or 'Ao' increases the outgoing long wave radiation and lowers the net mass balance profile. Increasing the continental long wave parameter, Ac, by 10% from its tuned value lowers the net balance profile by approximately 80 metres while reducing it by 10% raises the mass balance profile by approximately 65 metres (figure 3.23). The oceanic long wave component, Ao, is less sensitive. An increase of 10% from the tuned value lowers the net balance profile by 30 metres while reducing it by 10% raises the profile similarly (figure 3.24). The difference in sensitivity is attributed to the larger temperature range found in continental regions.

The parameter, B, relates the surface temperature to long wave radiation and is assigned the same value for both continental and oceanic regions. An increase in value of 10% lowers the net mass balance profile by approximately 25 metres and there is a comparable raising of the balance profile for a 10% reduction (figure 3.25).

The parameter, C, relates cloud cover to the long wave radiation, and again, is assigned the same value for both continental and oceanic regions. An increase of 10% lowers the balance profile by approximately 35 metres and there is a comparable raising of the balance profile for a 10% decrease (figure 3.26).

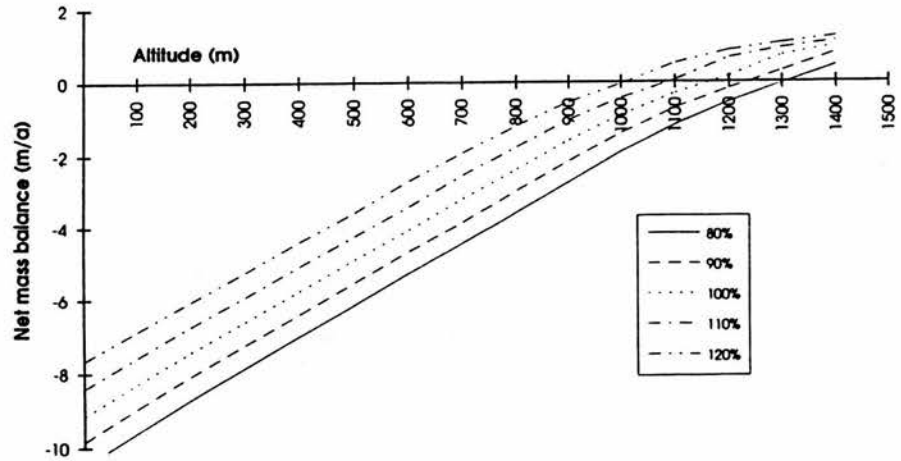

Figure 3.23 Sensitivity to the continental long wave parameter, Ac.

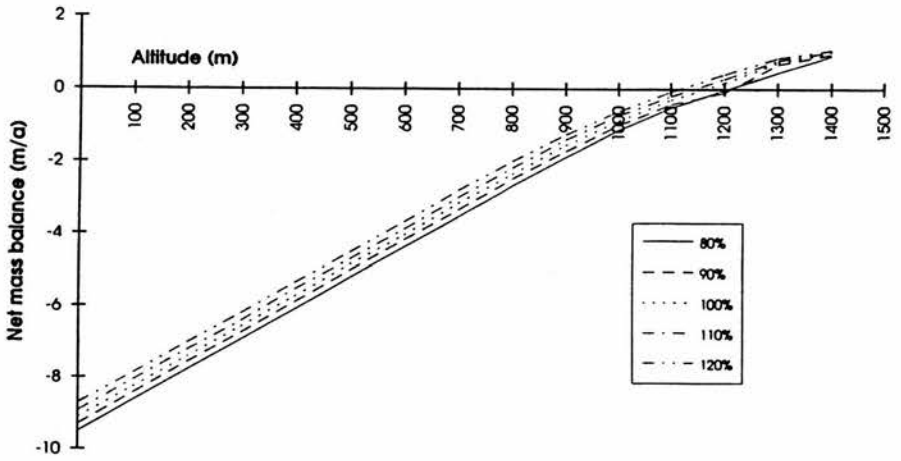

Figure 3.24 Sensitivity to the oceanic long wave parameter, Ao.

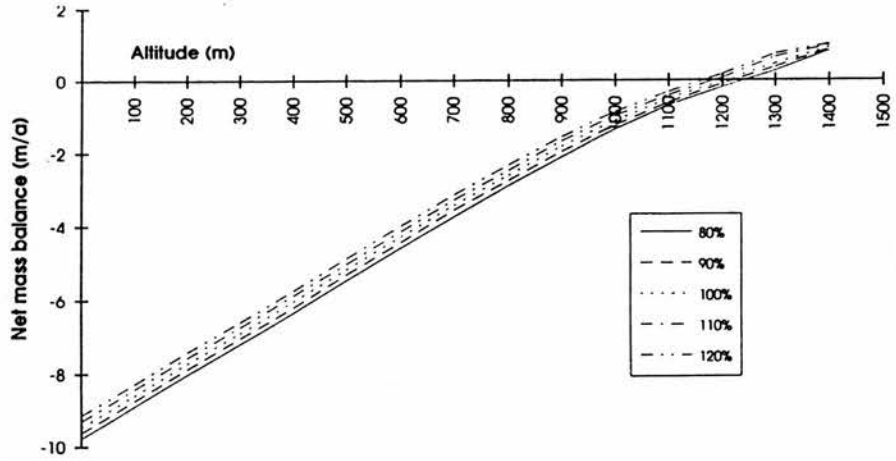

Figure 3.25 Sensitivity to the long wave parameter B.

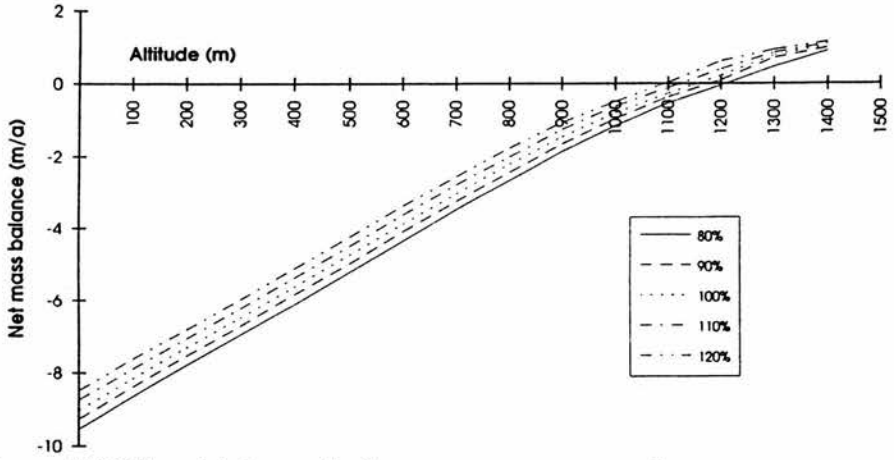

Figure 3.26 Sensitivity to the long wave parameter C.

3.4 The ice sheet model

The ice sheet model is derived from the models of Mahaffy (1976), Budd and Smith (1981), and Payne (1988). It has been tested on the current configurations of the Barnes Ice Cap (Mahaffy, 1976), the West Antarctic ice sheet (Payne et al.,1989), and the Loch Lomond re-advance (Payne and Sugden,1990) and as such its assets and limitations are well documented.

The features that limit the correct representation of the ice sheet system by the model are the prescribed conditions of bedrock topography, the climate, and the mathematical relationships for the deformation and sliding of ice. Paterson (1981,p271) describes the basic model as: "being useful for studying the growth and decay of ice caps, unless the bed topography is very rough." This point arises because assumptions used in the derivation of the ice flow equations, such as assuming longitudinal stresses are insignificant, break down in the presence of large bed slopes. By suitable smoothing of the bed topography on sufficiently large grid cells this problem can be suppressed, though at the expense of a discrepancy between real and modelled bed topography. This trade off between the representation of real bed topography and the mathematical requirements of the ice flow equations puts fundamental limits on what we can infer from model results. This is particularly apparent in peaked mountain areas where there is the greatest mismatch between reality and its representation in the model by a mean or maximum altitude in a grid cell. This leads to a misrepresentation of both the climatic input, which depends on the grid cell altitude, and the ice volume, which is influenced by bedrock gradients.

Furthermore, increasing the grid cell size leads to model output which is less constrained geographically and hence less testable. Decreasing the grid cell size introduces problems concerning the stability of the model because of steepening numerical gradients between grid cells.

Ice flow comprises two parts: the internal deformation of ice, which is derived from simplifying assumptions concerning the consequent strain on ice from an applied stress, and ice sliding, which is derived from an empirical relationship involving ice surface slope and ice thickness. These two processes primarily operate in different areas of ice sheets. The former reaches a maximum in areas with large surface slopes and ice thicknesses and a minimum at ice margins while the latter is most effective at ice margins where the ice thickness is small and the surface slope is large.

The assumptions employed in deriving the ice deformation term break down at ice margins and ice divides. In the case of ice margins, the deformational velocity is at a minimum since the ice thickness is small and most movement is assumed to occur by sliding. Weertman (1961) found that the effect of ignoring longitudinal stresses at ice divides was minimal on small ice caps and negligible on ice sheets. The most important limitation imposed by this formulation for ice deformation concerns the need for small bedrock gradients, which necessitates the use of a smoothed and somewhat artificial representation of the bedrock topography.

There is no attempt to understand the physics behind the processes of ice sliding. Instead, a simple relationship involving ice surface slope and ice thickness is used. This was originally derived using data from the West Antarctic ice sheet to simulate the low stress, high velocity regions found in marine ice sheets (Budd et al.,1984). It is arguable whether such a formulation can simulate ice sliding in non marine ice sheets. The justification is that maritime climates are a high energy, relatively warm environment which lead to warm based ice sheets with fast flowing outlet glaciers. The alternative is to use a sliding relation derived with data from polar ice sheets. However, this is likely to severely underestimate the role of sliding unless the thermodynamic equations are incorporated to determine areas of basal melting. However, in this model ice is assumed to be isothermal so no distinction can be made between areas of basal melting and freezing.

Both the terms for ice sliding and ice deformation rely on the spatial and temporal invariance of their empirically determined multipliers. These are the flow law exponential, n, and the flow law multiplier, A, in the deformation equation, and the sliding equation multiplier, κ_2. Clearly there will be localised variations from their optimum values but it is assumed that these variations do not significantly affect the overall evolution of the system. This approach is justifiable since ice sheet simulations in different geographical areas with these parameter values provide the best fit between modelled and observed or inferred ice sheet extent.

There are two topographic factors which have an indirect effect on ice sheet evolution but which are not incorporated into the model, and these are eustasy and isostasy. Eustasy is the average sea level within a particular region and changes can lead to two effects. Firstly, the relative height of the bedrock topography changes, and this has a bearing on the mass balance because of the high temperature and precipitation lapse rates in the atmosphere. Secondly, the stresses on ice floating in water are such that the

ice breaks up or thins and forms ice shelves. The grounding line, which is the point where the buoyancy of ice exceeds its weight in water, is determined by the sea level relative to the land. Although a eustatic change primarily affects marine ice sheets, which have a substantial area of ice resting below sea level, it also influences ice sheets terminating in coastal areas. These may have large outlet glaciers which reach sea level and eustatic changes will influence the discharge of ice from such glaciers.

By choosing to model the evolution of maritime ice sheets, which are smaller than the large continental ice sheets, it is assumed that eustatic changes are imposed externally. This requires a knowledge of the regional sea level changes. Although global patterns of sea level variations are apparent, the regional nature of tectonic displacements ensures that there is no absolute sea level datum (Clark et al.,1978). The history of sea level change must be obtained from empirical evidence in the vicinity.

There are two reasons why the absence of eustasy does not materially affect model results. Firstly, the Loch Lomond stadial ice cap was primarily land based so ice is only likely to have reached sea level in confined valley glaciers. The modification of ice discharge caused by a eustatic change is likely to have been negligible compared to the net ice flux over the entire ice cap. If this was not the case, the model would have to be substantially modified to incorporate the variable ice discharge of glaciers which are below the grid scale of the model. Secondly, empirical evidence suggests that the variation of sea level was of the order of a few metres during the Loch Lomond stadial (Sutherland,1984). This is well within the error limits of model results.

The second indirect way in which topography influences ice sheet evolution is isostasy. Isostasy is the relative change in ground level with respect to a fixed point. The weight of an ice sheet depresses the earth's crust into the mantle leading to lower bedrock and ice surface elevations. This has important implications for the interaction of the regional climate and the ice sheet by reducing the accumulation area and increasing the ablation area. It has been postulated that this effect can account for the rapid reduction in ice volume observed at the end of glacial cycles in palaeoclimatic records (Peltier,1982; Oerlemans,1980a).

Isostasy does not materially affect model results because the Loch Lomond case study concerns a small ice cap which grew and decayed over a period of approximately 3000 years. The response of the lithosphere over such short temporal, and small spatial, scales is likely to have been negligible.

A detailed derivation of ice calving is not included in the model for two reasons. Firstly, the Loch Lomond stadial ice cap was primarily land based. The modification of the ice cap extent and thickness caused by fluctuations in ice calving from confined valley glaciers is likely to have been negligible. Secondly, the physics of calving is poorly understood. Although calving obviously depends on the stress field at the glacier termini, recent theories (eg.Hughes,1992) are not sufficiently constrained by testing to justify their inclusion.

The two primary empirical simplifications within the ice sheet model are, firstly, the multiplier (A) and exponential (n) in the ice deformation equations, and secondly, the multiplier (κ_2) in the ice sliding equation. These factors influence the extent to which ice flows from areas with a positive mass balance to areas with a negative mass balance. Reduced sliding or deformational velocities decrease ice sheet extent but increase ice thickness at the centre, and vice versa. This process is complicated by the feedback between net mass balance, ice thickness, and surface elevation. The climatic forcing over a rising ice surface will depend on the altitudinal mass balance gradient. The effect of this feedback will modify ice sheet extent and ice volume during the evolution of the ice sheet, especially over complex bed topography where the altitude and geometry of mountains strongly influences areas of growth (Payne and Sugden, 1990).

Payne (1988) used the same ice flow formulation and bedrock topography and examined the sensitivity of the deformation (A) and sliding (κ_2) multipliers by changing their optimum value by 50%. A 50% decrease in κ_2 was found to produce a 17% increase in maximum ice volume while a 50% increase reduces maximum ice volume by 11%. The increase in ice volume is a result of the thicker ice in the centre and the aforementioned feedback loop which favours small, thick ice sheets rather than large, thin ones for maximising mass input. A 50% increase or decrease in the value of 'A' has a minimal effect on the ice volume.

Although deformation is assumed to have been the dominant form of ice flow on the land based ice sheet the model is less sensitive to it than to the sliding relation. Payne (1988) attributes this to the natural variability of the two parameters; the deformation parameter varies by an order of magnitude (Paterson, 1981) so a 50% change is comparatively minor while the observations from which the sliding parameter is derived are more constrained (though paradoxically there are more serious doubts concerning its applicability!).

The effect of a change in the flow law exponential, n, is more substantial than for the deformation multiplier, A, but the conclusion is similar: increasing n increases the plasticity of ice, making it more 'sticky', which reduces ice sheet extent and increases ice thickness in the centre, and vice versa. Its value is important but there is no evidence that a value different from 3 would produce a better modelled fit to a real or inferred ice sheet extent. In general, the ice flow parameters are substantially less sensitive than climatic parameters such as precipitation and temperature.

3.5 Summary

All the models have been tested previously so this thesis is concerned with assessing their applicability to the present case studies. The relative sensitivity of the parameters in the climate models is shown in table 3.1.

The regional energy balance model can only be used meaningfully as a means of assessing the sensitivity of components of the regional climate. The model has little internal freedom to adapt realistically to new climatic conditions because of the large number of pre-determined empirical relationships. Its most sensitive parameters are the poleward energy flux parameter, k, and the long wave radiation parameters, Ac and Ao. These parameters, along with the zonal energy flux, are used to tune the model to simulate annual temperature cycles in specified regions.

The annual temperature cycle is one of six prescribed inputs to the surface energy balance model, which calculates more detailed derivations of the surface energy budget to obtain glacial mass balance profiles. This process - oriented approach allows an explicit study of the factors which influence glacial mass balance, so the effect of inferred climatic changes can be calculated and compared with independent evidence of the actual events. The limitations of the model stem from two quarters. The first concerns the prescribed climatic inputs. Clearly, there is insufficiently detailed knowledge of these inputs for either case study. However, by applying the model only to regions with similar climatic settings to the mid-latitude alpine glaciers for which it was developed, these inputs are likely to be closely matched. In addition, poorly constrained inputs such as cloud cover and the mean height of the cloud base are insensitive parameters. Overall, when the sensitivity of parameter values in the model is combined with their natural variability in nature the most sensitive inputs include the mean temperature, annual temperature range and precipitation totals. The second limitation of the model stems from the empirical relationships which formulate the energy budget. The least constrained formulations are

the surface albedo and the turbulent fluxes. The former parameter varies geographically and seasonally and there is little scope for obtaining a more accurate value. The latter parameter cannot accurately account for effects such as sublimation, which is an important process at temperatures well below freezing. In addition, refreezing of surface meltwater is not incorporated and the combined effect of these latter parameters constrains the model to mid latitude glaciers and ice caps.

The glacial mass balance profile obtained by the surface energy balance model is used as the climatic input to the ice sheet model. The model calculates ice sheet extent and thickness from a prescribed bed topography, the climate, and mathematical relationships for the deformation and sliding of ice. The limitations of the model stem from the representation of the bedrock topography on the model grid, and the sensitivity of model output to the empirically- determined parameters in the ice flow equations. However, the sensitivity of the ice flow parameters is less than that of climatic parameters. This justifies retaining a simple ice sheet model and examining the climatic forcing in more depth.

Parameter:	**Natural sensitivity (+/-)**	**Change in parameter value**	**Change in modelled ELA (m)**
Mean temperature	5°C	1°C	120
Precipitation, P	100%	20%	80
Latitudinal heat flux coefficient, k	100%	100%	350
Temperature lapse rate	2°C/km	1°C	150
Total albedo, α	50%	10%	60
Sliding law multiplier, κ_2	10%	50%	-
Flow law power, n	50%	50%	-
Snow albedo, α_{sn}	50%	10%	50
Atmospheric emittance, ε_a	20%	10%	120
Continental longwave parameter, Ac	30%	10%	80
Precipitation lapse rate, dP/dh	50%	10%	40
Continental albedo, α_{cont}	20%	10%	100
Outgoing longwave parameter, I_o	10%	10%	150
Black body radiation, f	50%	10%	30
Atmospheric transmissivity, τ_a	50%	10%	30
Cloud transmissivity, τ_c	50%	10%	30
Cloud height	5000m	1000m	25
Cloud cover, n	50%	10%	25
Solar constant, S	2%	2%	100
Exchange coefficient, C	20%	50%	rotation about ELA
Oceanic longwave parameter, Ao	30%	10%	30
Background albedo, α_b	50%	10%	<20
Cloud emittance, α_{cl}	20%	10%	40
Activation energy, Q	20%	10%	-
Longwave parameter, C	20%	10%	35
Oceanic albedo, α_{oc}	20%	10%	30
Longwave parameter, B	20%	10%	25
Flow law multiplier, A	50%	50%	-
Ice density, ρ	10%	5%	-
Zonal heat flux coefficient, E	100%	100%	25
Exchange coefficient gradient, dC/dh	20%	50%	rotation about ELA

Table 3.1 Sensitivity of parameters in the climate models in order of importance.

Chapter Four:
Climate Experiments

THE SENSITIVITY OF THE SOUTH CHILEAN SNOWLINE TO CLIMATIC CHANGE

Summary

Inferred climatic changes in southern Chile during the Last Glacial Maximum are modelled to investigate the role of the southern Westerlies on the region's glacial history. This is accomplished with a numerical model of the surface energy balance which is calibrated to derive glacial mass balance profiles from existing climatic stations. The model is then used to predict the equilibrium line altitude based on estimates of palaeoclimate. This provides an independent measure of the regional snowline which can be compared with evidence of former snowlines.

The modelled snowline mirrors the latitudinal trend of current glacier equilibrium line altitudes. It is most sensitive to temperature changes in regions with high precipitation (46° - 50°S) and sensitive to precipitation changes in regions with lower precipitation totals (south of 50° and north of 40°). This differential in sensitivity with latitude implies that glacial expansion in the region depends on a delicate interplay between cooling induced by the equatorward movement of the oceanic Antarctic Polar Front, and access to precipitation, comparable to or greater than that of today. The main conclusion is that glacial expansion in southern Chile is associated with the migration of the southern westerlies towards the equator. The importance of migrating precipitation belts in permitting glacier growth carries the implication that maximum depression of the snowline is unlikely to have been contemporaneous from latitude to latitude.

INTRODUCTION

The aim of this paper is to use a climate model to reconstruct the climate in southern Chile during the Last Glacial Maximum (LGM). The paper focuses on the role of the southern westerlies in determining the glacial history of the area. We examine the effect of the inferred climatic changes on glacial mass balance profiles (net gain or loss of snow at different altitudes) by using a numerical model of the surface energy balance developed by Oerlemans (1992). The model calculates the glacial mass balance from existing climatic stations and thus provides an independent measure of the regional snowline which can be compared with evidence of former snowlines.

The climate of southern South America is influenced by the location of the Andean Cordillera lying athwart the dominant westerlies. There is a marked contrast between the maritime climate of the western coastal ranges and the dry climate of the plains of Argentinian Patagonia in the east. Miller (1976) sub-divides southern Chile into a cool temperate band south of 42°S and a warm temperate band to the north. The southern band comprises prevailing westerlies all year round with little seasonality. The north-south pressure gradient, the westerlies, and precipitation are at a maximum around 50°S, with over 300 days of rainfall in places and mean annual cloud cover of more than 0.85. The west-east transition of rainfall is pronounced with variations of the order of metres/year occurring over distances of tens of kilometres. The annual temperature range is typically small for a maritime climate and the mean temperature ranges from 5.5°C in the extreme south to 11°C at 42°S. Further north, mean temperatures rise and precipitation drops as a result of the decreasing frequency of fronts crossing the coasts, and the climate becomes increasingly seasonal.

There has been much debate concering the changes in climate that have taken place in southern South America during the Pleistocene, usually from a palaeoecological perspective (Heusser,1989c; Markgraf,1989a; Markgraf et al.,1992) or a geomorphological perspective (Clapperton,1983; Rabassa and Clapperton,1990). All are agreed that the southern Westerlies which circulate the globe between Antarctica and the southern hemisphere land masses play a crucial role in determining the climate to the west of the Andean Cordillera (Miller,1976; Prohaska,1976; Pittock and Salinger,1991). Lamb (1959) suggested that the southern wind system acts as a 'flywheel' of the general atmospheric circulation, and changes in it entail an adjustment of the atmosphere at a global scale. However, there has been disagreement as to the latitudinal changes that

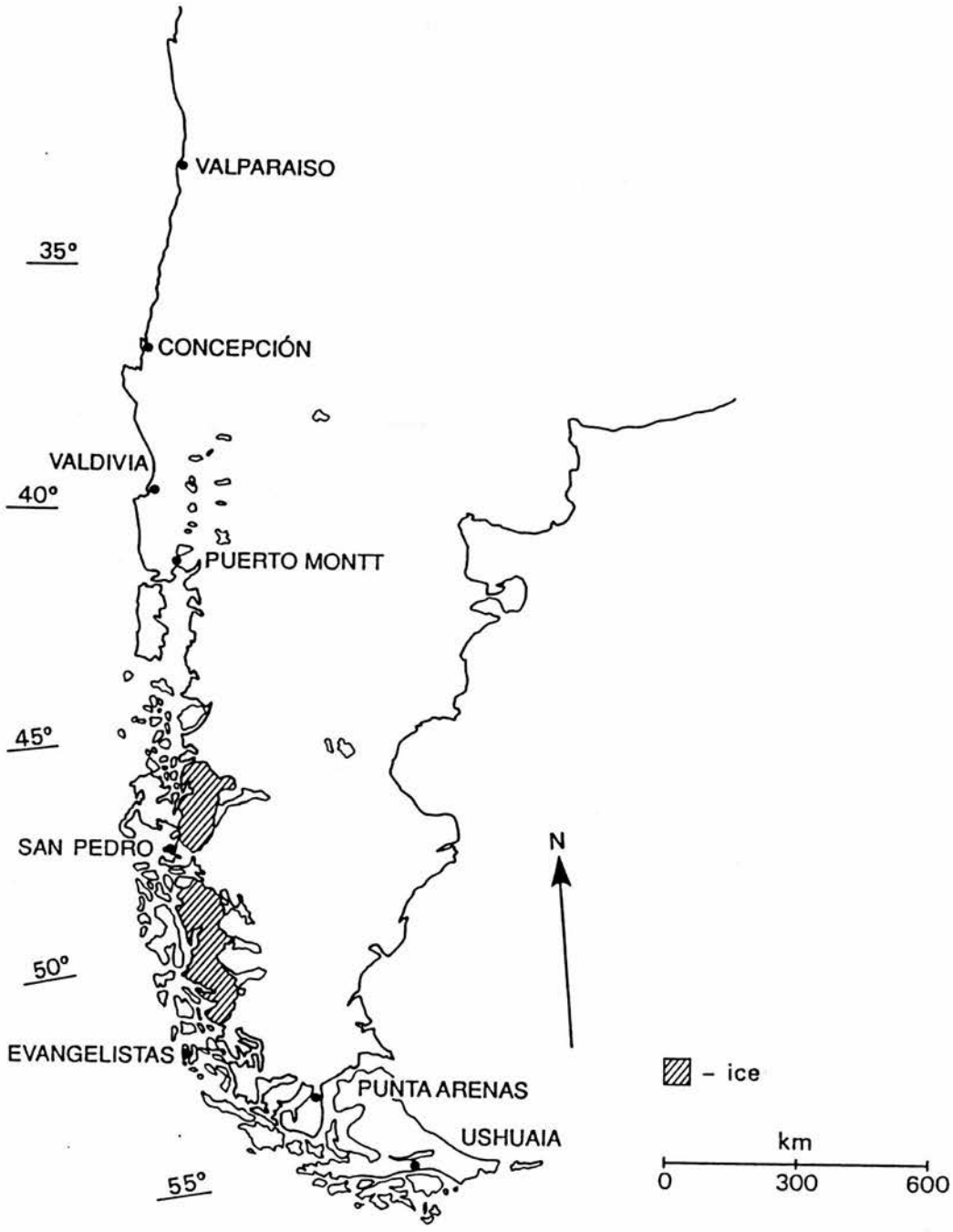

Figure 1. A map of southern South America showing the location of the climate stations and the current ice fields.

occurred during glacial conditions, a time when the oceanic Antarctic Polar Front shifted north by a few degrees of latitude (Morley and Hays,1979). Markgraf (1989a; 1989b) and Markgraf et al. (1992) maintain that former vegetation patterns and certain global circulation models (Kutzbach and Guetter,1986) indicate a poleward shift of the subtropical and westerly circulation, with a zonal intensification of the wind systems between 43° and 50°S. Meanwhile, Heusser (1983; 1989b; 1989c) claims that the former vegetation patterns in Chile reflect an equatorward migration of the wind belts, citing the requirements for large increases in precipitation to nourish the glaciers of north and central Chile (Hastenrath,1971; Caviedes and Paskoff,1975). The effect of a change in the wind systems has also been investigated using a regression model which relates air and sea temperatures to precipitation and snowline elevation (Caviedes,1990). The model indicates a substantial increase in precipitation for a small drop in sea temperature, leading to a depression in the snowline which is most significant to the south of latitude 35°S.

This paper attempts a more complete examination of the inferred climatic changes by using a process-oriented model to assess the role of different components of the climatic system. The model is calibrated by current meteorological data and the predicted altitude of the snowline in different latitudes is compared with the altitude observed today. Given good agreement, the model is then used to calculate the envelope of change in temperature and precipitation derived from independent palaeoecological evidence of the climate at the Last Glacial Maximum. These reconstructions are tested by applying the climate model to climate stations which are representative of the main latitudinal climate regions in the area: Puerto Montt (41°S) in the warm temperate zone, San Pedro (47°S) in the moist temperate zone, and Ushuaia (54°S) in the cold temperate zone (Figure 1). The modelled snowline is compared with evidence of the snowline depression during the Last Glacial Maximum thought to range from 900 metres at 40°S (Porter,1981) to 500 metres in the far south (Garfield and Stingl,1988).

THE MODEL

The altitude of the snowline can be estimated by the surface energy balance model developed by Oerlemans (1992), which is a natural extension of the model developed by Oerlemans and Hoogendoorn (1989). The amount of snow, M, accumulated or ablated in

a specific region and at a particular altitude is obtained by integrating the surface energy budget, B, and the precipitation, P, over one year:

$$M = \int [-B/L + P]\, \delta t$$

where L is the latent heat of melt at 0°C. The precipitation is assumed to fall as snow below a threshold temperature of 2°C. Unless there is a specific seasonal maximum, precipitation is assumed to fall uniformly during specific 'events' on every fifth day and is adjusted to match the annual precipitation total at sea level. Snow melts if the energy budget, -B/L, is negative, and once snow melts it is assumed not to refreeze. If more snow falls than melts over each time step then there is a net accumulation of snow.

The daily cycle of temperature and radiation is an integral part of the energy balance and is obtained by integrating with a time step of 30 minutes. The calculation of the integral depends on the value of the surface energy budget, B, which can be partitioned into specific energy fluxes as follows:

$$B = Q(1-\alpha) + I_t - I_O + F_S + F_l$$

where Q is the incoming shortwave radiation, α is the surface albedo, I_t and I_O are the incoming and outgoing longwave radiation, and F_S and F_l are the turbulent fluxes of sensible and latent heat respectively.

The direct incoming shortwave radiation, Q, depends on the solar output, S, the angular position of the sun, γ, (Walraven,1978) and the transmissivity of the atmosphere, which is obtained by separating the absorption of air, τ_a, and clouds, τ_c. The air transmissivity term is schematically represented in terms of altitude and solar elevation and the cloud transmissivity in terms of cloud cover:

$$Q = [\, S \sin\gamma \,]\, \tau_a\, \tau_c$$

where $S = 1353.\, [\, 1 + 0.034\cos(\, 2\pi N/365 \,)\,]\ W/m^2$

$\tau_a = (\, 0.79 + 0.000024h \,)\, [1 - 0.009\, (\, 90 - \gamma \,)]$

$\tau_c = 1 - (\, 0.41 - 0.000065h)\, n - 0.37\, n^2$

where h is the altitude in metres, n is cloud cover in tenths, and N is number of days.

An appraisal of the surface albedo, α, is important for an accurate determination of the energy budget. It depends on a large number of spatially and temporally heterogeneous variables, and as a result can only be calculated schematically. In the model the albedo is linked to a regional background albedo, α_b, which depends on altitude relative to the snowline:

$$\alpha_b = 0.115 \text{ arctg } (h - E + 300 / 200) + 0.48$$

where E is the glacial equilibrium line altitude in metres. The surface albedo is obtained by perturbing the background albedo in terms of the snow depth, δ, and the seasonally accumulated snowmelt, Mn:

$$\alpha = \max [0.12; \alpha_{sn} - (\alpha_{sn} - \alpha_{b)} e^{-5\delta} - 0.015Mn]$$

where α_{sn} is the albedo of snow which is taken to be 0.72.

The formulation of the longwave radiation comprises two parts. The outgoing radiation is set to that of a melting ice surface. The incoming radiation is assumed to depend on two factors: the contribution from clouds, I_{cl}, and that from the atmosphere, I_{at}. Both depend on the temperature of the emitting surface and are schematically formulated in terms of the surface air temperature, Θ_a, the mean height of the cloud base (which determines the temperature of the cloud base, Θ_{cl}), and the mean cloud cover, n:

$$I_{at} = \varepsilon_a \sigma \Theta^4_a$$
$$I_{cl} = nf\sigma\Theta^4_{cl}$$

where $\varepsilon_a = 0.7 - 0.000025h$

$$f = 0.6732 + 0.0024\Theta_{cl} - 0.914\times10^{-5}\Theta^2_{cl}$$

where f is the fraction of black body radiation in the 'effective' window band and σ is the Stefan-Boltzmann constant.

The final components of the energy budget are the turbulent fluxes of sensible, F_s, and latent heat, F_l. Since the relevant parameters are rarely measured, an altitudinally dependent exchange coefficient, C, is utilized, which is assumed to mimic the gross

features of the fluxes. It is related to the climatic snowline and the fluxes are represented in terms of the difference between the atmospheric and surface temperature and humidity:

$$C = C_E + (E - h) \, dC/dh$$
$$F_s = C (\Theta_a - \Theta_s)$$
$$F_l = C L (q_a - q_s) / c_p$$

where L is the latent heat of melt, q is the specific humidity, subscripts a and s refer to the atmosphere and surface respectively, and c_p is the heat capacity of water.

In order to obtain the glacial mass balance profile the energy budget is integrated with precipitation for three years. This output is independent of the initial prescription of the snowline required to calculate the surface albedo and turbulent fluxes. Seven climatic inputs are required: annual mean and range of temperature, daily temperature range, annual precipitation, altitudinal variation of precipitation, mean cloud cover, mean height of cloud base, and temperature lapse rate.

The limitations of the model stem from the necessarily schematic representation of the energy fluxes. Two problems can be distinguished. The first concerns the lack of climatic data over the appropriate averaging periods. For example, the long wave radiation calculation requires knowledge of mean cloud cover and the mean height of the cloud base, both of which vary substantially over time and space. It has to be assumed that the variance from the mean value does not materially affect the overall calculation. Fortunately in this instance, the model output appears to be relatively insensitive to this assumption. The second problem concerns the overall formulation of the energy fluxes. The most poorly constrained formulations are those of the surface albedo and the turbulent fluxes. A model of the spatial and temporal variation of the surface albedo does not exist, so the only alternative is to use a scheme which broadly matches empirical observations. Oerlemans developed this model for mid-latitude Alpine glaciers and thus the application of the model to the Andes carries the assumption that there is a similar climatic and topographic setting. The turbulent fluxes determine the transfer of energy from the free atmosphere to the surface and depend on the stability of the atmospheric boundary layer and surface conditions such as temperature, humidity, and roughness (Kuhn,1979; 1987). Clearly, these variables can only be quantified at a local scale with in situ measurements, so such refinements cannot be incorporated into the model. Instead, a

scheme is utilised which averages empirical observations at a broad scale (Kuhn,1979; Gruell and Oerlemans,1986).

There are likely to be two main problems when applying the model to the Andes. Firstly, mean wind speeds are high Schwerdtfeger (1976) and thus the transfer of sensible heat may be underestimated. Secondly, the role of sublimation is not incorporated in a meaningful manner. Sublimation depends on both the specific humidity gradient across the surface and wind speed. It is important in snow ablation at temperatures near to and below freezing and is therefore likely to be an important factor in the high arid regions of the Andean mountains north of 33°S (Kuhn,1980). Since this paper deals with the temperate regions well to the south of 33°S, the role of sublimation is likely to be less important.

A model of this type, which relies on empirically simplified processes, depends on careful calibration. In practice, the components of the model which can be calibrated from empirical data are the altitudinal variation of precipitation, the temperature lapse rate and the humidity. In general, precipitation increases with altitude to a maximum at an altitude of approximately 650 metres on the windward side of the Andean crest (Fujiyoshi et al.,1987). In the model it is assumed that there is a constant increase of precipitation with elevation from the annual mean value at sea level. In reality, precipitation will vary markedly over small horizontal and vertical distances depending on the surrounding topography and, at higher elevations, the inability of high-altitude cold air to hold as much moisture as warmer air at low altitudes. A constant temperature lapse rate of 6.5° C/km is used throughout the year despite the complex variability observed over glaciers. Synoptic features such as the contrast in lapse rate between sunny and rainy periods, or temperature inversions, are not incorporated into the model. The region is influenced by moist maritime air and high values of relative humidity of nearly 80% are observed close to the ice fields (Inoue et al.,1987).

TESTING THE MODEL

The uncertainties in construction means that the model must be tested to see if it is a sufficiently accurate representation of the present climate system. One way to do this is to compare the model predictions with independent evidence. An appropriate test is to simulate and compare the current configuration of the regional snowline.

Climatic data from various stations in Chile and Argentina (Table 1) were used as input to the model, and the resulting mass balance profiles are shown in figure 2 for altitudes ranging from sea level to 2800 metres. The altitude of the snowline, where the mass balance equals zero, is predicted for each station. In a maritime environment such as this the snowline is approximately equivalent to the equilibrium line altitude of glaciers.

The most comprehensive account of observed snowlines comes from Nogami (1976), Schwerdtfeger (1976), and Kuhn (1980). The topographic and climatic nature of the region means there is considerable uncertainty attached to the reported snowline altitudes, which are usually derived from cirque floor altitudes. The glaciers are highly dependent on the moisture provided by the westerlies so the equilibrium line altitude (ELA) rises steeply away from the Pacific coast as precipitation decreases. Since there are only a few reported snowline altitudes on the Pacific coast south of Puerto Montt we carried out a fresh survey of the regional snowline.

Andrews and Miller (1972) showed that the accumulation-area ratio (AAR) of a glacier in steady state is usually around 0.65. Under such circumstances the equilibrium line altitude can be estimated as the altitude of the contour that divides the glacier into accumulation and ablation zones in a ratio of 2:1. To be fully effective it is necessary to know the hypsometry of a glacier basin in detail and to exclude anomalies such as glaciers which are largely nourished by avalanches or losing mass by calving. An advantage of the technique is that it assumes the glacier is in steady state and thus represents a measure of equilibrium line altitudes over some years. Kuhn (1984) and Oerlemans and Hoogendoorn (1989) have shown that the response of glaciers to climate depends on the climatic setting and hence the glacial mass balance gradient, as well as the equilibrium line altitude. This suggests that the AAR technique is not ideal when comparing regions with diverse climates. However, the climatic setting of the region in question is sufficiently similar over its latitudinal extent to warrant use of this method.

The measurements were made from maps at a scale of 1: 250,000 with a contour interval of 1000 feet (303m). Glaciers were excluded (a) if their topographic drainage basin could not be identified unambiguously, as is the case with divergent flow in most ice caps, (b) if the glacier is small and occupied a cirque likely to experience snow drifting (which would yield an anomalously low ELA), and (c) if the glacier calves into the sea. One hundred and forty glaciers from a spread of latitudes were accepted as offering good estimates of the regional equilibrium line altitude.

The errors in this approach stem from three sources: firstly, even assuming the maps are accurate, the large contour interval means the snowlines in our survey are accurate to less than ±150 metres. Secondly, the steep snowline gradient away from the coast, and the variation of the snowline within a confined area, due to the extreme variability of precipitation, means the latitudinal variation of the snowline can only be represented by very general trends (figure 3). Thirdly, the model derived snowline is determined from only a small number of stations so the latitudinal variation shown in figure 4 is meant only to show the general trend, rather than indicate an exact snowline for a particular latitude. This best fit line accounts for the fact that Punta Arenas and Ushuaia are to the lee of the main crest while Evangelistas and San Pedro are to windward.

With such poorly constrained test data it is unsurprising that there is a good fit, even though the model was not optimised in any way, with both sets of results showing a decline from 1500-1700m in the north to 550m in the south. The glaciers in the survey are separated into windward, main crest, and lee side glaciers to distinguish the effect of the west-east ELA gradient, which is approximately 420m/ °longitude at 47°S. In the south the modelled snowline is similar to the observed altitude on the main crest of the Andes. In the north it tends to be lower, probably reflecting the model's inability to simulate a more seasonal climate.

	Latitude (°S)	Longitude (°W)	Mean Annual Temperature (°C)	Daily Temperature Range (°C)	Annual Precipitation (mm)	Mean cloud cover (tenths)	Mean wind Speed (m/s)
Concepcion	3640'	73°03'	13.0	11.5	1,293	0.44	4
Valdivia	39°48'	73°14'	11.9	9.4	2,489	0.51	2
Puerto Montt	41°28'	72°57'	11.1	7.5	1,982	0.69	4
San Pedro	47°43'	74°55'	8.2	5.7	4,485	0.81	7
Evangelistas	52°24'	75°06'	6.4	4.2	2,570	0.84	12
Punta Arenas	53°10'	70°54'	6.7	6.7	448	0.69	4
Ushuaia	54°48'	68°19'	5.5	7.7	574	0.62	3.9

Table 1 Climatic data from selected stations.

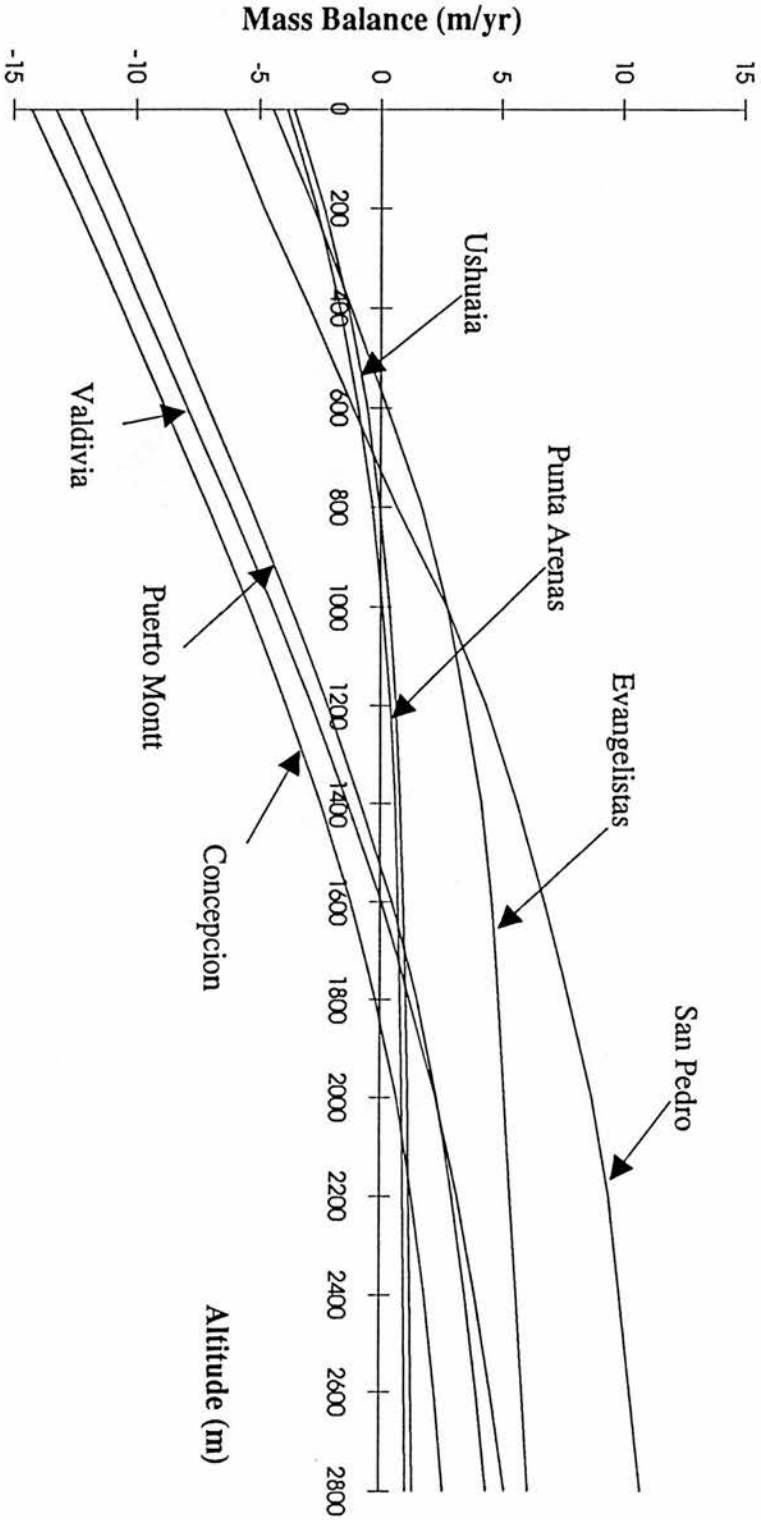

Figure 2. The glacial mass balance profiles calculated by the climate model for the climate stations.

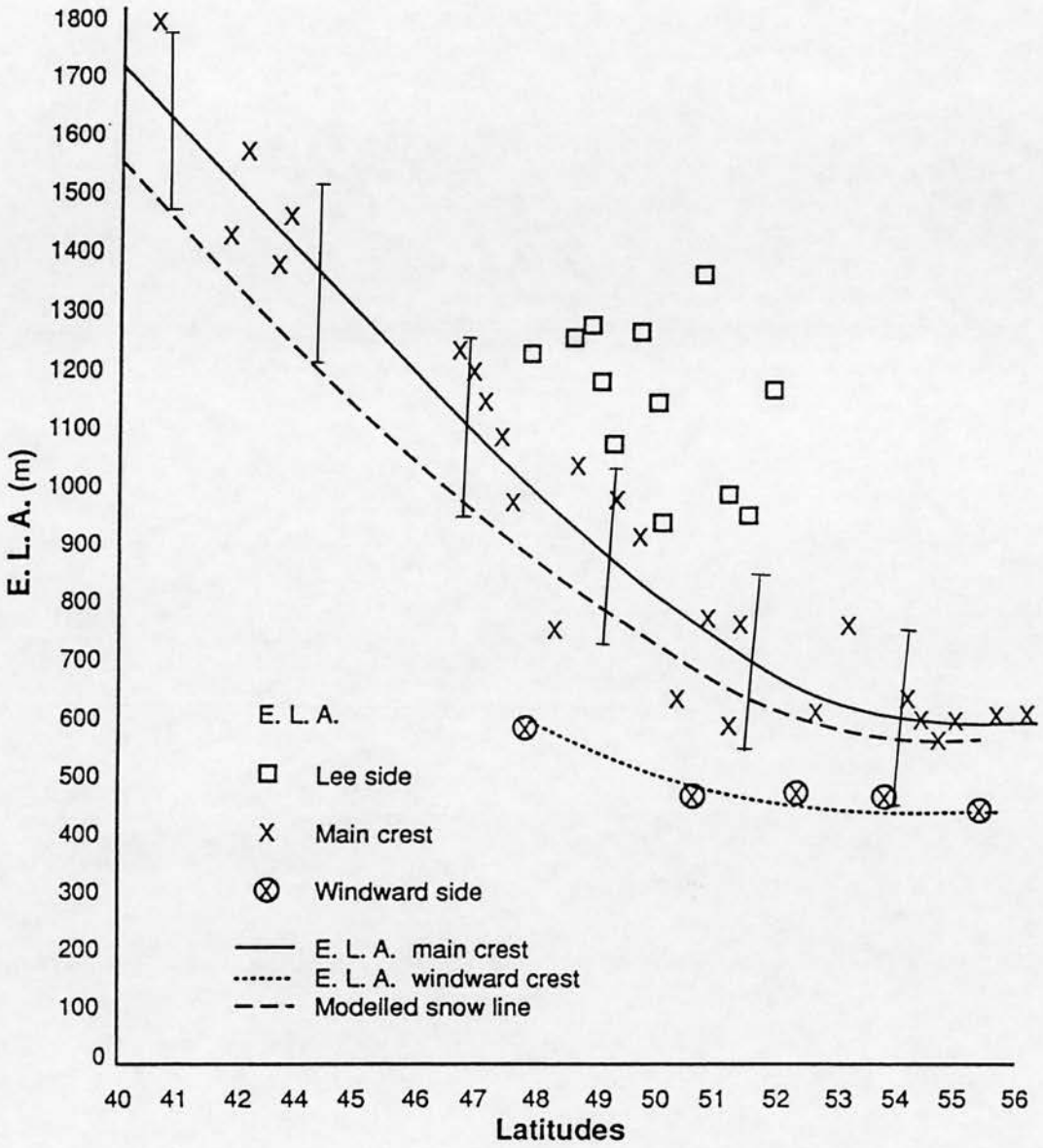

Figure 3. The latitudinal variation of the modelled snowline and the empirically - derived equilibrium line altitude (ELA). The ELA is plotted as a mean of 5° latitudinal bands and is distinguished between glaciers on the windward, crest and lee of the main Andean mountain crest. Details of glacier locations are in Hulton et al. (1993).

SENSITIVITY OF THE CURRENT CLIMATE

The major controls on the glacial mass balance profile in maritime climates are mean annual temperature and total annual precipitation (Kuhn,1984; Oerlemans and Hoogendoorn,1989; Kerr,1992). Mean annual temperature is strongly dependent on the sea surface temperature in maritime climates and it drops linearly with increasing latitude. Annual sea-level precipitation is almost 2 metres at 40°S and rises to 4 metres and possibly over 6 metres at its maximum in the south around 50°S. Fujiyoshi et al. (1987) suggest annual precipitation reaches 10 metres on the Patagonian ice fields, but such estimates are based on few measurements.

The effect of temperature and precipitation on the glacial mass balance is shown in figure 4. The snowline is governed primarily by the annual mean temperature and secondarily by precipitation. In general there is a drop of 0.4°C/ °latitude in the mean annual temperature and this is reflected in a drop of approximately 80m/ °latitude in the regional snowline to the south. An increase of precipitation increases the volume of winter precipitation falling as snow and depresses the snowline. This effect is amplified at lower latitudes where the seasonal precipitation falls mainly during the winter months. More importantly it steepens the mass balance gradient,which increases glacier extent. The effect of precipitation can be most clearly seen at the stations which are not located on the west coast. Puerto Montt lies to the south of Valdivia but is located to the lee of the coastal hills and hence has lower precipitation. As a result it has a higher modelled snowline than would be expected for its latitudinal position. Similarly, Punta Arenas and Ushuaia are both situated to the lee of the Andean crest and consequently have less precipitation which is reflected in their higher than average snowlines.

The effect on the glacial mass balance of a change in the mean annual temperature and precipitation can best be shown by sensitivity analysis. Temperature and precipitation are examined at three stations which are representative of the different climatic regions in the area. Puerto Montt (41°S) represents the warm temperate zone, San Pedro (47°S) the moist temperate zone, and Ushuaia (54°S) the cold temperate zone. In the experiments the mean annual temperature is changed by ±2°C and the precipitation by ± 50% while all other climatic components remain the same.

At Puerto Montt, the effect of a drop of 2°C in the mean annual temperature is to reduce the snowline altitude by 295 metres, while a rise of 2°C raises the snowline by 310

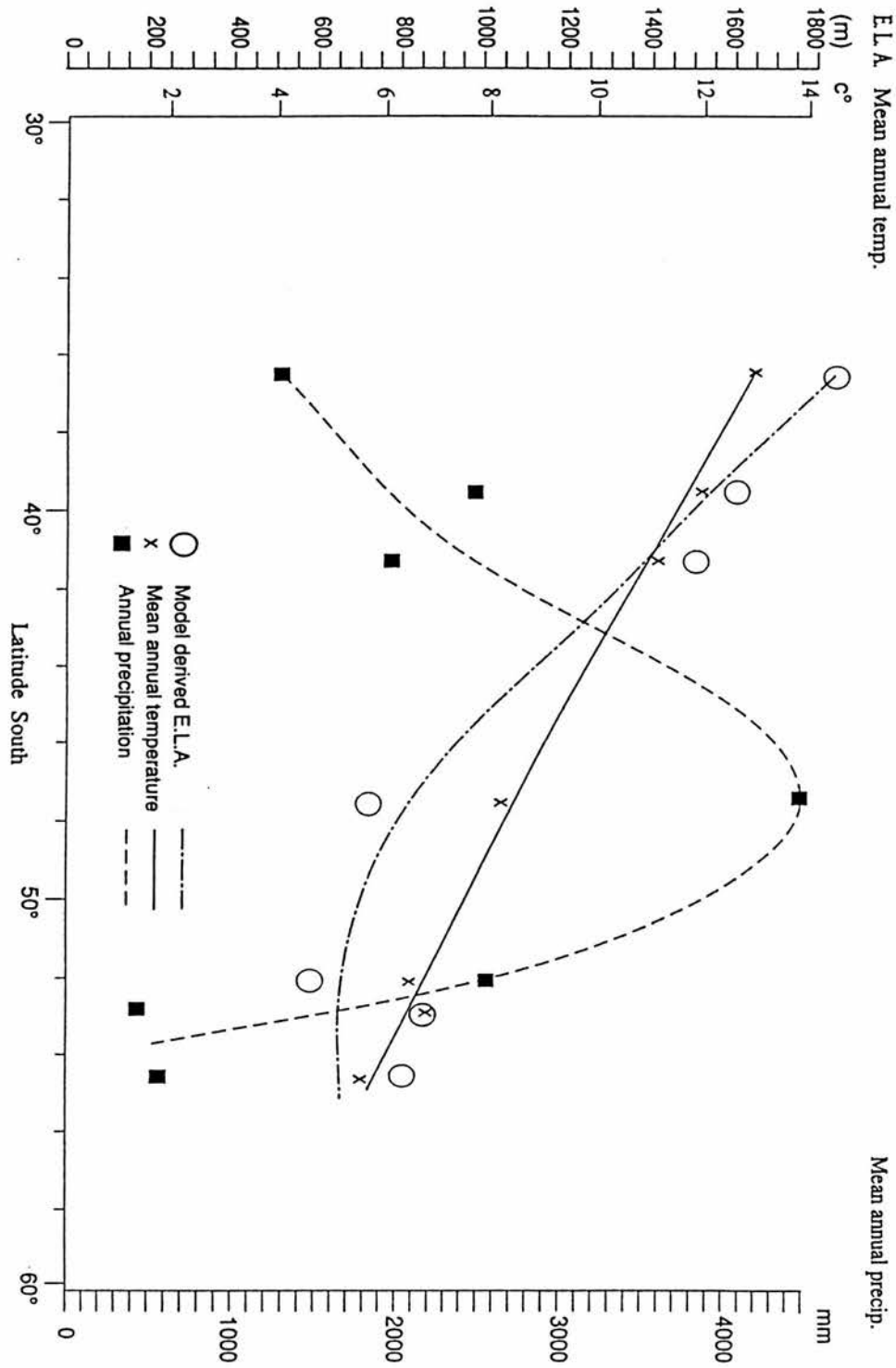

Figure 4. The variation of mean annual temperature, annual precipitation totals, and model - derived snowline altitude with latitude.

metres (figure 5a). An increase of precipitation by 50% lowers the snowline altitude by 120 metres and, more importantly, steepens the gradient of the mass balance profile. A decrease of precipitation by 50% has the reverse effect and raises the snowline by 205 metres. At San Pedro, a 2°C reduction in the mean annual temperature lowers the snowline altitude by 315 metres while a 2°C increase raises it by 320 metres (figure 5b). An increase of precipitation by 50% lowers the snowline altitude by 95 metres, and steepens an already steep mass balance gradient. A reduction of precipitation by 50% raises the snowline altitude by 160 metres. At Ushuaia, a 2°C reduction in the mean annual temperature decreases the snowline altitude by 290 metres while a 2°C increase raises the snowline altitude by 320 metres (figure 5c). An increase of precipitation by 50% lowers the snowline altitude by 120 metres while a decrease raises it by 205 metres, and reduces an already small positive mass balance.

This analysis shows the altitude of the modelled snowline is most sensitive to temperature changes in the area of maximum precipitation and least sensitive in drier areas. Conversely, it is most sensitive to precipitation changes in the area of low precipitation and less sensitive in areas of high precipitation. These two factors are related because the temperature determines the amount of precipitation falling as snow.

MODELLING THE INFERRED CLIMATIC CHANGES

The purpose of this section is to simulate the glacial climate inferred from pollen data in each climatic zone to reconstruct the former regional snowlines. Unfortunately, while estimates of the maximum lowering of the snowline are usually possible, there are, as yet, poor chronological constraints on glacial history so the maximum snowline lowering may not have been contemporaneous. The model is applied to the same three climate stations: Puerto Montt, in the north; San Pedro, close to the central belt of the Westerlies; and Ushuaia, in Tierra del Fuego.

Heusser et al. (1981) apply regression equations relating present day pollen to temperature and precipitation and hence to fossil pollen data from Taiquemo (42°S), close to Puerto Montt on Isla Chiloe. They infer a 4°C cooling compared to present values during glacial conditions between 31,000 and 14,000 years B.P., accompanied by a 50% reduction of precipitation. However, Markgraf (1989a) claims this falls short of explaining the full glacial climate and interprets the taxa to suggest a climate with summer

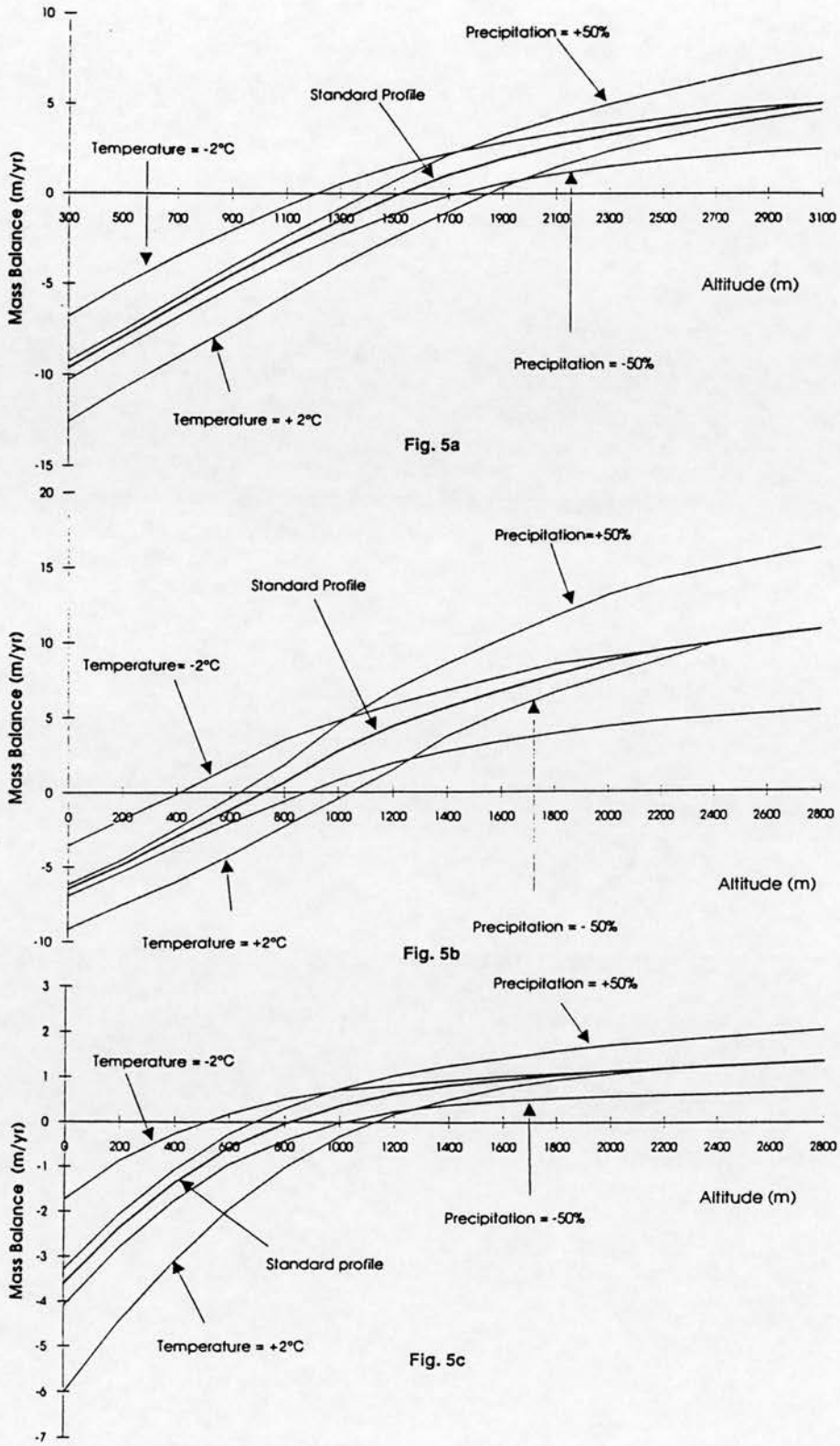

Figure 5. The sensitivity of the present glacial mass balance profiles at (a) Puerto Montt, (b) San Pedro, and (c) Ushuaia.

moisture stress related to a decreased influence of the westerlies. At the same latitude on Isla Chiloe, Villagran (1988) provides evidence of increased precipitation and cooler temperatures reflected in the expansion of moorland vegetation. Figure 6a shows the modelled mass balance profile for the present climate and three profiles corresponding to a 4°C drop in temperature combined with a change of precipitation of -50% and +50%, and a 6°C drop with a -50% change in precipitation . The latter values correspond to the inferred climatic change postulated by Markgraf (1989b) for the subtropical lowlands to the north. The climatic change inferred by Heusser et al. (1981) at the Last Glacial Maximum (LGM) results in a drop in the snowline altitude of less than 270 metres. This compares with the LGM snowline which is postulated to have been 900 metres below the present snowline by means of a simplified accumulation-area ratio approximation (Porter,1981). This is a substantial discrepancy, even allowing for a substantial error in both the model and the determination of the LGM snowline.

Figure 6b shows the modelled mass balance profile for the present day at San Pedro and the effect of a 3°C drop in mean annual temperature, combined with a change in precipitation of -30%, 0%, and +30%. These values have been arbitrarily chosen to reflect the reduction in temperature that may have occurred and a comparison of the effect of both increased moisture and aridity. The conclusion is that the model is sensitive to temperature at this location and, given the high precipitation, a reduction in mean annual temperature of 3-4°C is sufficient to lower the snowline sufficiently to initiate substantial glaciation.

In the extreme south in Tierra del Fuego, the climate is inferred to be very dry and much colder although no pollen record extends back to the Last Glacial Maximum (Heusser,1989b; Heusser,1989c) . Figure 6c shows the modelled profile for the present climate at Ushuaia and the effect of reducing the temperature by 3°C combined with a change in precipitation of ±50%. This is the inferred temperature reduction for the Late Glacial (Heusser,1989b) and, combined with arbitrary changes in precipitation, indicates the importance of precipitation on both the snowline altitude and the mass balance gradient. Clearly, a drop in temperature of the order of 6°C (Heusser,1989b) is sufficient to depress the snowline by the 500 metres suggested by Markgraf et al. (1992). However such a decrease in precipitation reduces the mass balance gradient to the unlikely climatic setting of a polar desert. The sensitivity of the modelled snowline altitude to precipitation implies that a less severe reduction in temperature coupled to a smaller reduction in precipitation is perhaps more likely. This would lower the snowline altitude by an

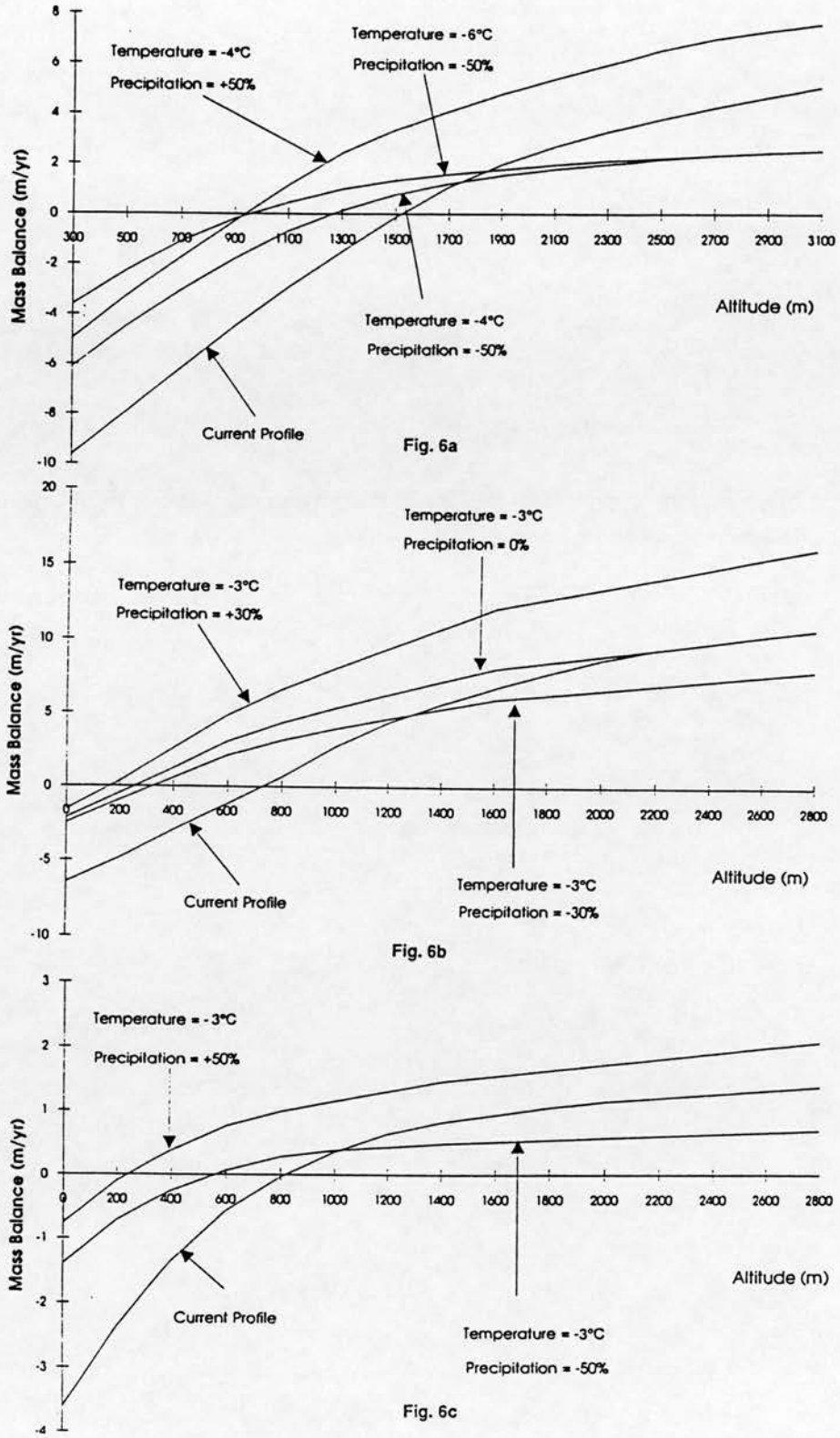

Figure 6. The glacial mass balance profiles calculated from inferred climatic changes at (a) Puerto Montt, (b) San Pedro, and (c) Ushuaia.

equivalent amount and retain a sufficiently steep mass balance gradient to permit glacial expansion.

DISCUSSION

The climate model allows the palaeoclimate inferred from pollen records to be reconstructed. There are two alternative interpretations. First, the Westerlies zonally intensified between 43° and 50°S as a consequence of the equatorward migration of the Antarctic Polar Front and the poleward migration of the subtropical Pacific high pressure cell (Markgraf et al.,1992). Second, the Westerlies moved equatorward in response to the movement of the Antarctic Polar Front and zonal intensification was negligible (Heusser,1989a; Caviedes,1990).

In Tierra del Fuego, Heusser (1989b) suggests that the temperature depression of the Late Glacial was >3°C and estimates the temperature depression at the Last Glacial Maximum to be 6-6.5°C. It is assumed that it was arid during the Late Glacial and during the LGM, though it is acknowledged that precipitation variation is difficult to assess. This magnitude of climatic change is sufficient to depress the snowline by 500 metres below the present day value. There are two potential problems with such a severe temperature depression. Firstly, if it is assumed that sea surface temperatures govern mean annual temperatures on land then a large reduction in the sea surface temperature is required. However, reconstruction of the sea surface temperatures at the LGM (CLIMAP Project Members,1981) indicates that the water in close proximity to Tierra del Fuego was only approximately 2°C colder, which is consistent with the small latitudinal change of the Antarctic Polar Front south of Cape Horn (Morley and Hays,1976). Secondly, the assumed aridity in the region further reduces an already small mass balance gradient which would have an adverse effect on ice sheet growth, yet the region is one of the seeding areas for the former Patagonian ice sheet (Rabassa and Clapperton,1990).

These two points, combined with the sensitivity of the modelled snowline altitude, suggest that there is an alternative interpretation of a less cold and less arid environment. If the precipitation reduction is less severe, then a 500 metre snowline depression can be obtained in conjunction with a 3° or 4°C cooling. In such a case the aridity inferred from cores located in Tierra del Fuego and further north to the east of the Andes could be related to local effects associated with the growth of the ice sheet. If so, the expansion of the ice caps in southern-most South America would then depend on the delicate interplay

between cooler temperatures and eventual precipitation starvation, as postulated for other maritime ice sheets (Payne and Sugden,1990).

Further north at 42°S, Heusser (1989a) and Villagran (1988) agree that the climate at the LGM was cooler and moister. Markgraf (1989a) argues that the west coast of Chile between 43° and 54°S was effectively moister prior to 12,000 yr BP. and this is qualified by Markgraf et al. (1992) who regard the narrow band (43° to 45°S) as an anomaly and in marked contrast to increased aridity elsewhere. However, there is some disagreement as to how this is interpreted in relation to the movement of the Westerlies. Markgraf (1989b) argues that this increase in moisture is the result of an intensification of the Westerlies at these latitudes. However, one might also argue that since the zone of maximum precipitation and the highest north-south pressure gradient lie around 50°S (Miller,1976) then an increase in moisture at 42°S implies an equatorward shift of the band of maximum precipitation. By either definition, the climate at San Pedro does not provide a critical test of the movement of the Westerlies since the net result of either interpretation is a substantial lowering of the snowline and an increased mass balance gradient, both of which induce expanded glaciation.

The crux of the argument concerning the movement of the Westerlies is to be found in the Chilean Lake District close to Puerto Montt. As the model experiments show (Figure 6a) neither the explanation of Markgraf (1989a) or Heusser et al. (1981) concurs with the estimated snowline depression of the Last Glacial Maximum of 900m. A 4°C temperature lowering combined with a 50% reduction of precipitation (Heusser et al.,1981) falls far short of the estimated snowline depression required for maximum glaciation. The 6°C temperature lowering combined with increased aridity inferred further north (Markgraf,1989b) goes further towards redressing the discrepancy but still only depresses the snowline by 560 metres. Moreover it reduces the mass balance gradient which makes it more difficult to initiate a substantial glaciation. The model suggests that either a temperature depression of >5°C with an accompanying increase of precipitation or a >8°C temperature depression with increased aridity, is required to depress the snowline by about 900m. The former interpretation is more consistent with inferred temperature changes elsewhere in South America and thus the implication is that during the Last Glacial Maximum the climate at 42°S was significantly more humid than at present.This is most easily explained if the migration of the westerlies towards the equator is associated with a general cooling.

CONCLUSIONS

1. The climate model successfully simulates the observed north-south decrease in altitude of the regional snowline.

2. The modelled snowline is most sensitive to temperature changes in regions of high precipitation (46° - 50°S), and most sensitive to precipitation changes in regions of low precipitation (south of 50°S and north of 40°S).

3. South of 50°S, expanded glaciation appears to depend on the subtle interplay between decreased temperature and precipitation starvation induced by the equatorward movement of the oceanic Antarctic Polar Front.

4. Expansion of the current Patagonian ice fields seems ensured by either a small equatorward movement, or by the zonal intensification of the Westerlies, accompanied by cooling.

5. Glaciation of the Chilean Lake District suggests an equatorward shift of the Westerlies since cooling accompanied by precipitation is crucial for the glacial expansion at these latitudes.

6. The postulated migration of precipitation belts carries the implication that the maximum depression of the snowline is unlikely to have been contemporaneous in different latitudes.

7. The Chilean snowline is very sensitive to relatively small movements of the atmospheric and oceanic fronts in the region. This implies that this is a fine location for studying climatic change in the Southern Hemisphere.

THE INITIATION OF MARITIME ICE SHEETS

Summary

Quantitative estimates of the climate change necessary to initiate maritime ice sheets are obtained by relating climatic parameters to glacier mass balance. A numerical, coupled climate-ice sheet model is used at a regional scale to investigate the behaviour of former British ice sheets. The climate model is driven by changes in solar radiation, precipitation, and ocean circulation, such as the migration of the North Atlantic polar front. The resulting mass balance is used in the ice sheet model which predicts the extent, velocity and thickness of ice during a glacial cycle.

Sea temperature, topography, and precipitation levels play key roles in the dynamics of ice sheet growth, while variations in solar radiation are insignificant. The maritime influence affects land temperatures and reduces the annual temperature range, while high lapse rates make the altitude and geometry of the topography important in ice sheet growth. Precipitation levels, which are vital in determining the threshold and rate of growth of mid-latitude maritime ice sheets, are related to topographic altitude and sea temperatures. For example, a 4°C mean annual temperature drop lowers the equilibrium line altitude by the same value as a 7°C drop with an associated 50% reduction in precipitation. The conclusion is that the dynamics of ice sheet initiation are highly sensitive to offshore marine temperatures and the geometry of upland topography.

INTRODUCTION

This paper investigates the set of possible climatic configurations that can initiate an ice sheet in a maritime climate. It uses coupled numerical models of climate and ice sheets to obtain quantitative estimates of the necessary climate deterioration to grow an ice sheet. The experiments were carried out for the former Scottish ice sheet and are of interest since the abrupt change from an interglacial to a glacial climate, when large ice sheets covered areas which are currently unglaciated, is poorly understood.

There are two advantages in investigating the maritime ice sheets of Britain in relation to global climatic change. Firstly, they are likely to be particularly sensitive to ocean temperature variation, and thus changes in North Atlantic circulation, which is believed to be crucial in global climate change. This is a result of high accumulation and high ablation values leading to steep net mass balance gradients, which are sensitive to changes in precipitation and temperature (Pelto et al.,1990). The crux of the problem is the delicate balance between the cooling required to initiate glaciers and that which limits the flow of moisture and thus precipitation into the area (Lamb,1964).

Secondly, there is a large body of data concerning the Late Devensian climate for Britain and the North Atlantic (Ruddiman et.al.,1980). Climatic estimates are useful in constraining model input data, while field evidence provides independent tests of the model assumptions. Normally, testing theories about the growth of an ice sheet is difficult since evidence is destroyed by a later maximum. However, the Younger Dryas glaciation in Scotland (c.10500 yrs BP) appears to represent a truncated glaciation and provides a useful reference with which to compare results.

Intuitively there are three possible mechanisms that could initiate an ice sheet in a maritime climate:

a. Insolation variation

b. Seasonal climatic changes

c. Sea surface temperature changes

Early numerical modelling (Andrews and Mahaffy,1976) examined the conditions for growth of the Laurentide ice sheet and concluded that moisture availability and transport was vital. This agrees with work by Ruddiman and MacIntyre (1980) and Johnson and Andrews (1979) concerning the balance between the need for warm sea surface temperatures for precipitation and high latitude cooling, from insolation reduction, to initiate growth. This paper is an extension of the work of Payne and Sugden (1990)

which investigated the Younger Dryas glaciation of Scotland in terms of the complex link between ocean surface cooling and moisture starvation during ice sheet growth.

METHOD

To obtain the set of possible climatic configurations required to initiate an ice sheet, the climatic parameters must be related to some measure of glacier mass balance. This is achieved using the mass balance model developed by Oerlemans (1992), and an energy balance model which simulates the changing regional climate of the United Kingdom for use as input to the mass balance model (see North et.al.,1981).

The first two mechanisms for initiation, insolation variations and seasonal climatic change, can be investigated by sensitivity analysis of the climate models to determine the components most effective in reducing the equilibrium line altitude. There is less confidence in the model when investigating the third possibility, ocean temperature changes, since the underlying assumptions of the regional energy balance model, which is tuned with the present day climate, become invalid. In this case the mean land temperatures are assumed to change roughly in proportion with the change in ocean temperature; the energy fluxes are not explicitly modelled. The variation in equilibrium line altitude can be obtained for different climates once the important climatic components have been identified. This can then be coupled to the ice sheet model to examine the effect of climate variation on real topography.

THE MASS BALANCE MODEL

The mass balance, M, of the surface can be obtained by integrating the equation:

$$M = \int [-B/L + P] \, \delta t$$

where B is the energy balance of the surface; L is the latent heat of melt at 273K; and P is the precipitation falling in solid form, which is assumed to occur below a critical temperature. The energy balance can be written:

$$B = Q(1-\alpha) + I\iota + Io + Fs + Fl$$

where Q is the shortwave radiation; I is the longwave radiation; Fs and Fl are turbulent fluxes; and α is the albedo.

The mass balance model contains two major feedbacks: an ice-albedo-temperature feedback and an altitude-mass balance feedback. The mass balance equation is integrated with a time step of 30 minutes (to resolve the daily cycle) for a period of one year at 15 different elevations. This is then repeated to allow the equilibrium line altitude to converge at a stable value. The model is applied to different climatic regions of the United Kingdom to obtain the equilibrium line altitude and net mass balance. The required inputs are: seasonal temperature range and mean, daily temperature range, annual precipitation, precipitation lapse rate, cloudiness, mean height of cloud base, and temperature lapse rate.

As a first approximation the input parameters are based on present day values since the aim is to establish the climate perturbations required to move from an interglacial to a glacial stage. Broad simplifications are required since many parameters exhibit complex geographical and seasonal variations from their average value. However, maritime climates have characteristically little variation in cloud cover and daily temperature range.

THE REGIONAL ENERGY BALANCE CLIMATE MODEL

The model calculates the energy balance for a particular latitude band (here 50-60°) and the latitudinal and zonal (land-sea) advection of energy fluxes to obtain a seasonal temperature curve for a particular climatic region of the United Kingdom:

$$C_o \, . \, \partial\theta/\delta t = R_o - k\theta + \mu E(T - \theta)$$
$$C_l \, . \, \partial T/\delta t = R_l + k'T + E(\theta - T)$$

where C is the heat capacity; θ is the ocean temperature; T is the land temperature; R is the surface energy balance; k is the latitudinal heat flux coefficient; E is the zonal heat flux coefficient; μ is the zonal land-sea fraction; and subscripts l and o refer to land and ocean respectively.

The regional energy balance model is tuned to present day observations of sea level temperature (over a one year cycle) for particular regions of the United Kingdom. The characteristically complex temperature variation is simplified to regional values with a correction for altitude. The mass balance model can then be tested against current day observations of seasonal snow cover.

THE ICE SHEET MODEL

The climate models are coupled to the ice-sheet model which is derived from those of Mahaffy (1976), Budd & Smith (1981), and Payne et.al.(1989). It is based on the continuity equation for ice thickness which is calculated using:

$$dZ/dt = b - \nabla.[\, Z(Us+Ud) \,]$$

where Z is ice thickness; t is time; b is net balance; Ud is the vertically averaged deformation velocity; and Us is sliding velocity. The model equations are approximated using finite differences over a rectangular grid with 5 x 5 km elements. Two feedback loops form the crux of the model. The first is the mass balance/ ice thickness/ ice surface elevation feedback which provides the mechanism for ice sheet growth. The second, ice

thickness/ ice flow/ ice velocity, allows the ice to spread in extent. Isostasy is also included. Inputs required for each element are topography, sea level and mass balance.

CLIMATE SENSITIVITY

Sensitivity experiments help to establish the climatic parameters which can reduce the equilibrium line altitude sufficiently to initiate an ice sheet. One parameter in each model run was changed systematically and indicates the relative importance of that parameter within the model.

The most sensitive parameters are the mean annual temperature, precipitation, and annual temperature range. Varying the solar constant by the magnitudes calculated for the Quaternary is not sufficient to initiate an ice sheet, although in sensitive areas it may reduce the equilibrium line sufficiently to create mountain glaciers. This is a result of the dominance of the ocean heat flux holding land temperatures higher than for non-maritime areas at similar latitudes. Similarly, other climatic parameters are unable to lower the equilibrium line sufficiently (over their likely range of values) so the first two mechanisms for initiating an ice sheet, insolation variations and seasonal climatic changes, can be discounted. The third, a change in the sea surface temperature, is more problematic to model since the regional climate model is tuned with present day conditions and thus based on invalid assumptions of cloud cover and albedo values for latitude bands. Dynamic changes in ocean circulation are outside the scope of the regional model but appear to be vital in reducing mean annual temperatures on land. To overcome this, mean annual temperatures are assumed to drop in proportion to the sea surface temperatures, but the actual energy fluxes are not explicitly modelled.

Reducing the mean annual temperature reduces the equilibrium line altitude by approximately 135m/K (Fig.1). A reduction in precipitation leads to a rise in the equilibrium line altitude of approximately 70m/10%, but the rise is non-linear for large variations of precipitation (Fig.2). The results again show that the response of the equilibrium line altitude to changes in climate, which is related to the balance gradient close to the equilibrium line, is closely related to the precipitation regime (Oerlemans,1992). In general, a more maritime climate leads to a steeper balance gradient and thus is more sensitive to changes in climatic variables.

One characteristic of maritime climates is the rapid increase in continentality with distance from the coast. There are two combined effects; firstly the increased annual temperature range, and secondly, the reduction in precipitation inland. This is emphasised in Scotland by the mountains on the windward coast. These processes lead to a substantially higher equilibrium line over the east coast compared to the west coast of Scotland (a difference of 300m). In general, the climate gradient is larger from west to east than from north to south in the British Isles.

One can combine the results to obtain a three dimensional plot which shows how the equilibrium line altitude varies with particular climatic parameters (Fig.3). It is important to note that the balance gradients are not identical above and below this trend surface but are dependent on the relative values of precipitation and mean annual temperature. Here, a temperature depression of 4°K has an equivalent equilibrium line altitude drop to a temperature depression of approximately 7°K with an associated precipitation reduction of 50%.

Since the climate is a coupled system the process of separating climatic components for sensitivity tests must be undertaken with care. However, since we do not know the palaeoclimate we must rely on intuitive assumptions of the coupled values; for example, that an increase of in precipitation was coupled to an increase in cloud cover. Oerlemans (1992) found that the effects of the coupled climatic perturbations on the equilibrium line altitude appeared to be additive but the overall increase was less than 10%.

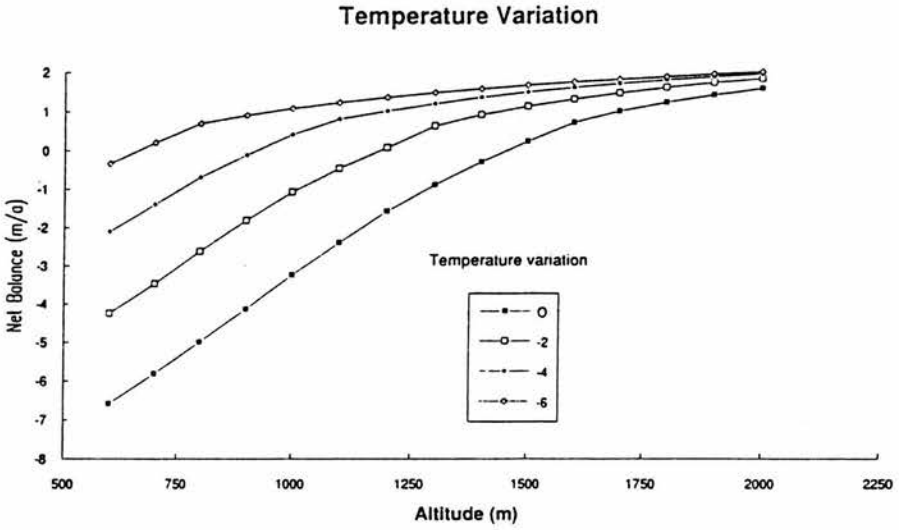

Figure 1. Mass balance curves for different mean annual temperatures in the western region. The balance gradient at the equilibrium line remains the same for different temperature regimes.

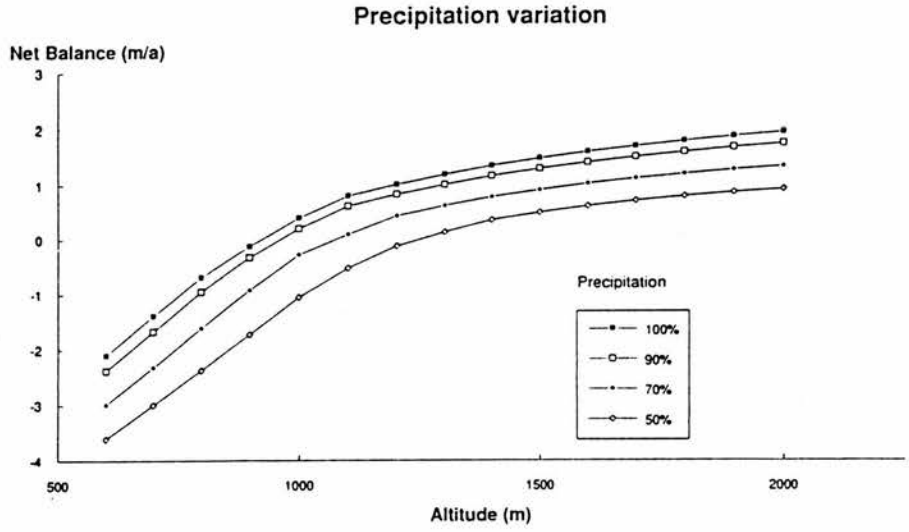

Figure 2. Mass balance curves for different annual precipitation in the western region. The balance gradient at the equilibrium line varies with different precipitation regimes.

ICE SHEET GROWTH

1. Precipitation

The role of precipitation in the ice sheet system is worth emphasising. A reduction in air temperature reduces ablation and increases solid precipitation but simultaneously reduces atmospheric moisture content and thus precipitation. The exact balance between these two contrasting effects on the equilibrium line altitude is complicated to model and depends on many factors, such as the fetch and temperature of water over which the prevailing wind is travelling. The approach of this paper avoids these problems by merely calculating the overall effect of a reduction in precipitation, rather than trying to calculate specifically the precipitation reduction that occurred in the past; a notoriously difficult parameter to estimate.

2. Topography

From a theoretical point of view, as the equilibrium line altitude falls below the mountain summits small ice caps will form. In reality it will depend on the geometry of the summit (Manley,1955) and factors such as exposure (Ahlmann,1948). Individual mountains are below the resolution of this model but the process remains identical for the grid cells. At a particular equilibrium line altitude the mountain ice caps reach a size where they flow into the valleys and coalesce. Continuing growth produces a positive feedback between the rising ice-filled valley floor, lower temperatures, and more positive mass balance, which creates an explosive growth of ice (Payne and Sugden,1990). This critical point depends on the topography of the region as a whole while the initiation of mountain ice caps depends on the height and geometry of the individual mountain massifs. In general, plateaux-like topography requires a smaller drop in the equilibrium line to grow large ice sheets than Alpine topography. This is the basis of the "instantaneous glaciation" of Northern Canada in initiating the Laurentide ice sheet (Andrews and Mahaffy,1975; Williams,1979).

Figure 4 shows the abrupt threshold between small mountain ice caps and a large ice sheet for variations in precipitation and mean annual temperature. The threshold is a unique function of the topography of a region. It is important to note that the sensitivity of the model is such that the error in calculating the equilibrium line altitude is larger than the sensitivity of the topographic threshold we are trying to investigate. In other words,

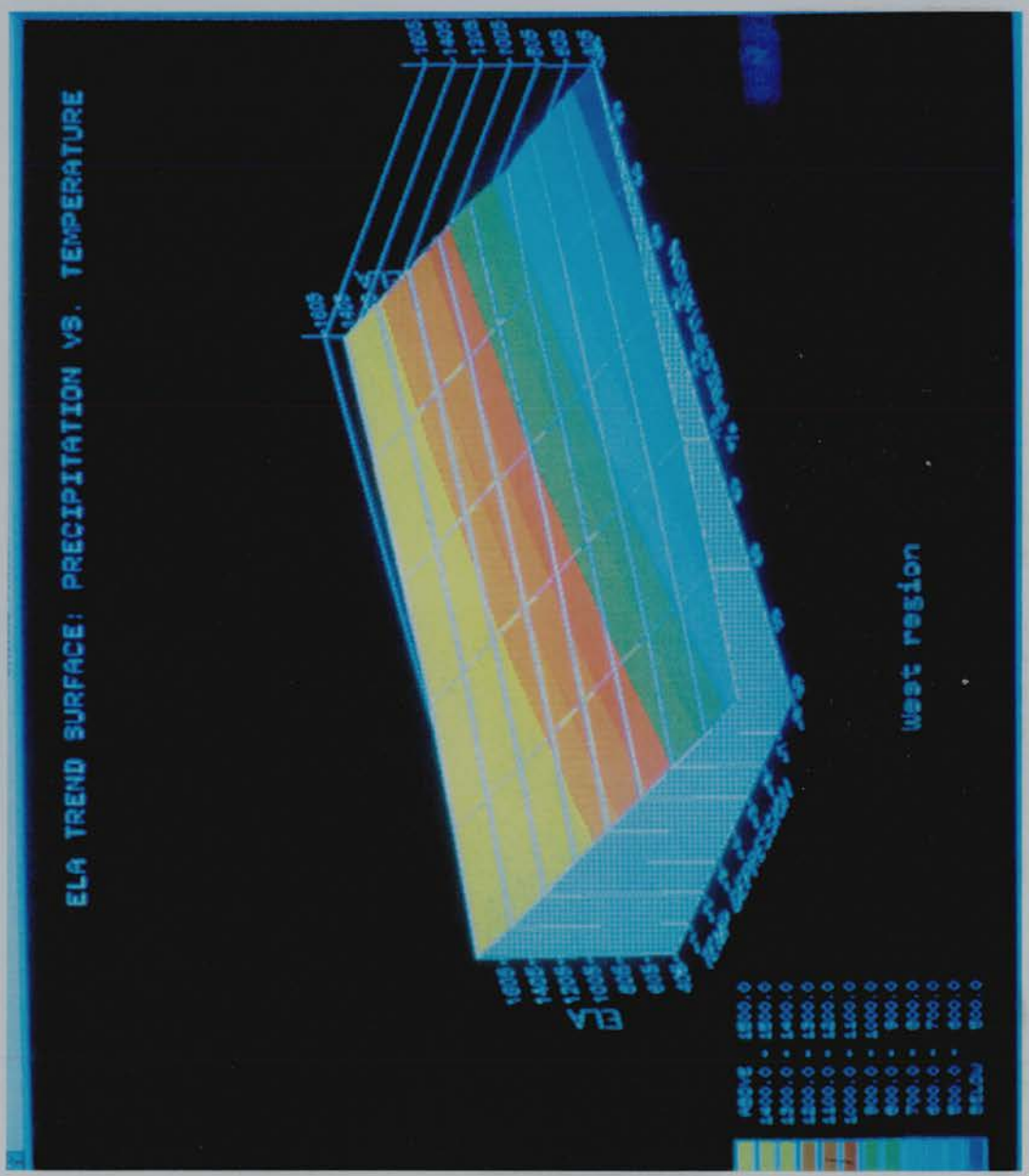

Figure 3. The equilibrium line altitude surface as a function of annual precipitation and mean annual temperature in the western region. Shaded regions are of equal altitude.

we do not have the ability to measure the palaeoclimate accurately enough to determine when the threshold would be crossed.

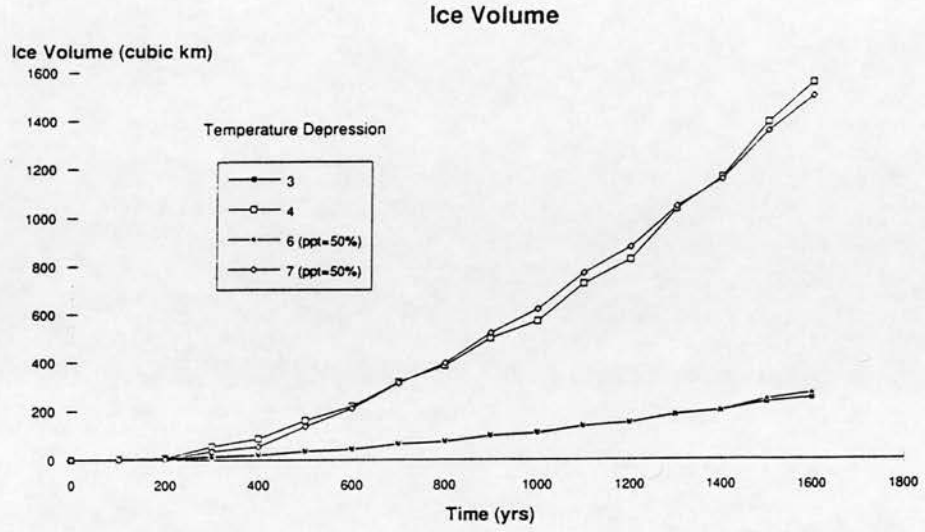

Figure 4. Ice volume through time for changes in annual precipitation and mean annual temperature. The equilibrium line depression is similar in the case of a 3°C and a 6°C drop with 50% precipitation and likewise with a 4°C and a 7°C drop with 50% precipitation.

THE LOCH LOMOND ICE SHEET

Using as a reference case the Younger Dryas (or Loch Lomond) ice sheet, model results can be compared with field evidence of ice sheet extent. The reference case climate is a 7°C drop in mean annual temperature combined with a 50% reduction in precipitation. Figure 5 shows the geographical location of the ice sheet for this experiment. It can be seen that although the highest, plateaux type mountains are in the east (and therefore most susceptible to ice growth), no ice has built up there. This is because the east has substantially less precipitation than the west, assuming broadly similar prevailing winds from the Atlantic rather than from the east, and a more continental climate, which results in a higher equilibrium line altitude. The north is climatically most susceptible to ice sheet growth but topographically is less suited with

lower, more peaked, dispersed mountains. The west is climatically and topographically suitable for ice sheet growth.

The results appear to confirm that ice sheet initiation is a function of the balance between the climatic and topographic susceptibility of a particular region. In this example, the west is the most favourable region and the east is the least favourable.

It is important to recognise the assumptions which underpin this work and to examine other possibilities. The sea-level precipitation for each region is assigned before the model run and the precipitation pattern across Scotland is assumed to be broadly similar to the present day. Thus, the west has almost twice the precipitation of the east. It has been suggested that the prevailing winds during the Loch Lomond stadial were from the south west (Sissons,1981; Payne & Sugden,1990) which would lead to a reduction in precipitation in the north; the model would therefore over-predict the volume of ice in the northern region. In common with the work of Payne & Sugden (1990), a comparison of the model results with the field evidence of the extent of the Loch Lomond glaciation (Sissons,1981) suggests that this may well be the case.

Figure 5. Ice sheet growth in Scotland for a 7°C temperature drop and a 50% reduction in precipitation. The captions are taken every 400 years. Ice grows in the west and north but not in the east, despite high plateaux mountains.

CONCLUSIONS

1. Insolation variations cannot initiate maritime ice sheets directly although in mountainous areas of maritime regions glaciers may form.

2. Changes in ocean temperature affects the delicate balance between precipitation and mean annual temperatures and drive maritime ice sheet growth. Increased continentality leads to an increased annual temperature range and lowers susceptibility to ice sheet growth. Reduced precipitation with distance from prevailing oceanic winds emphasises this climatic gradient.

3. Changes in the net balance gradient at the equilibrium line affect the rate of ice sheet growth, and are determined by the relative values of precipitation and mean annual temperature.

4. The configuration and altitude of the upland topography determines the point of initiation and the threshold between stable upland glaciers and the growth of an ice sheet.

5. In the case of Britain, ice sheets appear to be triggered by the southward movement of the North Atlantic polar front. This would lead to cooler temperatures with, initially, enhanced precipitation as the belt of maximum precipitation migrated south with the oceanic front. Further southward movement would continue to reduce the temperature but the precipitation would decrease, raising the spectre of precipitation starvation in the far north. Thus the initiation and evolution of the British ice sheets appears to depend on the extent of the movement of the oceanic and atmospheric fronts. Abrupt changes in ocean circulation, as postulated for the Younger Dryas cooling, would lead to the apparent truncated glaciation, and abrupt changes between glacial and interglacial conditions.

CHAPTER FIVE:
TOPOGRAPHY EXPERIMENTS

TOPOGRAPHY, CLIMATE AND ICE MASSES: A REVIEW

Summary

Topography acts as a filter between regional climate and the consequent response of a glacier or ice sheet. It influences the mass and energy inputs and modifies the ice dynamics. The evolution of the ice sheet surface and, over longer time scales, of the bed topography modulates the climatic forcing.

Until we have a better understanding of these topographic linkages, the use of geophysical signals from former ice masses to determine palaeoclimates must be regarded as fundamentally flawed.

INTRODUCTION

The aim of this paper is to review the role of topography on the relationship between climate and ice volume. Topography plays a fundamental role because it acts as a filter between the regional climate and the response of the glacier or ice sheet. This response ultimately yields a geological or geophysical signal which is then used inversely to obtain information about regional palaeoclimates. The topographic filter encompasses a number of complex linkages which act both externally to the system, through localised variations in energy and mass input, and internally, by modifying ice flow dynamics (figure1).

Theoretical and observational studies of glaciers and ice sheets have been performed for many years and are often concerned with the relationship between climatic change and ice sheet evolution, especially with regard to the Pleistocene ice ages. This relationship is highly complex and an understanding requires delineating the important processes at different spatial and temporal scales. Topography is one aspect of this relationship but it underlies a number of related factors including isostasy, the relative position of the land surface to sea level, and eustasy, a change in sea level; both of which have been studied in detail with relation to glacial cycles.

Ice masses are arbitrarily classified in this paper by distinguishing the way ice interacts with the underlying topography: first, mountain glaciers and ice caps which are constrained by topography and depend on the effect of bed topography on regional climate for their mass and energy balances; and second, ice sheets which largely submerge the underlying topography and are less constrained by it except at the margins.

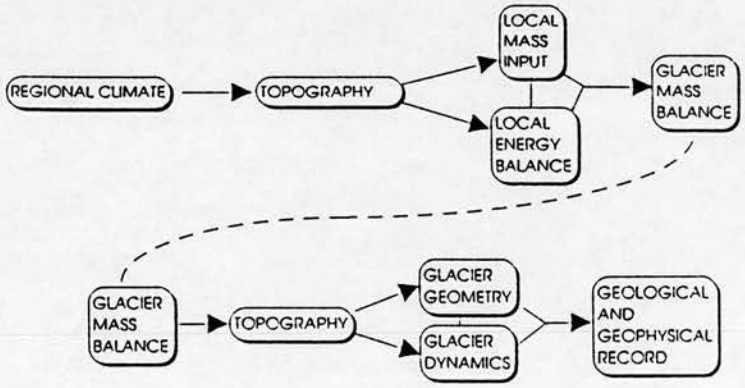

Figure 1. Topographic linkage between regional climate, glacial response, and the geophysical record. Figure taken from Furbish and Andrews (1984).

TOPOGRAPHY AND GLACIERS

Bed topography plays a rather more dominant role on valley glaciers and mountain ice caps than it does on large ice sheets since the former are dependent on the surrounding topography for their existence. At large scales it is the altitude and morphology of the mountains that determines both the potential size of the glaciers and ice caps, and the glacial mass balance, which is the balance between the supply (accumulation) and loss (ablation) of ice. In addition, the geometry of the bedrock affects the motion of the glacier.

i) Topography and Climate

Large scale topography such as a mountain range acts in two distinct ways to influence glaciers: first, the energy and mass inputs to the glacial system depend on how the regional climate interacts with the surface topography. Second, the morphology of the topography defines the geometrical limits of a glacier.

The regional climate is dependent on geographical variables such as latitude, altitude, and continentality (the distance from an ocean to windward), which determine the energy and precipitation received in any one area. The interaction between regional climate and mountains is complicated by the localised nature of the mass and energy exchange between the atmosphere and the surface, with its variable altitude, relief, and aspect. One of the primary difficulties in delineating this problem has been the lack of systematic data in mountainous regions (with the notable exception of certain Alpine and Scandinavian records). Barry (1981) provides a summary of the physics involved as an atmospheric flow crosses mountains.

The relationship between glaciers and climate is primarily determined by two parameters. The equilibrium line is the boundary between the accumulation area, where there is a net gain of mass over the year, and the ablation area, where there is a net loss. The accumulation area encompasses both areas of permanent snow cover and superimposed ice, where snow melts and refreezes. In temperate glaciers, the superimposed ice zone is insignificant and the climatic snowline is approximately equivalent to the glacial equilibrium line. The altitudinal mass balance profile is the amount of snow accumulated or ablated over one year at different altitudes (figure 2). This latter parameter is more useful for determining the climatic setting and hence the glacial response to a climatic change.

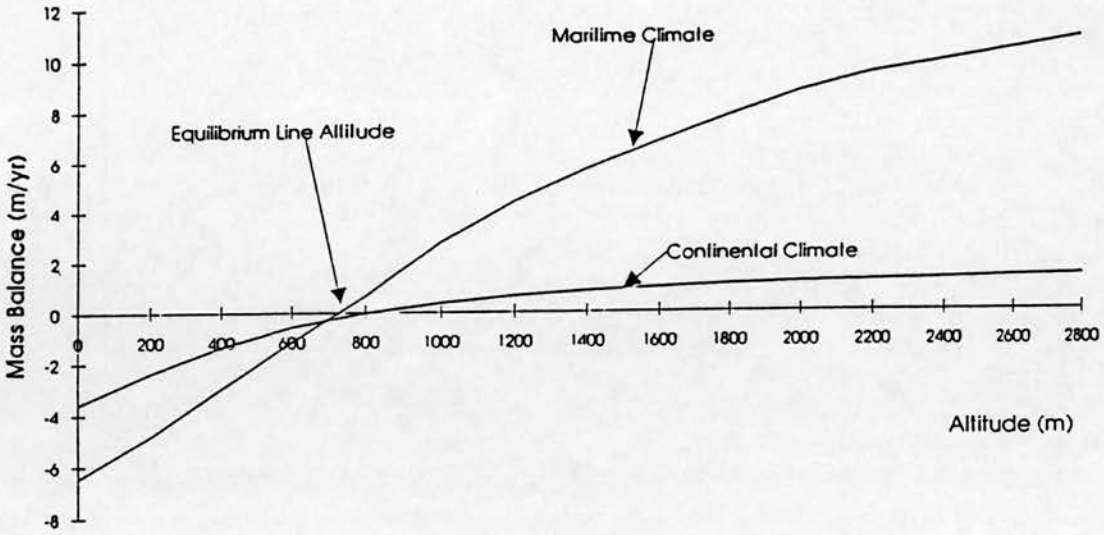

Figure 2. Glacial mass balance profile showing the contrast between maritime and continental environments. Although the equilibrium line altitudes are similar, the maritime climate has a much steeper balance gradient because of the higher values of accumulation and ablation. Hence, there is a much faster throughput of ice which results in glacier termini reaching lower elevations before melting.

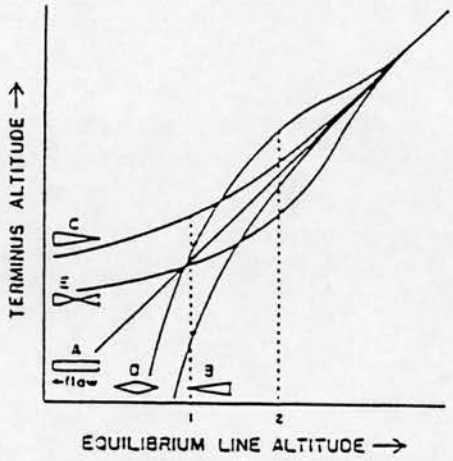

Figure 3. Relationship between the glacier terminus altitude (TA) and the equilibrium line altitude (ELA) for five glaciers, A-E, of different idealised shapes. Changing the ELA modifies the area of accumulation and ablation, and hence the response of the terminus. For ELA position 1, the terminus altiude of B<A≈D≈E<C; for position 2, E<B<A<C<D. Figure taken from Furbish and Andrews (1984).

Ahlmann (1948) noted the importance of the mass balance profile (and its altitudinal gradient) on glacial response while Schytt (1967) related the ablation gradient to climatic variables. The seminal work on the subject was the analytical formulation of the sensitivity of the mass balance profile to climatic variables (Kuhn 1979,1981,1984,1989). The factors contributing to the energy and mass budgets, such as the radiation budget, temperature, precipitation, and turbulent fluxes, have contrasting sensitivities depending on the climatic regime. Snow accumulation, especially in summer, plays a decisive role in maritime climates while the length of the ablation season is important in polar areas. In dry, continental regions the mass balance profile is sensitive to albedo changes close to the equilibrium line, and in alpine regions climate sensitivity is less dependent on altitude.

This work indicates that common assumptions concerning the conservation of mass balance gradients under climatic change (eg. Lliboutry, 1974) are doubtful. Further work (Oerlemans and Hoogendoorn, 1989; Oerlemans, 1990) concurs and has led to a refining of the formulation and sensitivity of climatic variables; for example, by incorporating precipitation into a surface energy balance model.

The problems associated with measuring a glaciers mass balance profile led to work on the statistical correlation between this and other parameters which are more easily measured, such as the equilibrium line altitude (Braithwaite, 1984). However, it was concluded that accurate calculations were impossible without further climatic information. Similarly, observations of glacier mass balance and meterological data (Letreguilly, 1988; Letreguilly and Reynaud, 1989) indicate the problems involved in statistical correlation.

The two overriding conclusions are, first, that the sensitivity of glacial mass balance depends on the prevailing climatic regime. Pelto et al. (1990) noted that the climatic regime will change over a glacial cycle and hence so will the sensitivity of the glacial mass balance. Second, the climatic sensitivity of glacial mass balance must be distinguished from the variation in glacial extent. Observational evidence (Hoinkes, 1968; Reynaud et al., 1984) and theory agree that mass balance profiles are useful indicators of climatic change but that glacial extent is not because glacial fluctuations depend on the surrounding topography. The high frequency atmospheric forcing is filtered by the glacier. Any attempt to invert this signal to obtain specific climatic variables such as temperature or precipitation from fluctuations of glacial extent is fundamentally flawed.

The broad theoretical understanding of the response of a glacier to climate was developed by Nye (1960,1961,1963a, 1963b,1965a,1965b) and neatly summarised by

Paterson (1981). A glacier responds to a perturbation in mass balance by the propagation of diffusive kinematic waves down the glacier to re-establish a steady state ice volume and length. Strictly speaking the theory is only valid for temperate glaciers on simple bed topography since the consequent effect of complex topography or a temperature change on ice flow is ignored. The perturbations from steady state are also assumed to be small. More recently, Johannesson et al. (1989a, 1989b) have adapted Nye's work and used the geometric similarity of glacial profiles to show more robust estimates of the time for a glacier or ice cap to respond to climatic change: of the order of tens of years for valley glaciers.

The second effect of large scale topography is to delimit the potential size of glaciers and ice caps for a specified climate. It is intuitively obvious that glacial extent depends on the morphology of the bedrock topography. This was articulated by Manley (1955) who estimated the relative importance of the breadth and height of a mountain summit in determining whether it could carry a glacier for a specified equilibrium line altitude. For example, an alpine aiguille may never carry a glacier because it is too steep while a mountain plateau, such as those found in the Cairngorms in Scotland, can potentially carry a glacier if the equilibrium line is just below the summit. Conversely, plateaux surfaces are poor accumulators of snow in windy conditions. The wind blown snow accumulates in bedrock depressions or in the lee of the plateau where cirques develop. The reliance of these cirque glaciers on wind blown snow and cornice avalanches for their nourishment means they can exist well below the regional equilibrium line.

These local climatic and morphological effects ensure there is no simple way of obtaining regional equilibrium lines, and hence a measure of climate, from observations of glacial extent (eg.Andrews et al.,1970). This has serious implications for an understanding of regional climate in remote areas and more especially for reconstructing palaeoclimates. Various approximations of the glacial level have been used such as defining the glaciation level as being between the lowest suitable mountain carrying a glacier and the highest suitable mountain without one. Ahlmann (1937) applied this idea to Vatnajökull while Østrem (1966) extended it to calculate the glaciation level in British Columbia.

Palaeoclimatic studies use a variety of methods to estimate former equilibrium line altitudes by means of geometrical arguments. For example, it is possible to use a shape ratio since there is approximately one third of a glacier in the ablation zone and two thirds

in the accumulation zone, so in theory the equilibrium line altitude can be estimated for a steady state glacier from geological records. Meierding (1982) assessed six methods for inferring equilibrium lines and concluded that the shape ratio had the smallest statistical mean error of 80 metres for current glaciers in the Colorado Front mountain range. However, this type of areal relationship does not appear to hold uniformly for glaciers in widely differing climates. As Williams (1975) points out, the estimation of climatic deterioration from terminal moraines or small cirques assumes certain climatic factors, such as the altitudinal temperature lapse rate (which is highly variable (Harding, 1978)), remains invariant even though the climate has changed dramatically.

Furbish and Andrews (1984) used topographic hypsometry (area-height profile) to examine the long term stability and response of glaciers to changes in mass balance. They derive a simple equation relating the mass balance and hypsometry of a glacier to the glacial response to climate change and show that the amplitude of glacier response is dependent on valley geometry (figure 3). This is taken a step further by Oerlemans (1989) who used a numerical model to examine the response of a glacier to changing climatic conditions on different topographies. There are three important conclusions: first, the longitudinal bed profile is very important. Beds with smaller slopes are more sensitive to climatic change since a change in the (near horizontal) equilibrium line affects a larger part of the glacier (figure 4), but glaciers with small bed slopes react more slowly to climatic change; a consequence of the smaller mass throughput of these glaciers. Second, the presence of reverse slopes leads to the possibility of multiple steady states for a specific range of climate. The actual ice volume depends on the history of mass balance fluctuations (Letreguilly and Oerlemans, 1990). Finally, the mass balance gradient on long valley glaciers is partly determined by along valley changes in width and albedo. These latter factors link topography, climate, and glacial dynamics.

ii) Topography and Glacial Dynamics

Climatic forcing of glaciers depends on the interaction with regional topography and the areal extent of the glaciers. This depends on the morphology of the topography and ice dynamics, which comprises two parts: ice deformation and basal sliding (figure 5). Both are strongly determined by the underlying topography.

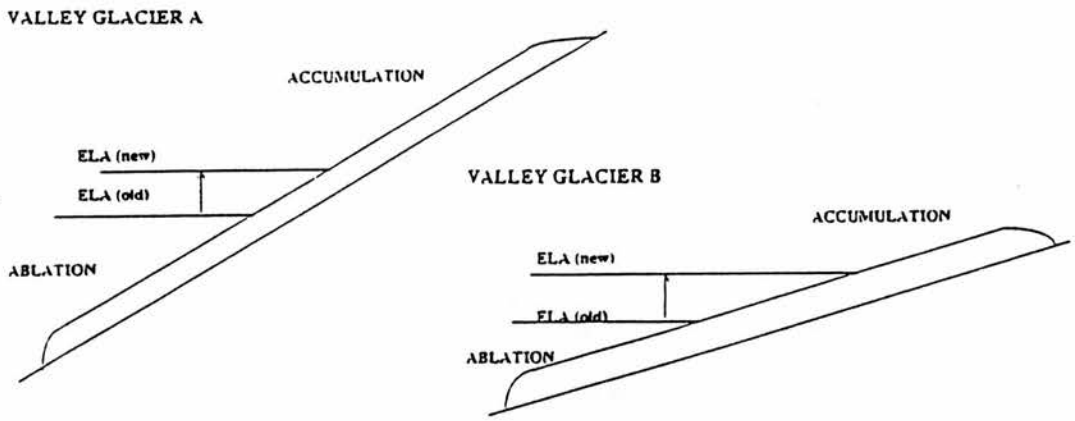

Figure 4. A sketch of two glaciers which respond differently to an identical change in the equilibrium line altitude because of their differing bed slopes. The accumulation/ ablation ratio of Glacier A is less affected than glacier B by the change in equilibrium line altitude, so glacier A will have a smaller response to the climatic change.

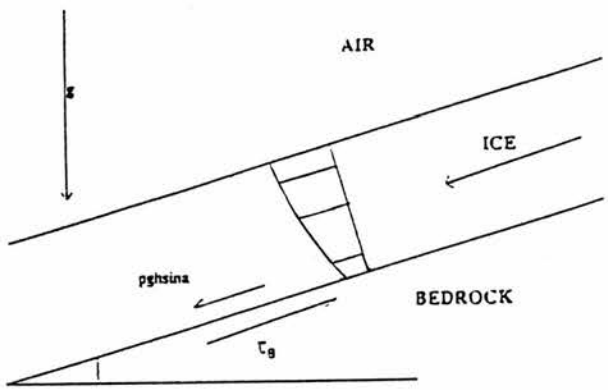

Figure 5 shows the motion of a glacier, which is a combination of ice deforming under its own weight and sliding over the bed. Ice deformation is mainly determined by ice surface slope.

Topography affects ice deformation in a glacier by altering the stresses acting on the ice mass. The fundamental problem has been to derive a complete set of equations which describe deforming ice under known mechanical laws and complex boundary conditions. Polycrystalline ice deforms plastically and this understanding (Orowan,1949;Nye,1951) and subsequent work (Glen,1955;Nye,1957) showed that the relationship between the effective strain rate, $\dot{e}$, and the effective stress, t, was non-linear and had the form:

$$\dot{e} = A.\tau^n$$

over the range of stresses usually found in a glacier. Different values of n and A have been found in various studies; n is usually taken to be 3 while A is temperature dependent. Using the generalised flow law analytical solutions of the equilibrium profiles of glaciers and ice sheets become possible under certain simplifying assumptions (Nye,1952;Vialov,1958). The ice is assumed to deform under its own weight in simple shear and the basal shear is found to be mainly determined by ice surface slope:

$$\tau_b = \rho.g.h.\sin\alpha$$

where α is the surface slope, and h is the ice thickness.

Glacial flow is affected by valley walls and by bedrock irregularities. The former effect can be approximately taken into account by multiplying by a shape factor, F, which depends on the valley half width and ice thickness (Nye,1965c). A more recent analysis suggests F has a simple physical interpretation and that it varies as the glacial profile approaches steady state (Johannesson et al.,1989b). The latter effect requires additional correction terms to the basal shear equation and these depend on the scale over which calculations are averaged. At small scales all terms must be taken into account while at large scales, perhaps twenty times the ice thickness, the correction terms can be ignored. Observationally it is very difficult to verify the basal stress approximation because accurate surface velocity measurements are required but Bindschadler et al. (1977) found on Variegated Glacier, Alaska, that the correction terms could be ignored if the surface slope was averaged over long enough length scales. It may be that, in general, the large scale longitudinal slope is the important factor for longitudinal stresses (Budd,1970b).

The second process which affects ice extent is basal sliding but the formulation of a generally applicable sliding law has proved beyond mathematical analysis. There are three potential mechanisms for basal sliding in temperate glaciers. The first is regelation

which occurs when ice melts in high pressure areas upstream of obstacles and refreezes downstream, with the concurrent transfer of latent heat upstream through the obstacle forcing ice melting. The second process involves enhanced creep caused by additional stresses induced by the obstacle which leads to ice preferentially moving over and around obstacles. The former process operates over small obstacles while the latter occurs over larger bedrock irregularities (Weertman,1957). Lliboutry (1968) suggested a third important process, that of sliding over water and air filled cavities between the ice and bedrock, since there is less friction in these areas.

The mathematical formulation of this problem is extremely complex and has been tackled, not altogether successfully, in a number of different ways. Kamb (1970) and Nye (1969) generalised the Weertman ideas for variable bedrock roughness by statistically calculating the bed roughness using Fourier methods and assuming no cavitation. Morland (1976) extended this to include gravity by using a sloping bed while Lliboutry (1976,1987) continued on the problem of cavitation by extending the concept of effective pressure: the difference between the downward pressure of ice and upward pressure of basal water. This could explain seasonal variations in sliding velocity through fluctuations in melt water. The problem was reformulated into two parts by Fowler (1981,1987): the flow in the basal boundary layer and the flow in the bulk of the glacier. This work again emphasised the importance of bedrock topography on the sliding law.

However, this work generally failed to deal with the effects of factors such as rock debris in the basal layers which increases friction (Boulton,1974; Hallet,1981; Schweizer and Iken,1992), or the possibility of glaciers moving over deformable sediments as postulated for the southern areas of Pleistocene ice sheets (Boulton and Jones,1979).

A generally applicable sliding law is still not in sight so current mathematical models use crude relations postulated years ago between basal stress, sliding velocity and overburden pressure. The justification is that the glacier or ice sheet evolution appears less sensitive to basal sliding relations than to variations in mass balance. In any case, the bed geometry in models is usually too simplified to justify more complex derivations.

TOPOGRAPHY AND ICE SHEETS

Ice sheets submerge underlying topography and it is the evolving ice surface which interacts with the climate. Ice flow is less affected than in glaciers but bed topography becomes increasingly important at ice sheet margins.

i) Topography and Climate

The main interest in the relationship between ice surface topography and climate concerns the extent and stability of the ice sheet, and the modification of the regional climate by the evolving ice sheet.

Early investigations into the effect of climate were based on analytical work of ice flow in steady state ice sheets; in other words, the mass input to the ice sheet is just balanced by ice flow. In this instance, the height of the ice sheet is only nominally dependent on the absolute values of accumulation and ablation. In the theoretical case of plastic ice the ice sheet height depends only on ice sheet extent which depends on the geographical slope of the equilibrium line and regional topography. Similarly, the position of ice divides and centres is poorly dependent on the variation of accumulation over the ice sheet (Weertman,1973).

The effect of a climate change is to grow or decay an ice sheet. Weertman (1964) used a dynamic model to examine the time required for this change in ice volume assuming plastic ice and simplifying assumptions concerning the equilibrium line. There is an asymmetry in the time for growth and decay because of the discrepancy between accumulation rates and the larger ablation rates. Derivations by Hindmarsh (1990) re-emphasised the importance of the accumulation/ablation ratio (not the absolute rates) and the slope of the equilibrium line on the ice sheet profile.

Bodvarsson (1955) was the first to consider the stability of ice sheets in relation to climate and showed that if the equilibrium line is horizontal a steady state ice sheet is unstable. If the ice sheet grows the accumulation/ablation area ratio increases over the ice sheet leading to continued growth. Similar arguments apply to ablation when the ice sheet shrinks. This point was addressed mathematically by Weertman (1961) who found a series of stable and unstable states, such that a critical size of ice cap existed which, when exceeded, could allow unstable growth.

To examine the role of more complex boundary conditions, such as time dependent mass balance or bed topography, numerical methods are required. The

increasing power and sophistication of computers has led to rash of models for different applications but they are broadly of two types: a two or three dimensional model incorporating the continuity equation of ice, where the change in ice height is a function of the mass balance and the divergence of flow, and simplified relations are used for ice flow and sliding, such as the Mahaffy (1976) model; or a one dimensional flow line model which can incorporate more complex bed topography and stress relations.

Later models improved the mathematical formulation of ice flow and environmental interactions (eg.Budd and Smith,1981) but too often still relied on poor parameterisation of bed topography or naive formulations for climate; typically the Milankovitch variations of insolation were directly linked to the north-south movement of the equilibrium line. Concurrently, the formulation of equilibrium energy balance models for heat fluxes between latitude zones (North et al.,1981) and at the ice surface were improved to give a more reasonable coupling of the climate to an evolving ice sheet.

Unfortunately, these models rely on broad simplifying assumptions and empirically derived parameters such that a rough simulation of glacial growth and decay in a particular region may provide less insight into the physical processes involved than into the limitations of the model (Saltzman,1985); often there is a lack of data to test the model at different periods of ice sheet evolution (Porter,1989).

More positively, quantitative results of important feedbacks within the climate-ice sheet system have been identified. One such process related to the ice sheet profile is the mass balance-altitude feedback. The atmosphere is characterised by high vertical gradients of climatic variables which favour ice sheet growth at higher altitudes. Ice sheet growth leads to a rising ice surface, and to increased mass input, and hence to more growth, until limited by factors such as coastlines or precipitation starvation which occurs in the cold, high altitude air (figure 6). This feedback was articulated by Oerlemans (1980) and found to be more important than the albedo-temperature feedback originally postulated by Budyko (1969) and Sellers (1969).

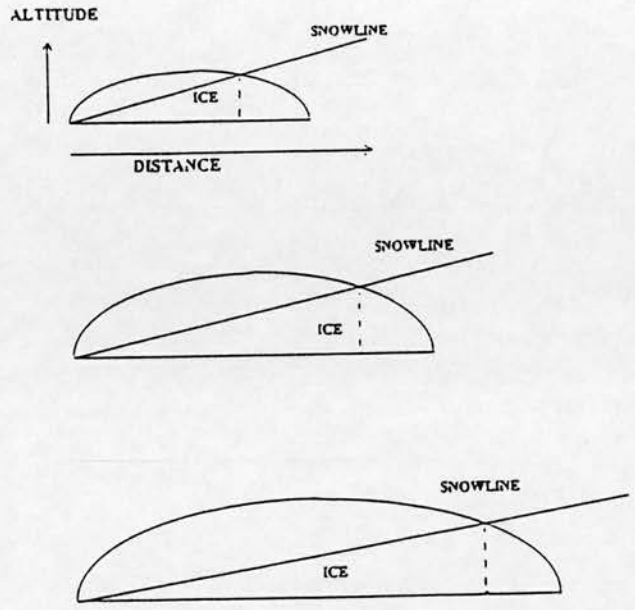

Figure 6. A schematic illustration of the height - mass balance feedback. A small modification of the snowline causes a dramatic change in ice sheet extent because of the effect of the increasing ice sheet surface elevation on the accumulation/ablation ratio.

A major complication of the climate-ice sheet interaction is the modification of regional climate by the ice sheet. Small ice caps can have a dramatically different surface energy balance from surrounding land by virtue of increased cloudiness and a larger albedo (Bradley and Serreze,1987). Large ice sheets can influence planetary atmospheric circulation and consequently affect precipitation patterns to leeward. Experiments by Cook (1990) indicate the Laurentide ice sheet could also have affected North Atlantic sea surface temperatures. These effects have a bearing on the evolution of ice sheets in Europe though dating techniques are insufficiently accurate to test hypotheses concerning phase lags between major ice sheets.

The climate-ice sheet interaction leads to questions on the stability of ice sheets: the Milankovitch insolation variations appear too small to account for the apparent ice volume changes during the Pleistocene. We require instabilities within the system for ice caps to grow beyond a critical size and decouple themselves from the regional

topography and climate. The increasing surface height and the modification of regional climate by an ice sheet may provide part of the answer.

Oerlemans and van der Veen (1984) and Hindmarsh (1990) both note the existence of fold catastrophes in the climate-ice sheet system due to the coupled effect of a dropping equilibrium line and a rising ice surface. Examples include the transition from valley glaciers to ice sheets, medium scale topography (Payne and Sugden,1990), and the coalescence of ice sheet domes. The catastrophic jumps at these topographic thresholds occur as the system moves to more stable states (figure 7). Although in theory the topographic thresholds can be calculated, the time lags within the system mean the glacial response to climatic forcing is unpredictable at these points.

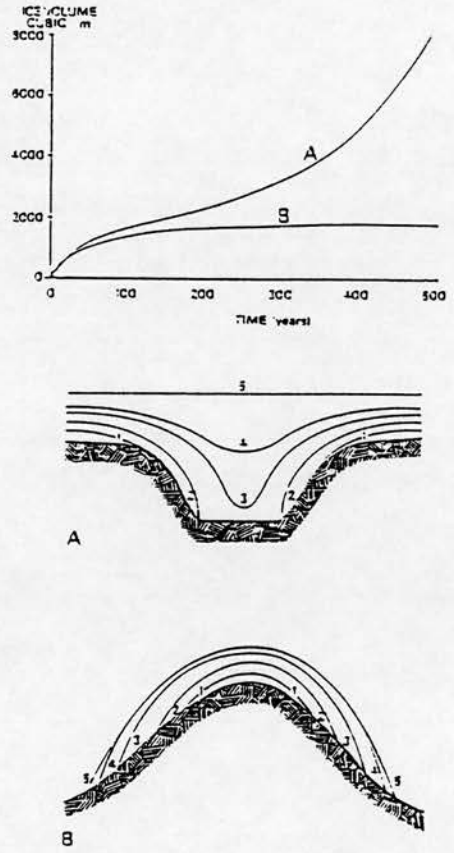

Figure 7. A lowering of the equilibrium line altitude results in a very different history of ice growth (denoted by stages 1-5) on A and B. After stage 2 there is an explosive increase of ice volume at A because of the rising ice surface while B approaches a steady state. Figure adapted from Payne and Sugden (1990).

ii) Topography and Glacial Dynamics

Ice flow in ice sheets is comparatively unaffected by bed topography except at the margins. The ice sheet surface can be approximated with analytical solutions of equilibrium profiles, where ice is assumed to deform under its own weight. Weertman (1961) showed that in small ice caps longitudinal stresses modified the equilibrium profile by flattening the ice divide but they were negligible in large ice sheets.

Although these theoretical profiles broadly represent the large scale features of an ice sheet surface, observational discrepancies became apparent (Robinson, 1966). Robin (1967) pointed out that Nye's approximation of basal shear stress to ice surface slope was not sensitive locally because of longitudinal stresses resulting from ice movement over varying bottom topography, and there began a long series of attempts to derive correction terms for the resulting effects. Collins (1968) mathematically justified certain assumptions used by Robin (1967) and was followed by a series of theoretical analyses (Nye,1969; Budd, 1970a, 1970b, 1971) to explain the waves apparent on the ice surface. Budd (1970b) concluded that particular bedrock wavelengths were damped differentially, with wavelength undulations of approximately 3.3 times the ice thickness preferentially transmitted to the surface. This appeared to be confirmed by observations (Budd and Carter,1971) and later analysis (Hutter et al.,1981) agreed that a distinct wavelength may exist while questioning some of the assumptions used in the analysis.

More recent work has entailed using more sophisticated mathematical techniques (Hutter et al.,1981; Hutter,1983; Morland and Johnson,1982), or extensions of previous theory (Whillans and Johnsen,1983) to demonstrate the importance of longitudinal stress gradients on basal shear stress over various scales of longitudinal averaging. Kamb and Echelmeyer (1986) and related papers develop a simple general formulation to describe how ice thickness and bed mass translate into a particular pattern of longitudinal flow.

Unfortunately these ideas invariably involve simplifying assumptions which may invalidate some of the conclusions. For example, Hutter et al. (1981) assume the ice and bed surface are approximately parallel, while Kamb and Echelmeyer (1986) linearize the longitudinal variations of ice flow. In addition, most previous work required that basal boundary conditions were known, or could be fitted to the theoretical surface values for the solution. An alternative approach was adopted by Van der Veen and Whillans (1989a, 1989b) and Whillans et al. (1989) who calculated the inverse (and more practical) result of deriving stress and strain rates at depth from surface measurements, and tested the theory on Byrd Glacier, Antarctica in 2- and 3- dimensions. The results reiterate the

importance of longitudinal stresses on ice flow variation close to ice sheet margins. It may be that this inverse approach leads to a more general understanding of the relevant stresses which contribute to variations in ice flow over complex bedrock terrain.

While bed topography does not predominantly affect ice flow in ice sheets, on smaller scales and in areas where the magnitude of bed topography waves approaches the ice depth it plays an increasingly important role. For example, marine ice sheets rest on land that is generally below sea level, and the transition from ice sheet to ice shelf at the grounding line is very sensitive to bedrock topography (Thomas,1979). The grounding line limits the ice sheet size and in retreat can theoretically destabilise an ice sheet though recent fears concerning the West Antarctic ice sheet appear unfounded at present (Van der Veen,1985). The transition from ice sheet to ice stream flow is also abrupt and occurs at a step in the subglacial topography, with rapid ice flow through subglacial topography leading to characteristic over-deepened troughs (McIntyre,1985). There is also geological evidence that the southern ice lobes of the former Scandinavian ice sheet were topographically controlled (Punkari,1980). Furthermore, ice berg calving glaciers are found to be partially decoupled from the regional climate by local topography. The glacier may be pinned before a deepening expanse of water or it may advance on its own terminal moraine across deep water. This leads to glacial oscillations which bear no resemblance to climatic trends (Warren,1992).

LONG TERM TOPOGRAPHIC EVOLUTION

Over the time scales of glacial cycles topographic evolution modifies the climatic forcing of ice sheets. For example, the time lagged effect of isostasy can partially explain the saw-tooth shape observed in proxy data of ice volume while eustastic sea level rises can destabilise marine ice sheets (Payne et al.,1989; Huybrechts,1990). Both processes are extensively reviewed elsewhere. On longer time scales tectonic uplift may have initiated the late Cenozoic cooling which led to the growth of continental ice sheets. Raymo and Ruddiman (1992) review these ideas and conclude that the uplift of the Tibetan plateau is crucial to explain observed climatic change while acknowledging that a better understanding of the linkages between uplift, weathering and climate is required. A complementary argument is put forward by Molnar and England (1990) who hypothesise that climatic change contribute to tectonic uplift. This seemingly surprising result is

obtained by considering the climatically forced high denudation rates of mountain ranges which leads to compensatory isostatic uplift; although the mean elevation drops the peak elevation increase. They argue that the inferred acceleration of late Cenozoic uplift can equally be explained by climatic change. It is widely acknowledged (Chalikov and Verbitsky,1990;Birchfield et al.,1982;Abe-Ouchi and Blatter,1992) that a necessary but not sufficient requirement for the inception of the ice ages is large uplifted regions at high latitudes. The weakness in their argument revolves around the erosive power of glaciers required to move sufficient material from the mountains and transport it long distances.

The erosion of bed topography is poorly understood, depending as it does on regional geology, preglacial elevations and the basal thermal regime of ice. Mazo (1989) developed a model of the eroding glacier and the eroded bed which indicates that a specific erosive scale preferentially develops into the morphological form of the cirque bed profile while Harbor et al. (1988) derive a more comprehensive model of landform development. However further work is required to understand the development of glacially eroded landscapes under changing climatic conditions.

CONCLUSION

The fundamental effect of topography is to decouple the response of a glacier or an ice sheet from the climate. It influences the mass and energy inputs to glaciers and modifies the ice dynamics. Ice sheets are less constrained by bed topography but by nature have a finite width, and at the margin topography influences outlet glaciers and ice streams. The evolving ice sheet profile is crucial in determining the interaction with the climate.

Bed topography also evolves over long time scales. It is driven by regional tectonics, isostasy, eustasy and erosion, and this evolution affects the climatic forcing. Topography must be considered a dynamic variable in the earths climate system if we are to understand long term climatic trends.

Examples of fold catastrophes appear to be very common in the ice sheet system and the unstable jumps of ice volume to more stable states puts fundamental limits on the predictability of ice sheet evolution.

In this context, the use of geological or geophysical signals from former glaciers or ice sheets to determine palaeoclimates must be regarded as fundamentally flawed. In essence we require a measure of the effect that an arbitrary topography has on the response of an ice mass to an arbitrary climatic change. To determine this measure future work requires an interdisciplinary approach that encompasses glaciologists, geomorphologists, and climatologists to examine the complex linkages between the evolution of topography, climate, and ice sheets.

THE GLACIER - ICE SHEET TRANSITION

Introduction

This paper examines the critical transition from stable mountain glaciers to ice sheets by assessing the consequence of climatic forcing over different bedrock slopes. The explosive growth of ice observed in figure 4 (paper II) resulting from a small change in the climatic forcing appears to be a function of the topography. Topography is poorly resolved in the ice sheet model so there is little appreciation of the factors responsible for this sudden growth in ice volume. Further investigation is warranted to determine whether such behaviour is a function of the model's construction or is inherent in the real world. This is accomplished by linking highly simplified models of the climate and ice sheet dynamics and performing sensitivity experiments of climatic forcing over simplified yet different topographic configurations. Since simple models appear to produce qualitatively similar results to more complex models (Oerlemans,1981) they are preferable to the more detailed models of climate and ice sheets derived earlier in the thesis for two reasons. First, an examination of one facet of a complex coupled system, such as that of topography, climate and ice, is best achieved by simplifying the components which are not directly related to the investigation. Second, the assumptions used to derive the ice sheet model are not necessarily applicable on the topography used in this section.

THE TOPOGRAPHY MODEL

The topography model is based on four assumptions. First, the climate forcing can be represented by a mass balance profile which consists of linear accumulation and ablation gradients about a horizontal equilibrium line. The presence of a horizontal equilibrium line means that stable glaciers are only possible when there are mountains (Bodvarsson,1955; Oerlemans,1981). A climatic change is assumed to raise or lower the equilibrium line altitude but leave the ablation and accumulation gradients unchanged. Sensitivity experiments with the full climate model indicate that this is equivalent to a change in the mean annual temperature rather than annual precipitation, which modifies the mass balance gradient.

Second, ice deforms as a perfectly plastic substance. This assumption has been widely used as a means of simplifying ice mechanics and reconstructing ice surfaces (Denton and Hughes,1981), and implies that there is a specific yield stress at which ice flows. Motion in a parallel sided slab of ice is assumed to occur only by deformation caused by the weight of the ice, and this is balanced by the shear stress at the base, τ_b:

$$\tau_b = \rho g h \sin\alpha \qquad (5.1)$$

where ρ is the ice density (assumed constant), g is the acceleration due to gravity, h is the ice thickness, and α is the ice surface slope which is parallel to the bedrock slope. The basal shear stress has been calculated for a range of glaciers and found to be between 50 and 150 kilopascals (kPa). By assuming a mean value of 100 kPa for the yield stress, τ_o, the ice thickness can be calculated from the bedrock slope (Paterson,1981). The assumption that the ice surface is parallel to the bedrock can be relaxed for small slopes and it is found that the basal shear stress is still dependent on the ice surface slope. This latter approximation is used when the bedrock is horizontal. The assumptions used in deriving these approximations break down when the slopes are large, such as near the margin, but the discrepancies are negligible for the purposes of this work. Orowan (1949) showed that perfectly plastic ice in equilibrium has a maximum ice thickness, H, of:

$$H = \sqrt{(2\tau_o L/\rho g)} \qquad (5.2)$$

where L is the length of the glacier. Equivalently, the height, h, along the parabolic profile of a glacier can be calculated using:

$$h^2 = (2\tau_o/\rho g)(L - x) \qquad (5.3)$$

where x is the distance from the centre to the margin (figure 5.1).

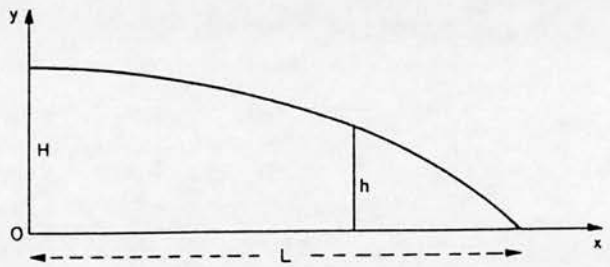

Figure 5.1 The equilibrium profile of an ice sheet.

The third assumption in the model is that glaciers retain their geometrical profile while advancing or retreating under the influence of a small climatic change. Hindmarsh (1990) and Jóhannesson et al. (1989b) have noted that the geometrical profiles of glaciers are relatively insensitive to fluctuations in the ice discharge, not only in steady state, but also in advance and retreat.

The fourth assumption is that the ice surface evolves to its equilibrium state instantaneously as the climate changes. This assumption avoids the requirement of building time into the model and simplifies it substantially. Time is only important in determining the length of time of each mass balance fluctuation since this influences the proximity of the glacier profile to its equilibrium form. By ignoring time we are saying that the climatic change is slow enough that the glacier is always close to its equilibrium size.

In the model the glacier always attains an equilibrium state so the length of the glacier is determined directly by the climate, or more specifically, by the need for the mass

accumulated over the surface of the glacier to be exactly balanced by the mass ablated over the glacier. The glacier conforms to the balance:

$$\zeta_a/\zeta_b = \Lambda\eta_b/\beta\eta_a \qquad (5.4)$$

where ζ is the mass balance gradient, Λ is the accumulation area, β is the ablation area, η is the altitudinally weighted depth of snow, and subscripts a and b refer to the accumulation and ablation areas respectively.

The derivation of this equation (Furbish and Andrews, 1984) requires that the accumulation and ablation gradients are linear. In reality, the most obvious departure from this assumption is around the equilibrium line though at this altitude the mass accumulated and ablated are at a minimum.

The formulation of the model reflects the need for simplicity in order to examine one facet of a complex, coupled system. The limitations stem from the associated simplifying assumptions. Perhaps the most important limitation involves coupling the climate to perfectly plastic ice. Morland and Johnson (1980,1982) argue that over long periods of time ice behaves as an incompressible, non-linearly viscous fluid. If this is so, and the balance gradient increases without an increase in the glacier's mass balance, equivalent to a simultaneous and comparable rotation of the accumulation and ablation gradients, then a larger shear stress is required to force the increased ice volume through the system, and the surface profile of the glacier steepens. However, in the model the flow of perfectly plastic ice adjusts itself to changes in the balance gradient without a change in the shear stress and the ice surface profile. Boulton et al. (1984) argue that coupling balance gradients to plastically deforming ice effectively decouples a highly coupled system which lies at the heart of climatically-forced ice sheet dynamics. The following experiments circumvent this problem by, firstly, assuming that a climatic change raises or lowers the equilibrium line but leaves the mass balance gradients unchanged, and secondly, assuming that the climatic change is sufficiently small for glaciers to retain their geometrical profile.

MODEL EXPERIMENTS

A formal test of the model against reality is difficult to perform because of the inherent simplifications. Hence the model should not be seen as a simulation of the real world but rather as an aid to understanding one particular problem; the transition from upland glaciers to an ice sheet. The manner in which the model demonstrates the non-linear nature of the changes in ice volume can perhaps be best illustrated by applying it to a trial slope and lowering the equilibrium line. An equilibrium line altitude (ELA) of 1000m yields a stable glacier with the characteristic parabolic profile in the upper half of the slope (figure 5.2a). Dropping the ELA to 900m results in a small response from the glacier terminus down the steep, central slope and little change in ice volume (figure 5.2b). A further drop in the ELA of 100m provides a sufficiently large accumulation area for the terminus to extend into the lowest plain and attain its equilibrium profile (figure 5.2c), thus leading to a substantial increase in ice volume.

However, the limitations of the model can be exemplified by applying it to complex topography, such as a series of truncated sine waves (figure 5.3). Once the ice sheet threshold has been crossed, the maximum ice volume is limited by the restrictions placed on ice dynamics rather than by the equilibrium line altitude or the model boundary. On flat surfaces, maximum ice height is totally determined by the length of the surface, so the infilling of valleys and subsequent submergence of bed topography by ice is not possible.

Sensitivity experiments were carried out, firstly, to assess different values of the yield stress, and secondly, to assess different topographic configurations. The value of the yield stress was varied from 50 to 150 kPa while the model was applied to the same bed topography. The effect of such a change is to modify the ice thickness and hence the ice volume for a given bed slope. However, the equilibrium line altitude at which the jumps occur are the same. Since the yield stress is a proxy parameter for the flow law multiplier and exponent, A and n, these results imply that the topographic thresholds are independent of the formulation of ice flow. However, using a model incorporating the flow law of ice, Oerlemans (1981) found there was a dependence but that it was rather weak.

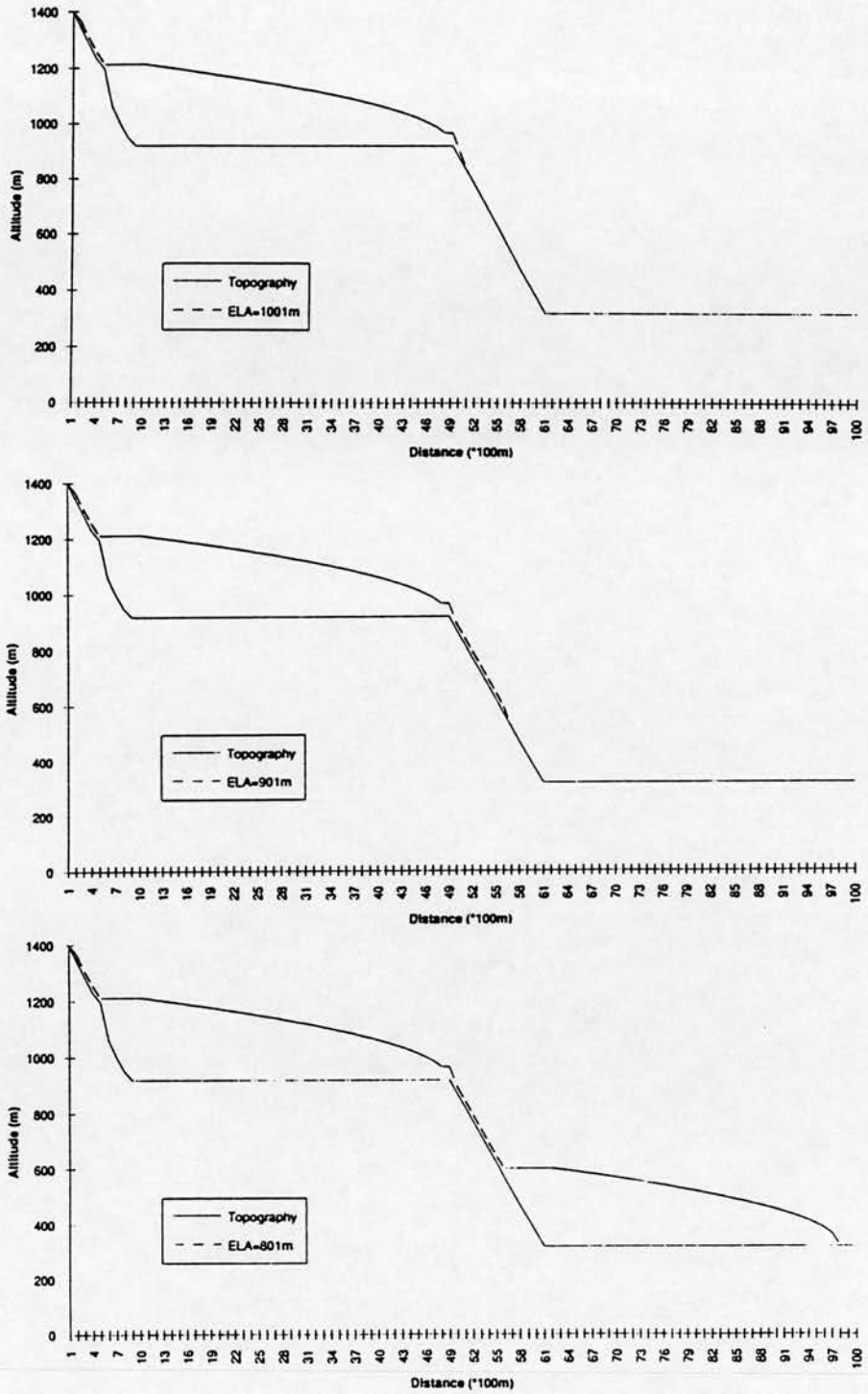

Figure 5.2 The result of lowering the equilibrium line altitude from (a) 1000m, to (b) 900m, and finally to (c) 800m. The response of the ice volume is non-linear.

The second set of sensitivity experiments was run with different bed topographies. The topographic configurations are truncated sine waves which are compressed or expanded in the flow line direction (figure 5.4). Hence each bed topography has a different slope and hypsometry (area - height ratio). The equilibrium line altitude was lowered until the glacier - ice sheet threshold was crossed, and ice grew to the model boundary, and then raised progressively until all the ice had disappeared. The model results are shown in figure 5.5. There are three points of interest; firstly, the maximum ice volume attained in each example, secondly, the difference in ice volume between lowering and raising the equilibrium line altitude, and thirdly, the altitude at which there is a jump in the ice volume.

Considering the first point, since plastic ice flow is assumed, the maximum ice height, and thus the ice volume, is set by the width of the ice sheet which is the same in each case. The maximum ice volume obtained over different topographies is therefore the difference between this maximum value and the volume occupied by the bedrock.

Characteristically, on lowering the equilibrium line altitude there is a threshold altitude at which the equilibrium ice volume jumps from a small value to the maximum value. On raising the equilibrium line altitude, the volume of ice reduces, though with a less pronounced or non-existent threshold. The respective changes in ice volume that occur on raising and lowering the equilibrium line altitude do not coincide: a hysteresis loop occurs.

Finally, the altitudes at which there is a jump in the ice volume depend on the relative positions of the equilibrium line altitude and the ice surface, which depends on the bedrock slope. The consequent hysteresis loop is caused by the different surface configurations in the case of a falling, and of a rising, equilibrium line altitude. In the latter case, ice is present and hence the surface topography is different. The climate 'sees' the top surface (ice + bedrock) as its boundary for mass exchange while the ice 'sees' the bedrock as the boundary for constraining ice thickness.

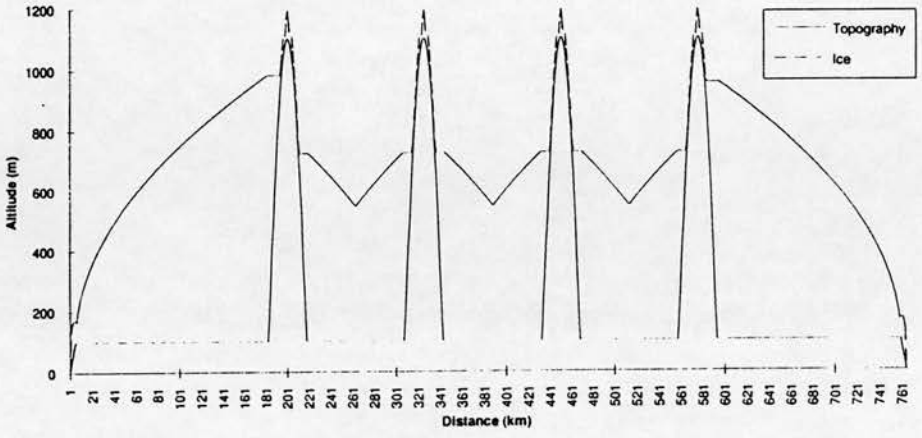

Figure 5.3 An example of bed topography which is too complex for the model.

INTERPRETATION

The nature of the hysteresis loop depends on the topography. This is best illustrated by looking at two extreme cases which are, firstly, an infinitely long flat surface, and secondly, an infinitely long regular slope (figure 5.7). In the flat case there is no ice until the equilibrium line reaches the surface whereupon there is unrestrained growth. On raising the equilibrium line above the old bed topography there is now a sufficiently high accumulation surface so ice volume is retained. In the second, sloping case, there is a unit increase in ice volume for a unit lowering in the equilibrium line; the actual volume will depend on the ice thickness, and thus on the steepness of the bedrock. If the equilibrium line is raised there is a unit decrease in the ice volume. The former case leads to a large hysteresis loop while the latter displays no hysteresis. In between these two extreme cases lie different configurations of bed topography, such as those used in the model experiments (figure 5.5). Here, the maximum altitude of the topography is 1100 metres so ice begins to grow when the equilibrium line is initially lowered to this altitude. The volume of ice depends on the gradient of the bed at 1100 metres. The topography with the shallowest gradient, $|\sin x|^{0.1}$, has the largest ice volume at this

point while the bed with the steepest gradient, $|\sin x|^{10}$, has the least. When the equilibrium line altitude is lowered to 1000 metres the former bed topography has a high enough accumulation area, because of the ice surface, to allow the ice to grow to the model boundary. In the latter case, the equilibrium line altitude needs to be lowered to 500 metres for the same effect. Similarly, on raising the equilibrium line the former bed topography has an abrupt transition from an ice sheet to a glacial system, while the latter case is smoother, reflecting the different ice surfaces resulting from the underlying bed. In theory, it is possible to plot equilibrium ice volumes for any arbitrary climate (equilibrium line altitude) and topography and so determine the characteristics of the hysteresis loop.

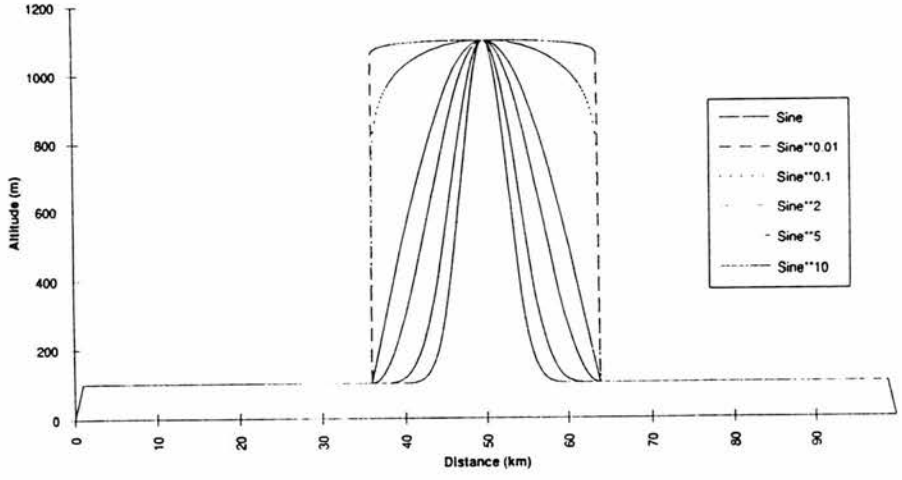

Figure 5.4 Bed topography used in the model experiments

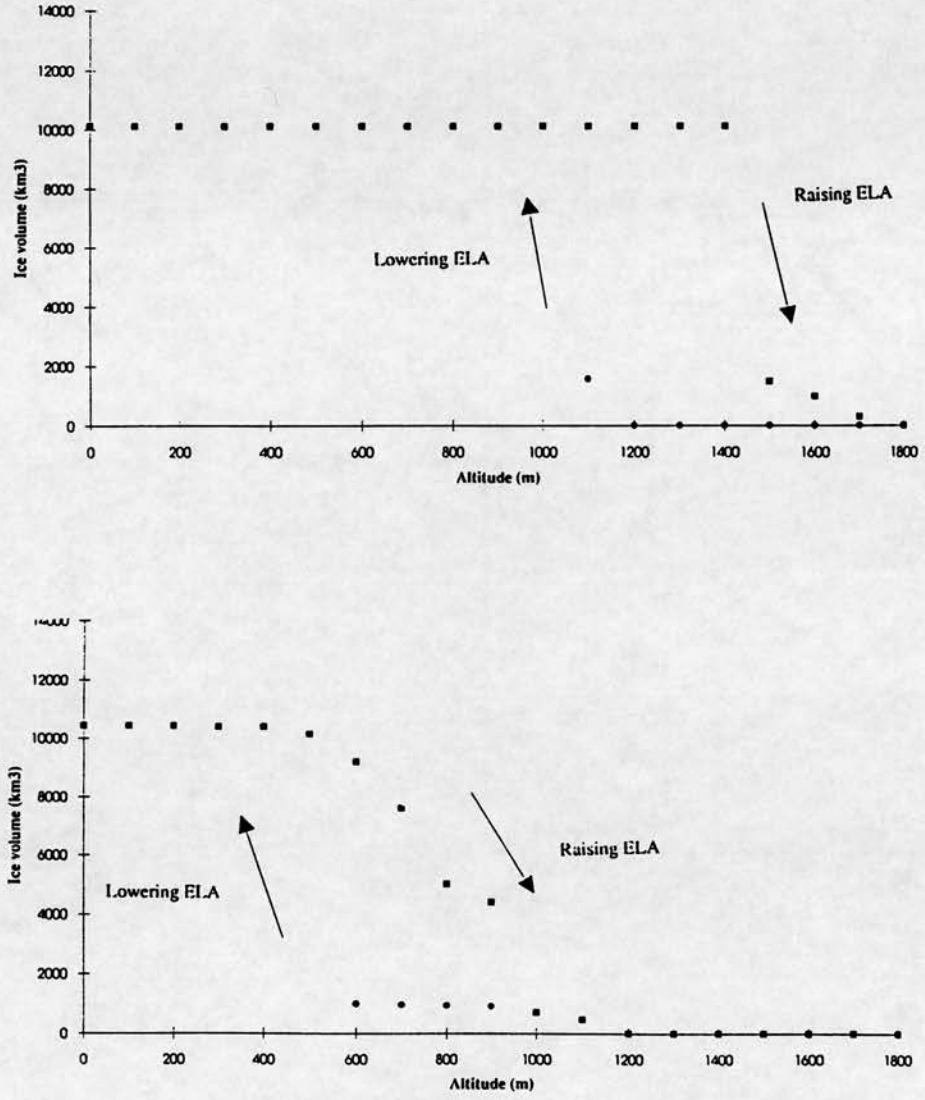

Figure 5.5 Modelled ice volumes obtained when the equilibrium line was lowered and then raised between 1800 and 0 metres over bed topographies $|\sin x|^{0.1}$ and $|\sin x|$ respectively.

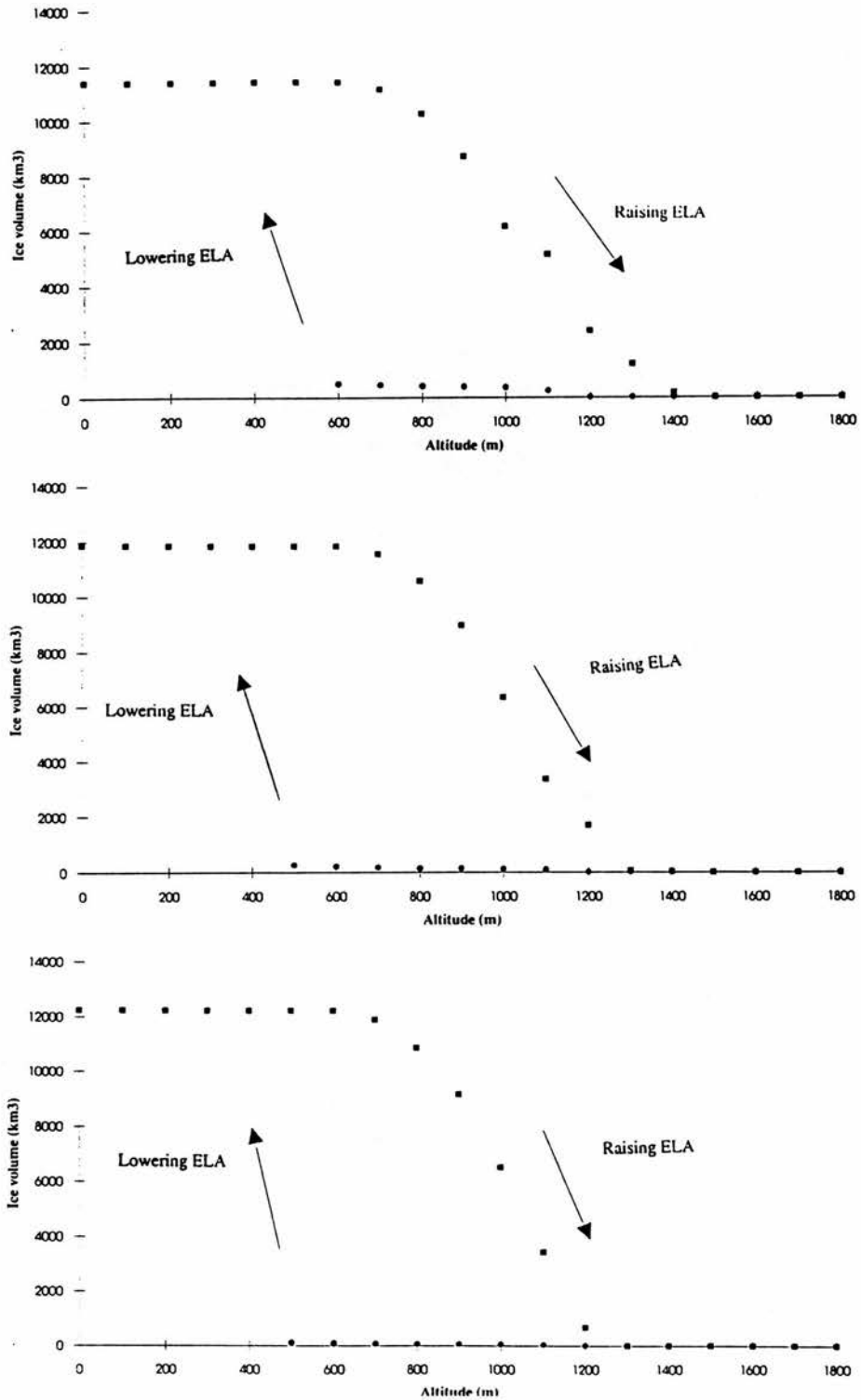

Figure 5.5 Modelled ice volumes obtained when the equilibrium line was lowered and raised between 1800 and 0 metres over bed topographies $|\sin x|^2$, $|\sin x|^5$, and $|\sin x|^{10}$ respectively.

This behaviour at the topographically forced transition between a mountain glacier system and an ice sheet system has been ascribed to a fold catastrophe (Oerlemans and van der Veen,1984; Hindmarsh,1990). Catastrophe theory was developed by Thom (1975) to explain how gradually changing forces produce sudden effects. The simplest elementary catastrophe is the fold-catastrophe as exemplified by the hysteresis loop in equilibrium ice volumes for a specific range of ELA's (figure 5.6). However, Zeeman (1977) notes that when qualitative features such as hysteresis, divergence, or sudden jumps are present in nature then it is likely that a cusp-catastrophe is present. If this is the case then the equilibrium ice volume for any arbitrary climate (ELA) and topography can be calculated once the cusp control point, which is the point where the two folds meet, is found. However, catastrophe theory cannot be formally applied here because the underlying functions (bedrock slopes and mass balance profiles) are not continuous; they do not possess derivatives of all orders. In figure 5.7, the equilibrium surface is ice volume, and the two horizontal axes are the climate, defined in terms of the ELA, and topography. This implies different topographic configurations will be situated at different points on the axis depending on the size of the hysteresis loop.

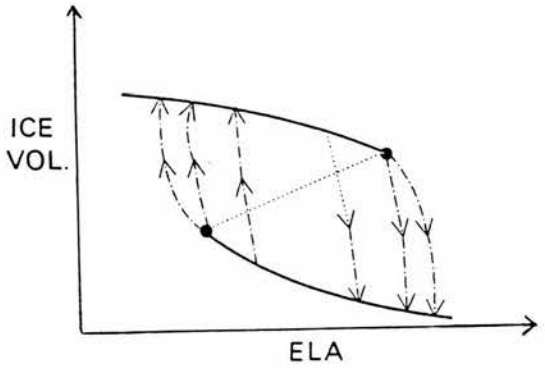

Figure 5.6 Fold catastrophe of ice volume and climate.

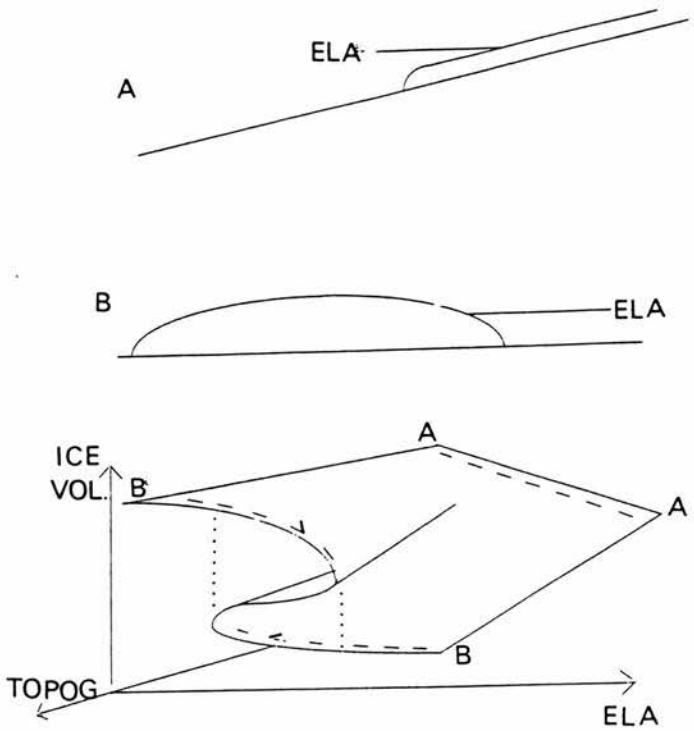

Figure 5.7 Cusp catastrophe of ice volume, climate and topography.

Unfortunately, the topographic axis is poorly defined, and it requires a more detailed look at the configuration and geometry of topography. Since there is a jump in ice volume there must be an increase in accumulation such that it exceeds the glaciers ability to lose mass by ablation. Clearly, the ratio of accumulation area to ablation area is very sensitive at this point, and the sudden increase in accumulation area caused by the lowering equilibrium line leads to a necessary adjustment of the glacier size to obtain the required ablation area. Since this accumulation area is dependent on the ice thickness, and thus the bed topography, it is possible to identify the 'potential for accumulation' as being the maximum possible mass input for a given bed configuration. Similarly, the 'potential for ablation' is the maximum possible mass output. The accumulation potential is only dependent on bed slope since, in the absence of time, this will define the maximum possible ice thickness at any given point. The ablation potential is more difficult to determine since it must balance the accumulation potential. Thus it depends on altitudinal gradients of accumulation and ablation which determine the climatic setting and the ice flow, the bedrock slope at different altitudes, and the accumulation potential. The jump in

ice volume must correspond to the point at which the potential for accumulation exceeds the potential for ablation, so the glacier grows until it reaches its next stable point or, in the simple geometry of these experiments, the model boundary. The size of this jump depends on the relative potentials of accumulation and ablation within a given area, and this determines the hysteresis loop and, ultimately, the position of the topography on the topographic axis.

DISCUSSION

The foregoing results and interpretations depend on the stringent assumptions on which the model is based. It is important to determine the effect of relaxing these conditions, and assess the wider implications of the transition between a glacial and an ice sheet system.

The assumption that the ice surface instantaneously attains an equilibrium state with the climate is clearly false. Glacier response lags climatic change because of the time taken to re-distribute the newly acquired mass over the glacier. If the climate forcing is changing quickly the glacier will not have re-equilibrated before a further adjustment is required. The final ice surface will be a function of the time interval of each climatic forcing, integrated with respect to the response time for that particular system to re-equilibrate. This means that there are multiple steady state solutions of ice volume for a particular geographical region (Letreguilly and Oerlemans, 1990). The particular solution which occurs depends on the past history of climate change, and since this is likely to be below our limit of resolution it will be unpredictable.

In the model the ice is assumed to flow under plastic deformation. Changing the yield stress, or adding a shape factor to account for valley walls leads to a change of ice thickness for a given bed slope and a change in ice volume. The results of the sensitivity experiments with different yield stresses were that the jump and fall in ice volume occurred at the same equilibrium line altitude. In terms of a cusp catastrophe, the effect of a change in yield stress is thus a translation of the vertical axis (ice volume) while retaining the structure of the equilibrium surface. The weak dependence of topographic thresholds on the flow law found by Oerlemans (1981) implies that this jump in ice volume only occurs at the same equilibrium line altitude if there is an identical throughput of ice, and ultimately a similar climatic setting. Of course, during the evolution of an ice

sheet local climate is modified through albedo, temperature and precipitation feedbacks, so the flow characteristics of the ice changes. This process couples climate, topography, and ice dynamics (Boulton et al.,1984) and undermines the assumption that glaciers retain their geometrical profile while advancing or retreating.

Different geographical regions have different topographic signatures and, in terms of a cusp catastrophe, are represented at different points on the topographic axis. As the climate deteriorates and glaciers form, the equilibrium ice volumes will follow trajectories towards the cusp axis. The bulk properties of ice force the geometrical profiles of evolving ice sheets which is why the parabolic approximation of the profile of a glacier is widely applicable. The volume of an ice sheet is found to be proportional to its area over four orders of magnitude (Paterson,1981) and this simplicity was utilised by early, analytical analyses of ice sheets. This implies that there is a powerful attractor on the upper fold of the cusp corresponding to the point on the topographic axis of an ice sheet deforming plastically. The trajectory of the equilibrium ice volumes will tend towards this point on the topographic axis from their initial positions as the growing ice sheet approaches a parabolic profile. Any climatic change which leads to a rising equilibrium line altitude will force the trajectory back towards the cusp, ultimately forcing a jump to the lower fold surface, and a divergence of trajectories back to the initial topography. One might expect the saw-tooth shape observed in palaeoclimatic reconstructions of ice volume to be a natural consequence of a steady lowering of the equilibrium line altitude, with the consequent merging of glaciers and ice caps to form an ice sheet, followed by a steady rise.

With regard to the bedrock surface there are three possible processes which affect the climate - ice system; isostasy, eustasy, and long term topographic evolution. The effect of isostasy is to reduce the surface height of an ice sheet and hence the potential for accumulation. Oerlemans (1980b) showed that this effect could be enough to destabilise an ice sheet and lead to catastrophic collapse. Since Weertman (1961) showed that the equilibrium profile of an ice sheet incorporating isostasy was to lower the surface but retain the profile, in terms of a cusp catastrophe this is equivalent to a trajectory moving perpendicular to the climate axis until it reaches the cusp fold and then dropping to the lower fold. A eustatic change is simply equivalent to a vertical change in the equilibrium line altitude. Longer term topographic evolution, which results from glacial and fluvial erosion and deposition and consequential tectonic underplating (Summerfield,1991), leads to a change in the surface area at higher altitudes and of the potential for

accumulation. Assuming that over a glacial cycle the change in topography is small compared with the change in climate, in terms of a cusp catastrophe this effect is equivalent to a region changing its initial position on the topographic axis between glacial cycles. A climatic forcing of the same magnitude as before will force ice volume along a different trajectory to the previous one, and this will meet the fold at a different equilibrium line altitude. This implies a different climatic deterioration is required to obtain a comparable ice volume. As a formerly plateau area becomes glacially incised with the development of over-deepened troughs and cirque formation leading, eventually, to more Alpine topography, the topographic signature of a region changes. This produces a powerful feedback (over Quaternary time scales) between climatic forcing and the resultant ice volume.

The natural extension of this work is to re-run the experiments with bedrock topography and climatic profiles which are mathematically continuous, and thus differentiable at all orders. This would provide a means of quantifying the influence of topography in an arbitrary region.

CONCLUSION

A simple model of glaciers in equilibrium with the climate and deforming plastically appears to be able to qualitatively reproduce the fold catastrophe noted by various authors. The critical thresholds are the points where a disequilibrium in the system caused by a change in the accumulation leads to a large change in ice volume as the glacier jumps to a new equilibrium. The concept of a potential for accumulation and ablation can be introduced for any arbitrary glacier, with the crucial height-mass balance feedback derived from the assumptions of plasticity of ice flow for bed slope angles. Thus, in theory, for any arbitrary topography and climate it is possible to determine the critical thresholds of growth and decay. However, since glaciers will not necessarily reach an equilibrium profile the actual evolution of a glacier will be unpredictable.

CHAPTER SIX:
SUMMARY AND IMPLICATIONS

6.1 Summary

This chapter briefly summarises the objectives and attainments of this thesis and assesses the wider implications for global climate. The aim was to investigate the influence of climate and topography on ice sheets in maritime environments. This was accomplished by using appropriate models of the climate and ice dynamics to simulate events from two case studies. Such an approach provides a means of understanding the dominant processes and relationships operating within each system, and by inference to the global climate system. The objectives were:

1) To simulate the climate of southern Chile to investigate the role of the Southern Westerlies in determining the climatic modification at the Last Glacial Maximum.

2) To simulate the Loch Lomond stadial ice cap in Scotland to examine the climatic and topographic conditions which facilitate ice sheet initiation.

3) To explore the sensitivity of ice sheet evolution to the regional configuration of mountains by examining the topographic threshold between stable upland glaciers and ice sheets.

6.2 The Models

The numerical models were chosen because they are the most appropriate models to answer the questions posed by the thesis objectives. The models of ice dynamics and the surface energy balance are adapted from Payne (1988) and Oerlemans (1992) respectively. The regional energy balance model is a simplified version of similar models developed in the 1970's (North et al.,1981).

The regional energy balance model calculates the annual temperature cycle at sea level in specified regions by relating the radiation at the surface to a schematic representation of the energy fluxes occurring between latitude bands and across coastal boundaries. This results in a regional temperature cycle which is input to the surface energy balance model. The surface energy balance model represents a maritime climate in terms of the glacial input to, and output from, an ice sheet. At a specified location climatic variables are related to an annually-averaged budget of snow accumulation and ablation at different altitudes. This glacial mass balance profile is the climatic forcing of the ice sheet model. The ice sheet model is based on the continuity equation for ice thickness which states that the change in ice thickness of a column of ice over time depends on the mass balance at the surface and the ice flux through the column. The ice flux depends on ice deformation and sliding. The former is proportional to ice surface

slope and hence basal shear stress while the latter is also proportional to surface slope but is inversely proportional to ice thickness, so the two processes predominate in different regions of ice sheet.

To have any confidence that these models are applicable to the case studies an appropriate modelling methodology is utilised. Model construction involves three different stages: choosing the variables, assigning values to the variables, and tuning the variables to simulate independent evidence. Since the models are taken from the literature, the first two stages were already completed. Each model is based on the perceived mathematical representation of the physical system in question. Where there are no mathematical derivations from the fundamental laws of conservation and motion, or where such derivations are only available at an inappropriate spatial or temporal scale, empirical relations are used. Model output was tuned to simulate independent evidence from the pertinent region. Such an approach assumes that the underlying physical processes which lead to the tuned values do not markedly vary through time. The validity of such assumptions was later examined in the sensitivity analysis when the sensitivity of individual components was assessed. Sensitive parameters occurred either because they were inherently sensitive or because the value of the parameter was poorly constrained. For example, the formulation of the surface albedo and turbulent fluxes in the surface energy balance model are only rough approximations of the complex small scale processes which operate in practice. Overall, the most sensitive climatic parameters are the mean annual temperature, the temperature range, and the precipitation while the ice sheet model is more sensitive to climatic forcing than to ice dynamics. The most sensitive parameter in the regional energy balance model is the tuning parameter which determines the latitudinal flow of heat. Finally, the assumptions and limitations of each model was explored to set the results and their implications in context. The models were chosen for their applicability to particular case studies which, given the nature of the system under investigation, involves processes operating between and within different climatic domains. The subjectivity of model construction ensures that the results are not unique but, rather, must be assessed with the models' limitations in mind.

6.3 Climate

The influence of the climate on ice sheets in maritime environments was investigated by applying the models to two case studies. Maritime areas are strongly influenced by the adjacent ocean so the zonal heat flux dominates the energy balance. This implies that in maritime regions which are close to glacial initiation, a change in the solar radiation on its own will be insufficient to initiate ice sheets. Instead, ice sheet initiation is strongly influenced by ocean temperature which affects the delicate balance between decreasing precipitation, which inhibits glacial expansion, and decreasing temperature, which promotes it. This balance is exemplified by figure 3 (page 93) which displays the equilibrium line altitude for different values of temperature and precipitation in the west of Scotland. A fall of temperature of 4°C, with the same precipitation distribution as now, lowers the regional equilibrium line altitude by approximately 500 metres. However, if precipitation was also reduced by 50%, as a result of the migration of the belts of maximum precipitation, the temperature would need to fall by 7°C to lower the equilibrium line by the same amount. Different regions will have different sensitivities to a climatic change depending on initial values of precipitation and temperature, since these primarily determine the mass balance gradient. The modelled equilibrium line is most sensitive to temperature changes in regions of high precipitation and most sensitive to precipitation in regions of low precipitation. These factors are related because the temperature determines the 'efficiency' of the precipitation falling as snow. Increased seasonality also affects the balance. A higher temperature range increases the period of melting in the summer while doing little to increase the 'efficiency' of snow falling in winter since it already falls as snow. Similarly, decreased seasonality which leads to decreased winter snowfall raises the snowline since less energy is required to melt the thinner snow cover during the summer.

Ultimately, glacial initiation and expansion is more dependent on the net mass balance gradient than the equilibrium line (Kuhn,1984; Oerlemans and Hoogendoorn,1989). These results re-emphasise this point since both the rate of ice sheet growth and the ice flux to lower altitudes depend on the balance gradient. Increased aridity inferred at the last glacial maximum (Jouzel et al.,1989) suggests that ice sheet decay was initiated or augmented by precipitation depletion. A further implication of the importance of precipitation is that maximum lowering of the snowline is unlikely to be contemporaneous over a wide latitudinal range.

The case studies of southern Chile and Scotland share many similarities. The regions have a comparable latitude, a maritime climate, a mountainous region on the windward side, and steep climatic gradients across the region. The results of the case study also suggest a great deal of similarity in the phases of ice sheet initiation and expansion. Both depend on the delicate interplay between precipitation and temperature, implicitly assumed to occur as a result of the movement of the respective oceanic polar fronts. In Chile, the southern-most region lies to the south of the belt of maximum precipitation. Expanded glaciation appears to depend on the balance between decreased temperature and precipitation starvation induced by the equatorward movement of the Antarctic polar front. Alternatively, a poleward movement of the belt of maximum precipitation with no increase in temperature would also reduce the equilibrium line and steepen the mass balance gradient which are prerequisites for glacial initiation. However, the relationship between the belt of maximum precipitation and the oceanic polar front makes this possibility climatically less likely. The region closest to the central belt of the Westerlies, where the current Patagonian ice fields are situated appears to be a prime region for glacial expansion. Either of the two postulated climatic modifications, an equatorward shift or a zonal intensification of the Westerlies accompanied by cooling, lowers the snowline and steepens the balance gradient. Precipitation is crucial for glacial expansion in the Chilean Lake District. An excessive temperature reduction, uncorroborated by other evidence, is required if the precipitation starvation inferred from pollen data occurred. The implication is that glaciation reflects an equatorward movement of the Westerlies, causing the belt of maximum precipitation to move north. The enhanced precipitation, coupled with cooler temperatures, provide the necessary conditions for the inferred glacial expansion in the Chilean Lake District.

Scotland lies to the south of both the Atlantic polar front and the zone of maximum precipitation. A southward movement of the polar front will therefore raise precipitation and lower temperature. However, southward movement beyond a critical point will lead to precipitation starvation in the north and a situation analogous to the present climatic regions in Chile will develop.

The three regions in Scotland have different susceptibilities to glacial initiation and expansion. The north is climatically most favourable while the east is the least favourable. The latter region is influenced both by increased continentality, which increases the temperature range, and reduced precipitation. Both factors raise the equilibrium line and reduce susceptibility to ice sheet growth.

6.4 Topography

The influence of topography on ice sheets in maritime environments was investigated by applying models to the Scottish case study, and subsequently developing an explicit topography model to provide a more rigorous analysis.

In Scotland, the eastern region is topographically most susceptible to ice sheet growth while the north is least so. Climatically, the reverse occurs and yet it is the western region which develops an ice cap. Clearly, ice sheet growth is determined by both climate and topography. It appears that the role of altitude, and the configuration of upland topography, is to determine the point of initiation of an ice mass, and to control the threshold between stable upland glaciers and the growth of an ice sheet. The glacial system becomes very sensitive at this threshold, which is a function of the accumulation and ablation areas, the bedrock slopes, and the climatic gradients. Sensitivity experiments indicate a fold catastrophe occurs, and imply that it is theoretically possible to calculate the topographic glacier - ice sheet threshold for any arbitrary configuration of topography.

Glacial initiation in susceptible regions requires suitable topography; high plateaux are best, since only a small lowering of the equilibrium line altitude to below the plateaux surfaces can lead to an explosive growth of ice. However, over the course of a glacial cycle isostatic depression provides a powerful negative feedback to the surface altitude of a growing ice sheet, while fluctuations in eustasy influence both the ice surface altitude and ice discharge from outlet, calving glaciers. On longer time scales, glacial and fluvial erosion provide a strong feedback between climate, topography, and ice volume. Environments most susceptible to glacial initiation will have repeated glaciations and this will modify the topography. Glacially incised troughs or the development of characteristic alpine landscapes are less susceptible to glacial initiation and expansion, so each succeeding glacial cycle would be expected to have a smaller maximum ice volume than the previous one.

6.5 The contribution of this thesis

Three sets of experiments were carried out to accomplish the three stated objectives of this thesis. The experiments involved numerical models of the three subsystems under investigation: maritime climates, subglacial topography, and ice sheets.

Maritime climates are strongly influenced by the temperature of the adjacent ocean and have relatively warm, wet environments. These experiments indicate that the

balance between ocean cooling and the retention of precipitation is critical for ice sheet growth. In reality, this depends on the relative positions of the oceanic and atmospheric polar fronts, and the land mass. Furthermore, the subglacial topography must be susceptible to ice sheet growth. These experiments indicate that ice sheet evolution is non-linear and depends, in part, on the configuration of subglacial topography. There is a critical balance between regions of accumulation and ablation and the falling equilibrium line altitude. However, the fold catastrophe observed in experiments has yet to be formally quantified.

From this work, two necessary conditions are inferred for the initiation and growth of ice sheets in maritime environments. The adjacent oceans' temperature must cool, since experiments indicate that the other plausible mechanism, the Milankovitch orbital variations, appears insufficient to reduce the temperature by the required amount. In addition, the land must have a surface topography conducive to ice sheet growth, and it is this topographic configuration which ultimately determines whether a small or large ice mass exists for an arbitrary climate.

The limitations of the experiments revolve around the assumptions used in the numerical models. In particular, the regional energy balance model relies on the spatial and temporal invariance of optimised parameters. Given the climatic changes involved, this assumption may well be invalid, in which case the inferred role of Milankovitch orbital variations may be underestimated. The surface balance model is more process oriented, and the assumptions depend on the applicability of the model, originally designed for the Alps, being applied to maritime environments of many thousands of years ago. In mitigation, weaknesses of the model, such as the formulation of the turbulent fluxes and factors such as cloud cover and cloud height, are less variable in such environments than in more continental areas. The major weakness of the ice sheet model is the requirement of a smooth, subglacial topography. This requirement limits understanding of the importance of the subglacial topography in determining ice sheet evolution.

Despite these limitations, and the consequent problems with conclusions inferred from model results, numerical modelling provides the best approach for tackling the interactions of climatic subsystems which operate over long time, and large, spatial scales. Empirical work is not sufficiently constrained to provide us with a good understanding of the physical mechanisms in operation. This understanding will be enhanced when better empirical data is obtained to more tightly constrain numerical models.

6.6 Conclusion

The two primary implications of this work are, firstly, a necessary condition for the initiation or expansion of an ice sheet in a maritime region is the reduction in temperature of the adjacent ocean. Since the seeding areas of the Laurentide and Scandinavian ice sheets are in maritime regions, this implies that substantial ocean current changes occurred repeatedly, as postulated by Broeker and Denton (1989), as a necessary condition for the Pleistocene glacial cycles. Furthermore, this possibility means that either the Milankovitch cycles are irrelevant, though this appears unlikely (Hays et al.,1976), or that the orbital forcing is being filtered by the changes in ocean currents. Further work clearly needs to focus on the relationship between ocean dynamics and orbital variations.

The second implication is that the effect of topography is to decouple the response of ice from the climate. Thus proxy data for ice volume should not be used as proxy data for climate until there is a quantitative understanding of the role played by topography. One approach is to formally apply catastrophe theory to relate the two physical controls of climate and topography to ice volume. This entails analysing climate and bedrock functions which are continuous (possessing derivatives of all orders), and these can be obtained by the use of Fourier analysis.

REFERENCES

Abe-Ouchi A. and Blatter H. 1992. On the initiation of ice sheets. *Abstract for IGS* Symposium on Snow and Snow-Related Problems, Japan.

Ahlmann H.W. 1937. Vatnajokull in relation to other present day Iceland glaciers. *Geogr. Annl.*,19, 146-231.

Ahlmann H.W. 1948. Glaciological research on the North Atlantic coasts. *Roy. Geog. Soc. Research Series 1*, 83pp.

Ambach W. and Kuhn M. 1989. Altitudinal shift of the equilibrium line in Greenland calculated from heat balance characteristics. In Oerlemans J. (ed) *Glacier fluctuation and climatic change.* Kluwer Acad. Publ., Dordrecht. 281-288.

Andrews J.T., Barry R.G., and Draper L. 1970. An inventory of the present and past glacierization of Home Bay and Okoa Bay, east Baffin Island, NWT, Canada, and some climatic and palaeoclimatic considerations. *J. Glaciol.*, 9(57), 337-362.

Andrews, J.T.and Mahaffy M.A.W. 1976. Growth rate of the Laurentide ice sheet and sea level lowering (with emphasis on the 115,000 BP sea level low). *Quat. Res.* 6 167-183.

Barry R.G. 1981. *Mountain weather and climate.* Methuen and Co. Ltd. London. 313pp.

Barry R.G. and Chorley R.J. 1987. *Atmosphere, weather and climate (5th ed).* Methuen and Co. Ltd. London. 460pp

Bindschadler R., Harrison W.D., Raymond C.F., and Crosson R. 1977. Geometry and dynamics of a surge-type glacier. *J. Glaciol.*, 18, 181-194.

Birchfield G.E. 1977. A study of the stability of a model continental ice sheet subject to periodic variations in heat input. *J. Geophys. Res.* 82 4909-4913.

Birchfield G.E., Weertman J., and Lunde A.T. 1981. A paleoclimate model of northern hemisphere ice sheets. *Quat. Res.* 15 126-142.

Birchfield G.E., Weertman J., and Lunde A.T. 1982. A model study of the role of high latitude topography in the climatic response to orbital insolation anomalies. *J. Atmos. Sci.*, 39, 71-87.

Bodvarsson G. 1955. On the flow of ice sheets and glaciers. *Jokull*, 5, 1-8.

Boulton G.S. 1974. Processes and patterns of glacial erosion. In Coates D.R. (ed), *Glacial geomorphology*, State University of New York, NY, 41-87.

Boulton G.S. and Jones A.S. 1979. Stability of temperate ice caps and ice sheets on beds of deformable sediments. *J. Glaciol.*, 24(90), 29-43.

Boulton G.S., Smith G.D., and Morland L. 1984. The reconstruction of former ice sheets and their mass balance characteristics using a non-linearly viscous flow model. *J. Glaciol.*, 30(105), 140-152.

Bradley R.S. and Serreze M.C. 1987. Topoclimatic studies of a high arctic plateau ice cap. *J. Glaciol.*, 33(114), 149-158.

Braithwaite R.J. 1984. Can the mass balance of a glacier be estimated from its equilibrium line altitude? *J. Glaciol.*, 30(106), 364-368.

Braithwaite R.J. and Olesen O.B. 1989. Calculation of glacier ablation from air temperature, West Greenland. In Oerlemans J. (ed) *Glacier fluctuation and climatic change*. Kluwer Acad. Publ., Dordrecht, 219-233.

Broeker W.S. and Denton G.H. 1989. The role of ocean-atmosphere reorganisations in glacial cycles. *Geochim. Cosmochim. Acta,* 53, 2465-2501.

Budd W.F. 1970a. The longitudinal stress and strain-rate gradients in ice masses, *J. Glaciol.*, 9(55), 19-27.

Budd W.F. 1970b. Ice flow over bedrock perturbations, *J. Glaciol.*, 9(55), 29-48.

Budd W.F. 1971. Stress variation with ice flow over undulations, *J. Glaciol.*, 10(59), 177-195.

Budd W.F. and Carter D.B. 1971. An analysis of the relation between the surface and bedrock profiles of ice caps, *J. Glaciol.*, 10(59), 197-209.

Budd W.F. and Jenssen D. 1975. Numerical modelling of glacier systems. *I.A.S.H. Publ.104*, (Proceedings of Moscow Symposium - Snow and Ice), 257-291.

Budd W.F., Jenssen D., and Smith I.N. 1984. A three dimensional time-dependent model of the West Antarctic ice sheet. *Annals Glaciol.* 5, 29-36.

Budd, W.F.and Smith I.N. 1981. The growth and retreat of ice sheets in response to orbital radiation changes. *I.A.H.S. Publ.131.* (Symposium at Canberra 1979 - Sea Level, Ice and Climate Change), 369-409.

Budd, W.F.and Smith I.N. 1982. Large scale numerical modelling of the Antarctic ice sheet. *Annals Glaciol.*, 3, 42-49.

Budyko M.I. 1969. The effect of solar radiation variations on the climate of the Earth. *Tellus*, 21(5), 609-619.

Caviedes, C.N. 1990. Rainfall variation, snowline depression and vegetational shifts in Chile during the Pleistocene. *Climatic Change,* 16, 99-114.

Caviedes, C.N. and Paskoff R. 1975. Quaternary glaciations in the Andes of north-central Chile. *J. Glaciol.* 14(70) 155-170.

Chalikov D.V. and Verbitsky M.Y.A. 1990. Modeling the Pleistocene ice ages. *Advances in Geophysics*, 32, 75-131.

Clapperton, C.M. 1983. The glaciation of the Andes. *Quat Sci.Rev.*, 2, 83-155.

Clark J.A., Farrell W.E., and Peltier W. 1978 Global changes in post-glacial sea level: A numerical calculation. *Quat. Res.*, 9, 265-287.

CLIMAP Project Members. 1981. Seasonal reconstruction of the Earth's surface at the last glacial maximum. (R. Cline, ed.) *Geol. Soc. Am. Map Charts Ser. 36.*

Collins I.F. 1968. On the use of the equilibrium equations and flow law in relating the surface and bed topography of glaciers and ice sheets. *J. Glaciol.*, 7(50), 199-204.

Cook K.H. 1990. The atmosphere's response to the ice sheets of the last glacial maximum. *Annals Glaciol.*, 14, 32-38.

Crowley T.J. and North G.R. 1991. *Paleoclimatology*. Clarendon Press. Oxford. 339pp

Denton G.H. and Hughes T. (eds.) 1981. *The Last Great Ice Sheets*. John Wiley & Sons, N.Y.

Fowler A.C. 1981. A theoretical treatment of the sliding of glaciers in the absence of cavitation. *Phil. Trans.of the Roy. Soc. London, Ser. A*, 298, 673-681.

Fowler A.C. 1987. Sliding with cavity formation. *J.Glaciol.*, 33(115), 255-267.

Fujiyoshi, Y., Kondo H., Inoue J., and Yamada T. 1987. Summer climate of the Northern Patagonia icefield. ***Bulletin of Glacier Research,*** 4, 15-23.

Furbish D.J. and Andrews J.T. 1984. The use of hypsometry to indicate long term stability and response of valley glaciers to changes in mass transfer. *J. Glaciol.*, 30(105), 199-211.

Garfield, K. and Stiegl H. 1988. Geomorphologische Untersuchungen in der nivalen und subnivalen Stufe der Argentinischen Anden. *Tagungsbericht und wissenschaftl Abhandl 46 Deutscher Geographentag* Munchen 1987. (M. Schneider,ed.) Franz Steiner, Weisbaden pp 419-425.

Ghil M. and LeTreut H. 1981. A climate model with cryodynamics and geodynamics. *J. Geophys. Res.*, 86, 5262-5270.

Glen J.W. 1955. The creep of polycrystalline ice. *Proc. Roy. Soc. London, Ser.A*, 228, 519-538.

Glen J.W. 1958. The flow law of ice. A discussion of the assumptions made in glacier theory, their experimental foundations and consequences. *I.A.S.H.*, 47, 171-183.

Greuell, W. and Oerlemans J. 1986. Sensitivity studies with a mass balance model including temperature profile calculations inside the glacier. *Z. Gletscherk. Glazialgeol.* 22 101-124.

Hallet B. 1981. Glacial abrasion and sliding: their dependence on the debris concentration in basal ice. *Ann. Glaciol.*, 2, 23-28.

Harbor J.M., Hallet B., and Raymond C. 1988. A numerical model of landform development by glacial erosion. *Nature*, 333, 347-349.

Harding R.J. 1978. The variation of the altitudinal gradient of temperature within the British Isles. *Geog. Annal.*, 60A, 43-49.

Hastenrath, S.L. 1971. On the Pleistocene snow-line depression in the arid regions of the South American Andes. *J.Glaciol.*, 10(59), 255-267.

Hays J.D., Imbrie J., and Shackleton N.J. 1976. Variations in the Earth's orbit: Pacemaker or the last ice ages. *Science,* 194, 1121-1132.

Heusser, C.J. 1983. Quaternary pollen record from Laguna de Tagua Tagua, Chile. *Science,* 219, 1429-1432.

Heusser, C.J. 1989a. Late Quaternary vegetation and climate of Southern Tierra del Fuego. *Quat. Res.*, 31, 396-406.

Heusser, C.J. 1989b. Southern Westerlies during the last glacial maximum. *Quat. Res.*, 31, 423-425.

Heusser, C.J. 1989c. Polar perspective of Late-Quaternary climates in the Southern Hemisphere. *Quat. Res.*, 32, 60-71.

Heusser, C.J., Streeter S.S. and Stuiver M. 1981. Temperature and precipitation record in southern Chile extended to ~ 43,000 yr ago. *Nature,* 294, 65-67.

Hindmarsh R.C.A. 1990. Time scales and degrees of freedom operating in the evolution of continental ice sheets. *Trans.Roy.Soc.Edinburgh: Earth Sciences*, 81, 371-384.

Hoinkes H. 1968. Glacier variation and weather. *J. Glaciol.*, 7(49), 3-19.

Hughes T. 1992. Theoretical calving rates from glaciers along ice walls grounded in water of variable depths. *J.Glaciol.*, 38, 282-294.

Hulton, N.R.J., Sugden D.E., Payne A.J., and Clapperton C.M. 1993. Glacier modelling and the climate of Patagonia during the Last Glacial Maximum. *Quat. Res.* (submitted)

Hutter K. 1983. *Theoretical glaciology.* Reidel Publishing, Dordrecht, pp510.

Hutter K., Legerer F. and Spring U. 1981. First order stresses and deformations in glaciers and ice sheets. *J. Glaciol.*, 27(96), 227-270.

Huybrechts P. 1990. The Antarctic ice sheet during the last glacial-interglacial cycle: a 3-D model experiment. *Ann. Glaciol.*,14, 115-119.

Inoue J., Kondo H., Fujiyoshi Y., Yamada T., Fukami H., and Nakajima C. 1987. Summer climate of the Northern Patagonian icefield. *Bulletin of Glacier Research,* 4, 7-11.

James I.N. and James P.M. 1989. Ultra-low frequency variability in a simple atmospheric circulation model. Nature, 342, 53-55.

Jóhannesson T., Raymond C.F. and Waddington E.D. 1989a. A simple method for determining the response time of glaciers. In: *Glacier Fluctuations and Climatic Change* (ed. by J. Oerlemans), 343-352, Kluwer Academic publishers, Dordrecht.

Jóhannesson T., Raymond C.F. and Waddington E.D. 1989b. Time scale for adjustments of glaciers to changes in mass balance. *J. Glaciol.*, 35(121), 355-369.

Johnson, R.G. and Andrews J.T. 1979. Rapid ice-sheet growth and initiation of the last glaciation. *Quat. Res.*, 12, 119-134.

Jouzel J., Lorius C., Merlivat L., Petit J-R. 1989. A comparison of deep Antarctic ice cores and their implications for climate between 65,000 and 15,000 years ago. *Quat. Res.*, 31, 135-150.

Källen E., Crafoord C. and Ghil M. 1979. Free ocsillations in a climate model with ice sheet dynamics. *J Atmos. Sci.*, 36(12), 2292-2303.

Kamb B. 1970. Sliding motion of glaciers: theory and observation. *Rev. Geophys. Space Phys.*, 8(4), 673-728.

Kamb B. and Echelmeyer K.A. 1986. Stress-gradient coupling in glacier flow: I longitudinal averaging of the influence of ice thickness and surface slope. *J. Glaciol.*, 32(111), 267-284.

Kerr, A. 1990. The initiation of maritime ice sheets. *Z. Gletscherk. Glazialgeol.*, 26(1), 69-79.

Kirkby M.J., Naden P.S., Burt T.P., and Butcher D.P. 1987. *Computer simulation in physical geography.* J. Wiley & Sons, Chichester. 227pp.

Kondo J. and Sata T. 1988. A simple model of drainage flow on a slope. *Bound. Layer Meteor.*, 43, 103-123.

Kuhn, M. 1979. On the computation of heat transfer coefficients from energy-balance gradients on a glacier. *J. Glaciol.*, 22(87), 263-272.

Kuhn, M. 1980. Vergletscherung, nullgradgrenze, und niederschlag in den Anden. *Sonderdruck aus Jahresbericht des Sonnblick - Vereines 1978-1980.*

Kuhn M. 1981. Climate and glaciers. *Int. Assoc. Hydrol. Sci. Publ., 131,* (Symposium at Canberra 1979 - Sea level, ice and climate change), 3-20.

Kuhn, M. 1984. Mass budget imbalances as criterion for a climatic classification of glaciers. *Geogr. Annlr.*, 66A, 229-238.

Kuhn, M. 1987. Micro-meteorological conditions for snow melt. *J. Glaciol.*, 33(113), 24-26.

Kuhn M. 1989. The response of the ELA to climate fluctuations: theory and observations. In: *Glacier Fluctuations and Climatic Change* (ed. by J. Oerlemans), 407-417, Kluwer Academic publishers, Dordrecht.

Kutzbach, J.E. and Guetter P.J. 1986. The influence of changing orbital parameters and surface boundary conditions on climate simulations for the past 18,000 years. *J. of the Atmos.Sci.*, 43(16), 1726-1759.

Lamb, H.H. 1959. The Southerly Westerlies: a preliminary survey; main characteristics and apparent associations. *Quart.J.Roy.Met.Soc.*, 85(363), 1-23.

Lamb, H.H. 1964. The role of atmosphere and oceans in relation to climatic changes and the growth of ice sheets on land. (NATO Advanced Studies Institute Symposium on Palaeoclimates) in *Problems of Palaeoclimatology*, Nairn(ed). 332-348pp. London, New York and Sydney, John Wiley and Sons Ltd.

Letreguilly A. 1988. Relationships between mass balance of West Canadian mountain glaciers and meteorological data. *J. Glaciol.*, 34(116), 11-18.

Letreguilly A. and Oerlemans J. 1990. Climate sensitivity: the significance of the altitude mass balance feedback on glaciers and ice sheets. *Annals Glaciol.*, 14, 345.

Letreguilly A. and Reynaud L. 1989. Spatial patterns of mass balance fluctuations of North American glaciers. *J. Glaciol.*, 35(120), 163-168.

Lliboutry L. 1968. General theory of subglacial cavitation and sliding of glaciers. *J. Glaciol.*, 7(49), 21-58.

Lliboutry L. 1974. Multivariate statistical analysis of glacier annual balances. *J. Glaciol.*, 13(69), 371-392.

Lliboutry L 1976. Physical processes in temperate glaciers. *J. Glaciol.*, 16(74), 151-158.

Lliboutry LA. 1987. *Very Slow Flows of Solids,* Martinus Nijhoff Publishers, Dordrecht, 510pp.

Lowe J.J. and Walker M.J.C. 1987. *Reconstructing Quaternary environments (2nd ed.)* Longman, London. 389pp.

Mahaffy, M.A.W. 1976. A three dimensional numerical model of ice sheets: tests on the Barnes Ice Cap, Northwest Territories. *J. Geophys. Res.,* 81(6), 1059-1066.

Manley G. 1955. On the occurence of ice domes and permanently snow covered summits. *J. Glaciol.*, 2(17), 453-456.

Markgraf, V. 1989a. Palaeoclimates in Central and South America since 18000 BP based on pollen and lake-level records. *Quat. Sci. Rev.,* 8, 1-24.

Markgraf, V. 1989b. Reply to C.J.Heusser's 'Southern Westerlies during the Last Glacial Maximum'. *Quat. Res.,* 31, 426-432.

Markgraf, V., Dodson J.R., Kershaw A.P.,McGlone M.S., and Nicholls M. 1992. Evolution of late Pleistocene and Holocene climates in the circum - South Pacific land areas. *Climate Dynam.*, 6, 193-211.

Mazo V.L. 1989. Waves on glacier beds. *J. Glaciol.*, 35(120), 179-182.

McIntyre N.F. 1985. The dynamics of ice sheet outlets. *J. Glaciol.*, 31(108), 99-107.

Meierding T.C. 1982. Late Pleistocene glacial equilibrium line altitudes in the Colorado Front Range: a comparison of methods. *Quat. Res.*, 18, 289-310.

Miller, A. 1976. The climate of Chile. In '*World Survey of Climatology*'. Vol.12, 'Climates of Central and South America' (W.Schwerdtfeger,ed) pp113-145. Elsevier, Amsterdam.

Molnar P. and England P. 1990. Late Cenozoic uplift of mountain ranges and global climate change: chicken or egg? *Nature*, 346, 29-34.

Monin A.S. 1986. *An introduction to the theory of climate.* D. Reidel Publ. Co., 261pp.

Morland L.W. 1976. Glaciers sliding down an inclined wavy bed. *J. Glaciol.*, 17(77), 447-462.

Morland L.W. and Johnson I.R. 1980. Steady motion of ice sheets. *J. Glaciol.*, 25(92), 229-246.

Morland L.W. and Johnson I.R. 1982. Effects of bed inclination and topography on steady state isothermal ice sheets. *J. Glaciol.*, 28 (98), 71-90.

Morley, J.J. and Hays J.D. 1979. Comparison of Glacial and Interglacial oceanographic conditions in the South Atlantic from variations in calcium carbonate and radiolarian distributions. *Quat. Res.*, 12, 396-408.

Nogami, M. 1976. Altitude of the modern snowline and Pleistocene snowline in the Andes. *Tokoyo Metrop. Univ. Geogr. Rep.*, 11, 71-86.

North G.R., Cahalan R.F., and Coakley J.A. 1981. Energy balance climate models. *Rev. Geophys. Space Phys.*, 19(1), 91-121.

Nye J.F. 1951. The flow of glaciers and ice sheets as a problem in plasticity. *Proc. Roy. Soc. London, Series A*, 207, 554-572.

Nye J.F. 1952. A method of calculating the thickness of the ice sheets. *Nature*, 169, 529-530.

Nye J.F. 1957. The distribution of stress and velocity in glaciers and ice sheets. *Proc. Roy. Soc. London, Series A*, 239, 113-133.

Nye J.F. 1959. The motion of ice sheets and glaciers. *J. Glaciol.*, 3(26), 493-507.

Nye J.F. 1960. The response of glaciers and ice sheets to seasonal and climatic changes. *Proc. Roy. Soc. London, Series A*, 256, 559-584.

Nye J.F. 1961. The influence of climatic variations on glaciers. *Int. Assoc. Scient. Hydrol., 54*, 397-404.

Nye J.F. 1963a. On the theory of the advance and retreat of glaciers. *Geophys. J. Roy. Astron. Soc.*, 7, 431-456.

Nye J.F. 1963b. The response of glaciers to changes in the rate of nourishment and wastage. *Proc. Roy. Soc. London, Series A*, 275, 87-112.

Nye J.F. 1965a. The frequency response of glaciers. *J. Glaciol.*, 5(41), 567-587.

Nye J.F. 1965b. A numerical method of infering the budget history of a glacier from its advance and retreat. *J. Glaciol.*, 5(41), 589-607.

Nye J.F. 1965c. The flow of a glacier in a channel of rectangular, elliptic or parabolic cross-section. *J. Glaciol.*, 5 (41), 661-690.

Nye J.F. 1969. The effect of longitudinal stress on the shear stress at the base of an ice sheet. *J. Glaciol.*, 8(53), 207-213.

Oerlemans J. 1980a. Continental ice sheets and the planetary radiation budget. *Quat. Res.*, 14, 349-359.

Oerlemans J. 1980b. Model experiments on the 100,000 year glacial cycle. *Nature*, 287, 430-432.

Oerlemans J. 1980c. On zonal asymmetry and climate sensitivity. *Tellus*, 32, 489-499.

Oerlemans J. 1981. Some basic experiments with a vertically - integrated ice sheet model. *Tellus,* 33, 1-11.

Oerlemans J. 1989. On the response of valley glaciers to climatic change. In: *Glacier Fluctuations and Climatic Change* (ed. by J. Oerlemans), 407-417, Kluwer Academic publishers, Dordrecht.

Oerlemans J. 1991. Modelling the mass balance of the Greenland ice sheet. *The Holocene*, 1(1), 40-49.

Oerlemans, J. 1992. A model for the surface balance of ice masses: part 1: Alpine Glaciers. *Z. Gletscherk. Glazialgeol.* 26 (2)

Oerlemans, J. and Hoogendorn N.C. 1989. Mass - balance gradients and climatic change. *J. Glaciol.*, 35(121), 399-405.

Oerlemans J. and van der Veen C.J. 1984. ***Ice sheets and climate.*** D.Reidel Publ. Dordrecht.

Orowan E. 1949. At "Joint meeting of the British Geological Survey, the British Rheologists Club and the Institute of Metals". *J.Glaciol.*, 1(5), 231-240.

Østrem G. 1966. The height of the glaciation limit in southern British Columbia and Alberta. *Geogr. Ann.*, 48A(3), 126-138.

Østrem G. and Brugman M. 1991. Glacier mass balance measurements. ***Natural Hydrology Research Institute,*** 4. 224pp.

Paterson W.S.B. 1980. Ice sheets and ice shelves. In *Dynamics of Snow and Ice Masses.* (ed.Colbeck S.C.) Academic Press. N.Y. 1-78.

Paterson W.S.B. 1981. *The Physics of Glaciers* (2nd edn.). Pergamon Press, Oxford, 380pp.

Payne A.J. 1988. Modelling former ice sheets. ***PhD Thesis (unpubl.)*** Univ. of Edinburgh.

Payne, A.J. and Sugden D.E. 1990a. Climate and the initiation of maritime ice sheets. *Annals Glaciol.*, 14, 232-237.

Payne A.J. and Sugden D.E. 1990b. Topography and ice sheet growth. *Earth Surf. Processes Landforms,* 15, 625-639.

Payne A.J., Sugden D.E., and Clapperton C.M. 1989. Modelling the growth and decay of the Antarctic peninsular ice sheet. *Quat. Res.*, 31, 119-134.

Peltier W.R. 1982. Dynamics of the ice age Earth. *Advan. Geophys.*, 24, 2-139.

Pelto, M.S., Higgins S.M., Hughes T.J., and Fastook J.L. 1990. Modelling mass balance changes during a glacial cycle. *Annals Glaciol.*, 14, 238-241.

Pittock, A.B. and Salinger M.J. 1991. Southern Hemishere climate scenarios. *Climatic Change,* 18, 205-222.

Pollard D. 1982. A simple ice sheet model yields realistic 100kyr glacial cycles. *Nature*, 296, 334-338.

Porter, S.C. 1981. Pleistocene Glaciation in the Southern Lake District of Chile. *Quat. Res.*, 16, 263-292.

Porter S.C. 1989. Some geological implications of average Quaternary glacial conditions. *Quat. Res.*, 32(3), 245-261.

Prohaska, F. 1976. The climate of Argentina, Paraguay and Uruguay. In '*World Survey of Climatology*'. Vol.12, 'Climates of Central and South America' (W.Schwerdtfeger, ed.) pp13-112. Elsevier, Amsterdam.

Punkari M. 1980. The ice lobes of the Scandinavian ice sheet during the deglaciation in Finland. *Boreas*, 9, 307-310.

Rabassa, J. and Clapperton, C.M. 1990. Quaternary Glaciations of the Southern Andes. *Quat. Sci. Rev.*, 9, 153-174.

Raschke E., Vonder Haar T.H., Bandeen W.R., and Pasternak M. 1973. The annual radiation balance of the earth-atmosphere system during 1969-70 from Nimbus-3 measurements. *J. Atmos. Sci.*, 30, 341-364.

Raymo M.E. and Ruddiman W.F. 1992. Tectonic forcing of the late Cenozoic climate. *Nature*, 359, 117-122.

Reynaud L., Vallon M., Martin S., and Letreguilly A. 1984. Spatio temporal distribution of the glacial mass balance in the Alpine, Scandinavian and Tien Shan areas. *Geogr. Ann.*, 66A(3), 239-247.

Robin G.de Q. 1967. Surface topography of ice sheets. *Nature*, 215, 1029-1032.

Robinson E.S. 1966. On the relationship of ice surface topography to bed topography on the south polar plateau. *J. Glaciol.*, 6(43), 43-54.

Ruddiman, W.F., McIntyre A., Niebler-Hunt V., and Durrazzi J.T. 1980. Oceanic evidence for the mechanism of rapid Northern Hemisphere glaciation. *Quat. Res.*, 13, 33-64.

Saltzman B. 1983. Climate systems analysis. *Advan. Geophys.*, 25, 173-233.

Saltzman B. 1985. Paleoclimatic modelling. In: *Paleoclimatic Analysis and Modelling*, (ed. A.D. Hecht), Wiley- Interscience publishers. 341-396.

Saltzman B., Hansen A.R. and Maasch K.A. 1984. The Late Quaternary glaciations as the response of a three - component feedback system to Earth orbital forcing. *J. Atmos. Sci.*, 41(23), 3380-3389.

Saltzman B. and Sutera A. 1984. A model of the internal feedback system involved in Late Quaternary climatic variations. *J. Atmos. Sci.*, 41(5), 736-745.

Schweizer J. and Iken A. 1992. The role of bed seperation and friction in sliding over an undeformable bed. *J. Glaciol.*, 38(128), 77-92.

Schwerdtfeger, W. 1976. The atmospheric circulation over Central and South America. In '*World Survey of Climatology*'. Vol.12, 'Climates of Central and South America' (W.Schwerdtfeger, ed.) pp1-12. Elsevier, Amsterdam.

Sellers W.D. 1965. *Physical Climatology*. Univ. of Chicago Press. 272pp.

Sellers W.D. 1969. A global climate model based on the energy balance of the earth-atmosphere system. *J. Applied Meteorology*, 8, 392-400.

Schytt V. 1967. A study of 'ablation gradient'. *Geogr. Ann.*, 49A(2-4), 327-332.

Sergin V. Ya. 1979. Numerical modelling of the glaciers-ocean-atmosphere global system. *J. Geophys. Res.*, 84(C6), 3191-3204.

Sissons J.B. 1981. The last Scottish ice-sheet: facts and speculative discussion. *Boreas*, 10, 1-17.

Summerfield M.A. 1991. *Global Geomorphology*. Longman, Singapore. 537pp.

Sutherland D.G. 1984. Modern glacial characteristics as a basis for inferring former climate with particular reference to the Loch Lomond stadial. *Quat. Sci. Rev.*, 3, 291-309.

Thom R. 1975. *Structural stability and morphogenesis*. Benjamin, Reading, MA.

Thomas R.H. 1979. The dynamics of marine ice sheets. *J. Glaciol.*, 24(90), 167-177.

Van den Dool H.M. 1980. On the role of cloud amount in an energy balance model of the Earth's climate. *J. Atmos. Sci.*, 37(5), 939-946.

Van der Veen C.J. 1985. Response of a marine ice sheet to changes in the grounding line. *Quat. Res.*, 24(3), 257-267.

Van der Veen C.J. and Whillans I.M. 1989a. Force budget: I: theory and numerical methods. *J. Glaciol.*, 35(119), 53-60.

Van der Veen C.J. and Whillans I.M. 1989b. Force budget: II: application to two-dimensional flow along Byrd Station strain network, Antarctica. *J. Glaciol.*, 35(119), 61-67.

Vialov S.S. 1958. Regularities of glacial shield movements and the theory of plastic viscous flow. *Int. Assoc. Scient. Hydrol.*, 47, 266-275.

Villagran, C. 1988. Expansion of Magellanic moorland during the Late Pleistocene: Palynological evidence from northern Isla de Chiloe, Chile. *Quat. Res.*, 30, 304-314.

Walraven, R. 1978. Calculating the position of the sun. *Solar Energy,* 20, 393-397.

Warren C.R. 1992. Iceberg calving and the glacio-climatic record. *Progress in Physical Geography*, 16(3), 253-282.

Weertman J. 1957. On the sliding of glaciers. *J. Glaciol.*, 3(21), 33-38.

Weertman J. 1961. Equilibrium profile of ice caps. *J. Glaciol.*, 3(30), 953-964

Weertman J. 1964. Rate of growth or shrinkage of non-equilibrium ice sheets. *J. Glaciol.*, 5(38), 145-158.

Weertman J. 1973a. Position of ice divides and ice centres on ice sheets. *J. Glaciol.*, 12(66), 353-360.

Weertman J. 1973b. Creep of ice. In Walley E., Jones S.J., and Gold L.W. (eds.) *Physics and chemistry of ice*. Royal Soc. of Canada, Ottawa, Canada. 320-337.

Weertman J. 1976. Milankovitch solar radiation variations and ice age ice sheet sizes. *Nature,* 261, 17-20.

Weertman J. 1979. The unsolved general glacier silding problem. *J. Glaciol.*, 23(89), 97-115.

Whillans I.M. and Johnsen S. J. 1983. Longitudinal variations in glacier flow: theory and test using data from the Byrd Station strain network, Antarctica. *J. Glaciol.*, 29(101), 78-97.

Whillans I.M., Chen Y.H., van der Veen C.J. and Hughes T.J. 1989. Force budget III: application to three dimensional flow of Byrd glacier, Antarctica. *J. Glaciol.*,35(119), 68-80.

Williams L.D. 1975 The variation of corrie elevation and equilibrium line altitude with aspect in Eastern Baffin Island, N.W.T., Canada. *Arctic and Alpine Res.*, 7(2), 169-181.

Williams, L.D. 1979. An energy balance model of potential glacierization of Northern Canada. *Arctic and Alpine Res.*, 11(4), 443-456.

Zeeman E.C. 1977. *Catastrophe Theory: Selected Papers 1972-1977.* Addison-Wesley Publ. Co., Reading, MA.

APPENDIX 1:
MATHEMATICAL SYMBOLS AND PARAMETER VALUES USED IN THESIS

A. The Surface Energy Balance Model

M		metres	Snow accumulated or ablated
B		W/m^2	Energy at surface
L	334000	J/kg	Latent heat of melt
P		metres	Precipitation
Q		W/m^2	Incoming shortwave radiation
α		-	albedo (reflectance) of surface
I_ι		W/m^2	Incoming longwave radiation
I_o	316	W/m^2	Outgoing longwave radiation
F_s		W/m^2	Turbulent flux of sensible heat
F_l		W/m^2	Turbulent flux of latent heat
S	1353	W/m^2	Solar constant
N		-	Number of days
τ_a		-	Atmospheric transmissivity
τ_c		-	Cloud transmissivity
h	0-1400	metres	Altitude above mean sea level
γ		radians	Angular position of sun
n		-	Cloud cover (tenths)
I_{at}		W/m^2	Longwave radiation contributed by the atmosphere
ε_a		-	Emittance of the atmosphere
σ	5.7×10^{-8}	$W/m^2/K^4$	Stefan Boltzman constant
Θ_a		K	Atmospheric temperature
I_{cl}		W/m^2	Longwave radiation contributed by clouds
ε_{cl}	0.7	-	Emittance of clouds
Θ_{cl}		K	Cloud temperature
f		-	Fraction of emitted black body radiation
α_b		-	Background albedo of region
E		metres	Altitude of equilibrium line

α_{sn}	0.72	-	Albedo of snow
δ		metres	Depth of snow through year
Mn		metres	Accumulated seasonal melt of snow
C		$W/(m^2K)$	Exchange coefficient for turbulent fluxes
Θ_s		K	Temperature at the surface
C_E	10	$W/(m^2K)$	Exchange coefficent at the equilibrium line
dC/dh	0.002	$W/(m^2K)$	Altitudinal gradient of the exchange coefficient
L	2478000	J/kg	Latent heat of vapourisation
q_a		-	Mixing ratio of water vapour in the atmosphere
q_s	4.3×10^{-3}	-	Mixing ratio of water vapour at the surface
c_p	1005	J/kg/K	Heat capacity of air
Tδ	Tuned	K	Daily temperature range
•T/dh	7.5	K/km	Temperature lapse rate
•P/dh	150	%/km	Altitudinal precipitation gradient
N_c	Tuned	-	Mean fraction of cloud cover
N_h	Tuned	metres	Mean height of cloud base
T		K	Annual temperature cycle

B. The Regional Energy Balance Model

R		W/m^2	Regional surface radiation budget
Q		W/m^2	Averaged daily quantity of shortwave radiation
I		W/m^2	Net longwave radiation emitted to space
Io		W/m^2	Longwave radiation emitted from the oceanic region
Ic		W/m^2	Longwave radiation emitted from the continental region
Ao	180	W/m^2	Empirically derived longwave constant
Ac	189	W/m^2	Empirically derived longwave constant
Θ		K	Surface temperature of the oceanic region

T		K	Surface temperature of the continental region
B	2.04	$W/(m^2K)$	Empirically derived longwave constant
C	-38.8	W/m^2	Empirically derived longwave constant
N_o		-	Cloud cover as a function of latitude in oceanic regions
N_c		-	Cloud cover as a function of latitude in continental regions
C_o	1.0×10^{-3}	J/kg/K	Heat capacity of the oceanic region
C_l	2.38×10^{-4}	J/kg/K	Heat capacity of the continental regions
k	Tuned	$W/(m^2K)$	Latitudinal heat flux coefficient for the oceanic region
k'	0.6 x k	$W/(m^2K)$	Latitudinal heat flux coefficient for the continental region
E	Tuned	$W/(m^2K)$	Zonal heat flux coefficient
μ	0.1	-	Zonal fraction of land area to total area
α_s		-	Clear sky albedo
	0.61	-	- snow cover
	0.56	-	- ice cover
	0.22	-	- bare land
	0.13	-	- open sea
α_{cl}	0.48	-	Cloud albedo

C. The Ice Sheet Model

h		metres	Ice thickness
b		metres	Annual net mass balance at surface
q_x		m^3/year	Ice flux in the subscripted direction
ε		-	Effective strain rate
A	5.3×10^{-33}	$/s/kPa^3$	Flow law multiplier
n	3	-	Flow law power
τ		kPa	Effective stress
A_o		-	Arrhenius relation multiplier

Q	139	kJ/mol	Activation energy for creep in ice
R	8.314	J/mol/K	Gas constant
T		K	Temperature of material
σ		kPa	Normal stress on a body of ice
τ		kPa	Shear stress on a body of ice
ρ	870	kg/m^3	Density of ice (assumed constant)
g	9.81	m/s/s	Acceleration due to gravity
h_s		metres	Ice surface elevation
x,y,z		-	Coordinate system
α		radians	Surface ice slope in the direction of flow
U_s		m/s	Sliding velocity
κ_2	5.0×10^6	$m^3/(kPa.a)$	Sliding law multiplier
τ_b		kPa	Basal shear stress
Z*		m	Normal load at the base of ice

C. The Computer Model

H		metres	Ice surface elevation
i,j	5	km	Grid unit denoting the x- and y-direction
G		m^3/year	Horizontal variation of ice flux
t	1	years	Time step
α'		radians	Maximum surface slope
U'	2.0	km/a	Maximum deformation velocity
Z'		metres	Maximum ice thickness
x,y,z		-	Coordinate system subscripts

E. The Topography Model

τ_b		kPa	Basal shear stress
ρ	870	kg/m^3	Density of ice (assumed constant)
g	9.81	m/s/s	Acceleration due to gravity
h		metres	Ice thickness

α		radians	Ice surface slope parallel to the bedrock
H		metres	Maximum ice thickness
τ_o	100	kPa	Yield stress (above which ice flows)
L		metres	Length of glacier
x		metres	Distance from centre to margin of glacier
ζ		m/a/m	Mass balance gradient
Λ		m^2	Accumulation area
β		m^2	Ablation area
η		metres	Altitudinally weighted depth of snow

APPENDIX 2:
EQUATIONS USED IN THESIS

A. The Surface Energy Balance Model

(2.1) $$M = \int [-B/L + P]\, \delta t$$

(2.2) $$B = Q(1-\alpha) + I_t + I_o + F_s + F_l$$

(2.3) $$S = 1353. [\, 1 + 0.034\cos (2\pi N/365) \,]$$

(2.4) $$\tau_a = (0.79 + 0.000024h) [1 - 0.009 (90 - \gamma)]$$

(2.5) $$\tau_c = 1 - (0.41 - 0.000065h) n - 0.37 n^2$$

(2.6) $$Q = [\, S \sin\gamma \,] \tau_a \tau_c$$

(2.7) $$I_{at} = \varepsilon_a \sigma \Theta^4_a$$

(2.8) $$\varepsilon_a = 0.7 - 0.000025h$$

(2.9) $$I_{cl} = n\varepsilon_{cl} \sigma f \Theta^4_{cl}$$

(2.10) $$f = 0.6732 + 0.0024\Theta_{cl} - 0.914\times10^{-5}\Theta^2_{cl}$$

(2.11) $$I_t = I_{at} + I_{cl}$$

(2.12) $$\alpha_b = 0.115 \operatorname{arctg} (h - E + 300 / 200) + 0.48$$

(2.13) $$\alpha = \max [\, 0.12; \alpha_{sn} - (\alpha_{sn} - \alpha_{b)}\, e^{-5\delta} - 0.015Mn \,]$$

(2.14) $$F_s = C (\Theta_a - \Theta_s)$$

(2.15) $$C = C_E + (E - h)\, dC/dh$$

(2.16) $$F_l = C L (q_a - q_s) / c_p$$

B. The Regional Energy Balance Model

(2.17) $Q(1 - \alpha) + \text{div} (\text{horizontal heat fluxes}) = I$

(2.18) $R = Q (1 - \alpha) + I$

(2.19) $I_o = A_o + B\theta + CN_o$

(2.20) $I_c = A_c + BT + CN_c$

(2.21) $C_o \partial\theta/\delta t = R_o - k\theta + \mu E(T - \theta)$

(2.22) $C_l \partial T/\delta t = R_l - k'T + E(\theta - T)$

C. The Ice Sheet Model

(2.23) $\partial h/\partial t = b - [\partial q_x/\partial x + \partial q_y/\partial y]$

(2.24) $\varepsilon = A\tau^n$

(2.25) $A = A_o \exp(-Q/RT)$

(2.26) $\partial\sigma_x/\partial x + \partial\tau_{xy}/\partial y = 0$

(2.27) $\partial\sigma_y/\partial y = \rho g$

(2.28) $\partial\tau_{yz}/\partial z + \partial\sigma_z/\partial z = 0$

(2.29) $\sigma_y = \sigma_x = \sigma_z = -\rho g (h_s - y)$

(2.30) $\tau_{xy} = -\rho g (h_s - y) (\partial h_s/\partial x)$

(2.31) $\tau_{yz} = -\rho g (h_s - y) (\partial h_s/\partial z)$

(2.32) $q_{x,z} (x,z,t) = (-2A/(n+1)) (\rho g)^n \alpha^{n-1} (\partial h_s/\partial x,\partial z) h^{n+2} + hU_s (x,z,t)$

(2.33) $\alpha = \sqrt{[\ (\partial h_s/\partial x)^2 + (\partial h_s/\partial z)^2\ ]}$

(2.34) $Us = \kappa_2 . \tau_b / Z^{*2}$

D. The Computer Model

(2.35) $\partial H/\partial x \Rightarrow (\ H_{i+1} - H_{i-1}\ )/\Delta x$

(2.36) $\partial H/\partial t = G \quad \Rightarrow \quad H_{t+1} = H_t + \Delta t.G$

(2.37) $\Delta t_{max} = (\Delta x)^2 |\ \alpha'|\ /\ (2U'Z'n)$

E. The Topography Model

(5.1) $\tau_b = \rho g h \sin\alpha$

(5.2) $H = \sqrt{(2\tau_o L/\rho g)}$

(5.3) $h^2 = (2\tau_o/\rho g)(L - x)$

(5.4) $\zeta_a/\zeta_b = \Lambda\eta_b/\beta\eta_a$

APPENDIX 3:
COMPUTER PROGRAMME LISTINGS

A. Surface energy balance model

```
      Program Balance
      implicit none
      integer day,min,count,prectime,stable,z,rundata
      real skyemiss,height,f,cltemp,Lv,Lm,n2,dtemp,ttemp,
     *  surftemp,lapse,clheight,n,mexco,dCdh,exco,Cp,totprec,
     *  transa,transc,solel,q,S,alback,ela,pi,preclapse,
     *  albedo,albsnow,depth,melt,iin,iout,icl,solar,massbal,
     *  solrad,clemitt,alb,pvo,pva,mixing,daytemp,whenprec,
     *  acmelt,Fs,Fl,B,precip,precipitation,initela,pvaz,
     *  htela(16),y,sbc,hpela(16),seasurftemp,soldeg,rad,
     *  converge
      character*60 balfile,tempfile
      logical first,fst
      parameter (clemitt=0.7,mexco=10.0,dCdh=0.002,solar=
     *  1353.0,iout=316.0,clheight=1500.0,n=0.7,pi =
     *  3.1415927,albsnow=0.72,n2=n*n,dtemp=6.0,
     *  Cp=1005,pvo=4.3E-3,Lm=334000.0,Lv=2478000.0,
     *  whenprec=5.0,rad=0.017453293,pva=4.2E-3,sbc=5.67E-8)
c_____ for details of variables see Oerlemans(1990)
c_____ Energy balance model: B=Q(1-alb)+iin+iout+Fs+Fl
c_____ surftemp is temp at surface, not surface temp!
c_____ glacier surface temp assumed = 0 degrees for turbulent
c_____ flux calc. Precip varies with altitude and falls in
c_____ constant events every 5 days
      first = .true.
      fst = .true.
      z = 1
      type*,' Output file? '
      read(*,21)balfile
21    format(a)
      type*,' Temperature file? '
      read(*,21)tempfile
      write(*,10)
10    format( '  Model run : ', $)
      read*,rundata
      write(*,11)
11    format( '  Tot prec : ', $)
```

```
      read*,totprec
      initela = 1500.0
      open(unit=9,file=balfile,status='new',
     *     form='formatted')
      open(unit=12,file=tempfile,status='old',form
     *     ='formatted')
      write(9,*)rundata,totprec
      do 301 converge = 1,2
      do 300 height = 600,2000,100
      day = 220
      min = 0
  100 continue
      if (first) then
        do 101 ttemp = 0,219
          read(12,*)seasurftemp
  101     continue
      endif
      read(12,*)seasurftemp
c     prectime = int(day/whenprec)
c     if (day.eq.prectime*whenprec) then
c       precipitation = precip/3504.0
c     else
c       precipitation = 0.0
c     endif
      if (day.le.75.or.day.gt.335) then
        lapse = 0.006
      else
        if (day.gt.75.and.day.lt.90) then
          lapse = 0.006 +((day-75)*0.000066)
        else
          lapse = 0.007
        endif
      endif
c_____ do 200 min = 0,1410,30
  200 continue
      daytemp = (seasurftemp+273.15) - (lapse*height)
      if (first) then
        ela = initela
        first = .false.
      endif
c_____ dtemp is daily temp range to give diurnal temp variations
        surftemp = daytemp + (dtemp/2)*sin(0.0043633*
     *       (min-525))
```

```
c_____ solar radiation calculated every half hour
      call elevation(day,min,solel)
      S = solar*(1 + 0.034*cos(2*pi*day/365.25))
      if (solel.lt.0.0) then
        solel = 0.0
      endif
      q = S*sin(solel)
      soldeg = solel/rad
      transa = (0.79 + 0.000024*height) * (1 - 0.009*
     *       (90 - soldeg))
      transc = 1 - (0.41 - 0.000065*height)*n - 0.37*n2
      solrad = q*transa*transc
c_____ longwave radiation from sky & clouds calculated
      cltemp = (seasurftemp+273.15) - (lapse*clheight)
      skyemiss = 0.7 + 0.000025*height
      f =-0.6732 + 0.00624*cltemp - (0.914E-5*cltemp**2)
      icl = clemitt*n*f*sbc*cltemp**4
      iin = skyemiss*sbc*surftemp**4 + icl
c_____ calc. for background & actual albedo at surface
      alback = 0.115*atan((height - ela + 300)/200) + 0.48
      alb = albsnow - alback
      albedo = albsnow - (alb*exp(-5*depth)
     *                    + (0.015*acmelt))
      if (albedo.lt.0.12) then
        albedo = 0.12
      endif
c_____ turbulent fluxes set proportional to air temp. Glacier
c_____ surface is assumed to = 0 degrees(melting).Lv is latent
c_____ heat of vaporisation,Cp is specific heat capacity of air
c_____ exco is exchange coeff.,dependent on height,mixing is
c_____ water vapour density difference(surface/air).See Kuhn(1984)
c_____ pvaz is pva changing with height
      exco = mexco + ((ela-height)*dCdh)
      Fs = exco*(surftemp-273.15)
      pvaz = pva + (-1.5E-6*(height-ela))
      mixing = pvaz - pvo
      Fl = (Lv*exco*mixing)/Cp
c_____ energy balance
c_____ melt is snow melted (always -ve)
      B = solrad*(1-albedo) + iin - iout + Fs + Fl
      melt = -B/Lm
      if (melt.gt.0.0) then
        melt = 0.0
```

```
      endif
c_____ precipitation amount every 5 days and adjusted for
c_____ height
      prectime = int(day/whenprec)
       preclapse = 0.0005 * totprec
       precip = totprec + (height*preclapse)
       if ((day.eq.prectime*whenprec).and.(surftemp-273.15)
     *     .lt.2.0) then
           precipitation = precip/3504.0
         else
           precipitation = 0.0
       endif
       massbal = massbal + melt + precipitation
       acmelt = acmelt + melt
       depth = depth + precipitation + melt
       if (depth.lt.0.0) then
         depth = 0.0
       endif
c_____ end minute loop
       min = min + 30
       if (min.eq.1440) then
         min = min - 1440
       else
         goto 200
       endif
c_____ end day loop
       day = day + 1
       if (day.eq.365) then
         day = day - 365
         rewind(unit=12)
       end if
       if (day.eq.219) then
           goto 109
         else
           goto 100
       end if
c_____ adjust ela to glaciation line
109    continue
       htela(z) = massbal
       if (fst) then
         if (massbal.gt.0.0) then
           hpela(z) = htela(z) - htela(z-1)
           y = -htela(z-1)/hpela(z)
```

```
            ela = (height-100) + (y*100)
            fst = .false.
          endif
        endif
        if (z.eq.15) then
          z = z - 15
          fst = .true.
        endif
        z = z + 1
        write(9,*)height,massbal,ela
        massbal = 0.0
        acmelt = 0.0
        precipitation = 0.0
        depth = 0.0
300     continue
301     continue
        close(9,disp='save')
        close(12,disp='save')
        end

c       Calculate solar elevation through year
        subroutine elevation(day,min,solel)
        implicit none
        integer day,min
        real theta,g,el,eps,sel,decl,h,phi,e,rad,ra,st,
     *    q,pi,lat,a1,a2,pi2,long,time,solel,
     *    locals,t
        parameter (pi=3.1415927,pi2=2*pi,rad=0.017453293,
     *     lat=55.0,long=0.0)
c_____ el-longitude of sun,g-mean anomaly of earth,eps-angle
c_____ between plane of ecliptic & celestial equator,decl-
c_____ declination of sun,h-hour angle,e-local elevation of
c_____ sun,phi-local lat.,st-siderial time,locals-local
c_____ siderial time
        t = min/60
        time = day + t/24
        theta = 360.0*(time/365.25)*rad
        g = -0.031271 - 4.53963E-7*time + theta
        el = 4.900968 + 3.67474E-7*time + (0.033434 - 2.3E-9
     *     *time) * sin(g) + 0.000349*sin(2.0*g) + theta
        eps = 0.409140 - 6.2149E-9*time
        sel = sin(el)
        a1 = sel * cos(eps)
```

```
      a2 = cos(el)
      ra = atan2(a1,a2)
      if (ra.lt.0.0) ra = ra + pi2
      decl = asin(sel*sin(eps))
c_____ st is siderial time,locals is local time relative
c_____ to GMT
      st = 1.759335 + pi2*(time/365.25) + 3.694E-7*time
      if (st.ge.pi2) st = st - pi2
      locals = st + 1.0027379*t*15.0*rad
      if (locals.ge.pi2) locals = locals - pi2
      h = ra - locals
      phi = lat*rad
c_____ e is sun elevation
      e = asin(sin(phi)*sin(decl) + cos(phi)*cos(decl)*
     *                              cos(h))
      if (sin(e).ge.sin(decl)/sin(phi)) solel = e
c____  solel = solel/rad
      continue
      return
      end
```

B. Regional energy balance model

```
    Program Energy
    implicit none
    integer i,j,rundata,loop
    real Ac,Ao,c,b,seacl,landcl,seaca,landca,albcl,albsea,
     *   oceanalb,albland,contalb,eqtemp,dampings,htcapo,u,E,
     *   k,htcapc,oexco,cexco,insl,initc,inito,ltemp,stemp,
     *   ocins,ocir,contins,contir,dsea,dcont,icont,iocean,Eo,
     *   q,k1,dampingl,eqtemps,eqtempl,inpl,sol
      logical first,choice
      common/log/first
     *    /solar/sol
      parameter (C=-38.8,seacl=0.78,Ao=180.0,Ac=189.0,landcl=
     *   0.66,B=2.04,albcl=
     *   0.48,albsea=0.13,oceanalb=albcl*seacl+albsea*0.22,
     *   u=0.1,htcapo=2.38E-4,htcapc=1.00E-3,
     *   initc=6.0,inito=8.0)
      write(*,5)
5     format( ' E= ',$)
```

```
      read(*,*)E
      write(*,7)
7     format( ' k= ',$)
      read(*,*)k
c     write(*,6)
c     format( ' Model run: ',$)
c     read*,rundata
      seaca=Ao+C*seacl
      landca=Ac+C*landcl
      Eo=u*E
      k1= 0.6*k
      open(unit=8,file='temp.dat',status='new',form=
     *     'formatted')
c     write(8,*)rundata,E,k,Ao,Ac
      first=.true.
      stemp=inito
      ltemp=initc
c____ do 200 i=1,2
      do 100 j=0,728
c_____ obtain insolation values from subroutine
      loop = loop + 1
      choice=.true.
      call solar(j,q,choice)
c_____ calc. insolation for ocean & continent; cont. depends
c_____ on whether snow is present(for albedo)
      ocins = q*(1-oceanalb)
      if (ltemp.lt.0.0) then
        albland = 0.61
       else
        if (ltemp.ge.0.0.and.ltemp.le.2.0) then
          albland = 0.61 - (0.195*ltemp)
         else
          albland = 0.22
        end if
      end if
      contalb = albcl*landcl+albland*(1-landcl)
      contins = q*(1-contalb)
c_____ longwave radiation is found for sea &land
      ocir = seaca+B*stemp
      contir = landca+B*ltemp
c_____ heat input from NH is calculated (from 35 degrees)
      call equiltemp(j,eqtemps,eqtempl)
      dampings = k*(eqtemps-stemp)
```

```
      dampingl = k1*(eqtempl-ltemp)
c_____ calc. exchange of heat between land & sea
      oexco = Eo*(ltemp-stemp)
      cexco = E*(stemp-ltemp)
c_____ calc. gradient of temp change for land &sea
c_____ and find new temp for following day
      dsea = htcapo*((ocins-ocir)+(dampings)+oexco)
      dcont = htcapc*((contins-contir)+dampingl+cexco)
      stemp = stemp+dsea
      ltemp = ltemp+dcont
      if (loop.gt.364) then
      write(8,*)ltemp
      end if
c_____ format(i4,x,2f6.3)
100   continue
c00   continue
      close(unit=8,disp='save')
      end

      subroutine solar(j,q,choice)
      implicit none
      integer j
      real time,theta,g,el,eps,sel,decl,inpl,h,phi,
     *     e,rad,b,b1,b2,q,pi,day,lat,sol
      logical choice
      common/solar/sol
      rad=0.017453293
      pi = 3.1415927
      sol=1353.0
      if (choice) then
        lat = 55.0
       else
        lat = 35.0
      endif
c_____ for details of variables see Walraven(1978) & Monin(198?)
      day = j
      time = day + 0.5
      theta = 360.0*(time/365.25)*rad
      g = -0.031271-4.53963E-7*time+theta
      el = 4.900968+3.67474E-7*time+(0.033434-2.3E-9*time)
     *     *sin(g)+0.000349*sin(2.0*g)+theta
      eps = 0.409140-6.2149E-9*time
      sel = sin(el)
```

```
      decl = asin(sel*sin(eps))
      b1 = tan(decl)
      phi = lat*rad
      b2 = -tan(phi)
      h = acos(b1*b2)
      e = h*sin(phi)*sin(decl)+cos(phi)*cos(decl)*sin(h)
      inpl = sol*(1+ 0.034*cos((2*pi*day)/365.25))
c_____ q is the insolation at the top of the atmosphere for any
c_____ given day of the year(j) at lat. 55  N
      q = inpl*e/pi
      continue
      return
      end

      subroutine equiltemp(j,eqtemps,eqtempl)
      implicit none
      integer j
      real startemps,eqtemps,eqtempl,eqocins,eqocir,eqcontir,
     *     heatcapo,heatcapc,startempl,eqcontins,eqocalb,avq,
     *     eqcontalb,eqseaca,eqcontca,B,eqoexco,eqcexco,eqEo,
     *     eqE,eqdsea,eqdcont
      logical first,choice
      common/log/first
      parameter (eqocalb=0.301,eqcontalb=0.307,startemps=13.0,
     *      eqseaca=209.3,eqcontca=215.2,eqE=10.0,startempl=
     *      10.0,eqEo=0.4*eqE,heatcapo=2.38E-4,heatcapc=2.38E-3,
     *      B=2.04)
c_____ oc,o,sea=ocean;cont,c=continent;eq,av=NH equil value;
c_____ alb=albedo,cld=cloud,ca=Ax+C*N N-cld(from I)
c_____ values taken from van den Dool(1980)
c_____ sets equilibrium temp with an initial value
      if (first) then
        eqtemps=startemps
        eqtempl=startempl
        first=.false.
      endif
c_____ calls subroutine solar & calculates q for 35 degrees
      choice = .false.
      call solar(j,avq,choice)
c_____ av.radiation balance for land & sea at 35 degrees
c_____ as above: temp change = (q(1-alb)-Io)*1/heatcap
c_____ insolation for land & sea
      eqocins =avq*(1-eqocalb)
```

```
      eqcontins =avq*(1-eqcontalb)
c_____ longwave radiation for sea & land
      eqocir = eqseaca + B*eqtemps
      eqcontir = eqcontca + B*eqtempl
c_____ calc. exchange between land & sea
      eqoexco = eqEo*(eqtempl-eqtemps)
      eqcexco = eqE*(eqtemps-eqtempl)
c_____ grad. of temp change
      eqdsea=heatcapo*((eqocins-eqocir)+eqoexco)
      eqdcont=heatcapc*((eqcontins-eqcontir)+eqcexco)
      eqtemps = eqtemps + eqdsea
      eqtempl = eqtempl + eqdcont
      continue
      return
      end
```

C. Coupled climate - ice sheet model

```
      program budd
      implicit none
      integer region(91,81)
      real ice1(91,81),ice2(91,81),mbtop(91,81),ice3(91,81),
     +    precip(91,81),
     +    thick(91,81,2),topog(91,81),nrtopog(91,81),
     +    strain(91,81,2),velbar(91,81,2),intopog(91,81),
     +    acvol,b,calved,calvol,delsea,deltemp,timelp,time,
     +    topel,tsea,ttemp,vol,avelev,inelev,newsea,oldsea,
     +    dtin,dt,number,whenpt,whenpr,whensmth,whensea,
     +    w,meltcnt,meltmax,meltmin,ro,row,pi,romiw,wsq,
     +    whentmp,elevscale,maxmelt,yy,
     +    clime,whenclime,netbal,regbal(4,16),ela
      integer i,j,k,l,maxx,maxy,nosea,notemp,perimno,plot,print,
     +       sea,smth,temp
      logical flag,floater(91,81),first/.true./
      character*40 topnam,prenam,outnam,tempnam,nmbnam,zednam,
     +           stdnam1,stdnam2,stdnam3,seanam
      parameter (dtin=0.0,dt=2.5,number=2000.0,
     +         whenpt=200.0,whenpr=50.0,
     +         whensmth=200.0,whensea=100.0,
     +         w=5.0,wsq=w*w,pi=3.14159,whenclime=100.0,
     +         meltcnt=0.5e-3,meltmin=meltcnt*dt,
```

```
     +        ro=870.0,row=1025.0,maxmelt=meltcnt*dt*4,
     +        romiw=1.0-ro/row,elevscale=1.0)
      common /iandj/ i,j
     +     /grdsz/ maxx,maxy
     +     /kandl/ k,l
     +     /fltlog/ floater
     +     /balance/ topel,deltemp
     +     /netmass/ netbal
     +     /volume/ vol,avelev,newsea
     +     /calving/ calved,calvol,acvol
     +     /icesheet/ thick
     +     /updown/ intopog
     +     /ground/ topog
     +     /nground/ nrtopog
     +     /area/yy
     +     /balela/ela
c     get relevant data files
      write(6,10)
10    format(//' Programme to determine icesheet dynamics '/
     +' from topography,climate,ocean temperature'/
     +' history and sea level history.'//
     +' Flow topography file name : ',$)
      read(5,20)topnam
20    format(a)
      write(6,30)
30    format(' Mass balance topography file name : ',$)
      read(5,20)nmbnam
c     reads in flow topography, net mass balance
c     topography
      flag=.true.
      call gdfil(topnam,topog,flag)
      call gdfil(nmbnam,mbtop,flag)
      do 50 i=1,maxx
        do 60 j=1,maxy
          mbtop(i,j)=topog(i,j)+elevscale*(mbtop(i,j)-topog(i,j))
60      continue
50    continue
      write(6,70)
70    format(' Ice thickness file name (n if none) : ',$)
      read(5,20)zednam
      if (zednam.eq.'N') zednam='n'
c     allows start-up icesheet
      if (zednam.ne.'n') then
```

```
      call gdfil(zednam,ice1,flag)
      do 80 i=1,maxx
        do 90 j=1,maxy
          if (ice1(i,j).lt.0) then
            thick(i,j,1)=0.
          else
            thick(i,j,1)=ice1(i,j)
          end if
90        continue
80      continue
      end if
       write(6,100)
100   format(' File for thickness output : ',$)
      read(5,20)stdnam1
      write(6,110)
110   format(' File for velocity output : ',$)
      read(5,20)stdnam2
      write(6,115)
115   format(' File for bedrock output : ',$)
      read(5,20)stdnam3
      write(6,120)
120   format(' File for ice fluxes : ',$)
      read(5,20)outnam
       write(6,140)
140   format(' File with sea level history : ',$)
      read(5,20)seanam
c     the sea level files are opened
      open(unit=10,file=seanam,type='old',form='formatted')
      read(10,*)nosea
      write(6,145)
145   format(' Original topography : ',$)
      read(5,20)topnam
      call gdfil(topnam,intopog,flag)
c     calculates INELEV which is an estimate of the area above -0.2
c     km and writes this to screen
      do 85 i=2,maxx-1
       do 95 j=2,maxy-1
         if (intopog(i,j).gt.-0.2)
     +       inelev=inelev+intopog(i,j)
95      continue
85    continue
      write(6,105)inelev
105   format(/' Sea level avelev=',f12.3)
```

```
c     opens output file for ice fluxes
      open(unit=8,file=outnam,type='new',form='formatted')
      write(8,*)int(number/whenpr+1)
       k=2
      l=1
      timelp=dtin
       flag=.false.
c     main loop starts
c     k and l refer to two layers in thick grid
c     swapping them is necessary for integration
c     round loop variable as wanders
 330  continue
       if (k.eq.1) then
         k=2
         l=1
      else
         k=1
         l=2
      end if
      time=nint(timelp/dt)*dt
c     if time for another sea level and not
c     at end of file then reads it
       sea=int(time/whensea)
      if (time.eq.sea*whensea.and.
     +    tsea.lt.nosea*whensea) then
190     read(10,170)tsea,newsea
170     format(2f12.3)
        delsea=newsea-oldsea
        oldsea=newsea
        if (tsea.lt.dtin) goto 190
        do 200 i=1,maxx
          do 210 j=1,maxy
            topog(i,j)=topog(i,j)+delsea
            mbtop(i,j)=mbtop(i,j)+delsea
210         continue
200       continue
      end if
c____ define region(i,j) depending on sea-level
c____ and topography: continentality.
       do 305 i = 1,maxx
        do 306 j = 1,maxy
          if (topog(i,j).ge.0.0) then
            if (i.lt.45.and.j.gt.40) then
```

```
            region(i,j) = 1
            yy = 1
          else
            if (i.ge.45.and.j.gt.40) then
              region(i,j) = 3
              yy = 3
                else
              region(i,j) = 2
              yy = 2
            end if
          end if
        end if
306     continue
305   continue
c____ if time to call climate change subroutine
      clime = int(time/whenclime)
      if (time.eq.0) then
        continue
      else
      if (time.eq.clime*whenclime) then
        call climate(regbal)
      end if
      end if
c     basal melt function determined internally.It is
c     either 0.5m/a (sub-polar) or 2m/a(polar).
     if (time.le.7000.0) then
        meltmax=meltmax
      else
        if (time.ge.15000.0.and.time.le.30000.0) then
          meltmax=meltmin
        else
          meltmax=meltmax
        end if
      end if
c     if at end of file or end of run then closes file
      if (tsea.eq.nosea*whensea.or.
     +    time.eq.number) close(unit=10,disp='save')
      smth=int(time/whensmth)
      if (time.ne.dtin.and.time.eq.smth*whensmth) then
        call smther
        call bedsmth
      end if
c     if time for volume output calculate volume
```

```
c     and output to file and screen
      print=int(time/whenpr)
      if (time.eq.print*whenpr) then
        if (first) then
          write(6,150)
150         format(///' output :'//
     +     '      time      volume    delsea
     +      acvol   calvol   bedrock'/)
          first=.false.
        end if
        call volcalc
        acvol=acvol*wsq
        calvol=calvol*wsq
        write(6,240)time,vol,newsea,
     +          acvol/1000.0,calvol/1000.0,avelev/inelev
240     format(6f12.3)
        write(8,240)time,vol,newsea,
     +          acvol/1000.0,calvol/1000.0,avelev/inelev
        acvol=0.0
        calvol=0.0
      end if
      plot=int(time/whenpt)
      if (time.ne.dtin.and.time.eq.plot*whenpt) then
        write(6,245)
245     format('              <<<<< output created >>>>>')
        do 310 i=1,maxx
          do 320 j=1,maxy
            ice3(i,j)=(newsea+topog(i,j)*1000.0)
            if (thick(i,j,k).le.0.or.
     +          i.eq.1.or.j.eq.1.or.i.eq.maxx.or.j.eq.maxy) then
              ice1(i,j)=0.0
              ice2(i,j)=0.0
            else
              ice1(i,j)=thick(i,j,k)*1000.0
              ice2(i,j)=1000.0*sqrt(velbar(i,j,1)**2
     +                  +velbar(i,j,2)**2)
            end if
320       continue
310     continue
        call gdfil(stdnam1,ice1,flag)
        call gdfil(stdnam2,ice2,flag)
        call gdfil(stdnam3,ice3,flag)
      end if
```

```
      call dipstick
c     deals with velocity side
      do 250 i=2,maxx-1
        do 260 j=2,maxy-1
c         if ice there
          if (thick(i,j,k).gt.0) then
            if (floater(i,j)) then
              call velcalc(thick(i,j,k),topog(i,j),
     +                     velbar(i,j,1),velbar(i,j,2),
     +                     thick(i,j+1,k),thick(i,j-1,k),
     +                     thick(i-1,j,k),thick(i-1,j,k),
     +                     topog(i,j+1),topog(i,j-1),
     +                     topog(i-1,j),topog(i+1,j))
              strain(i,j,1)=0.0
              strain(i,j,2)=0.0
            else
              velbar(i,j,1)=0.0
              velbar(i,j,2)=0.0
            end if
          end if
260       continue
250     continue
      do 270 i=2,maxx-1
        do 280 j=2,maxy-1
          if (thick(i,j,k).gt.0.and.
     +                floater(i,j).eq..false.) then
            call strncalc(strain(i,j,1),strain(i,j,2),
     +                    velbar(i-1,j,1),velbar(i+1,j,1),
     +                    velbar(i,j+1,2),velbar(i,j-1,2))
            velbar(i,j,1)=0.0
            velbar(i,j,2)=0.0
          else
            strain(i,j,1)=0.0
            strain(i,j,2)=0.0
          end if
280       continue
270     continue
      do 290 i=2,maxx-1
        do 300 j=2,maxy-1
          velbar(i,j,1)=velbar(i,j,1)+strain(i,j,1)
          velbar(i,j,2)=velbar(i,j,2)+strain(i,j,2)
300       continue
290     continue
```

```
c    continuity equation loop
c    integrates ice thickness continuity equation
c    (with velocity and mass balance) then
c    uses new thickness to determine next velocity
     do 220 i=2,maxx-1
       do 230 j=2,maxy-1
c         determines surface elevation and net
c         mass balance, if surface above sea level
c         option allows ice and flow topography to
c         over run mass balance topography (max)
          if (topog(i,j).lt.0.0) then
           if (thick(i,j,k).eq.0.0) then
              topel=0.0
            calved=meltmax
           else
             call calver(thick(i,j,k),thick(i,j+1,k),
     +             thick(i,j-1,k),thick(i-1,j,k),thick(i+1,j,k),
     +             thick(i,j+2,k),thick(i,j-2,k),
     +             thick(i-2,j,k),thick(i+2,j,k),
     +             topog(i,j),topog(i,j+1),topog(i,j-1),
     +             topog(i-1,j),topog(i+1,j),
     +             topog(i,j+2),topog(i,j-2),
     +             topog(i-2,j),topog(i+2,j))
            if (floater(i,j)) then
              topel=max(mbtop(i,j),topog(i,j)+thick(i,j,k))
            else
              topel=thick(i,j,k)*romiw


             end if
          end if

        else
           topel=max(mbtop(i,j),topog(i,j)+thick(i,j,k))
          calved=0.0
        end if
        if (topel.gt.0.0) then
          if (thick(i,j,k).lt.ela) then
             goto 201
          else
            call snowput(topel,netbal)
          end if
        else
```

```
          netbal = 0.0
        end if
201       continue
        if (thick(i,j,k).ne.0.or.thick(i-1,j,k).ne.0.or.
     +      thick(i+1,j,k).ne.0.or.thick(i,j-1,k).ne.0.or.
     +      thick(i,j+1,k).ne.0.or.netbal.gt.0) then

          call conteq(thick(i,j,k),thick(i,j,l),
     +      thick(i,j+1,k),thick(i,j-1,k),thick(i-1,j,k),
     +      thick(i+1,j,k),velbar(i,j,1),velbar(i,j,2),
     +      velbar(i-1,j,1),velbar(i+1,j,1),
     +      velbar(i,j+1,2),velbar(i,j-1,2))
        else
          thick(i,j,l)=0
        end if
230     continue
220     continue
c     end of main loop, outside closes volume output file
      if (timelp.le.number) then
        timelp=timelp+dt
        goto 330
      end if
      close(unit=8,disp='save')
      end


      subroutine volcalc
c     finds icesheet volume in km cubed
      implicit none
      real thick(91,81,2),w,vol,wsq,
     +    topog(91,81),intopog(91,81),avelev,newsea
      integer i,j,maxx,maxy,k,l
      parameter (w=25.0,wsq=w*w)
      common  /grdsz/ maxx,maxy
     +      /kandl/ k,l
     +      /volume/ vol,avelev,newsea
     +      /icesheet/ thick
     +      /ground/ topog
     +      /updown/ intopog
      vol=0.0
      avelev=0.0
      do 1000 i=2,maxx-1
        do 1010 j=2,maxy-1
```

```
        vol=vol+thick(i,j,k)
        if (intopog(i,j).gt.-0.2) avelev=avelev+topog(i,j)+newsea
1010    continue
1000  continue
      vol=vol*wsq
      return
      end

      subroutine alphcalc(thicku,thickd,thickl,thickr,
     +          topogu,topogd,topogl,topogr)
c     finds surface slope
c     if possible takes centred 3 point average
c     else single point
c     finds x and y components then resultant magnitude
      implicit none
      real thicku,thickd,thickl,thickr,topelu,topeld,topell,
     +    topelr,topogu,topogd,topogl,topogr,w,alpha,alphx,
     +    alphy,w2,ro,row,romiw
      integer i,j
      logical floater(91,81)
      parameter (w=25.0,w2=-2.0*w,
     +          ro=870.0,row=1025.0,
     +          romiw=1.0-ro/row)
      common /slope/ alpha,alphx,alphy
     +      /fltlog/ floater
     +      /iandj/ i,j
      if (floater(i+1,j)) then
        topelr=thickr+topogr
      else
        topelr=thickr*romiw
      end if
       if (floater(i-1,j)) then
        topell=thickl+topogl
      else
        topell=thickl*romiw
      end if
       alphx=(topelr-topell)/w2
       if (floater(i,j+1)) then
        topelu=thicku+topogu
      else
        topelu=thicku*romiw
      end if
       if (floater(i,j-1))then
```

```
        topeld=thickd+topogd
      else
        topeld=thickd*romiw
      end if
      alphy=(topelu-topeld)/w2
      alpha=sqrt(alphx**2+alphy**2)
      return
      end


      subroutine smther
c     smooths in one direction , noting initial volume,
c     then in other, noting final volume, then
c     redistributes lost volume to edge points
      implicit none
      real factor,thick(91,81,2),cperim,volaft,volbfr
      integer i,j,k,l,maxx,maxy
      common /grdsz/ maxx,maxy
     +      /kandl/ k,l
     +      /icesheet/ thick
     cperim=0.0
      volaft=0.0
      volbfr=0.0
       do 2000 i=3,maxx-2
         do 2010 j=3,maxy-2
           if (thick(i,j,l).ne.0) then
             thick(i,j,k)=(10*thick(i,j,l)-thick(i-2,j,l)
     +                  -thick(i+2,j,l)+4*(thick(i-1,j,l)
     +                  +thick(i+1,j,l)))/16
             volbfr=volbfr+thick(i,j,l)
           else
             thick(i,j,k)=0
           end if
2010     continue
2000   continue
       do 2020 i=3,maxx-2
         do 2030 j=3,maxy-2
           if (thick(i,j,l).ne.0) then
             thick(i,j,l)=(10*thick(i,j,k)-thick(i,j-2,k)
     +                  -thick(i,j+2,k)+4*(thick(i,j-1,k)
     +                  +thick(i,j+1,k)))/16
             volaft=volaft+thick(i,j,l)
             if (thick(i-1,j,l).eq.0.or.thick(i+1,j,l).eq.0.or.
```

```
     +          thick(i,j-1,l).eq.0.or.thick(i,j+1,l).eq.0.or.
     +          thick(i-2,j,l).eq.0.or.thick(i+2,j,l).eq.0.or.
     +          thick(i,j-2,l).eq.0.or.thick(i,j+2,l).eq.0)
     +        cperim=cperim+1
           else
             thick(i,j,l)=0
           end if
2030     continue
2020   continue
       if (cperim.gt.0) factor=(volbfr-volaft)/cperim
       do 2040 i=3,maxx-2
         do 2050 j=3,maxy-2
           if (thick(i,j,l).ne.0) then
             if (thick(i-1,j,l).eq.0.or.thick(i+1,j,l).eq.0.or.
     +          thick(i,j-1,l).eq.0.or.thick(i,j+1,l).eq.0.or.
     +          thick(i-2,j,l).eq.0.or.thick(i+2,j,l).eq.0.or.
     +          thick(i,j-2,l).eq.0.or.thick(i,j+2,l).eq.0)
     +        thick(i,j,l)=thick(i,j,l)+factor
           end if
2050     continue
2040   continue
       return
       end


       subroutine gdfil(name,grid,flag)
c      input/output of arrays
       implicit none
       real grid(91,81)
       integer maxx,maxy,i,j
       character*40 name
       character*3 type
       logical flag
       common /grdsz/ maxx,maxy
        if (flag) then
         type='old'
       else
         type='new'
       end if
       open(unit=7,file=name,type=type,form='unformatted')
       if (flag) then
         read(7)maxx,maxy,grid
         do 3000 i=1,maxx
```

```
          do 3010 j=1,maxy
            grid(i,j)=grid(i,j)/1000.
3010       continue
3000     continue
       else
         write(7)maxx,maxy,grid
       end if
       close(unit=7,disp='save')
       return
       end

       subroutine snowput(topel,netbal)
c____ calcs snow depth from region and specific
c____ net balance array for a given elevation
       implicit none
       integer i,j,yy
       real zz,topel,netbal,netspbal(4,15)
       common/specific/netspbal
       zz = int(topel/100)
       netbal = netspbal(yy,zz) + ((topel-zz)/100)*
      *       (netspbal(yy,(zz+1))-netspbal(yy,zz))
c      ...should be ((topel-(zz*100)/100)* etc above....
       continue
       return
       end


       subroutine climate(regbal)
c      calculates changing regional climate
       implicit none
       integer yy,z
       real  n,lapse,Ao,Ac,k,E,precip,netspbal(16),
      *   totprec,regbal(4,16)
       common/area/yy
         do 1050  yy = 1,4
           if (yy.eq.1) then
             n = 0.7
             Ao = 180.0
             Ac = 189.0
             k = 6.0
             E = 10.0
             totprec = 1.0
           end if
```

```
          if (yy.eq.2) then
            n = 0.6
            Ao = 180.0
            Ac = 189.0
            k = 6.0
            E = 10.0
            totprec = 0.6
          end if
          if (yy.eq.3) then
            n = 0.7
            Ao = 180.0
            Ac = 189.0
            k = 14.0
            E = 10.0
            totprec = 0.8
          end if
          if (yy.eq.4) then
            n = 0.65
            Ao = 180.0
            Ac = 189.0
            k = 10.0
            E = 5.0
            totprec = 0.7
          end if
        call energy(Ac,Ao,k,E)
        call balance(n,totprec,netspbal)
        regbal(yy,z) = netspbal(z)
1050    continue
      continue
      return
      end

c     produce linear interpolation of glaciation line and
c     mass balance from arrays calculated by balance &
c     energy subroutines for regions of UK

      subroutine energy(Ac,Ao,k,E)
      implicit none
      integer i,j
      real Ac,Ao,c,b,seacl,landcl,seaca,landca,albcl,albsea,
     *  oceanalb,albland,contalb,eqtemp,dampings,htcapo,u,E,
     *  k,htcapc,oexco,cexco,insl,initc,inito,ltemp,stemp,
     *  ocins,ocir,contins,contir,dsea,dcont,icont,iocean,Eo,
```

```
     *  q,k1,dampingl,eqtemps,eqtempl,inpl
      character*40 tempnam
      logical first,choice
      common/log/first
      parameter (C=-38.8,seacl=0.78,landcl=
     *  0.66,B=2.04,albcl=
     *  0.48,albsea=0.13,oceanalb=albcl*seacl+albsea*0.22,
     *  u=0.1,htcapo=2.38E-4,htcapc=2.38E-3,
     *  initc=2.5,inito=6.0)
      open(unit=12,file=tempnam,status='new',form=
     *       'unformatted')
      first=.true.
      stemp=inito
      ltemp=initc
      Eo=u*E
      seaca = Ao + C*seacl
      landca = Ac + C*landcl
c_____do 200 i=1,2
        do 100 j=0,364
c____ insolation calculations
        choice = .true.
        call solar(j,q,choice)
        ocins = q*(1 - oceanalb)
        if (ltemp.lt.0.0) then
          albland = 0.61
        else
          if (ltemp.ge.0.0.and.ltemp.le.2.0) then
            albland = 0.61 - (0.195*ltemp)
          else
            albland = 0.22
          endif
        endif
        contalb = albcl*landcl + albland*(1 - landcl)
        contins = q*(1 - contalb)
c____ longwave radiation & heat exchange
        ocir = seaca + B*stemp
        contir = landca + B*ltemp
        call equiltemp(j,eqtemps,eqtempl)
        dampings = k*(eqtemps - stemp)
        dampingl = k1*(eqtempl - ltemp)
        oexco = Eo*(ltemp-stemp)
        cexco = E*(stemp-ltemp)
c____ calc. gradient of temp change
```

```
        dsea = htcapo*((ocins-ocir)+dampings+oexco)
       dcont = htcapc*((contins-contir)+dampingl+cexco)
       stemp = stemp + dsea
       ltemp = ltemp + dcont
        write(12)ltemp
 100    continue
c____ continue
      close(unit=12,disp='save')
      continue
      return
      end

      subroutine solar(j,q,choice)
      implicit none
      integer j
      real time,theta,g,el,eps,sel,decl,inpl,h,phi,
     *  e,rad,b,b1,b2,q,pi,day,lat,sol
      logical choice
      rad = 0.017453293
      pi = 3.1415927
      sol = 1300.0
      if (choice) then
        lat = 57.0
      else
        lat = 35.0
      endif
c____ see Walraven(1978) for variable details
      day = j
      time = day + 0.5
      theta = 360.0*(time/365.25)*rad
      g = -0.031271 - 4.53963E-7*time + theta
      el = 4.900968 + 3.67474E-7*time + (0.033434 - 2.3E-9
     *  *time)*sin(g) + 0.000349*sin(2.0*g) + theta
      eps = 0.409140 - 6.2149E-9*time
      sel = sin(el)
      decl = asin(sel*sin(eps))
      b1 = tan(decl)
      phi = lat*rad
      b2 = -tan(phi)
      h = acos(b1*b2)
      e = h*sin(phi)*sin(decl) + cos(phi)*cos(decl)*sin(h)
      inpl = sol*(1 + 0.034*cos((2*pi*day)/365.25))
c____ q is insolation at top of atmosphere during year
```

```
      q = inpl*e/pi
      continue
      return
      end


      subroutine equiltemp(j,eqtemps,eqtempl)
      implicit none
      integer j
      real startemps,eqtemps,eqtempl,eqocins,eqocir,eqcontir,
     *  heatcapo,heatcapc,startempl,eqcontins,eqocalb,avq,
     *  eqcontalb,eqseaca,eqcontca,B,eqoexco,eqcexco,eqEo,
     *  eqE,eqdsea,eqdcont
      logical first,choice
      common/log/first
      parameter (eqocalb=0.301,eqcontalb=0.307,startemps=13.0,
     *  eqseaca=209.3,eqcontca=215.2,eqE=10.0,startempl=10.0,
     *  heatcapo=2.38E-4,heatcapc=2.38E-3,B=2.04)
c____ values taken from van den Dool (1978)
      if (first) then
        eqtemps = startemps
        eqtempl = startempl
        first = .false.
      endif
c____ calls insol. subroutine & calcs. radiation
      eqEo = eqE*0.4
      choice = .false.
      call solar(j,avq,choice)
      eqocins = avq*(1 - eqocalb)
      eqcontins = avq*(1 - eqcontalb)
      eqocir = eqseaca + B*eqtemps
      eqcontir = eqcontca + B*eqtempl
      eqoexco = eqEo*(eqtempl - eqtemps)
      eqcexco = eqE*(eqtemps - eqtempl)
c____ gradient of temperature change
      eqdsea = heatcapo*((eqocins-eqocir)+eqoexco)
      eqdcont = heatcapc*((eqcontins-eqcontir)+eqcexco)
      eqtemps = eqtemps + eqdsea
      eqtempl = eqtempl + eqdcont
      continue
      return
      end
```

```
      subroutine balance(n,totprec,netspbal)
      implicit none
      integer day,min,count,prectime,stable,z,ht,i,j
      real skyemiss,height,f,cltemp,Lv,Lm,n2,dtemp,n,
     *  surftemp,lapse,clheight,mexco,dCdh,exco,Cp,totprec,
     *  transa,transc,solel,q,S,alback,ela,pi,preclapse,
     *  albedo,albsnow,depth,melt,iin,iout,icl,solar,massbal,
     *  solrad,clemitt,alb,pvo,pva,mixing,daytemp,whenprec,
     *  acmelt,Fs,Fl,B,precip,precipitation,initela,pvaz,
     *  netspbal(16),y,sbc,hpela(16),seasurftemp,soldeg,rad
      character*40 tempnam,balnam
      logical first,fst
      common/balela/ela
      parameter (clemitt=0.7,mexco=10.0,dCdh=0.002,solar=
     *  1300.0,iout=316.0,clheight=1500.0,pi=3.1415927,
     *  albsnow=0.72,lapse=0.007,dtemp=6.0,Cp=1005.0,
     *  pvo=4.3E-3,Lm=334000.0,Lv=2478000.0,whenprec=5.0,
     *  rad=0.017453293,pva=4.2E-3,sbc=5.67E-8)
      first=.true.
      fst=.false.
      z = 1
      n2 = n*n
      initela = 1500
      open(unit=9,file=balnam,status='new',form=
     *   'unformatted')
      open(unit=12,file=tempnam,status='old',form=
     *   'unformatted')
c_____do 600 stable = 0,2
      do 300 height = 1000,2500,100
        day = 0
      min = 0
100   continue
      read(12)seasurftemp
      prectime = int(day/whenprec)
      if (day.eq.prectime*whenprec) then
        precipitation = precip/3504
      else
        precipitation = 0.0
      endif
200   continue
      daytemp = (seasurftemp + 273.15) - (lapse*height)
```

```
      if (first) then
        ela = initela
        first = .false.
      endif
c____ dtemp is daily temp range to give diurnal temp variations
      surftemp = daytemp + (dtemp/2)*sin(0.0043633*(min-525))
c____ solar rad. every half hour
      call elevation(day,min,solel)
      S = solar*(1 + 0.034*cos(2*pi*day/365.25))
      if (solel.lt.0.0) then
        solel = 0.0
      endif
      q = S*sin(solel)
      transa = (0.79 + 0.000024*height) * (1 - 0.009*
     *      (90 - soldeg))
      transc = 1 - (0.41 - 0.000065*height)*n - 0.37*n2
      solrad = q*transa*transc
c____ longwave radiation
      cltemp = (seasurftemp+273.15) - (lapse*clheight)
      skyemiss = 0.7 + 0.000025*height
      f = -0.6732 + 0.00624*cltemp - (0.914E-5*cltemp**2)
      icl = clemitt*n*f*sbc*cltemp**4
      iin = skyemiss*sbc*surftemp**4 + icl
c____ albedo calculations
      alback = 0.115*atan((height - ela + 300)/200) + 0.48
      alb = albsnow - alback
      albedo = albsnow - (alb*exp(-5*depth) + (0.015*acmelt))
      if (albedo.lt.0.12) then
        albedo = 0.12
      endif
c____ turbulent fluxes,Fl & Fs
      exco = mexco + ((ela-height)*dCdh)
      Fs = exco*(surftemp-273.15)
      pvaz = pva + (1.5E-6*(height - ela))
      mixing = pvaz - pvo
      Fl = (Lv*exco*mixing)/Cp
c____ energy balance
      B = solrad*(1 - albedo) + iin - iout + Fs + Fl
      melt = -B/Lm
      if (melt.gt.0.0) then
        melt = 0.0
      endif
c____ precipitation every 5 days
```

```
      preclapse = 0.0005 * totprec
      if ((surftemp - 273.15).gt.2.0) then
        precip = 0.0
      else
        precip = totprec + (height*preclapse)
      endif
      massbal = massbal + melt + precipitation
      acmelt = acmelt + melt
      depth = depth + precipitation + melt
      if (depth.lt.0.0) then
        depth = 0.0
      endif
c____ end time loops
      min = min + 30
      if (min.eq.1440) then
        min = min -1440
      else
        goto 200
      endif
      day = day + 1
      if (day.eq.365) then
        day = day - 365
        rewind(unit=12)
      else
        goto 100
      endif
c____ adjust ela to glaciation line
      netspbal(z) = massbal
      if (fst) then
        if (massbal.gt.0.0) then
          hpela(z) = netspbal(z) - netspbal(z-1)
          y = -netspbal(z-1)/hpela(z)
          ela = (height-100) + (y*100)
          fst = .false.
        endif
      endif
      if (z.eq.16) then
        z = z - 16
        fst = .true.
      endif
      z = z + 1
      write(9)height,massbal,ela
      massbal = 0.0
```

```
      acmelt = 0.0
      precipitation = 0.0
      depth = 0.0
300   continue
c____ continue
      close(9)
      close(12)
      continue
      return
      end

      subroutine elevation(day,min,solel)
      implicit none
      integer day,min
      real theta,g,el,eps,sel,decl,h,phi,e,rad,ra,st,
     *  q,pi,lat,a1,a2,pi2,long,time,solel,locals,t
      parameter (pi=3.1515927,pi2=pi*2,rad=0.017453293,
     *  lat=57.0,long=6.0)
      t = min/60
      time = day + t/24
      theta = 360.0*(time/365.25)*rad
      g = -0.031271 - 4.53963E-7*time + theta
      el = 4.900968 + 3.67474E-7*time + (0.033434 - 2.3E-9
     *  *time) *sin(g) + 0.000349*sin(2.0*g) + theta
      eps = 0.409140 - 6.2149E-9*time
      sel = sin(el)
      a1 = sel * cos(eps)
      a2 = cos(el)
      ra = atan2(a1,a2)
      if (ra.lt.0.0) ra = ra + pi2
      decl = asin(sel*sin(eps))
      st = 1.759335 + pi2*(time/365.25) + 3.694E-7*time
      if (st.ge.pi2) st = st - pi2
      locals = st + 1.0027379*t*15.0*rad
      if (locals.ge.pi2) locals = locals - pi2
      h = ra - locals
      phi = lat*rad
      e = asin(sin(phi)*sin(decl) + cos(phi)*cos(decl)
     *                          *cos(h))
      if (sin(e).ge.sin(decl)/sin(phi)) solel = e
      continue
      return
      end
```

```
      subroutine conteq(thickold,thicknew,
     +          thicku,thickd,thickl,thickr,
     +          velbar1,velbar2,velbarl,
     +          velbarr,velbaru,velbard)
c     finds discharge derivatives in x and y,
c     discharge is product of average velocity and
c     thickness. derivative is centred, first find
c     discharges half way between grid points then
c     finite difference derivative
      implicit none
      real thickold,thicknew,thicku,thickd,thickl,thickr,
     +    velbar1,velbar2,velbaru,velbard,velbarl,velbarr,
     +    dt,dqxdx,dqydy,qxphf,qxmhf,qyphf,qymhf,w,
     +    calved,calvol,acvol,netbal
      parameter (w=5.0,dt=2.5)
      common /netmass/ netbal
     +      /calving/ calved,calvol,acvol
      qxphf=(velbar1+velbarr)*(thickold+thickr)*0.25
      qyphf=(velbar2+velbaru)*(thickold+thicku)*0.25
      qxmhf=(velbarl+velbar1)*(thickl+thickold)*0.25
      qymhf=(velbard+velbar2)*(thickd+thickold)*0.25
      dqxdx=(qxphf-qxmhf)/w
      dqydy=(qyphf-qymhf)/w
c     continuity equation new thickness is old plus
c     difference in ice fluxes, ensure thickness above zero
      thicknew=max(0.0,thickold+dt*(netbal-dqxdx-dqydy))
      acvol=acvol+thicknew-thickold
      if ((thicknew-calved).lt.0) then
        calvol=calvol+thicknew
        thicknew=0.0
      else
        calvol=calvol+calved
        thicknew=thicknew-calved
      end if
      return
      end


      subroutine velcalc(thick,topog,velbar1,velbar2,
     +          thicku,thickd,thickl,thickr,
     +          topogu,topogd,topogl,topogr)
```

```
      implicit none
      real thick,topog,velbar1,velbar2,
     +    thicku,thickd,thickl,thickr,
     +    topogu,topogd,topogl,topogr,
     +    alpha,alphx,alphy,factor1,factor2,slidx,slidy,
     +    ro,row,slimit,k2,velmax,a,g,roiw
      integer n,nm1,np1
      parameter (slimit=0.1,a=5.3e-24,
     +          g=9.81,k2=5.0e-5,n=3,nm1=n-1,np1=n+1,
     +          ro=870.0,row=1025.0,roiw=row/ro,velmax=2.0,
     +          factor1=(((ro*g)**n)*2*a*31536e12)/(n+2),
     +          factor2=k2*g*ro)
      common /slope/ alpha,alphx,alphy
c     find surface slope
      call alphcalc(thicku,thickd,thickl,thickr,
     +              topogu,topogd,topogl,topogr)
c     if ice thick enough to slide
c     find sliding velocity, differs
c     whether ice is above or below sea level
c     two layers of velbar refer to x,y velocity
      if (thick.gt.slimit) then
        if (topog.lt.0) then
          slidx=factor2*thick*alphx/
     +      ((thick+roiw*topog)**2)
          slidy=factor2*thick*alphy/
     +      ((thick+roiw*topog)**2)
        else
          slidx=factor2*alphx/thick
          slidy=factor2*alphy/thick
        end if
      else
        slidx=0.
        slidy=0.
      end if
c     find deformation velocity
      velbar1=factor1*(alpha**nm1)*alphx*
     +          (thick**np1)+slidx
      velbar2=factor1*(alpha**nm1)*alphy*
     +          (thick**np1)+slidy
      if (abs(velbar1).gt.velmax)
     +  velbar1=sign(velmax,velbar1)
      if (abs(velbar2).gt.velmax)
     +  velbar2=sign(velmax,velbar2)
```

```
 return
 end


 subroutine strncalc(strain1,strain2,velbarl,
+                velbarr,velbaru,velbard)
 implicit none
 real strain1,strain2,velbarl,velbarr,
+    velbaru,velbard,velmax,w,strnrt,veloc
 parameter (strnrt=0.001,velmax=2.0,w=10.0,veloc=strnrt*w)
 if (velbarl.gt.0.and.velbarr.lt.0) then
   strain1=velbarl+velbarr
   if (strain1.ne.0) strain1=
+     strain1+sign(veloc,strain1)
 else
   if (velbarl.gt.0) then
     strain1=velbarl+veloc
   else
     if (velbarr.lt.0) then
       strain1=velbarr-veloc
     else
       strain1=0.0
     end if
   end if
 end if
 if (abs(strain1).gt.velmax)
+  strain1=sign(velmax,strain1)
 if (velbard.lt.0.and.velbaru.gt.0) then
   strain2=velbard+velbaru
   if (strain2.ne.0) strain2=
+     strain2+sign(veloc,strain2)
 else
   if (velbard.lt.0) then
     strain2=velbard-veloc
   else
     if (velbaru.gt.0) then
       strain2=velbaru+veloc
     else
       strain2=0.0
     end if
   end if
 end if
 if (abs(strain2).gt.velmax)
```

```
     +  strain2=sign(velmax,strain2)
        return
        end


        subroutine calver(thick,thicku,thickd,thickl,thickr,
     +          thicku2,thickd2,thickl2,thickr2,
     +          topog,topogu,topogd,topogl,topogr,
     +          topogu2,topogd2,topogl2,topogr2)
        implicit none
        real thick,thicku,thickd,thickl,thickr,
     +    thicku2,thickd2,thickl2,thickr2,
     +    topog,topogu,topogd,topogl,topogr,
     +    topogu2,topogd2,topogl2,topogr2,
     +    dt,w,calved,dtw,calvmax,calvrt,calvol,acvol
        integer calvcnt
        parameter (dt=2.5,w=10.0,calvmax=20.0,calvrt=28.75,dtw=dt/w)
        common /calving/ calved,calvol,acvol
        calvcnt=0
        if (thickl.eq.0.and.topogl.lt.0.and.
     +    thickl2.eq.0.and.topogl2.lt.0)
     +    calvcnt=calvcnt+1
        if (thickr.eq.0.and.topogr.lt.0.and.
     +    thickr2.eq.0.and.topogr2.lt.0)
     +    calvcnt=calvcnt+1
        if (thickd.eq.0.and.topogd.lt.0.and.
     +    thickd2.eq.0.and.topogd2.lt.0)
     +    calvcnt=calvcnt+1
        if (thicku.eq.0.and.topogu.lt.0.and.
     +    thicku2.eq.0.and.topogu2.lt.0)
     +    calvcnt=calvcnt+1
        calved=thick*dtw*calvcnt*min(calvmax,calvrt*(-topog))
        return
        end


        subroutine dipstick
c---  floating- floater is false
c---  grounded- floater is true
c---  no ice,dry land- floater is false
c---  no ice,over sea- floater is true
        implicit none
        real roflt,row,ro,thick(91,81,2),topog(91,81)
```

```
      integer i,j,k,l,maxx,maxy
      logical floater(91,81)
      parameter (ro=870.0,row=1025.0,roflt=-row/ro)
      common /grdsz/ maxx,maxy
     +     /kandl/ k,l
     +     /icesheet/ thick
     +     /ground/ topog
     +     /fltlog/ floater
      do 10 i=1,maxx
        do 20 j=1,maxy
          if (thick(i,j,k).ge.roflt*topog(i,j)) then
            floater(i,j)=.true.
          else
            floater(i,j)=.false.
          end if
20      continue
10    continue
      return
      end
```

D. Topography model

```
      program budd
       implicit none
      real ice1(50),ice2(50),topel(50),
     +    thick(50),topog(50),oldthick(50),
     +    testpint,testhyps(15),mark,dmark,
     +    acvol,b,topell,topelr,topel2l,topel2r,
     +    vol,avelev,inelev,
     +    w,ro,pi,wsq,
     +    yy,hela(3),regela,
     +    nwtopel,nwtopell,nwtopelr,nwtopel2l,nwtopel2r,
     +     netbal,regbal(3,15),ela,
     +    initela,achypsom,abhypsom,
     +    zc,zb,totac,totab,ctalpha,m,alpha,alphx,alphy,
     +    terminus,totabzb,bnc,bnb,
     +    tag,tau,yield,totlen,
     +     newbal,oldbal,region,term
       integer i,j,l,maxx,maxy,plot,print,achyps(0:14),abhyps(0:14),
     +       smth,temp,topint,botint,stable,elaint,a,termela,
     +       abfraction
      logical flag,first/.true./
```

```
      character*40 topnam,prenam,outnam,zednam,
     +           stdnam1,stdnam2
      parameter (tag=9.09,
     +         w=0.1,wsq=w*w,pi=3.14159)
      common /iandj/ i,j
     +      /grdsz/ maxx,maxy
     +      /netmass/ netbal
     +      /volume/ vol
     +      /icesheet/ thick
     +      /ground/ topog
     +      /balela/regela,ela,elaint
     +      /specific/regbal
     +      /slope/alpha,alphx,alphy
     +      /balan/bnb,bnc
     +      /terminus/termela
     +      /ablatarea/abfraction
     +      /upper/topel
c     get relevant data files
      write(6,10)
10    format(' Topographic input file : ',$)
      read(5,20)topnam
20    format(a)
      flag=.true.
      call gdfil(topnam,topog,flag)
      do i=1,maxx
          if (topog(i).lt.0.0) then
            topog(i) = 0.0
          end if
      end do
      write(6,70)
70    format(' Ice thickness file name (n if none) : ',$)
      read(5,20)zednam
      if (zednam.eq.'N') zednam='n'
c     allows start-up icesheet
      if (zednam.ne.'n') then
        call gdfil(zednam,ice1,flag)
        do 80 i=1,maxx
            if (ice1(i).lt.0) then
              thick(i)=0.
            else
              thick(i)=ice1(i)
            end if
80        continue
```

```
      end if
     write(6,100)
100   format(' File for thickness output : ',$)
      read(5,20)stdnam1
c     write(6,115)
c15   format(' File for bedrock output : ',$)
c     read(5,20)stdnam2
      write(6,120)
120   format(' File for ice fluxes : ',$)
      read(5,20)outnam
      write(6,125)
125   format(' Yield Stress (50-150)? : ',$)
      read(*,*)tau
      yield = tau/tag
      write(6,130)
130   format(' ELA? : ',$)
      read(*,*)ela
      write(6,135)
135   format(' Accumulation balance gradient : ',$)
      read(*,*)bnc
      write(6,140)
140   format(' Ablation balance gradient : ',$)
      read(*,*)bnb
c     opens output file for ice fluxes
      open(unit=8,file=outnam,type='new',form='formatted')
      flag=.false.
c     main loop starts
c____ if time to call climate change subroutine
 c_____  call albcalc
c_______ call balance(region,regbal)
 c_____ determines elevation and net mass balance
      stable = 0
900   continue
      stable = stable + 1
      regela = ela/1000.0
      elaint = int(regela*10)
      do 201 i=2,maxx-1
         topel(i) = topog(i) + thick(i)
201   end do
      do 220 i=2,maxx-1
          if (regela.lt.topel(i)) then
            topint = int(topel(i)*10)
            achyps(topint) = achyps(topint) + 1
```

```
          call alphcalc(topel(i),
     *         topel(i-1),topel(i+1),alpha)
          if (alpha.ge.45) then
            thick(i) = 0.0
          else
            if (alpha.gt.5) then
              thick(i) = (yield/sind(alpha))/1000.0
            else
              call lencalc(totlen)
              thick(i) = (sqrt(2*yield*totlen*1000))/1000.0
            end if
          end if
        else
          botint = int(topel(i)*10)
          abhyps(botint) = abhyps(botint) + 1
        end if
220     continue
      call accum(achyps,zc,totac)
      totabzb = zc*totac*bnc/bnb
      call ablat(abhyps,totabzb,zb,totab,a)
      termela = elaint-a-1
      do 245 i=2,maxx-1
          botint = int(topel(i)*10)
          if (botint.le.elaint.and.botint.ge.termela) then
            if (botint.eq.termela.and.thick(i+1).le.0
     *          .and.thick(i-1).le.0) then
              go to 248
            else
              if (botint.eq.termela.and.abfraction.le.0) then
                go to 248
              else
                if (botint.eq.termela.and.abfraction.
     *              gt.0) then
                  abfraction = abfraction - 1
                end if
              end if
            end if
            call alphcalc(topel(i),
     *           topel(i-1),topel(i+1),alpha)
            if (alpha.gt.45) then
              thick(i) = 0.0
            else
              if (alpha.ge.5) then
```

```
                thick(i) = (yield/sind(alpha))/1000.0
              else
                call lencalc(totlen)
                thick(i) = (sqrt(2*yield*totlen*1000))/1000.0
              end if
            end if
          end if
248     continue
245     continue
246     continue
        do 260 i=2,maxx-1
          oldthick(i)=thick(i)
          nwtopel = topel(i)+thick(i)
          nwtopell = topel(i-1) + thick(i-1)
          nwtopel2l = topel(i-2) + thick(i-2)
          nwtopelr = topel(i+1) + thick(i+1)
          nwtopel2r = topel(i+2) + thick(i+2)
c          call smooth(topel(i),topel(i-1),topel(i-2),topel(i+1),
c     *          topel(i+2),thick(i),thick(i-1),thick(i-2),
c     *          thick(i+1),thick(i+2),topog(i),nwtopel,nwtopell,
c     *          nwtopel2l,nwtopelr,nwtopel2r)
          if (thick(i).ne.oldthick(i)) then
            go to 246
          end if
260     continue
        if (stable.lt.1) goto 900
c____ obtain output files
      call volcalc
      write(6,150)
150   format(///' Output :'//
     *     ' ela       volume      totac     totab '/)
      write(6,240)ela,vol*1000,totac*0.1,totab*0.1
240   format(4F12.3)
      write(8,240)ela,vol*1000,totac*0.1,totab*0.1
      do 310 i = 1,maxx
          if (thick(i).le.0.or.
     *       i.eq.1.or.i.eq.maxx) then
            ice1(i) = 0.0
            ice2(i) = 0.0
          else
            ice1(i) = thick(i)*1000.0
            ice2(i) = topog(i)*1000.0
          end if
```

```
310  continue
     call gdfil(stdnam1,ice1,flag)
c_____call gdfil(stdnam2,ice2,flag)
     close(unit=8,disp='save')
     end

     subroutine volcalc
     implicit none
     real thick(50),w,wsq,topog(50),vol
     integer i,j,maxx,maxy
     parameter(w=0.1,wsq=w*w)
     common/grdsz/maxx,maxy
    *     /volume/vol
     *     /icesheet/thick
     *     /ground/topog
     vol = 0.0
     do i=2,maxx-1
          vol = vol + thick(i)
     end do
     vol = vol*wsq
     return
     end

     subroutine alphcalc(topel,topell,topelr,
    *                    alpha)
c    finds bedrock slope
c    if possible takes centred 3 point average
c    else single point
c    finds x and y components then resultant magnitude
     implicit none
     real topelu,topeld,topell,topog,topel,
    +     topelr,topogu,topogd,topogl,topogr,w,alpha,alphx,
    +     alphy,w2,alp
     integer i,j
     parameter (w=0.1,w2=-2.0*w)
     common /iandj/ i,j
     alphx=(topelr-topell)/w2
     alpha=atand(alphx)
     return
     end

     subroutine lencalc(totlen)
     implicit none
```

```
      integer mark,i,j,a,b,c,topa,oldb,topc,maxx,maxy,
     *        abfraction,ablen,botint,termela
      real w,ang,topog(50),tanf,totlen,len,topel(50)
      parameter(w=0.1,tanf=0.087488663,ang=tanf*w)
      common/iandj/i,j
     *     /grdsz/maxx,maxy
     *     /ground/topog
     *     /terminus/termela
     *     /ablatarea/abfraction
     *     /upper/topel
c_____ Obtain length of flat surface
      a = 1
      b = 1
      ablen = abfraction
      do while
     *   (abs(topel(i+a)-topel(i+a-1)).lt.ang)
          if ((int(topel(i+a)*10)).eq.termela) then
            if (ablen.le.0) then
               go to 220
            end if
            ablen = ablen - 1
          end if
          if (i+a.ge.maxx-1) then
             go to 220
          end if
          a = a + 1
      end do
220   continue
      do while
     *   (abs(topel(i-b)-topel(i-b+1)).lt.ang)
          if ((int(topel(i-b)*10)).eq.termela) then
            if (ablen.le.0) then
               go to 320
            end if
            ablen = ablen - 1
          end if
          if (i-b.le.2) then
            go to 320
          end if
          b = b + 1
      end do
320   continue
      if (topel(i+a).gt.topel(i+a-1).and.topel(i-b).le.
```

```
*  topel(i-b+1)) then
   len = b - 1
 else
   if (topel(i-b).gt.topel(i-b+1).and.topel(i+a).le.
*     topel(i+a-1)) then
     len = a - 1
   else
     if (topel(i+a).lt.topel(i+a-1).and.topel(i-b).lt.
*       topel(i-b+1)) then
       len = min((a-1),(b-1))
     else
       if (topel(i+a).gt.topel(i+a-1).and.topel(i-b)
*          .gt.topel(i-b+1)) then
         len = max(a-1,b-1)
       else
         len = min(a-1,b-1)
       end if
     end if
   end if
 end if
 totlen = len*w
 return
 end

 subroutine smooth(topel,topell,topel2l,topelr,topel2r,
*         thick,thickl,thick2l,thickr,thick2r,topog,
*         nwtopel,nwtopell,nwtopel2l,nwtopelr,nwtopel2r)
 implicit none
 real topel,topelu,topeld,topell,topelr,thick,
*    thicku,thickd,thickl,thickr,nwtopel,nwtopel2r,
*    topel2l,topel2r,thick2l,thick2r,nwtopel2l,
*    nwtopelu,nwtopeld,nwtopell,nwtopelr,newtop,topog
     newtop = 0.0
     if (topell.lt.topel.and.thickl.gt.thick.and.
*       nwtopell.gt.nwtopel) then
       if (topel2l.le.topel.and.thick2l.gt.thick.and.
*         nwtopel2l.gt.nwtopel) then
         newtop = nwtopel2l
         thick = newtop - topog
         thickl = thick
       else
         newtop = nwtopell
         thick = newtop - topog
```

```
          end if
        else
          if (topell.eq.topel.and.topelr.gt.topel.and.
     *      nwtopell.gt.nwtopel.and.nwtopelr.gt.nwtopel) then
            newtop = nwtopell
            thick = newtop - topog
          end if
        end if
        if (topelr.lt.topel.and.thickr.gt.thick.and.
     *     nwtopelr.gt.nwtopel) then
          if (topel2r.le.topel.and.thick2r.gt.thick.and.
     *       nwtopel2r.gt.nwtopel) then
            newtop = nwtopel2r
            thick = newtop - topog
            thickr = thick
          else
            newtop = nwtopelr
            thick = newtop - topog
          end if
        else
          if (topelr.eq.topel.and.topell.gt.topel.and.
     *       nwtopell.gt.nwtopel.and.nwtopelr.gt.nwtopel) then
            newtop = nwtopelr
            thick = newtop - topog
          end if
        end if
      return
      end

      subroutine gdfil(name,grid,flag)
c     input/output of arrays
      implicit none
      real grid(50)
      integer maxx,maxy,i,j
      character*40 name
      character*3 type
      logical flag
      common /grdsz/ maxx,maxy
       if (flag) then
         type='old'
      else
         type='new'
      end if
```

```
      open(unit=7,file=name,type=type,form='formatted')
      if (flag) then
        read(7,*)maxx,grid
        do 3000 i=1,maxx
            grid(i)=grid(i)/1000.
3000    continue
      else
        write(7,5)grid
      end if
5     format( f9.3)
      close(unit=7,disp='save')
      return
      end

      subroutine accum(achyps,zc,totac)
      implicit none
      integer elaint,topint,achyps(0:14)
      real totac,achypsom,zc,grdwth,ela,regela,
     *    bnb,bnc
      common/size/grdwth
     *     /balela/regela,ela,elaint
     *     /balan/bnb,bnc
c____ 100's cancel in below equation
      do topint = 0,14
        totac = totac + achyps(topint)
        achypsom = achypsom + achyps(topint)*(topint-elaint+1)
     *           *100*bnc
      end do
      if (totac.eq.0.0) then
        zc = 0.0
      else
        zc = achypsom/totac
      end if
      return
      end

      subroutine ablat(abhyps,totabzb,zb,totab,a)
      implicit none
      integer botint,abhyps(0:14),elaint,a,abfraction
      real totab,abhypsom,zb,ela,totabzb,fred,grdwth,
     *    regela,bnb,bnc,frac,newab,newhyps
      common/size/grdwth
     *     /balela/regela,ela,elaint
```

```
*     /balan/bnb,bnc
*     /ablatarea/abfraction
      a = 0
      abfraction = 0
      do botint = elaint,0,-1
        totab = totab + abhyps(botint)
        abhypsom = abhypsom + abhyps(botint)*(elaint-botint+1)
*               *100*bnb
        if (totab.eq.0.0) then
          zb = 0.0
        else
          zb = abhypsom/totab
        end if
        fred = totab*zb
        if (fred.gt.totabzb) then
          newab = totab
          newhyps = abhypsom
          totab = totab - abhyps(botint)
          abhypsom = abhypsom - abhyps(botint)*
*               (elaint-botint+1)*100*bnb
          frac = (totabzb-abhypsom)/(newhyps-abhypsom)
          abfraction =int(frac*(newab-totab))
          goto 322
        end if
        a = a + 1
      end do
322   continue
      if (totab.eq.0.0) then
        zb = 0.0
      else
        zb = abhypsom/totab
      end if
      return
      end
```

APPENDIX 4:
PUBLISHED PAPERS

Kerr A.R. (1990) The initiation of maritime ice sheets.
Zeit. Gletscherk. Glazialgeol. 26(1) 69-79

Kerr A.R. (1993) Topography, climate, and ice masses: a review
Terra Nova 5 (in press)

Band 26, Heft 1 (1990), S. 69—79

ZEITSCHRIFT FÜR
GLETSCHERKUNDE
UND GLAZIALGEOLOGIE

THE INITIATION OF MARITIME ICE SHEETS

By A. KERR, Edinburgh

With 5 figures

ABSTRACT

Quantitative estimates of the climate change necessary to initiate maritime ice sheets are obtained by relating climatic parameters to glacier mass balance. A numerical, coupled climate-ice sheet model is used at a regional scale to investigate the behaviour of former British ice sheets. The climate model is driven by changes in solar radiation, precipitation, and ocean circulation, such as the migration of the North Atlantic polar front. The resulting mass balance is used in the ice sheet model which predicts the extent, velocity and thickness of ice during a glacial cycle.

Sea temperature, topography, and precipitation levels play key roles in the dynamics of ice sheet growth, while variations in solar radiation are insignificant. The maritime influence affects land temperatures and reduces the annual temperature range, while high lapse rates make the altitude and geometry of the topography important in ice sheet growth. Precipitation levels, which are vital in determining the threshold and rate of growth of mid-latitude maritime ice sheets, are related to topographic altitude and sea temperatures. For example, a 4° C mean annual temperature drop lowers the equilibrium line altitude by the same value as a 7° C drop with an associated 50 % reduction in precipitation. The conclusion is that the dynamics of ice sheet initiation are highly sensitive to offshore marine temperatures and the geometry of upland topography.

DIE BILDUNG VON MARITIMEN EISSCHILDEN

ZUSAMMENFASSUNG

Mit der Beziehung zwischen Klimaparametern und der Massenbilanz von Gletschern werden die Klimaänderungen quantitativ geschätzt, die notwendig sind, um maritime Eisschilde zu bilden. Mit einem numerischen Modell, das die Verbindung von Klima und Eisschilden im regionalen Scale darstellt, wird das Verhalten der früheren Vereisung Großbritanniens untersucht. Das Klimamodell hat als unabhängige Variable die Änderungen in der Sonnenstrahlung, im Niederschlag und bei der Ozeanzirkulation, wie zum Beispiel die nordatlantische Polarfront. Die dementsprechenden Änderungen in der Massenbilanz dienen als Eingangsgrößen in einem Eisschildmodell, das die Ausdehnung, Fließgeschwindigkeit und Dicke des Eises während eines Vereisungszyklus berechnet.

Meerestemperatur, Topographie und Niederschlagsmengen spielen die wichtigste Rolle bei der Entwicklung eines Eisschilds, wogegen die Änderungen in der solaren Bestrahlungsstärke unwichtig sind. Der maritime Einfluß betrifft die Landtemperaturen und ihre Jahresamplitude, starke vertikale Temperaturgradienten geben der Höhe und der Form der Landoberfläche größeres Gewicht beim Wachstum des Eises. Die Niederschlagsmenge, die eine kritische Größe für den Einsatz und die Geschwindigkeit des Eiswachstums ist, hängt von der Höhe über dem Meer und von der Meerestemperatur ab. Zum Beispiel hat nach diesem Modell eine Abkühlung der Jahresmitteltemperatur um 4° C die gleiche Wirkung auf die Höhe der Gleichgewichtslinie wie eine Abkühlung um 7° C zusammen mit einer Verminderung des Niederschlags um 50 %. Aus diesen

Modellrechnungen wird der Schluß gezogen, daß der Beginn einer Vereisung höchst sensibel auf die Meerestemperatur und auf die Topographie der Landoberfläche reagiert.

1. INTRODUCTION

This paper investigates the set of possible climatic configurations that can initiate an ice sheet in a maritime climate. It uses coupled numerical models of climate and ice sheets to obtain quantitative estimates of the necessary climate deterioration to grow an ice sheet. The experiments were carried out for the former Scottish ice sheet and are of interest since the abrupt change from an interglacial to a glacial climate, when large ice sheets covered areas which are currently unglaciated, is poorly understood.

There are two advantages in investigating the maritime ice sheets of Britain in relation to global climatic change. Firstly, they are likely to be particularly sensitive to ocean temperature variation, and thus changes in North Atlantic circulation, which is believed to be crucial in global climate change. This is a result of high accumulation and high ablation values leading to steep net mass balance gradients, which are sensitive to changes in precipitation and temperature (Pelto et al. 1990). The crux of the problem is the delicate balance between the cooling required to initiate glaciers and that which limits the flow of moisture and thus precipitation into the area (Lamb 1964).

Secondly, there is a large body of data concerning the Late Devensian climate for Britain and the North Atlantic (Ruddiman et al. 1980). Climatic estimates are useful in constraining model input data, while field evidence provides independent tests of the model assumptions. Normally, testing theories about the growth of an ice sheet is difficult since evidence is destroyed by a later maximum. However, the Younger Dryas glaciation in Scotland (c. 10.500 yrs BP) appears to represent a truncated glaciation and provides a useful reference with which to compare results.

Intuitively there are three possible mechanisms that could initiate an ice sheet in a maritime climate:

a) Insolation variation,
b) Seasonal climatic changes,
c) Sea surface temperature changes.

Early numerical modelling (Andrews and Mahaffy 1976) examined the conditions for growth of the Laurentide ice sheet and concluded that moisture availability and transport was vital. This agrees with work by Ruddiman et al. (1980) and Johnson and Andrews (1979) concerning the balance between the need for warm sea surface temperatures for precipitation and high latitude cooling, from insolation reduction, to initiate growth. This paper is an extension of the work of Payne and Sugden (1990) which investigated the Younger Dryas glaciation of Scotland in terms of the complex link between ocean surface cooling and moisture starvation during ice sheet growth.

2. METHOD

To obtain the set of possible climatic configurations required to initiate an ice sheet, the climatic parameters must be related to some measure of glacier mass balance. This is achieved using the mass balance model developed by Oerlemans (1992),

and an energy balance model which simulates the changing regional climate of the United Kingdom for use as input to the mass balance model (see North et al. 1981).

The first two mechanisms for initiation, insolation variations and seasonal climatic change, can be investigated by sensitivity analysis of the climate models to determine the components most effective in reducing the equilibrium line altitude. There is less confidence in the model when investigating the third possibility, ocean temperature changes, since the underlying assumptions of the regional energy balance model, which is tuned with the present day climate, become invalid. In this case the mean land temperatures are assumed to change roughly in proportion with the change in ocean temperature; the energy fluxes are not explicitly modelled. The variation in equilibrium line altitude can be obtained for different climates once the important climatic components have been identified. This can then be coupled to the ice sheet model to examine the effect of climate variation on real topography.

3. THE MASS BALANCE MODEL

The mass balance, M, of the surface can be obtained by integrating the equation:

$$M = -B/L + P$$

where B is the energy balance of the surface; L is the latent heat of melt at 273 K; and P is the precipitation falling in solid form, which is assumed to occur below a critical temperature. The energy balance can be written:

$$B = Q(1-a) + I_{in} + I_{out} + F_s + F_l$$

where Q is the shortwave radiation; I is the longwave radiation; F_s and F_l are turbulent fluxes; and a is the albedo.

The mass balance model contains two major feedbacks: an ice-albedo-temperature feedback and an altitude-mass balance feedback. The mass balance equation is integrated with a time step of 30 minutes (to resolve the daily cycle) for a period of one year at 15 different elevations. This is then repeated to allow the equilibrium line altitude to converge at a stable value. The model is applied to different climatic regions of the United Kingdom to obtain the equilibrium line altitude and net mass balance. The required inputs are: seasonal temperature range and mean, daily temperature range, annual precipitation, precipitation lapse rate, cloudiness, mean height of cloud base, and temperature lapse rate.

As a first approximation the input parameters are based on present day values since the aim is to establish the climate perturbations required to move from an interglacial to a glacial stage. Broad simplifications are required since many parameters exhibit complex geographical and seasonal variations from their average value. However, maritime climates have characteristically little variation in cloud cover and daily temperature range.

4. THE REGIONAL ENERGY BALANCE CLIMATE MODEL

The model calculates the energy balance for a particular latitude band (here 50—60°) and the latitudinal and zonal (land-sea) advection of energy to obtain a seasonal temperature curve for a particular climatic region of the United Kingdom:

$$C_o dO/dt = R_o + k_o O + uE(T - O)$$

$$C_l dT/dt = R_l + k_l T + E(O - T)$$

where C is the heat capacity; O is the ocean temperature; T is the land temperature; R is the surface energy balance; k is the latitudinal heat flux coefficient; E is the zonal heat flux coefficient; u is the zonal land-sea fraction; and subscripts l and o refer to land and ocean respectively.

The regional energy balance model is tuned to present day observations of sea level temperature (over a one year cycle) for particular regions of the United Kingdom. The characteristically complex temperature variation is simplified to regional values with a correction for altitude. The mass balance model can then be tested against current day observations of seasonal snow cover.

5. THE ICE SHEET MODEL

The climate models are coupled to the ice-sheet model which is derived from those of Mahaffy (1976), Budd & Smith (1981), and Payne et al. (1989). It is based on the continuity equation for ice thickness which is calculated using:

$$dZ/dt = b - \nabla \cdot [Z(U_s + U_d)]$$

where Z is ice thickness; t is time; b is net balance; U_d is the vertically averaged deformation velocity; and U_s is sliding velocity. The model equations are approximated using finite differences over a rectangular grid with 5×5 km elements. Two feedback loops form the crux of the model. The first is the mass balance /ice thickness/ ice surface elevation feedback which provides the mechanism for ice sheet growth. The second, ice thickness /ice flow/ ice velocity, allows the ice to spread in extent. Isostasy is also included. Inputs required for each element are topography, sea level and mass balance.

6. CLIMATE SENSITIVITY

Sensitivity experiments help to establish the climatic parameters which can reduce the equilibrium line altitude sufficiently to initiate an ice sheet. One parameter in each model run was changed systematically and indicates the relative importance of that parameter within the model.

The most sensitive parameters are the mean annual temperature, precipitation and annual temperature range. Varying the solar constant by the magnitudes calculated for the Quaternary is not sufficient to initiate an ice sheet, although in sensitive areas it may reduce the equilibrium line sufficiently to create mountain glaciers. This is a result of the dominance of the ocean heat flux holding land temperatures higher than for non-maritime areas at similar latitudes. Similarly, other climatic parameters are unable to lower the equilibrium line sufficiently (over their likely range of values) so the first two mechanisms for initiating an ice sheet, insolation variations and seasonal climatic changes, can be discounted. The third, a change in the sea surface temperature, is more problematic to model since the regional climate model is tuned with present day conditions and thus based on invalid assumptions of cloud cover and albedo values for latitude bands. Dynamic changes in ocean circulation are outside the scope

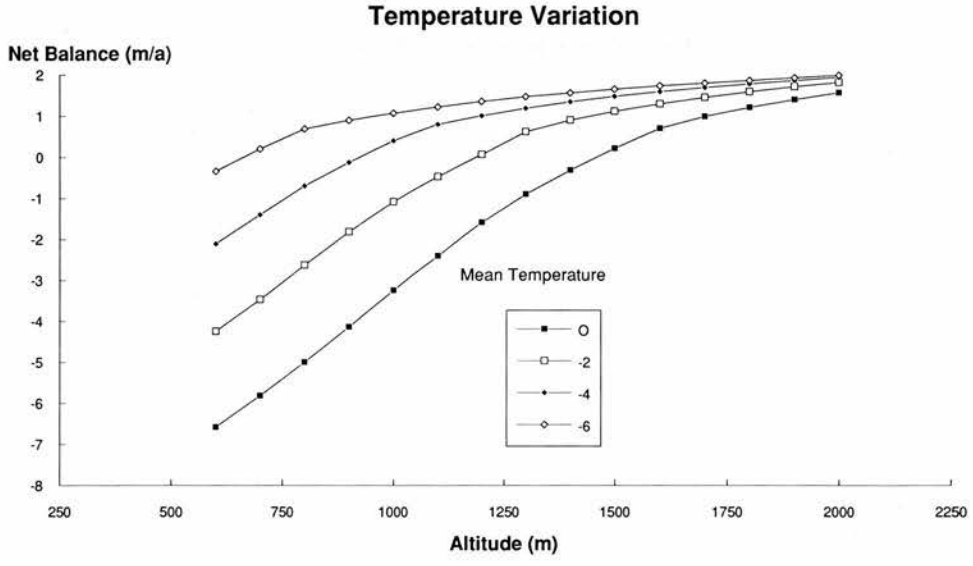

Fig. 1: Mass balance curves for different mean annual temperatures in the western region. The balance gradient at the equilibrium line remains the same for different temperature regimes

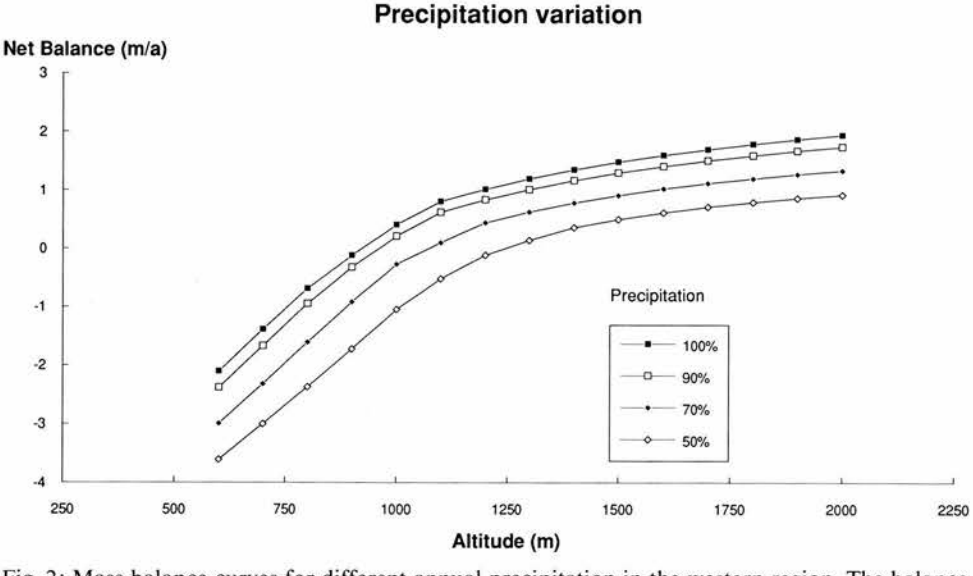

Fig. 2: Mass balance curves for different annual precipitation in the western region. The balance gradient at the equilibrium line varys with different precipitation regimes

of the regional model but appear to be vital in reducing mean annual temperatures on land. To overcome this, mean annual temperatures are assumed to drop in proportion to the sea surface temperatures, but the actual energy fluxes are not explicitly modelled.

Reducing the mean annual temperature reduces the equilibrium line altitude by approximately 135 m/K (fig. 1). A reduction in precipitation leads to a rise in the equilibrium line altitude of approximately 70 m/10 %, but the rise is non-linear for large variations of precipitation (fig. 2). The results again show that the response of the equilibrium line altitude to changes in climate, which is related to the balance gradient close to the equilibrium line, is closely related to the precipitation regime (Oerlemans 1992). In general, a more maritime climate leads to a steeper balance gradient and thus is more sensitive to changes in climatic variables.

One characteristic of maritime climates is the rapid increase in continentality with distance from the coast. There are two combined effects; firstly the increased annual temperature range, and secondly, the reduction in precipitation inland. This is emphasized in Scotland by the mountains on the windward coast. These processes lead to a substantially higher equilibrium line over the east coast compared to the west coast of Scotland (a difference of 300 m). In general, the climate gradient is larger from west to east than from north to south in the British Isles.

One can combine the results to obtain a three dimensional plot which shows how the equilibrium line altitude varies with particular climatic parameters (fig. 3). It is important to note that the balance gradients are not identical above and below this trend surface but are dependent on the relative values of precipitation and mean annual temperature. Here, a temperature depression of 4 K has an equivalent equilibrium line altitude drop to a temperature depression of approximately 7 K with an associated precipitation reduction of 50 %.

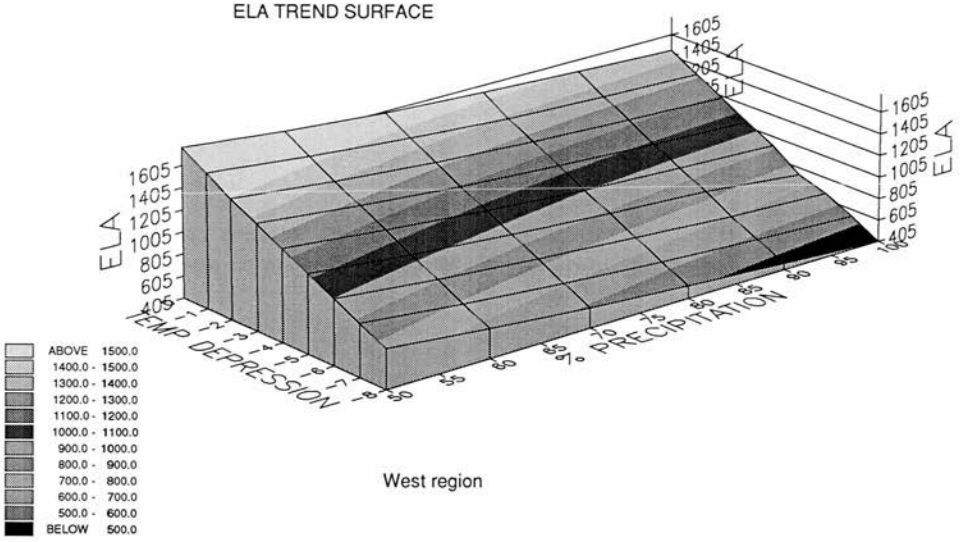

Fig. 3: The equilibrium line altitude surface as a function of annual precipitation and mean annual temperature in the western region. Shaded regions are of equal altitude

Since the climate is a coupled system the process of separating climatic components for sensitivity tests must be undertaken with care. However, since we do not know the palaeoclimate we must rely on intuitive assumptions of the coupled values; for example, that an increase of precipitation was coupled to an increase in cloud cover. Oerlemans (1992) found that the effects of the coupled climatic perturbations on the equilibrium line altitude appeared to be additive but the overall increase was less than 10 %.

7. ICE SHEET GROWTH

7.1 PRECIPITATION

The role of precipitation in the ice sheet system is worth emphasising. A reduction in air temperature reduces ablation and increases solid precipitation but simultaneously reduces atmospheric moisture content and thus precipitation. The exact balance between these two contrasting effects on the equilibrium line altitude is complicated to model and depends on many factors, such as the fetch and temperature of water over which the prevailing wind is travelling. The approach of this paper avoids these problems by merely calculating the overall effect of a reduction in precipitation, rather than trying to calculate specifically the precipitation reduction that occurred in the past; a notoriously difficult parameter to estimate.

7.2 TOPOGRAPHY

From a theoretical point of view, as the equilibrium line altitude falls below the mountain summits small ice caps will form. In reality it will depend on the geometry of the summit (Manley 1955) and factors such as exposure (Ahlmann 1948). Individual mountains are below the resolution of this model but the process remains identical for the grid cells. At a particular equilibrium line altitude the mountain ice caps reach a size where they flow into the valleys and coalesce. Continuing growth produces a positive feedback between the rising ice-filled valley floor, lower temperatures, and more positive mass balance, which creates an explosive growth of ice (Payne and Sugden 1990). This critical point depends on the topography of the region as a whole while the initiation of mountain ice caps depends on the height and geometry of the individual mountain massives. In general, plateaux-like topography requires a smaller drop in the equilibrium line to grow large ice sheets than Alpine topography. This is the basis of the "instantaneous glaciation" of Northern Canada in initiating the Laurentide ice sheet (Andrews and Mahaffy 1975, Williams 1979).

Fig. 4 shows the abrupt threshold between small mountain ice caps and a large ice sheet for variations in precipitation and mean annual temperature. The threshold is a unique function of the topography of a region. It is important to note that the sensitivity of the model is such that the error in calculating the equilibrium line altitude is larger than the sensitivity of the topographic threshold we are trying to investigate. In other words, we do not have the ability to measure the palaeoclimate accurately enough to determine when the threshold would be crossed.

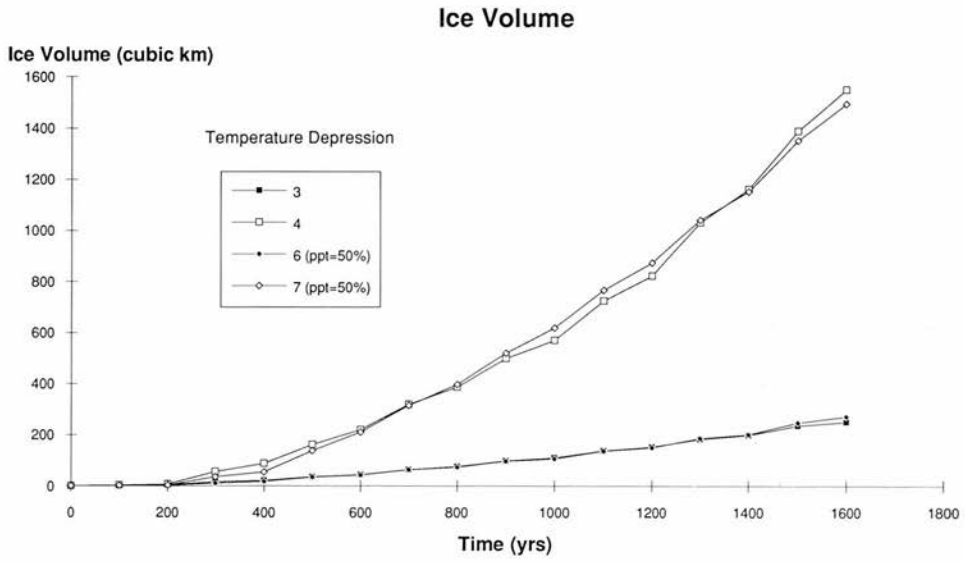

Fig. 4: Ice volume through time for changes in annual precipitation and mean annual temperature. The equilibrium line altitude depression is similar in the case of a 3° C and a 6° C drop with 50 % precipitation and likewise with a 4° C and a 7° C drop with 50 % precipitation

8. THE LOCH LOMOND ICE SHEET

Using as a reference case the Younger Dryas (or Loch Lomond) ice sheet, model results can be compared with field evidence of ice sheet extent. The reference case climate is a 7° C drop in mean annual temperature combined with a 50 % reduction in precipitation. Fig. 5 shows the geographical location of the ice sheet for this experiment. It can be seen that although the highest, plateaux type mountains are in the east (and therefore most susceptible to ice growth), no ice has built up there. This is because the east has substantially less precipitation than the west, assuming broadly similar prevailing winds from the Atlantic rather than from the east, and a more continental climate, which results in a higher equilibrium line altitude. The north is climatically most susceptible to ice sheet growth but topographically is less suited with lower, more peaked, dispersed mountains. The west is climatically and topographically suitable for ice sheet growth.

The results appear to confirm that ice sheet initiation is a function of the balance between the climatic and topographic susceptibility of a particular region. In this example, the west is the most favourable region and the east is the least favourable.

It is important to recognise the assumptions which underpin this work and to examine other possibilities. The sea-level precipitation for each region is assigned before the model run and the precipitation pattern across Scotland is assumed to be broadly similar to the present day. Thus, the west has almost twice the precipitation of the east. It has been suggested that the prevailing winds during the Loch Lomond sta-

dial were from the south west (Sissons 1981, Payne & Sugden 1990) which would lead to a reduction in precipitation in the north; the model would therefore over-predict the volume of ice in the northern region. In common with the work of Payne & Sudgen (1990), a comparison of the model results with the field evidence of the extent of the Loch Lomond glaciation (Sissons 1981) suggests that this may well be the case.

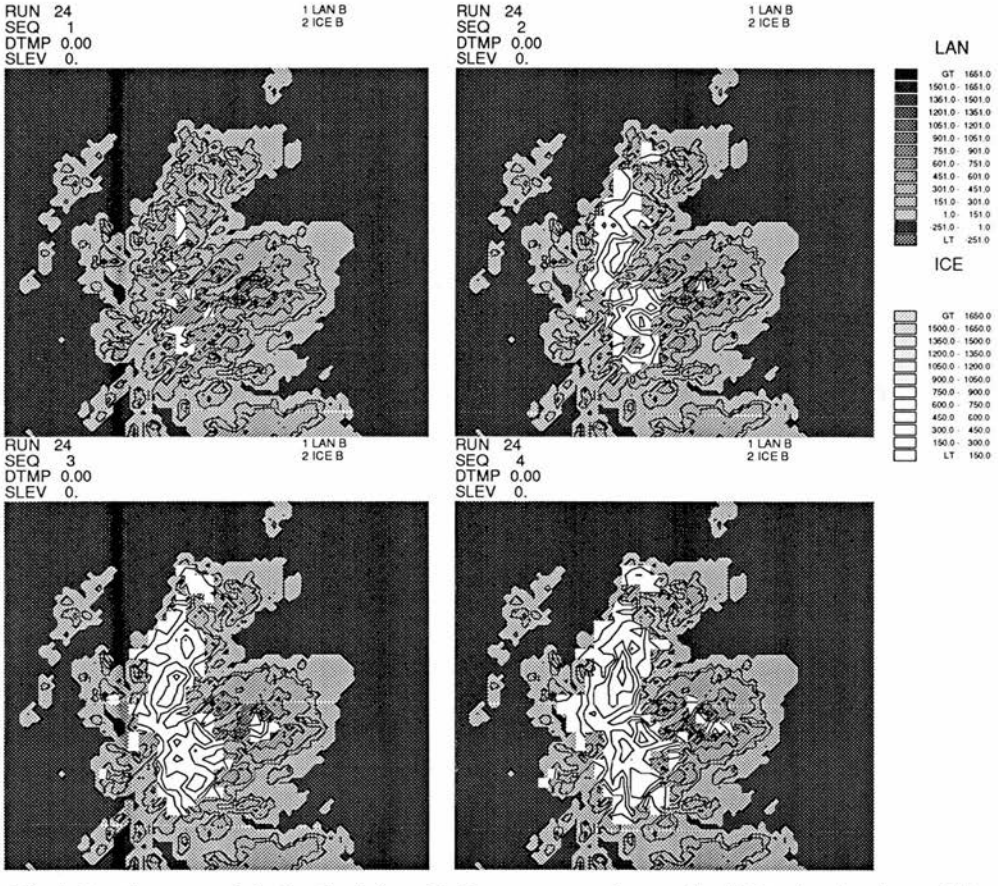

Fig. 5: Ice sheet growth in Scotland for a 7° C temperature drop and a 50 % reduction in precipitation. The captions are taken every 400 years. Ice grows in the west and north but not in the east, despite high plateaux mountains

9. CONCLUSIONS

1. Insolation variations cannot initiate maritime ice sheets directly although in mountainous areas of maritime regions glaciers may form.

2. Changes in ocean temperature affects the delicate balance between precipitation and mean annual temperatures and drive maritime ice sheet growth. Increased continentality leads to an increased annual temperature range and lowers susceptibility to ice sheet growth. Reduced precipitation with distance from prevailing oceanic winds emphasises this climatic gradient.

3. Changes in the net balance gradient at the equilibrium line affect the rate of ice sheet growth, and are determined by the relative values of precipitation and mean annual temperature.

4. The configuration and altitude of the upland topography determines the point of initiation and the threshold between stable upland glaciers and the growth of an ice sheet.

5. In the case of Britain, ice sheets appear to be triggered by the southward movement of the North Atlantic polar front.

ACKNOWLEDGEMENT

The author is indebted to J. Oerlemans of the Institute for Meteorology and Oceanography, University of Utrecht, for help and advice with the climate models, and A. Payne of the Grant Institute of Geology, University of Edinburgh, for help with the ice sheet model. This work was undertaken while the author was the recipient of a U. K. Natural Environment Research Council studentship.

REFERENCES

Ahlmann, H. W., 1948: Glaciological research on the North Atlantic coasts. London, Royal Geographical Society (R. G. S. Research Series 1).

Andrews, J. T. and M. W. Mahaffy, 1976: Growth Rate of the Laurentide Ice Sheet and Sea Level Lowering (with emphasis on the 115,000 BP sea level low). Quat. Res. 6, 167—183.

Budd, W. F. and I. N. Smith, 1981: The growth and retreat of ice sheets in response to orbital radiation changes. I A. H. S. Publ. 131. (Symposium at Canberra 1979 — Sea Level, Ice and Climate Change), 369—409.

Lamb, H. H., 1964: The Role of Atmosphere and Oceans in relation to climatic changes and the growth of ice sheets on land. (NATO Advanced Studies Institute Symposium on Palaeoclimates) in Problems of Palaeoclimatology, Nairn(ed). 332—348. London, New York and Sydney, John Wiley and Sons Ltd.

Johnson, R. G. and J. T. Andrews, 1979: Rapid Ice-Sheet Growth and Initiation of the Last Glaciation. Quat. Res. 12, 119—134.

Mahaffy, M. W., 1976: A three dimensional numerical model of ice sheets: tests on the Barnes Ice Cap, Northwest Territories. J. Geophys. Res. 81 (6), 1059—1066.

Manley, G., 1955: On the occurrence of ice domes and permanently snow-covered summits. J. Glaciol. 2 (17) 453—456.

North, G. R., R. F. Cahalan and J. A. Coakley, 1981: Energy Balance Climate Models. Reviews of Geophysics and Space Physics 19 (1), 91—121.

Oerlemans, J., 1992: A model for the surface balance of ice masses. Part I: Alpine Glaciers. Z. Gletscherk. Glazialgeol.

Payne, A. J. and D. E. Sugden, 1990: Climate and the initiation of maritime ice sheets. Annals of Glaciology 14, 232—237.

Payne, A. J., D. E. Sugden and C. M. Clapperton, 1989: Modelling the growth and decay of the Antarctic Peninsular ice sheet. Quat. Res. 31 (2), 119—134.
Pelto, M. S., S. M. Higgins, T. J. Hughes and J. L. Fastook, 1990: Modelling mass balance changes during a glacial cycle. Annals of Glaciology 14, 238—241.
Ruddiman, W. F., A. Mc Intyre, V. Niebler-Hunt and J. T. Durrazzi, 1980: Oceanic Evidence for the Mechanism of Rapid Northern Hemisphere Glaciation. Quat. Res. 13, 33—64.
Sissons, J. B., 1981: The last Scottish ice-sheet: facts and speculative discussion. Boreas 10, 1—17.
Williams, L. D., 1979: An Energy Balance Model of Potential Glacierization of Nothern Canada. Arctic and Alpine Res. 11 (4), 443—456.

Manuscript received 30th September 1991

Author's address: Andrew Kerr
Department of Geography
The University of Edinburgh
Drummond Street
Edinburg EH 8 9XP, Scotland

Topography, climate and ice masses: a review

Andrew Kerr

Department of Geography, University of Edinburgh, Drummond Street, Edinburgh EH8 9XP, UK

ABSTRACT Topography acts as a filter between regional climate and the consequent response of a glacier or ice sheet. It influences the mass and energy inputs and modifies the ice dynamics. The evolution of the ice sheet surface and, over longer time scales, of the bed topography modulates the climatic forcing.

Until we have a better understanding of these topographic linkages, the use of geophysical signals from former ice masses to determine palaeoclimates must be regarded as fundamentally flawed.

Terra Nova, **5**, 332–342, 1993.

INTRODUCTION

The aim of this paper is to review the role of topography on the relationship between climate and ice volume. Topography plays a fundamental role because it acts as a filter between the regional climate and the response of the glacier or ice sheet. This response ultimately yields a geological or geophysical signal which is then used inversely to obtain information about regional palaeoclimates. The topographic filter encompasses a number of complex linkages which act both externally to the system, through localized variations in energy and mass input, and internally, by modifying ice flow dynamics (Fig. 1).

Theoretical and observational studies of glaciers and ice sheets have been carried out for many years and are often concerned with the relationship between climatic change and ice sheet evolution, especially with regard to the Pleistocene ice ages. This relationship is highly complex and an understanding requires delineating the important processes at different spatial and temporal scales. Topography is one aspect of this relationship but it underlies a number of related factors including isostasy (the relative position of the land surface to sea level) and eustasy (a change in sea level), both of which have been studied in detail with relation to glacial cycles.

Ice masses are arbitrarily classified in this paper by distinguishing the way ice interacts with the underlying topography: first, mountain glaciers and ice caps which are constrained by topography and depend on the effect of bed topography on regional climate for their mass and energy balances; and second, ice sheets which largely submerge the underlying topography and are less constrained by it except at the margins.

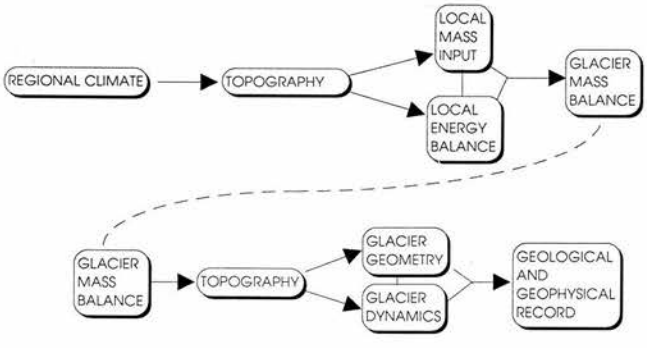

Fig. 1. *Topographic linkage between regional climate, glacial response, and the geophysical record. Figure taken from Furbish and Andrews (1984).*

TOPOGRAPHY AND GLACIERS

Bed topography plays a rather more dominant role on valley glaciers and mountain ice caps than it does on large ice sheets since the former are dependent on the surrounding topography for their existence. At large scales it is the altitude and morphology of the mountains that determines both the potential size of the glaciers and ice caps, and the glacial mass balance, which is the balance between the supply (accumulation) and loss (ablation) of ice. In addition, the geometry of the bedrock affects the motion of the glacier.

Topography and climate

Large-scale topography such as a mountain range acts in two distinct ways to influence glaciers: first, the energy and mass inputs to the glacial system depend on how the regional climate interacts with the surface topography. Secondly, the morphology of the topography defines the geometrical limits of a glacier.

The regional climate is dependent on geographical variables such as latitude, altitude, and continentality (the distance from an ocean to windward), which determine the energy and precipitation received in any one area. The interaction between regional climate and mountains is complicated by the localized nature of the mass and energy exchange between the atmosphere and the surface, with its variable altitude, relief, and aspect. One of the primary difficulties in delineating this problem has been the lack of systematic data in mountainous regions (with the notable exception of certain Alpine and Scandinavian records). Barry (1981) provides a summary of the physics involved as an atmospheric flow crosses mountains.

The relationship between glaciers and climate is determined primarily by two parameters. The equilibrium line is the boundary between the accumulation area, where there is a net gain of mass over the year, and the ablation area, where there is a net loss. The accumulation area encompasses both areas of permanent snow cover and superimposed ice, where snow melts and refreezes. In temperate glaciers, the superimposed ice zones is insignificant and the climatic snowline is approximately equivalent to the glacial equilibrium line. The altitudinal mass balance profile is the amount of snow accumulated or ablated over one year at different altitudes (Fig. 2). This latter parameter is more useful for determining the climatic setting and hence the glacial response to a climatic change.

Ahlmann (1948) noted the importance of the mass balance profile (and its altitudinal gradient) on glacial response while Schytt (1967) related the ablation gradient to climatic variables. The seminal work on the subject was the analytical formulation of the sensitivity of the mass balance profile to climatic variables (Kuhn, 1979, 1981, 1984, 1989). The factors contributing to the energy and mass budgets, such as the radiation budget, temperature, precipitation, and turbulent fluxes, have contrasting sensitivities depending on the climatic regime. Snow accumulation, especially in summer, plays a decisive role in maritime climates while the length of the ablation season is important in polar areas. In dry, continental regions the mass balance profile is sensitive to albedo changes close to the equilibrium line, and in alpine regions climate sensitivity is less dependent on altitude.

This work indicates that common assumptions concerning the conservation of mass balance gradients under climatic change (e.g. Lliboutry, 1974) are doubtful. Further work (Oerlemans and Hoogendoorn, 1989; Oerlemans, 1990) concurs and has led to a refining of the formulation and sensitivity of climatic variables; for example, by incorporating precipitation into a surface energy balance model.

The problems associated with measuring a glacier's mass balance profile led to work on the statistical correlation between this and other parameters which are more easily measured, such as the equilibrium line altitude (Braithwaite, 1984). However, it was concluded that accurate calculations were impossible without further climatic information. Similarly, observations of glacier mass balance and meterological data (Letreguilly, 1988; Letreguilly and Reynaud, 1989) indicate the problems involved in statistical correlation.

There are two overriding conclusions: first, that the sensitivity of glacial mass balance depends on the prevailing climatic regime. Pelto *et al.* (1990) noted that the climatic regime will change over a glacial cycle and hence so will the sensitivity of the glacial mass balance. Secondly, the climatic sensitivity of glacial mass balance

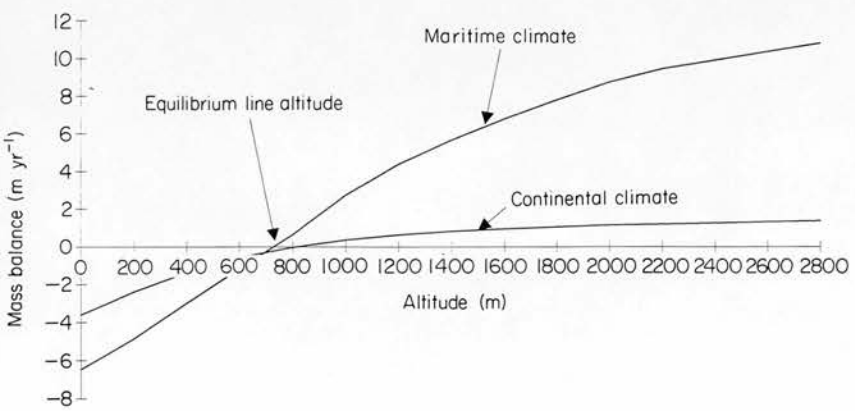

Fig. 2. *Glacial mass balance profiles showing the contrast between maritime and continental environments. Although the equilibrium line altitudes are similar, the maritime climate has a much steeper balance gradient because of the higher values of accumulation and ablation. Hence, there is a much faster throughput of ice which results in glacier termini reaching lower elevations before melting.*

must be distinguished from the variation in glacial extent. Observational evidence (Hoinkes, 1968; Reynaud *et al.*, 1984) and theory agree that mass balance profiles are useful indicators of climatic change but that glacial extent is not because glacial fluctuations depend on the surrounding topography. The high-frequency atmospheric forcing is filtered by the glacier. Any attempt to invert this signal to obtain specific climatic variables such as temperature or precipitation from fluctuations of glacial extent is fundamentally flawed.

The broad theoretical understanding of the response of a glacier to climate was developed by Nye (1960, 1961, 1963a, 1963b, 1965a, 1965b) and neatly summarized by Paterson (1981). A glacier responds to a perturbation in mass balance by the propagation of diffusive kinematic waves down the glacier to re-establish a steady-state ice volume and length. Strictly speaking the theory is valid only for temperate glaciers on simple bed topography since the consequent effect of complex topography or a temperature change on ice flow is ignored. The perturbations from steady state are also assumed to be small. More recently, Johannesson *et al.* (1989a, 1989b) have adapted Nye's work and used the geometric similarity of glacial profiles to show more robust estimates of the time for a glacier or ice cap to respond to climatic change: of the order of tens of years for valley glaciers.

The second effect of large-scale topography is to delimit the potential size of glaciers and ice caps for a specified climate. It is intuitively obvious that glacial extent depends on the morphology of the bedrock topography. This was articulated by Manley (1955) who estimated the relative importance of the breadth and height of a mountain summit in determining whether it could carry a glacier for a specified equilibrium line altitude. For example, an alpine aiguille may never carry a glacier because it is too steep while a mountain plateau, such as those found in the Cairngorms in Scotland, can potentially carry a glacier if the equilibrium line is just below the summit. Conversely, plateaux surfaces are poor accumulators of snow in windy conditions. The wind-blown snow accumulates in bedrock depressions or in the lee of the plateau where cirques develop. The reliance of these cirque glaciers on wind-blown snow and cornice avalanches for their nourishment means they can exist well below the regional equilibrium line.

These local climatic and morphological effects ensure that there is no simple way of obtaining regional equilibrium lines, and hence a measure of climate, from observations of glacial extent (e.g. Andrews *et al.*, 1970). This has serious implications for an understanding of regional climate in remote areas and more especially for reconstructing palaeoclimates. Various approximations of the glacial level have been used such as defining the glaciation level as being between the lowest suitable mountain carrying a glacier and the highest suitable mountain without one. Ahlmann (1937) applied this idea to Vatnajökull while Østrem (1966) extended it to calculate the glaciation level in British Columbia.

Palaeoclimatic studies use a variety of methods to estimate former equilibrium line altitudes by means of geometrical arguments. For example, it is possible to use a shape ratio since there is approximately one third of a glacier in the ablation zone and two thirds in the accumulation zone, so in theory the equilibrium line altitude can be estimated for a steady state glacier from geological records. Meierding (1982) assessed six methods for inferring equilibrium lines and concluded that the shape ratio had the smallest statistical mean error of 80 m for current glaciers in the Colorado Front mountain range. However, this type of areal relationship does not appear to hold uniformly for glaciers in widely differing climates. As Williams (1975) points out, the estimation of climatic deterioration from terminal moraines or small cirques assumes certain climatic factors, such as the altitudinal temperature lapse rate (which is highly variable; Harding, 1978), remains invariant even though the climate has changed dramatically.

Furbish and Andrews (1984) used topographic hypsometry (area–height profile) to examine the long-term stability and response of glaciers to changes in mass balance. They derive a simple equation relating the mass balance and hypsometry of a glacier to the glacial response to climatic change and show that the amplitude of glacier response is dependent on valley geometry (Fig. 3). This is taken a step further by Oerlemans (1989) who used a numerical model to examine the response of a glacier to changing climatic conditions on different topographies. There are three important conclusions: first, the longitudinal bed profile is very important. Beds with smaller slopes are more sensitive to climatic change since a change in the (near horizontal) equilibrium line affects a larger part of the glacier (Fig. 4), but glaciers with small bed slopes react more slowly to climatic change; a consequence of the smaller mass throughput of these glaciers. Second, the presence of reverse slopes leads to the possibility of multiple steady states for a specific range of climate; the actual ice volume depends on the history of mass balance fluctuations (Letreguilly and Oerlemans, 1990). Finally, the mass balance gradient on long valley glaciers is partly determined by along valley changes in width and albedo. These latter factors link topography, climate, and glacial dynamics.

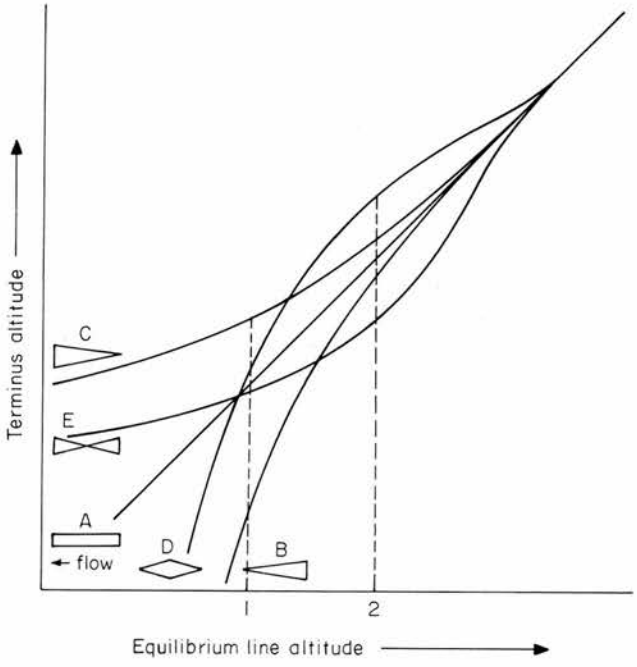

Fig. 3. *Relationship between the glacier terminus altitude (TA) and the equilibrium line altitude (ELA) for five glaciers, A–E, of different idealized shapes. Changing the ELA modifies the area of accumulation and ablation, and hence the response of the terminus. For ELA position 1, the terminus altitude of $B<A\approx D\approx E<C$; for position 2, $E<B<A<C<D$. Figure taken from Furbish and Andrews (1984).*

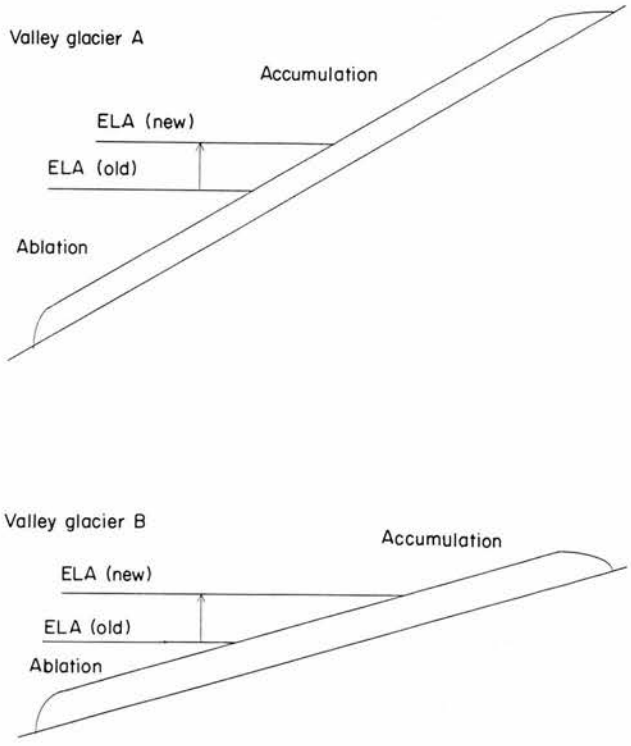

Fig. 4. *A sketch of two glaciers which respond differently to an identical change in the equilibrium line altitude because of their differing bed slopes. The accumulation/ablation ratio of Glacier A is less affected than glacier B by the change in equilibrium line altitude, so glacier A will have a smaller response to the climatic change.*

Topography and glacial dynamics

Climatic forcing of glaciers depends on the interaction with regional topography and the areal extent of the glaciers. This depends on the morphology of the topography and ice dynamics, which comprises two parts: ice deformation and basal sliding (Fig. 5). Both are strongly determined by the underlying topography.

Topography affects ice deformation in a glacier by altering the stresses acting on the ice mass. The fundamental problem has been to derive a complete set of equations which describe deforming ice under known mechanical laws and complex boundary conditions. Polycrystalline ice deforms plastically and this understanding (Orowan, 1949; Nye, 1951) and subsequent work (Glen, 1955; Nye, 1957) showed that the relationship between the effective strain rate, ε, and the effective stress, τ, was non-linear and had the form:

$$\epsilon = A \cdot \tau^n$$

over the range of stresses usually found in a glacier. Different values of n and A have been found in various studies; n is usually taken to be 3 while A is temperature dependent. Using the generalized flow law analytical solutions of the equilibrium profiles of glaciers and ice sheets become possible under certain simplifying assumptions (Nye, 1952; Vialov, 1958). The ice is assumed

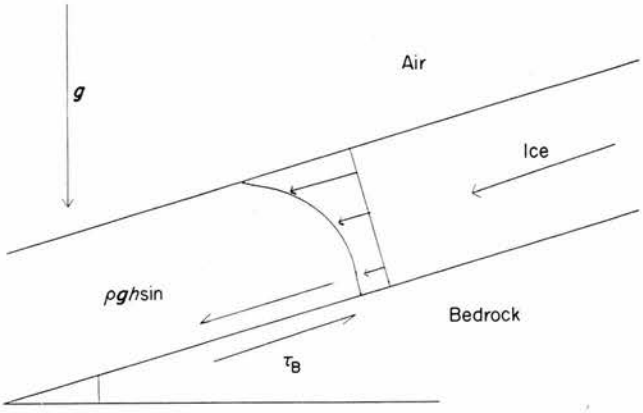

Fig. 5. *Schematic view of the motion of a glacier, which is a combination of ice deforming under its own weight and sliding over the bed. Ice deformation is determined mainly by ice surface slope.*

to deform under its own weight in simple shear and the basal shear is found to be determined mainly by ice surface slope:

$$\tau_b = \rho \cdot \mathbf{g} \cdot h \cdot \sin \alpha,$$

where α is the surface slope, and h is the ice thickness.

Glacial flow is affected by valley walls and by bedrock irregularities. The former effect can be approximately taken into account by multiplying by a shape factor, F, which depends on the valley half width and ice thickness (Nye, 1965c). A more recent analysis suggests F has a simple physical interpretation and that it varies as the glacial profile approaches steady state (Johannesson *et al.*, 1989b). The latter effect requires additional correction terms to the basal shear equation and these depend on the scale over which calculations are averaged. At small scales all terms must be taken into account while at large scales, perhaps twenty times the ice thickness, the correction terms can be ignored. Observationally it is very difficult to verify the basal stress approximation because accurate surface velocity measurements are required but Bindschadler *et al.* (1977) found on Variegated Glacier, Alaska, that the correction terms could be ignored if the surface slope was averaged over long enough length scales. It may be that, in general, the large-scale longitudinal slope is the important factor for longitudinal stresses (Budd, 1970b).

The second process which affects ice extent is basal sliding but the formulation of a generally applicable sliding law has proved beyond mathematical analysis. There are three potential mechanisms for basal sliding in temperate glaciers. The first is regelation which occurs when ice melts in high-pressure areas upstream of obstacles and refreezes downstream, with the concurrent transfer of latent heat upstream through the obstacle forcing ice melting. The second process involves enhanced creep caused by additional stresses induced by the obstacle which leads to ice preferentially moving over and around obstacles. The former process operates over small obstacles while the latter occurs over larger bedrock irregularities (Weertman, 1957). Lliboutry (1968) suggested a third important process, that of sliding over water- and air-filled cavities between the ice and bedrock, since there is less friction in these areas.

The mathematical formulation of this problem is extremely complex and has been tackled, not altogether successfully, in a number of different ways. Kamb (1970) and Nye (1969) generalized the Weertman ideas for variable bedrock roughness by statistically calculating the bed roughness using Fourier methods and assuming no cavitation. Morland (1976) extended this to include gravity by using a sloping bed while Lliboutry (1976, 1987) continued on the problem of cavitation by extending the concept of effective pressure: the difference between the downward pressure of ice and upward pressure of basal water. This could explain seasonal variations in sliding velocity through fluctuations in melt water. The problem was reformulated into two parts by Fowler (1981, 1987): the flow in the basal boundary layer and the flow in the bulk of the glacier. This work again emphasized the importance of bedrock topography on the sliding law.

However, this work failed in general to deal with the effects of factors such as rock debris in the basal layers which increases friction (Boulton, 1974; Hallet, 1981; Schweizer and Iken, 1992), or the possibility of glaciers moving over deformable sediments as postulated for the southern areas of Pleistocene ice sheets (Boulton and Jones, 1979).

A generally applicable sliding law is still not in sight so current mathematical models use crude relations postulated years ago between basal stress, sliding velocity and overburden pressure. The justification is that the glacier or ice sheet evolution appears less sensitive to basal sliding relations than to variations in mass balance. In any case, the bed geometry in models is usually too simplified to justify more complex derivations.

TOPOGRAPHY AND ICE SHEETS

Ice sheets submerge underlying topography and it is the evolving ice surface which interacts with the climate. Ice flow is less affected than in glaciers but bed topography becomes increasingly important at ice sheet margins.

Topography and climate

The main interest in the relationship between ice surface topography and climate concerns the extent and stability of the ice sheet, and the modification of the regional climate by the evolving ice sheet.

Early investigations into the effect of climate were based on analytical work of ice flow in steady state ice sheets; in other words, the mass input to the ice sheet is just balanced by ice flow. In this instance, the height of the ice sheet is only nominally dependent on the absolute values of accumulation and ablation. In the theoretical case of plastic ice the ice sheet height depends only on ice sheet extent which depends on the geographical slope of the equilibrium line and regional topography. Similarly, the position of ice divides and centres is poorly dependent on the variation of accumulation over the ice sheet (Weertman, 1973)

The effect of a climatic change is to grow or decay an ice sheet. Weertman (1964) used a dynamic model to

examine the time required for this change in ice volume assuming plastic ice and simplifying assumptions concerning the equilibrium line. There is an asymmetry in the time for growth and decay because of the discrepancy between accumulation rates and the larger ablation rates. Derivations by Hindmarsh (1990) re-emphasized the importance of the accumulation/ablation ratio (not the absolute rates) and the slope of the equilibrium line on the ice sheet profile.

Bodvarsson (1955) was the first to consider the stability of ice sheets in relation to climate and showed that if the equilibrium line is horizontal a steady-state ice sheet is unstable. If the ice sheet grows the accumulation/ablation area ratio increases over the ice sheet leading to continued growth. Similar arguments apply to ablation when the ice sheet shrinks. This point was addressed mathematically by Weertman (1961) who found a series of stable and unstable states, such that a critical size of ice cap existed which, when exceeded, could allow unstable growth.

To examine the role of more complex boundary conditions, such as time-dependent mass balance or bed topography, numerical methods are required. The increasing power and sophistication of computers has led to a rash of models for different applications but they are broadly of two types: 2D or 3D models incorporating the continuity equation of ice, where the change in ice height is a function of the mass balance and the divergence of flow, and simplified relations are used for ice flow and sliding, such as the Mahaffy (1976) model; or a one-dimensional flow line model which can incorporate more complex bed topography and stress relations.

Later models improved the mathematical formulation of ice flow and environmental interactions. (e.g. Budd and Smith, 1981) but too often still relied on poor parameterization of bed topography or naïve formulations for climate; typically the Milankovitch variations of isolation were directly linked to the N–S movement of the equilibrium line. Concurrently, the formulation of equilibrium energy balance models for heat fluxes between latitude zones (North *et al.*, 1981) and at the ice surface were improved to give a more reasonable coupling of the climate to an evolving ice sheet.

Unfortunately, these models rely on broad simplifying assumptions and empirically derived parameters such that a rough simulation of glacial growth and decay in a particular region may provide less insight into the physical processes involved than into the limitations of the model (Saltzman, 1985); often there is a lack of data to test the model at different periods of ice sheet evolution (Porter, 1989).

More positively, quantitative results of important feedbacks within the climate-ice sheet system have been identified. One such process related to the ice sheet profile is the mass balance–altitude feedback. The atmosphere is characterized by high vertical gradients of climatic variables which favour ice sheet growth at higher altitudes. Ice sheet growth leads to a rising ice surface, and to increased mass input, and hence to more growth, until limited by factors such as coastlines or precipitation starvation which occurs in the cold, high-altitude air (Fig. 6). This feedback was articulated by Oerlemans (1980) and found to be more important than the albedo-temperature feedback originally postulated by Budyko (1969) and Sellers (1969).

A major complication of the climate–ice sheet interaction is the modification of regional climate by the ice

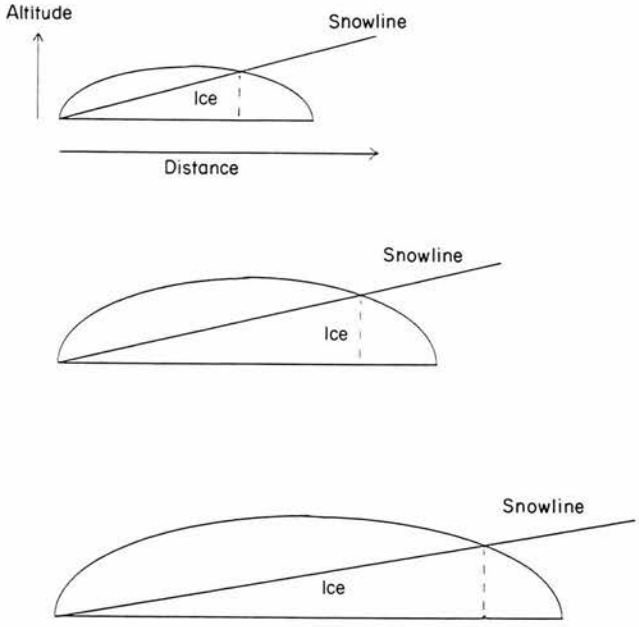

Fig. 6. *A schematic illustration of the height–mass balance feedback. A small modification of the snowline causes a dramatic change in ice sheet extent because of the effect of the increasing ice sheet surface elevation on the accumulation/ablation ratio.*

sheet. Small ice caps can have a dramatically different surface energy balance from surrounding land by virtue of increased cloudiness and a larger albedo (Bradley and Serreze, 1987). Large ice sheets can influence planetary atmospheric circulation and consequently affect precipitation patterns to leeward. Experiments by Cook (1990) indicate that the Laurentide ice sheet could also have affected North Atlantic sea surface temperatures. These effects have a bearing on the evolution of ice sheets in Europe though dating techniques are insufficiently accurate to test hypotheses concerning phase lags between major ice sheets.

The climate–ice sheet interaction leads to questions on the stability of ice sheets: the Milankovitch insolation variations appear too small to account for the apparent ice volume changes during the Pleistocene. We require instabilities within the system for ice caps to grow beyond a critical size and decouple themselves from the regional topography and climate. The increasing surface height and the modification of regional climate by an ice sheet may provide part of the answer. Oerlemans and van der Veen (1984) and Hindmarsh (1990) both note the existence of fold catastrophes in the climate–ice sheet system due to the coupled effect of a dropping equilibrium line and a rising ice surface. Examples include the transition from valley glaciers to ice sheets, medium-scale topography (Payne and Sugden, 1990), and the coalescence of ice sheet domes. The catastrophic jumps at these topographic thresholds occur as the system moves to more stable states (Fig. 7). Although in theory the topographic thresholds can be calculated, the time lags within the system mean the glacial response to climatic forcing is unpredictable at these points.

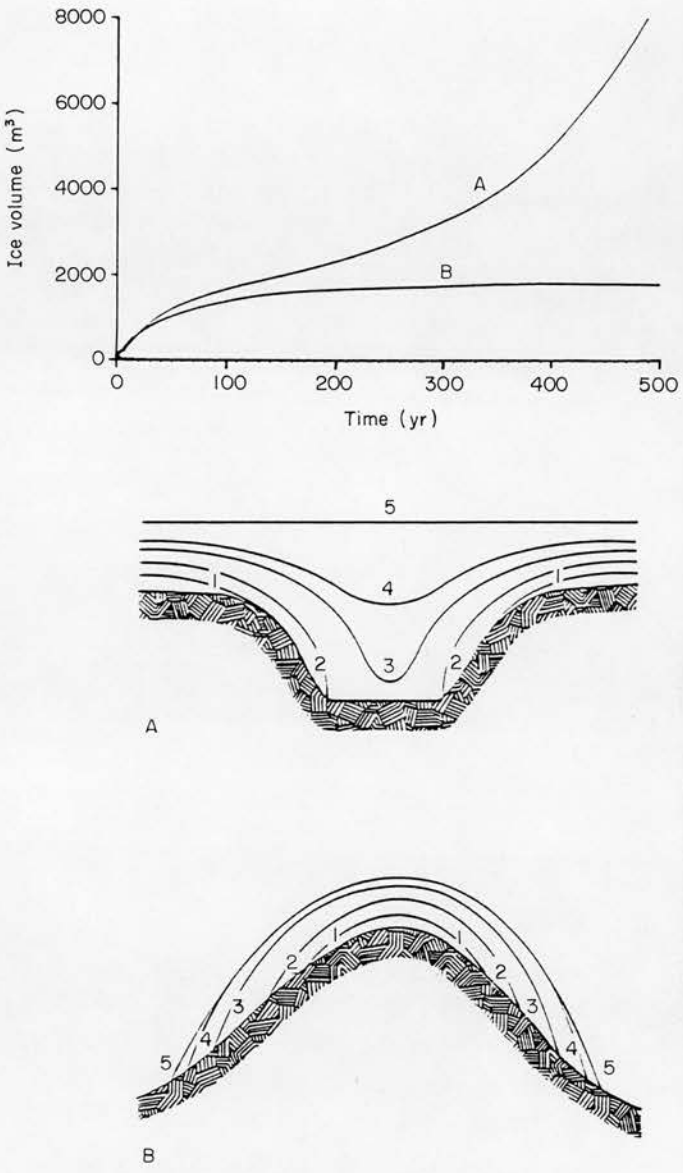

Fig. 7. *A lowering of the equilibrium line altitude results in a very different history of ice growth (denoted by stages 1–5) on A and B. After stage 2 there is an explosive increase of ice volume at A because of the rising ice surface while B approaches a steady state. Figure adapted from Payne and Sugden (1990).*

Topography and glacial dynamics

Ice flow in ice sheets is comparatively unaffected by bed topography except at the margins. The ice sheet surface can be approximated with analytical solutions of equilibrium profiles, where ice is assumed to deform under its own weight. Weertman (1961) showed that in small ice caps longitudinal stresses modified the equilibrium profile by flattening the ice divide but they were negligible in large ice sheets.

Although these theoretical profiles broadly represent the large-scale features of an ice sheet surface, observational discrepancies became apparent (Robinson, 1966). Robin (1967) pointed out that Nye's approximation of basal shear stress to ice surface slope was not sensitive locally because of longitudinal stresses resulting from ice movement over varying bottom topography, and there began a long series of attempts to derive correction terms for the resulting effects. Collins (1968) mathematically justified certain assumptions used by Robin (1967) and was followed by a series of theoretical analyses (Nye, 1969; Budd, 1970a, 1970b, 1971) to explain the waves apparent on the ice surface. Budd (1970b) concluded that particular bedrock wavelengths were damped differentially, with wavelength undulations of approximately 3.3 times the ice thickness preferentially transmitted to the surface. This appeared to be confirmed by observations (Budd and Carter, 1971) and later analysis (Hutter *et al.*, 1981) agreed that a distinct wavelength may exist while questioning some of the assumptions used in the analysis.

More recent work has entailed using more sophisticated mathematical techniques (Hutter *et al.*, 1983; Morland and Johnson, 1982), or extensions of previous theory (Whillans and Johnsen, 1983) to demonstrate the importance of longitudinal stress gradients on basal shear stress over various scales of longitudinal averaging. Kamb and Echelmeyer (1986) and related papers develop a simple general formulation to describe how ice thickness and bed mass translate into a particular pattern of longitudinal flow.

Unfortunately, these ideas invariably involve simplifying assumptions which may invalidate some of the conclusions. For example, Hutter *et al.* (1981) assume that the ice and bed surface are approximately parallel, while Kamb and Echelmeyer (1986) linearize the longitudinal variations of ice flow. In addition, most previous work required that basal boundary conditions were known, or could be fitted to the theoretical surface values for the solution. An alternative approach was adopted by Van der Veen and Whillans (1989a, 1989b) and Whillans *et al.* (1989) who calculated the inverse (and more practical) result of deriving stress and strain rates at depth from surface measurements, and tested the theory on Byrd Glacier, Antarctica in two- and three-dimensions. The results reiterate the importance of longitudinal stresses on ice flow variation close to ice sheet margins. It may be that this inverse approach leads to a more general understanding of the relevant stresses which contribute to variations in ice flow over complex bedrock terrain.

While bed topography does not predominantly affect ice flow in ice sheets, on smaller scales and in areas where the magnitude of bed topography waves approaches the ice depth it plays an increasingly important role. For example, marine ice sheets rest on land that is generally below sea-level, and the transition from ice sheet to ice shelf at the grounding line is very sensitive to bedrock topography (Thomas, 1979). The grounding line limits the ice sheet size and in retreat can theoretically destabilise an ice sheet though recent fears concerning the West Antarctic ice sheet appear unfounded at present (Van der Veen, 1985). The transition from ice sheet to ice stream flow is also abrupt and occurs at a step in the subglacial topography, with rapid ice flow through subglacial topography leading to characteristic over-deepened troughs (McIntyre, 1985). There is also geological evidence that the southern ice lobes of the former Scandinavian ice sheet were controlled topographically (Punkari, 1980). Furthermore, ice berg calving glaciers are found to be partially decoupled from the regional climate by local topography. The glacier may be pinned before a deepening expanse of water or it may advance on its own terminal moraine across deep water. This leads to glacial oscillations which bear no resemblance to climatic trends (Warren, 1992).

LONG-TERM TOPOGRAPHIC EVOLUTION

Over the time-scales of glacial cycles, topographic evolution modifies the climatic forcing of ice sheets. For example, the time-lagged effect of isostasy can partially explain the saw-tooth shape observed in proxy data of ice volume while eustastic sea-level rises can destabilize marine ice sheets (Payne *et al.*, 1989; Huybrechts, 1990). Both processes are reviewed extensively elsewhere. On longer time scales tectonic uplift may have initiated the late Cenozoic cooling which led to the growth of continental ice sheets. Raymo and Ruddiman (1992) review these ideas and conclude that the uplift of the Tibetan plateau is crucial to explain observed climatic change while acknowledging that a better understanding of the linkages between uplift, weathering and climate is required. A complementary argument is put forward by Molnar and England (1990) who hypothesize that climatic change contributes to tectonic uplift. This seemingly surprising result is obtained by considering the climatically forced high denudation rates of mountain ranges which lead to compensatory isostatic uplift; although the mean elevation drops the peak elevation increases. They argue that the inferred acceleration of late Cenozoic uplift can equally be explained by climatic change. It is widely acknowledged (Chalikov and Verbitsky, 1990; Birchfield *et al.*, 1982; Abe-Ouchi and Blatter, 1992) that a necessary but not sufficient requirement for the inception of the ice ages is large uplifted regions at high latitudes. The weakness in their argument revolves around the erosive power of glaciers required to move sufficient material from the mountains and transport it long distances.

The erosion of bed topography is poorly understood, depending as it does on regional geology, preglacial elevations and the basal thermal regime of ice. Mazo (1989) developed a model of the eroding glacier and the eroded bed which indicates that a specific erosive scale preferentially develops into the morphological form of the cirque bed profile while Harbor *et al.* (1988) derive a more comprehensive model of landform development. However further work is required to understand the development of glacially eroded landscape under changing climatic conditions.

CONCLUSION

The fundamental effect of topography is to decouple the response of a glacier or an ice sheet from the climate. It influences the mass and energy inputs to glaciers and modifies the ice dynamics. Ice sheets are less constrained by bed topography but by nature have a finite width, and at the margin topography influences outlet glaciers and ice streams. The evolving ice sheet profile is crucial in determining the interaction with the climate.

Bed topography also evolves over long time scales. It is driven by regional tectonics, isostasy, eustasy and erosion, and this evolution affects the climatic forcing. Topography must be considered a dynamic variable in the earth's climate system if we are to understand long-term climatic trends.

Examples of fold catastrophes appear to be very common in the ice sheet system and the unstable jumps of ice volume to more stable states puts fundamental limits on the predictability of ice sheet evolution.

In this context, the use of geological or geophysical signals from former glaciers or ice sheets to determine palaeoclimates must be regarded as fundamentally flawed. In essence we require a measure of the effect that an arbitrary topography has on the response of an ice mass to an arbitrary climatic change. To determine this measure future work requires an interdisciplinary approach that encompasses glaciologists, geomorphologists, and climatologists to examine the complex linkages between the evolution of topography, climate, and ice sheets.

ACKNOWLEDGEMENTS

This work was carried out while the author was the recipient of a NERC grant.

REFERENCES

Abe-Ouchi A. and Blatter H. (1992) On the initiation of ice sheets, *Abstracts for IGS Symposium on Snow and Snow-related Problems, Japan.*

Ahlmann H.W. (1937) Vatnajokull in relation to other present day Iceland glaciers, *Geogr. Annlr.*, **19,** 146–231.

Ahlmann H.W. (1948) Glaciological research in the North Atlantic coasts, *R. Geogr. Soc. Res. Ser.*, **1,** 83 pp.

Andrews J.T., Barry R.G. and Draper L. (1970) An inventory of the present and past glacierization of Home Bay and Okoa Bay, east Baffin Island, NWT, Canada, and some climatic and palaeoclimatic considerations, *J. Glaciol.*, **9**(57), 337–362.

Barry R.G. (1981) *Mountain Weather and Climate.* Methuen and Co. Ltd. London. 313 pp.

Bindschadler R., Harrison W.D., Raymond C.F. and Crosson R. (1977) Geometry and dynamics of a surge-type glacier, *J. Glaciol.*, **18,** 181–194.

Birchfield G.E., Weertman J. and Lunde A.T. (1982) A model study of the role of high latitude topography in the climatic response to orbital insolation anomalies, *J. Atmos. Sci.* **39,** 71–87.

Bodvarsson G. (1955) On the flow of ice sheets and glaciers, *Jökull,* **5,** 1–8.

Boulton G.S. (1974) Processes and patterns of glacial erosion. In: *Glacial Geomorphology* (ed. by D.R. Coates), pp. 41–87. State University of New York, NY .

Boulton G.S. and Jones A.S. (1979) Stability of temperate ice caps and ice sheets on beds of deformable sediments, *J. Glaciol.*, **24**(90), 29–43.

Bradley R.S. and Serreze M.C. (1987) Topoclimatic studies of a high arctic plateau ice cap, *J. Glaciol.*, **33**(114), 149–158.

Braithwaite R.J. (1984) Can the mass balance of a glacier be estimated from its equilibrium line altitude?, *J Glaciol.*, **30**(106), 364–368.

Budd W.F. (1970a) The longitudinal stress and strain-rate gradients in ice masses, *J. Glaciol.*, **9**(55), 19–27.

Budd W.F. (1970b) Ice flow over bedrock perturbations, *J. Glaciol.*, **9**(55), 29–48.

Budd W.F. (1971) Stress variation with ice flow over undulations, *J. Glaciol.*, **10**(59), 177–195.

Budd W.F. and Carter D.B. (1971) An analysis of the relation between the surface and bedrock profiles of ice caps, *J. Glaciol.*, **10**(59), 197–209.

Budd W.F. and Smith I.N. (1981) The growth and retreat of ice sheets in response to orbital radiation changes. In: *Sea Level, Ice and Climatic Change, Proc. Canberra Symp., Dec. 1979.* I.A.H.S. Publ. No. 131, pp. 441–471.

Budyko M.I. (1969) The effect of solar radiation variations on the climate of the Earth, *Tellus,* **21**(5), 609–619.

Chalikov D.V. and Verbitsky M.Y.A. (1990) Modeling the Pleistocene ice ages, *Adv. Geophys.* **32,** 75–31.

Collins I.F. (1968) On the use of the equilibrium equations and flow law in relating the surface and bed topography of glaciers and ice sheets, *J. Glaciol.*, **7**(50), 199–204.

Cook K.H. (1990) The atmosphere's response to the ice sheets of the last glacial maximum, *Ann. Glaciol.*, **14,** 32–38.

Fowler A.C. (1981) A theoretical treatment of the sliding of glaciers in the absence of cavitation, *Phil. Trans. R. Soc. A,* **298,** 673–681.

Fowler A.C. (1987) Sliding with cavity formation, *J. Glaciol.*, **33**(115), 255–267.

Furbish D.J. and Andrews J.T. (1984) The use of hypsometry to indicate long term stability and response of valley glaciers to changes in mass transfer, *J. Glaciol.*, **30**(105), 199–211.

Glen J.W. (1955) The creep of polycrystalline ice, *Proc. R. Soc. A,* **228,** 519–538.

Hallet B. (1981) Glacial abrasion and sliding: their dependence on the debris concentration in basal ice, *Ann. Glaciol.*, **2,** 23–28.

Harbor J.M., Hallet B. and Raymond C. (1988) A numerical model of landform development by glacial erosion, *Nature,* **333,** 347–349.

Harding R.J. (1978) The variation of the altitudinal gradient of temperature within the British Isles, *Geogr. Annl.*, **60A,** 43–49.

Hoinkes H. (1968) Glacier variation and weather, *J. Glaciol.*, **7**(49), 3–19.

Hindmarsh R.C.A. (1990) Time scales and degrees of freedom operating in the evolution of continental ice sheets, *Trans. R. Soc. Edinb.: Earth Sci.*, **81,** 371–384.

Hutter K. (1983) *Theoretical Glaciology.* Reidel, Dordrecht, 510 pp.

Hutter K., Legrerer F. and Spring U. (1981) First order stresses and deformations in glaciers and ice sheets, *J. Glaciol.*, **27**(96), 227–270.

Huybrechts P. (1990) The Antarctic ice sheet during the last glacial-interglacial cycle: a 3-D model experiment, *Ann. Glaciol.*, **14,** 115–119.

Johannesson T., Raymond C.F. and Waddington E.D. (1989a) A simple method for determining the response time of glaciers. In: *Glacier Fluctuations and Climatic Change* (ed. by J. Oerlemans), pp. 343–352. Kluwer, Dordrecht.

Johannesson T., Raymond C.F. and Waddington E.D. (1989b) Time scale for adjustments of glaciers to changes in mass balance, *J. Glaciol.*, **35**(121), 355–369.

Kamb B. (1970) Sliding motion of glaciers: theory and observation, *Rev. Geophys. Space Phys.*, **8**(4), 673–728.

Kamb B. and Echelmeyer K.A. (1986) Stress-gradient coupling in glacier flow: I longitudinal averaging of the influence of ice thickness and surface slope, *J. Glaciol.*, **32**(111), 267–284.

Kuhn M. (1979) On the computation of heat transfer coefficients for energy balance gradients, *J. Glaciol.*, **22,** 263–272.

Kuhn M. (1981) Climate and glaciers, *Int. Ass. Hydrol. Sci. Publ.*, **131** (*Symp. Canberra 1979—Sea level, ice and climate change*), 3–20.

Kuhn M. (1984) Mass budget imbalances as criterion for a climatic classification of glaciers, *Geogr. Annl.*, **66A**(3), 229–238.

Kuhn M. (1989) The response of the ELA to climate fluctuations: theory and observations. In: *Glacier Fluctuations and Climatic Change* (ed. by J. Oerlemans), pp. 407–417. Kluwer, Dordrecht.

Letreguilly A. (1988) Relationships between mass balance of West Canadian mountain glaciers and meteorological data. *J. Glaciol.*, **34**(116), 11–18.

Letreguilly A. and Oerlemans J. (1990) Climate sensitivity: the significance of the altitude mass balance feedback on glaciers and ice sheets, *Annals Glaciol.*, **14,** 345.

Letreguilly A. and Reynaud L. (1989) Spatial patterns of mass balance fluctuations of North American glaciers, *J. Glaciol.*, **35**(120), 163–168.

Lliboutry L. (1968) General theory of subglacial cavitation and sliding of glciers, *J. Glaciol.*, **7**(49), 21–58.

Lliboutry L. (1974) Multivariate statistical analysis of glacier annual balances, *J. Glaciol.*, **13**(69), 371–392.

Lliboutry L. (1976) Physical processes in temperate glaciers, *J. Glaciol.*, **16**(74), 151–158.

Lliboutry LA. (1987) *Very Slow Flows of Solids.* Martinus Nijhoff, Dordrecht, 510 pp.

McIntyre N.F. (1985) The dynamics of ice sheet outlets, *J. Glaciol.*, **31**(198), 99–107.

Mahaffy M.W. (1976) A three dimensional numerical model of ice sheets: tests on the Barnes ice cap, NW Territories, *J. geophys. Res.*, **81**(6), 1059–1066.

Manley G. (1955) On the occurence of ice domes and permanently snow covered summits, *J. Glaciol.*, **2**(17), 453–456.

Mazo V.L. (1989) Waves on glacier beds, *J. Glaciol.*, **35**(120), 179–182.

Meierding T.C. (1982) Late Pleistocene glacial equilibrium line altitudes in the Colorado Front Range: a comparison of methods, *Quat. Res.*, **18,** 289–310.

Molnar P. and England P. (1990) Late Cenozoic uplift of mountain ranges and global climate change: chicken or egg?, *Nature*, **346,** 29–34.

Morland L.W. (1976) Glaciers sliding down an inclined wavy bed, *J. Glaciol.*, **17**(77), 447–462.

Morland L.W. and Johnson I.R. (1982) Effects of bed inclinaiton and topography on steady state isothermal ice sheets, *J. Glaciol.*, **28**(98), 71–90.

North G.R., Cahalan R.F. and Coakley J.A. (1981) Energy balance climate models, *Rev. Geophys. Space Phys.*, **19**(1), 91–121.

Nye J.F. (1951) The flow of glaciers and ice sheets as a problem in plasticity, *Proc. R. Soc. A* **207,** 554–572.

Nye J.F. (1952) A method of calculating the thickness of the ice sheets, *Nature*, **169,** 529–530.

Nye J.F. (1957) The distribution of stress and velocity in glaciers and ice sheets, *Proc. R. Soc. A*, **239,** 113–133.

Nye J.F. (1960) The response of glaciers and ice sheets to seasonal and climatic changes, *Proc. R. Soc. A*, **256,** 559–584.

Nye J.F. (1961) The influence of climatic variations on glaciers, *J. Int. Ass. Sci. Hydrol.*, **54,** 397–404.

Nye J.F. (1963a) On the theory of the advance and retreat of glaciers, *Geophys. J. R. astr. Soc.*, **7,** 431–456.

Nye J.F. (1963b) The response of glaciers to changes in the rate of nourishment and wastage, *Proc. R. Soc. A*, **275,** 87–112.

Nye J.F. (1965a) The frequency response of glaciers, *J. Glaciol.*, **5**(41), 567–587.

Nye J.F. (1965b) A numerical method of infering the budget history of a glacier form its advance and retreat, *J. Glaciol.*, **5**(41), 589–607.

Nye J.F. (1965c) The flow of a glacier in a channel of rectangular, elliptic or parabolic cross-section, *J. Glaciol.*, **5**(41), 661–690.

Nye J.F. (1969) The effect of longitudinal stress on the shear stress at the base of an ice sheet, *J. Glaciol.*, **8**(53), 207–213.

Oerlemans J. (1980) Continental ice sheets and the planetary radiation budget, *Quat. Res.*, **14,** 349–359.

Oerlemans J. (1989) On the response of valley glaciers to climatic change. In: *Glacier Fluctuations and Climatic Change* (ed. by J. Oerlemans), pp. 407–417, Kluwer, Dordrecht.

Oerlemans J. (1990) A model for the surface balance of ice masses, Part 1: Alpine glaciers, *Z. Gletscherk. Glazialgeol.*, **26**(2).

Oerlemans J. and Hoogendoorn N.C. (1989) Mass-balance gradients and climate change, *J. Glaciol.*, **35**(121), 399–405.

Oerlemans J. and van der Veen C.J. (1984) *Ice Sheets and Climate.* Reidel, Dordrecht.

Orowan E. (1949) At "Joint meeting of the British Geological Survey, the British Rheologists Club and the Institute of Metals", *J. Glaciol.*, **1**(5), 231–240.

Østrem G. (1966) The height of the glaciation limit in southern British Columbia and Alberta, *Geogr. Annlr.*, **48A**(3), 126–138.

Paterson W.S.B. (1981) *The Physics of Glaciers*, 2nd edn. Pergamon, Oxford, 380 pp.

Payne A.J. and Sugden D.E. (1990) Topography and ice sheet growth, *Earth Surf. Proc. Landforms*, **15,** 625–639.

Payne A.J., Sugden D.E. and Clapperton C.M. (1989) Modelling the growth and decay of the Antarctic peninsular ice sheet, *Quat. Res.*, **31,** 119–134.

Pelto M.S., Higgins S.M., Hughes T.J. and Fastook J.L. (1990) Modelling-mass balance during a glaciation cycle, *Annals Glaciol.*, **14,** 328–241.

Porter S.C. (1989) Some geological implications of average Quarternary glacial conditions, *Quat. Res.*, **32**(3), 245–261.

Punkari M. (1980) The ice lobes of the Scandinavian ice sheet during the deglaciation in Finland, *Boreas*, **9,** 307–310.

Raymo M.E. and Ruddiman W.F. (1992) Tectonic forcing of the late Cenozoic climate, *Nature*, **359,** 117–122.

Reynaud L., Vallon M., Martin S. and Letreguilly A. (1984) Spatio temporal distribution of the glacial mass balance in the Alpine, Scandinavian and Tien Shan areas, *Geogr. Annlr.*, **66A**(3), 239–247.

Robin G. de Q. (1967) Surface topography of ice sheets, *Nature*, **215,** 1029–1032.

Robinson E.S. (1966) On the relationship of ice surface topography to bed topography on the south polar plateau, *J. Glaciol.*, **6**(43), 43–54.

Saltzman B. (1985) Paleoclimatic modelling. In: *Paleoclimatic Analysis and Modelling* (ed. by A.D. Hecht). Wiley, London.

Schweizer J. and Iken A. (1992) The role of bed seperation and friction in sliding over an undeformable bed, *J. Glaciol.*, **38**(128), 77–92.

Sellers W.D. (1969) A global climate model based on the energy balance of the earth–atmosphere system, *J. Appl. Meteorol.*, **8,** 392–400.

Schytt V. (1967) A study of 'ablation gradient', *Geogr. Annlr.*, **49A**(2–4), 327–332.

Thomas R.H. (1979) The dynamics of marine ice sheets, *J. Glaciol.*, **24**(90), 167–177.

Van der Veen C.J. (1985) Response of a marine ice sheet to changes in the grounding line, *Quat. Res.*, **24**(3), 257–267.

Van der Veen C.J. and Whillans I.M. (1989a) Force budget: I: theory and numerical methods, *J. Glaciol.*, **35**(119), 53–60.

Van der Veen C.J. and Whillans I.M. (1989b) Force budget: II: application to two-dimensional flow along Byrd Station strain network, Antarctica, *J. Glaciol.*, **35**(119), 61–67.

Vialov S.S. (1958) Regularities of glacial shield movements and the theory of plastic viscous flow, *J. Int. Ass. Sci. Hydrol.*, **47**, 266–275.

Warren C.R. (1992) Iceberg calving and the glacio-climatic record, *Progr. Phys. Geogr.*, **16**(3), 253–282.

Weertman J. (1957) On the sliding of glaciers, *J. Glaciol.*, **3**(21), 33–38.

Weertman J. (1961) Equilibrium profile of ice caps, *J. Glaciol.*, **3**(30), 953–964.

Weertman J. (1964) Rate of growth or shrinkage of non-equilibrium ice sheets, *J. Glaciol.*, **5**(38), 145–158.

Weertman J. (1973) Position of ice divides and ice centres on ice sheets, *J. Glaciol.*, **12**(66), 353–360.

Whillans I.M. and Johnsen S.J. (1983) Longitudinal variations in glacier flow: theory and test using data from the Byrd Station strain network, Antarctica, *J. Glaciol.*, **29**(101), 78–97.

Whillans I.M., Chen Y.H., van der Veen C.J. and Hughes T.J. (1989) Force budget III: application to three dimensional flow of Byrd glacier, Antarctica, *J. Glaciol.*, **35**(119), 68–80.

Williams L.D. (1975) The variation of corrie elevation and equilibrium line altitude with aspect in Eastern Baffin Island, N.W.T., Canada, *Arctic Alpine Res.*, **7**(2), 169–181.

Received 18 December 1992; revision accepted 7 April 1993